

**THE ROLE OF POTENTIAL DETERMINING IONS IN
CARBONATE ROCK-SEAWATER INTERACTIONS**

BY

MOSHOOD OLUWASEUN KASSIM

A Thesis Presented to the
DEANSHIP OF GRADUATE STUDIES

KING FAHD UNIVERSITY OF PETROLEUM & MINERALS

DHAHRAN, SAUDI ARABIA

1963 ١٣٨٣

In Partial Fulfillment of the
Requirements for the Degree of

MASTER OF SCIENCE

In

PETROLEUM ENGINEERING

SEPTEMBER 2012

KING FAHD UNIVERSITY OF PETROLEUM & MINERALS

DHAHRAN- 31261, SAUDI ARABIA

DEANSHIP OF GRADUATE STUDIES

This thesis, written by **MOSHOOD OLUWASEUN KASSIM** under the direction of his thesis advisor and approved by his thesis committee, has been presented and accepted by the Dean of Graduate Studies, in partial fulfillment of the requirements for the degree of **MASTER OF SCIENCE IN PETROLEUM ENGINEERING.**



Dr. Hasan S. Al-Hashim
(Advisor)



Dr. Abdullah Sultan
Department Chairman



Dr. Salam A. Zummo
Dean of Graduate Studies



Dr. Abdullah Sultan
(Member)



Dr. Reyad A. Shawabkeh
(Member)

13/10/12

Date



DEDICATION

This thesis is dedicated to my mother, who passed away during the course of this research.

May Almighty Allah(SWT) grant her Janat-Alfirdaus(Amin).

ACKNOWLEDGEMENT

My greatest gratitude goes to Almighty Allah (SWT) for bestowing on me his guidance, and mercies throughout this work.

Acknowledgment is due to King Fahd University of Petroleum & Minerals for providing me with the scholarship opportunity to pursue graduate studies. Saudi-Aramco is also appreciated for providing reservoir carbonate rocks and crude oil samples. I would also like to thank the former chairman of the Petroleum Engineering Department, Dr. Abdulaziz Al-Majed for his support.

My profound gratitude goes to my thesis advisor, Dr. Hasan S. Al-Hashim for the opportunity given to me to carry out this research, and for his support, suggestions, and constructive criticisms which were very handy throughout this research work. I am greatly indebted to my thesis committee members, Dr. Reyad A. Shawabkeh, and Dr. Abdullah Sultan for their consistent support, guidance, and motivations. Despite their very busy schedule, they were always willing to analyse and discuss results with so much enthusiasm. Special thanks also goes to Prof. Dr. Mehmet Sabri Celik of the Istanbul Technical University, Turkey, for patiently initiating me into this kind of experimental work.

My sincere gratitude goes to the members of staff of the Environmental Chemistry Analytical laboratory (ECAL) unit at the Center for Environment and Water (CEW), KFUPM Research Institute, specifically Mohammed Nazeeruddin Sayed, Buanafe Ricardo, Hassan Al-Heliyal, Hassan Al-Muhanna, Izzat Wajih, Tahir Zaidi, Dr. Shemsi,

and Muhammed Omer for the freedom given to me to work in their labs, and for the analysis of my brines. I will also like to thank the staff members of the Center for Petroleum and Minerals (CPM) for their support, and invaluable advices throughout this work.

I would like to extend my sincere appreciation to my friends and colleagues in the department, including Najimudeen, Jabbar, and others (too numerous to be mentioned) whose little chats and tips made the accomplishment of this thesis possible. Members of the Nigerian community at KFUPM are also appreciated for making Saudi Arabia for me home away from home.

I would like to thank my family, especially my parents and siblings for their never-ending encouragements, support, and prayers. Finally, my beloved patient wife is affectionately appreciated for her passionate prayers, support and understanding, which have to a great extent made the accomplishment of this thesis possible.

TABLE OF CONTENTS

ACKNOWLEDGEMENT.....	IV
TABLE OF CONTENTS	VI
LIST OF TABLES	X
LIST OF FIGURES	XI
ABSTRACT.....	XVIII
CHAPTER 1.....	1
INTRODUCTION.....	1
1.1 OBJECTIVE.....	3
CHAPTER 2.....	4
LITERATURE REVIEW	4
2.1 CARBONATES	4
2.1.1 Limestone.....	4
2.1.2 Dolomites.....	5
2.1.3 Chalk	5
2.2 WETTABILITY OF CARBONATE RESERVOIRS.....	5
2.2.1 Wettability Alteration in Carbonate Reservoirs.....	7
2.3 CARBONATE ROCK/BRINE INTERACTIONS	8
2.3.1 Impacts of Ca^{2+} , Mg^{2+} , and SO_4^{2-} in seawater on improved oil recovery in Chalk	8
2.3.2 Impacts of Ca^{2+} , Mg^{2+} , and SO_4^{2-} in seawater on improved oil recovery in Limestone.....	13
2.3.3 Impacts of NaCl in seawater on improved oil recovery in Chalk and Limestone	14

2.3.4	Impact of Low Saline Brines on Oil Recovery in Sandstones	15
2.3.5	Impact of Low Saline Brines on Oil Recovery in Carbonates	16
CHAPTER 3	19
EXPERIMENTAL METHODOLOGY	19
3.1	MATERIALS	19
3.1.1	Limestone sample	19
3.1.2	Precipitated Calcium carbonate (PCC) and other analytical grade reagents	20
3.1.3	Brines	23
3.1.4	Crude Oil.....	24
3.2	EXPERIMENTAL PROCEDURES AND EQUIPMENTS	25
3.2.1	Adsorption Experiments in the Absence of Crude Oil	25
3.2.2	Adsorption Experiments in the Presence of Crude Oil	27
3.2.3	Chemical Analysis of Brines.....	29
3.2.4	Adsorption density calculations	31
3.2.5	Adsorption Results Analysis on Limestone	32
3.2.6	Zeta Potential Measurements	33
CHAPTER 4	36
RESULTS AND DISCUSSION	36
4.1	EXPERIMENTAL RESULTS ON PRECIPITATED CALCIUM CARBONATE (PCC).....	36
4.1.1	Adsorption Results on PCC	36
4.1.1.1	Calcium ion adsorption onto PCC.....	36
4.1.1.2	Magnesium ion adsorption onto PCC	38
4.1.1.3	Sulfate ion adsorption onto PCC.....	41

4.1.2	Zeta Potential Results on PCC	42
4.1.2.1	Iso-Electric Point (IEP) of PCC	42
4.1.2.2	Impact of Sulfate, Calcium, and Magnesium ions on the Zeta Potential of PCC	44
4.1.2.3	Impact of Temperature on the Zeta Potential of PCC	45
4.2	EXPERIMENTAL RESULTS ON LIMESTONE.....	46
4.2.1	Static Adsorption studies on Limestone.....	48
4.2.1.1	Adsorption of Ca^{2+} , Mg^{2+} , SO_4^{2-} , and Cl^- on Limestone in the absence of crude oil at 25°C.....	48
4.2.1.2	Adsorption of Ca^{2+} , Mg^{2+} , SO_4^{2-} , and Cl^- on Limestone in the presence of crude oil at 25°C	60
4.2.1.3	Adsorption of Ca^{2+} , Mg^{2+} , SO_4^{2-} , and Cl^- on Limestone in the absence of crude oil at 90°C.....	72
4.2.1.4	Adsorption of Ca^{2+} , Mg^{2+} , SO_4^{2-} , and Cl^- on Limestone in the presence of crude oil at 90°C	84
4.2.1.5	Impact of crude oil on the adsorption of Ca^{2+} , Mg^{2+} , SO_4^{2-} , and Cl^- on Limestone at 25°C	96
4.2.1.6	Impact of crude oil on the adsorption of Ca^{2+} , Mg^{2+} , SO_4^{2-} , and Cl^- on Limestone at 90°C	108
4.2.1.7	Temperature effect on the adsorption of Ca^{2+} , Mg^{2+} , SO_4^{2-} , and Cl^- on Limestone in the absence of crude oil	120
4.2.1.8	Temperature effect on the adsorption of Ca^{2+} , Mg^{2+} , SO_4^{2-} , and Cl^- on Limestone in the presence of crude oil.....	130
4.2.1.9	Summary of adsorption results of Ca^{2+} , Mg^{2+} , SO_4^{2-} , and Cl^- on Limestone	142
4.2.2	Zeta Potential Results on Limestone.....	144
4.2.2.1	Iso-Electric Point (IEP) of Limestone.....	144

4.2.2.2	Impact of Calcium, Magnesium, Sulfate, Carbonate, and Bi-Carbonate ions on the Zeta Potential of limestone	146
4.2.2.3	Zeta potential of limestone in seawater	149
4.2.2.4	Impact of Temperature on the Zeta Potential of Limestone	153
CHAPTER 5	154
CONCLUSIONS AND RECOMMENDATIONS	154
5.1	CONCLUSIONS	154
5.2	RECOMMENDATIONS	157
APPENDIX	158
NOMENCLATURE	163
REFERENCES	166
VITA	174

LIST OF TABLES

Table 1: Chemical composition of carbonate samples used in this study.....	21
Table 2: Analytical grade reagents used in brine preparations	21
Table 3: Ionic Composition of Injection Seawater and 50% SW	23
Table 4: Initial brine compositions	24
Table 5: Factors and levels used in adsorption ANOVA.....	32
Table 6: Ionic concentrations of all factors considered in ANOVA.....	47
Table A1: Ca^{2+} raw experimental adsorption data on limestone	158
Table A2: Mg^{2+} raw experimental adsorption data on limestone	159
Table A3: SO_4^{2-} raw experimental adsorption data on limestone.....	160
Table A4: Cl^- raw experimental adsorption data on limestone	161

LIST OF FIGURES

Figure 1: Zeta potential measurements on an aqueous chalk suspension system by adding Sulfate and Calcium ions [24].....	9
Figure 2: Zeta potential measurements on an aqueous chalk suspension system by adding Magnesium ion [25]	10
Figure 3: Schematic model of the suggested mechanism for the wettability alteration induced by seawater. (A) Proposed mechanism when Ca^{2+} and SO_4^{2-} are active at lower and high temperature. (B) Proposed mechanism when Mg^{2+} and SO_4^{2-} are active at higher temperatures [27]	12
Figure 4: XRD pattern of Arab-D limestone powder	22
Figure 5: Effect of Solid/Liquid ratio on sulfate ion adsorption onto PCC	25
Figure 6: Equilibrium time for adsorption of ions onto limestone	28
Figure 7: Adsorption isotherms of Ca^{2+} onto PCC at 25°C and 90°C.....	38
Figure 8a: Adsorption isotherms of Mg^{2+} onto PCC at 25°C and 90°C.	40
Figure 8b: Desorption of Ca^{2+} in PCC- Mg^{2+} brine interactions at 25°C and 90°C.....	40
Figure 9: Adsorption isotherms of SO_4^{2-} onto PCC at 25°C and 90°C.....	41
Figure 10: Zeta Potential profile of PCC as a function of pH at 25°C.	43
Figure 11: Impact of Ca^{2+} , Mg^{2+} , and SO_4^{2-} on the zeta potential of PCC.....	44
Figure 12: Effect of temperature on the zeta potential of PCC	45
Figure 13: Main effects of $[\text{Ca}^{2+}]$, $[\text{Mg}^{2+}]$, $[\text{SO}_4^{2-}]$, and $[\text{Cl}^-]$ on the adsorption of Ca^{2+} by limestone at 25°C in the absence of crude-oil	49
Figure 14: Two-way interactions of $[\text{Ca}^{2+}]$, $[\text{Mg}^{2+}]$, $[\text{SO}_4^{2-}]$, and $[\text{Cl}^-]$ on the adsorption of Ca^{2+} by limestone at 25°C in the absence of crude-oil	50
Figure 15: Main effects of $[\text{Ca}^{2+}]$, $[\text{Mg}^{2+}]$, $[\text{SO}_4^{2-}]$, and $[\text{Cl}^-]$ on the adsorption of Mg^{2+} by limestone at 25°C in the absence of crude-oil	52

Figure 16: Two-way interactions of $[Ca^{2+}]$, $[Mg^{2+}]$, $[SO_4^{2-}]$, and $[Cl^-]$ on the adsorption of Mg^{2+} by limestone at 25°C in the absence of crude-oil.....	53
Figure 17: Main effects of $[Ca^{2+}]$, $[Mg^{2+}]$, $[SO_4^{2-}]$, and $[Cl^-]$ on the adsorption of SO_4^{2-} by limestone at 25°C in the absence of crude-oil.....	55
Figure 18: Two-way interactions of $[Ca^{2+}]$, $[Mg^{2+}]$, $[SO_4^{2-}]$, and $[Cl^-]$ on the adsorption of SO_4^{2-} by limestone at 25°C in the absence of crude-oil.....	56
Figure 19: Main effects of $[Ca^{2+}]$, $[Mg^{2+}]$, $[SO_4^{2-}]$, and $[Cl^-]$ on the adsorption of Cl^- by limestone at 25°C in the absence of crude-oil	58
Figure 20: Two-way interactions of $[Ca^{2+}]$, $[Mg^{2+}]$, $[SO_4^{2-}]$, and $[Cl^-]$ on the adsorption of Cl^- by limestone at 25°C in the absence of crude-oil.....	59
Figure 21: Main effects of $[Ca^{2+}]$, $[Mg^{2+}]$, $[SO_4^{2-}]$, and $[Cl^-]$ on the adsorption of Ca^{2+} by limestone at 25°C in the presence of crude-oil.....	61
Figure 22: Two-way interactions of $[Ca^{2+}]$, $[Mg^{2+}]$, $[SO_4^{2-}]$, and $[Cl^-]$ on the adsorption of Ca^{2+} by limestone at 25°C in the presence of crude-oil	62
Figure 23: Main effects of $[Ca^{2+}]$, $[Mg^{2+}]$, $[SO_4^{2-}]$, and $[Cl^-]$ on the adsorption of Mg^{2+} by limestone at 25°C in the presence of crude-oil.....	64
Figure 24: Two-way interactions of $[Ca^{2+}]$, $[Mg^{2+}]$, $[SO_4^{2-}]$, and $[Cl^-]$ on the adsorption of Mg^{2+} by limestone at 25°C in the presence of crude-oil.....	65
Figure 25: Main effects of $[Ca^{2+}]$, $[Mg^{2+}]$, $[SO_4^{2-}]$, and $[Cl^-]$ on the adsorption of SO_4^{2-} by limestone at 25°C in the presence of crude-oil.....	67
Figure 26: Two-way interactions of $[Ca^{2+}]$, $[Mg^{2+}]$, $[SO_4^{2-}]$, and $[Cl^-]$ on the adsorption of SO_4^{2-} by limestone at 25°C in the presence of crude-oil	68
Figure 27: Main effects of $[Ca^{2+}]$, $[Mg^{2+}]$, $[SO_4^{2-}]$, and $[Cl^-]$ on the adsorption of Cl^- by limestone at 25°C in the presence of crude-oil.....	70
Figure 28: Two-way interactions of $[Ca^{2+}]$, $[Mg^{2+}]$, $[SO_4^{2-}]$, and $[Cl^-]$ on the adsorption of Cl^- by limestone at 25°C in the presence of crude-oil	71
Figure 29: Main effects of $[Ca^{2+}]$, $[Mg^{2+}]$, $[SO_4^{2-}]$, and $[Cl^-]$ on the adsorption of Ca^{2+} by limestone at 90°C in the absence of crude-oil	73

Figure 30: Two-way interactions of $[Ca^{2+}]$, $[Mg^{2+}]$, $[SO_4^{2-}]$, and $[Cl^-]$ on the adsorption of Ca^{2+} by limestone at 90°C in the absence of crude-oil	74
Figure 31: Main effects of $[Ca^{2+}]$, $[Mg^{2+}]$, $[SO_4^{2-}]$, and $[Cl^-]$ on the adsorption of Mg^{2+} by limestone at 90°C in the absence of crude-oil	76
Figure 32: Two-way interactions of $[Ca^{2+}]$, $[Mg^{2+}]$, $[SO_4^{2-}]$, and $[Cl^-]$ on the adsorption of Mg^{2+} by limestone at 90°C in the absence of crude-oil	77
Figure 33: Main effects of $[Ca^{2+}]$, $[Mg^{2+}]$, $[SO_4^{2-}]$, and $[Cl^-]$ on the adsorption of SO_4^{2-} by limestone at 90°C in the absence of crude-oil	79
Figure 34: Two-way interactions of $[Ca^{2+}]$, $[Mg^{2+}]$, $[SO_4^{2-}]$, and $[Cl^-]$ on the adsorption of SO_4^{2-} by limestone at 90°C in the absence of crude-oil	80
Figure 35: Main effects of $[Ca^{2+}]$, $[Mg^{2+}]$, $[SO_4^{2-}]$, and $[Cl^-]$ on the adsorption of Cl^- by limestone at 90°C in the absence of crude-oil	82
Figure 36: Two-way interactions of $[Ca^{2+}]$, $[Mg^{2+}]$, $[SO_4^{2-}]$, and $[Cl^-]$ on the adsorption of Cl^- by limestone at 90°C in the absence of crude-oil	83
Figure 37: Main effects of $[Ca^{2+}]$, $[Mg^{2+}]$, $[SO_4^{2-}]$, and $[Cl^-]$ on the adsorption of Ca^{2+} by limestone at 90°C in the presence of crude-oil	85
Figure 38: Two-way interactions of $[Ca^{2+}]$, $[Mg^{2+}]$, $[SO_4^{2-}]$, and $[Cl^-]$ on the adsorption of Ca^{2+} by limestone at 90°C in the presence of crude-oil	86
Figure 39: Main effects of $[Ca^{2+}]$, $[Mg^{2+}]$, $[SO_4^{2-}]$, and $[Cl^-]$ on the adsorption of Mg^{2+} by limestone at 90°C in the presence of crude-oil	88
Figure 40: Two-way interactions of $[Ca^{2+}]$, $[Mg^{2+}]$, $[SO_4^{2-}]$, and $[Cl^-]$ on the adsorption of Mg^{2+} by limestone at 90°C in the presence of crude-oil	89
Figure 41: Main effects of $[Ca^{2+}]$, $[Mg^{2+}]$, $[SO_4^{2-}]$, and $[Cl^-]$ on the adsorption of SO_4^{2-} by limestone at 90°C in the presence of crude-oil	91
Figure 42: Two-way interactions of $[Ca^{2+}]$, $[Mg^{2+}]$, $[SO_4^{2-}]$, and $[Cl^-]$ on the adsorption of SO_4^{2-} by limestone at 90°C in the presence of crude-oil	92
Figure 43: Main effects of $[Ca^{2+}]$, $[Mg^{2+}]$, $[SO_4^{2-}]$, and $[Cl^-]$ on the adsorption of Cl^- by limestone at 90°C in the presence of crude-oil	94

Figure 44: Two-way interactions of $[Ca^{2+}]$, $[Mg^{2+}]$, $[SO_4^{2-}]$, and $[Cl^-]$ on the adsorption of Cl^- by limestone at 90°C in the presence of crude-oil	95
Figure 45: Main effects of $[Ca^{2+}]$, $[Mg^{2+}]$, $[SO_4^{2-}]$, and $[Cl^-]$ on the adsorption of Ca^{2+} by limestone at 25°C in the absence and presence of crude-oil	97
Figure 46: Two-way interactions of $[Ca^{2+}]$, $[Mg^{2+}]$, $[SO_4^{2-}]$, and $[Cl^-]$ on the adsorption of Ca^{2+} by limestone at 25°C in the absence and presence of crude-oil	98
Figure 47: Main effects of $[Ca^{2+}]$, $[Mg^{2+}]$, $[SO_4^{2-}]$, and $[Cl^-]$ on the adsorption of Mg^{2+} by limestone at 25°C in the absence and presence of crude-oil.....	100
Figure 48: Two-way interactions of $[Ca^{2+}]$, $[Mg^{2+}]$, $[SO_4^{2-}]$, and $[Cl^-]$ on the adsorption of Mg^{2+} by limestone at 25°C in the absence and presence of crude-oil	101
Figure 49: Main effects of $[Ca^{2+}]$, $[Mg^{2+}]$, $[SO_4^{2-}]$, and $[Cl^-]$ on the adsorption of SO_4^{2-} by limestone at 25°C in the absence and presence of crude-oil	103
Figure 50: Two-way interactions of $[Ca^{2+}]$, $[Mg^{2+}]$, $[SO_4^{2-}]$, and $[Cl^-]$ on the adsorption of SO_4^{2-} by limestone at 25°C in the absence and presence of crude-oil	104
Figure 51: Main effects of $[Ca^{2+}]$, $[Mg^{2+}]$, $[SO_4^{2-}]$, and $[Cl^-]$ on the adsorption of Cl^- by limestone at 25°C in the absence and presence of crude-oil	106
Figure 52: Two-way interactions of $[Ca^{2+}]$, $[Mg^{2+}]$, $[SO_4^{2-}]$, and $[Cl^-]$ on the adsorption of Cl^- by limestone at 25°C in the absence and presence of crude-oil	107
Figure 53: Main effects of $[Ca^{2+}]$, $[Mg^{2+}]$, $[SO_4^{2-}]$, and $[Cl^-]$ on the adsorption of Ca^{2+} by limestone at 90°C in the absence and presence of crude-oil.....	109
Figure 54: Two-way interactions of $[Ca^{2+}]$, $[Mg^{2+}]$, $[SO_4^{2-}]$, and $[Cl^-]$ on the adsorption of Ca^{2+} by limestone at 90°C in the absence and presence of crude-oil	110

Figure 55: Main effects of $[Ca^{2+}]$, $[Mg^{2+}]$, $[SO_4^{2-}]$, and $[Cl^-]$ on the adsorption of Mg^{2+} by limestone at 90°C in the absence and presence of crude-oil	112
Figure 56: Two-way interactions of $[Ca^{2+}]$, $[Mg^{2+}]$, $[SO_4^{2-}]$, and $[Cl^-]$ on the adsorption of Mg^{2+} by limestone at 90°C in the absence and presence of crude-oil	113
Figure 57: Main effects of $[Ca^{2+}]$, $[Mg^{2+}]$, $[SO_4^{2-}]$, and $[Cl^-]$ on the adsorption of SO_4^{2-} by limestone at 90°C in the absence and presence of crude-oil	115
Figure 58: Two-way interactions of $[Ca^{2+}]$, $[Mg^{2+}]$, $[SO_4^{2-}]$, and $[Cl^-]$ on the adsorption of SO_4^{2-} by limestone at 90°C in the absence and presence of crude-oil	116
Figure 59: Main effects of $[Ca^{2+}]$, $[Mg^{2+}]$, $[SO_4^{2-}]$, and $[Cl^-]$ on the adsorption of Cl^- by limestone at 90°C in the absence and presence of crude-oil	118
Figure 60: Two-way interactions of $[Ca^{2+}]$, $[Mg^{2+}]$, $[SO_4^{2-}]$, and $[Cl^-]$ on the adsorption of Cl^- by limestone at 90°C in the absence and presence of crude-oil	119
Figure 61: Main effects of $[Ca^{2+}]$, $[Mg^{2+}]$, $[SO_4^{2-}]$, and $[Cl^-]$ on the adsorption of Ca^{2+} by limestone at 25°C and 90°C in the absence of crude-oil	121
Figure 62: Two-way interactions of $[Ca^{2+}]$, $[Mg^{2+}]$, $[SO_4^{2-}]$, and $[Cl^-]$ on the adsorption of Ca^{2+} by limestone at 25°C and 90°C in the absence of crude-oil	122
Figure 63: Main effects of $[Ca^{2+}]$, $[Mg^{2+}]$, $[SO_4^{2-}]$, and $[Cl^-]$ on the adsorption of Mg^{2+} by limestone at 25°C and 90°C in the absence of crude-oil	124
Figure 64: Two-way interactions of $[Ca^{2+}]$, $[Mg^{2+}]$, $[SO_4^{2-}]$, and $[Cl^-]$ on the adsorption of Mg^{2+} by limestone at 25°C and 90°C in the absence of crude-oil	125
Figure 65: Main effects of $[Ca^{2+}]$, $[Mg^{2+}]$, $[SO_4^{2-}]$, and $[Cl^-]$ on the adsorption of SO_4^{2-} by limestone at 25°C and 90°C in the absence of crude-oil	126

Figure 66: Two-way interactions of $[Ca^{2+}]$, $[Mg^{2+}]$, $[SO_4^{2-}]$, and $[Cl^-]$ on the adsorption of SO_4^{2-} by limestone at 25°C and 90°C in the absence of crude-oil	127
Figure 67: Main effects of $[Ca^{2+}]$, $[Mg^{2+}]$, $[SO_4^{2-}]$, and $[Cl^-]$ on the adsorption of Cl^- by limestone at 25°C and 90°C in the absence of crude-oil	128
Figure 68: Two-way interactions of $[Ca^{2+}]$, $[Mg^{2+}]$, $[SO_4^{2-}]$, and $[Cl^-]$ on the adsorption of Cl^- by limestone at 25°C and 90°C in the absence of crude-oil	129
Figure 69: Main effects of $[Ca^{2+}]$, $[Mg^{2+}]$, $[SO_4^{2-}]$, and $[Cl^-]$ on the adsorption of Ca^{2+} by limestone at 25°C and 90°C in the presence of crude-oil	131
Figure 70: Two-way interactions of $[Ca^{2+}]$, $[Mg^{2+}]$, $[SO_4^{2-}]$, and $[Cl^-]$ on the adsorption of Ca^{2+} by limestone at 25°C and 90°C in the presence of crude-oil	132
Figure 71: Main effects of $[Ca^{2+}]$, $[Mg^{2+}]$, $[SO_4^{2-}]$, and $[Cl^-]$ on the adsorption of Mg^{2+} by limestone at 25°C and 90°C in the presence of crude-oil	134
Figure 72: Two-way interactions of $[Ca^{2+}]$, $[Mg^{2+}]$, $[SO_4^{2-}]$, and $[Cl^-]$ on the adsorption of Mg^{2+} by limestone at 25°C and 90°C in the presence of crude-oil	135
Figure 73: Main effects of $[Ca^{2+}]$, $[Mg^{2+}]$, $[SO_4^{2-}]$, and $[Cl^-]$ on the adsorption of SO_4^{2-} by limestone at 25°C and 90°C in the presence of crude-oil	137
Figure 74: Two-way interactions of $[Ca^{2+}]$, $[Mg^{2+}]$, $[SO_4^{2-}]$, and $[Cl^-]$ on the adsorption of SO_4^{2-} by limestone at 25°C and 90°C in the presence of crude-oil	138
Figure 75: Main effects of $[Ca^{2+}]$, $[Mg^{2+}]$, $[SO_4^{2-}]$, and $[Cl^-]$ on the adsorption of Cl^- by limestone at 25°C and 90°C in the presence of crude-oil	140
Figure 76: Two-way interactions of $[Ca^{2+}]$, $[Mg^{2+}]$, $[SO_4^{2-}]$, and $[Cl^-]$ on the adsorption of Cl^- by limestone at 25°C and 90°C in the presence of crude-oil	141

Figure 77: Zeta Potential profile of limestone in deionized water as a function of pH at 25°C.....	145
Figure 78: Impact of Ca^{2+} , Mg^{2+} , SO_4^{2-} , CO_3^{2-} , and HCO_3^- on the zeta potential of limestone at 25°C	147
Figure 79: Effect of varying $\text{SO}_4^{2-} / \text{Ca}^{2+}$ and $\text{SO}_4^{2-} / \text{Mg}^{2+}$ ratios on the zeta potential of limestone.....	148
Figure 80: Zeta potential of limestone in modified seawater brines in the presence and absence of crude oil at 25°C.....	150
Figure 81: Ca^{2+} raw experimental adsorption result on limestone	150
Figure 82: Mg^{2+} raw experimental adsorption result on limestone	151
Figure 83: SO_4^{2-} raw experimental adsorption result on limestone.....	152
Figure 84: Cl^- raw experimental adsorption result on limestone	152
Figure 85: Effect of temperature on the zeta potential of limestone	153
Figure A1: SEM image of Limestone	158

ABSTRACT

Full Name : Moshood Oluwaseun Kassim
Thesis Title : The Role of Potential Determining Ions in Carbonate Rock - Seawater Interactions
Major Field : Petroleum Engineering
Date of Degree : September, 2012

Water flooding has not been very efficient in carbonate reservoirs due mainly to the low water wetness of these reservoirs. Recently, extensive research through spontaneous imbibition and core-flooding experiments have demonstrated that the oil recovery from these carbonate reservoirs could be improved by modifying the ionic composition and salinity of the injected seawater. Although the underlying mechanisms are still a subject of debate, the improved oil recovery has been mostly attributed to the increased water-wetness of the rock through the interactions of specific ions like Ca^{2+} , Mg^{2+} , SO_4^{2-} , and Cl^- , which are present in seawater with the rock surface under favourable conditions.

In this thesis, static adsorption studies were extensively carried out to investigate the adsorption interactions of Ca^{2+} , Mg^{2+} , SO_4^{2-} , and Cl^- in the Arabian Gulf seawater with Arab-D carbonate reservoir rock composed mostly of dolomitized limestone in the absence and presence of crude oil from the same reservoir, at temperatures of 25°C and 90°C. This was carried out with the objective to identify the optimum parameters of the seawater that will trigger the adsorption and desorption of these ions under different conditions, which may lead to wettability alteration. In this study, surface charge of

carbonates-brines system was also studied using zeta potential technique in the absence and presence of crude oil.

Adsorption results revealed that the rock-fluid interactions of Ca^{2+} , Mg^{2+} , SO_4^{2-} , and Cl^- in Arabian Gulf seawater with carbonate rocks depends on a variety of conditions like the rock type and constituents, brine composition, presence of crude oil, and temperature. The various ways to promote adsorption or desorption of these ions under the different conditions have been extensively discussed. Zeta potential measurements confirmed that the carbonate rock is negatively charged in Arabian Gulf seawater, and this surface charge will vary depending on the brine ionic composition, presence of crude-oil and temperature. This research has shown that the interactions between the injection Arabian Gulf seawater, crude oil and the carbonate rock matrix is very complex but it can be optimized to obtain a favourable formulation that will eventually promote recovery of additional oil by simply adjusting the ionic composition of the seawater.

ملخص الرسالة

الاسم: مشهود اوليواسيون قاسم.

عنوان الأطروحة: دور و إمكانية تحديد الأيونات في تفاعلات الصخور المكمنية و مياه البحر.

التخصص: هندسة البترول.

تاريخ الدرجة العلمية: سبتمبر 2012 .

يعرف عن تقنية الغمر بالمياه أنها ليست ذات كفاءة عالية في المكامن الكربونية، وذلك لضعف خاصية التبلل المائي لصخور هذه المكامن. في الآونة الأخيرة، تم إجراء أبحاث مستفيضة لدراسة الإستخلاص النفطي بواسطة عمليات الغمر بالمياه و ذلك من خلال تجارب التشرب العفوي و الغمر الديناميكي لعينات من الصخور الكربونية. من خلال هذه البحوث لوحظ ان هنالك تحسن في نسبة إستخلاص النفط، وذلك بعد تعديل التركيب الأيوني و نسبة الملوحة لمياه البحر المستخدمة في هذه التجارب. على الرغم من أنه لا يوجد إجماع عام على آلية معينة يعزى اليها التحسن في استخلاص النفط، إلا أن زيادة التبلل المائي لسطح حبيبات الصخور الكربونية نتيجة لتفاعل أيونات الكالسيوم ، الماغنيسيوم و الكبريتات مع سطح الحبيبات الصخرية يلعب دورا رئيسيا في زيادة نسبة النفط المستخلص من هذه المكامن الكربونية وذلك في ظروف مكمنية معينة.

في هذه الأطروحة تم إجراء تجارب إمتزاز ساكن مكثفة لدراسة التفاعلات بين ايونات الكالسيوم، الماغنيسيوم، الكبريتات و الكلور الموجودة في مياه الخليج العربي و بين عينة من مكمّن عرب-د الكربوني في المملكة العربية السعودية ذو التركيبة الصخرية التي يطغى عليها الحجر الجيري بالإضافة الى الدولومايت. تم إجراء هذه التجارب في وجود و غياب عينات من النفط الخام من نفس الحقل و ذلك في درجتى حرارة ، 25 و 90 درجة مئوية. بصورة عامة، تم إجراء هذه التجارب لمعرفة المكونات الأساسية لمياه البحر التي تساعد على إمتزاز و إمتصاص الأيونات السابق ذكرها في ظروف مكمنية مختلفة، و من خلال ذلك يمكن معرفة الآلية التي تؤدي الى تغيير نوع التبلل

الصخري. إضافة الى تجارب الإمتزاز هذه، تم إجراء تجارب لدراسة الشحنات الكهربائية لسطح العينة الصخرية و ذلك بإستخدام تقنية جهد زيتا (زيتا بوتينشال) في وجود و غياب زيت المكن.

من خلال نتائج التجارب المذكورة أعلاه، تبين ان التفاعلات بين أيونات الكالسيوم، الماغنيسيوم، الكبريتات و الكلور الموجودة في مياه البحر ، و بين عينة الصخر الكربوني تختلف باختلاف التركيبة المعدنية للصخر، التركيبة الكيميائية للمحلول الملحي المستخدم، وجود النفط الخام و درجة الحرارة. في هذا البحث تم التطرق بإسهاب الى الطرق المختلفة التي تساعد على تعزيز إمتزاز و إمتصاص الأيونات السابقة و ذلك في ظروف مكنية مختلفة من خلال قياسات جهد زيتا (زيتا بوتينشال) للتأكد من أن عينة الصخر الكربوني تحمل شحنات سالبة عند وجودها في مياه البحر و لقد وُجد أن هذه الشحنات تختلف باختلاف التركيب الأيوني للمحلول المستخدم، وجود النفط الخام و درجة الحرارة. من خلال هذا البحث وُجد أن التفاعلات بين مياه البحر و عينة الصخور الكربونية المحتوية على النفط الخام غاية في التعقيد، إلا انه بالإمكان الوصول الى تركيبيية مثالية لمياه البحر يمكن من خلالها تعزيز إستخلاص النفط الخام من هذه الصخور، و ذلك بتعديل التركيب الأيوني لهذه المياه.

CHAPTER 1

INTRODUCTION

Many studies have been carried out to assess recovery from carbonate reservoirs, the reason being that more than 50% of the proven oil resources are trapped in these rocks [1]. Unfortunately, the average oil recovery from these carbonate reservoirs is less than 30% worldwide, which is very small compared to the sandstone reservoirs [2]. This has been mainly attributed to the structural heterogeneity in the porous media, natural fractures, and low water wetness.

Historically, waterflooding is often a cheap and commonly applied secondary recovery technique, with the aim of maintaining reservoir pressure, and driving of oil into the producing wells but it is not very effective due to microscopic oil trapping and macroscopic bypassing [3]. Recent laboratory studies have aimed at improving this oil recovery by attempting to understand the oil/brine/rock interactions that can alter the rock wettability. This has been done by injecting brines with tuned salinities and selected ionic compositions in both sandstone and carbonate reservoirs. Brine, which has been designed with a composition and salinity that supports maximum oil recovery is conventionally known as “smart water”.

From studies available in the literature, smart water can be designed and optimized both with regard to salinity and specific ionic compositions. Until just recently, one set of studies carried out mainly on chalk reservoirs believe that seawater rather than any kind of water will help in recovering additional oil from carbonate reservoirs. They have indicated that calcium ion (Ca^{2+}), magnesium ion (Mg^{2+}), and sulfate ion (SO_4^{2-}) present in seawater are the responsible ions for the improved oil recovery through wettability alteration. Contrary to this, brines with low salinity have also been identified as another type of smart water. The brine is prepared by reducing the salinity of the seawater by dilution up to a maximum of 5000 ppm [4]. Usage of the low saline brines has proven to be an effective improved oil recovery (IOR) technique in the laboratory and field for sandstone reservoirs. Research into its application for carbonate reservoirs was triggered by the recent findings of Yousef et al. [5], wherein they reported 18 - 19% tertiary oil recovery from coreflood experiments as a result of stepwise dilution of seawater. The improved oil recovery was attributed to the alteration of the rock wettability towards a more water-wet state. Even though studies on improving oil recovery by modification of the chemistry of the injected brine is currently on the increase as apparent from the growing number of related publications, the underlying mechanisms responsible for the improved oil recovery is still a subject of debate as many questions remain unanswered.

1.1 Objective

The main objective of this thesis is to experimentally investigate the interactions between Ca^{2+} , Mg^{2+} , SO_4^{2-} , and Cl^- which are present in the Arabian Gulf seawater with crushed Arab-D reservoir rock from Saudi Arabian carbonate reservoirs in the presence and absence of crude oil from the same reservoir. This objective was designed with a view to identify the optimum parameters of the seawater that will trigger the adsorption/desorption of these ions, which may eventually trigger wettability alteration.

CHAPTER 2

LITERATURE REVIEW

2.1 Carbonates

Carbonates are sedimentary rocks composed primarily of calcium carbonate, CaCO_3 . Two major types of carbonates are Limestone (CaCO_3), and Dolostone, which is composed of the mineral dolomite ($\text{CaMg}(\text{CO}_3)_2$). Chalk is a special type of carbonate rock. Carbonates generally form by precipitation of bicarbonate from marine muds, or accumulation of debris (grains of limestone, shells, etc.) [6]. It is estimated that almost two-thirds of the world's remaining oil reserves are contained in carbonate reservoirs [7]. Ghawar field, Saudi Arabia, and South Pars/North Dome field, Iran and Qatar are the world's largest oil and gas fields respectively and they are composed of carbonate rocks [8, 9].

2.1.1 Limestone

Limestone is a sedimentary rock composed primarily of calcium carbonate (CaCO_3) in the form of the mineral calcite. It most commonly forms in clear, warm, shallow marine waters. It is usually an organic sedimentary rock that forms from the accumulation of

shell, coral, algal and fecal debris [10]. Some limestones can form by direct precipitation of calcium carbonate from marine or fresh water. Limestones formed this way are chemical sedimentary rocks. They are thought to be less abundant than biological limestones.

2.1.2 Dolomites

Dolomite is a carbonate mineral composed of calcium magnesium carbonate $\text{CaMg}(\text{CO}_3)_2$. They are originally deposited as calcite/aragonite and transformed to dolomite during diagenesis in a process known as dolomitization.

2.1.3 Chalk

Chalk is a special case of carbonates. It is a soft, white, porous sedimentary rock composed of the mineral calcite (CaCO_3) with minor amounts of silt and clay. It is formed by the stacking of small single-cell algae called coccoliths [6]. The porosity of chalk is high, but the permeability in this carbonate is low or very low (about 1 mD), which is caused by the small pores, in the range of 0.2 to 2 microns [6].

2.2 Wettability of Carbonate Reservoirs

The reservoir rock wettability is an important property determining the success of waterflooding, because it influences greatly the location, flow and distribution of the fluids in the reservoir [11]. It is acknowledged that wettability is among the major factors which affect residual oil saturation, capillary pressures, electrical properties, relative permeabilities, and oil recovery.

In contrast to sandstone reservoirs, literature data indicate that about 80-90% of the world's carbonate reservoirs show a negative capillary pressure, that is, they are preferentially oil-wet [12]. This wetting state is as a result of adsorption of polar components from the crude oil onto the originally strong water-wet mineral surface [13]. Dubey et al. [14] explained that during the oil accumulation process in a reservoir, the oil and the mineral surfaces is separated by a water film whose thickness is determined by a balance of forces acting on it. These forces consequently result into a disjoining pressure, which resists thinning of the water film. A negative disjoining pressure will attract the two surfaces [15]. The Electrical or Zeta potential of the crude-oil/brine interface and the rock/brine interface is the most important factor in the stability of the water film. The crude oil- water interface is negatively charged as a result of dissociation of carboxylic material, while the rock-water interface is positively charged because of the high concentration of Ca^{2+} present in the initial brine [16]. These opposite charges will result into an attractive electrostatic force between the two interfaces, which will continuously thin the water film until it collapses, resulting into direct contact of the oil with the carbonate rock surface. The carboxylic group in the crude oil will then form strong bonds to the positively charged sites on the carbonate surface, thus making the water wetness to decrease as the amount of carboxylic material in the crude oil increases [16]. This carboxylic material can be quantified as an Acid number (AN), which is expressed in mg of KOH/g. The low oil recovery attributed to this low water wetness served as an impetus for research into how to increase the water wetness of our carbonate rocks.

2.2.1 Wettability Alteration in Carbonate Reservoirs

Two main approaches are used for wettability alteration in originally oil-wet carbonate rocks.

The first approach involves chemical treatment by surfactant flooding, altering the wettability from oil-wet to intermediate or to a more water-wet state, by solubilizing adsorbed hydrophobic components, thereby enhancing imbibition [17]. Though the mechanism of wettability alteration has not been fully understood, it has been generally reported that oil recovery has been increased by usage of these surfactants, some have even reported up to 60 to 70% recovery based on laboratory experiments [18, 19]. Although the surfactants have proven to increase the recovery, their application on reservoir scale is hampered by their high prices, and their instability under harsh conditions like high temperature and high salinity. Each reservoir usually requires a particular surfactant, for which specific production may not be advantageous for the chemical industry.

The second approach involves the injection of brines with compositions and salinities that can increase the water wetness of carbonate rocks. Smart water flooding is an emerging improved/enhanced oil recovery method that has attracted the attention of the petroleum industry. It has demonstrated the capability to alter the wettability of reservoir rocks advantageously. Smart water flooding has several advantages compared to other Enhanced Oil Recovery (EOR) methods which are highlighted below [20]:

- It can achieve higher ultimate oil recovery with minimal investment in current operations, assuming that a water-flooding infrastructure is already in place.
- Unlike conventional EOR, it can be applied during the early life cycle of the reservoir
- The payback is faster, even with small incremental oil recovery.

In spite of the large body of experimental evidence available on smart water flooding, it can be said that it is still in the R&D stage, as there are still many uncertainties and many questions which remain unanswered with regards to the mechanisms leading to the additional oil recovery.

2.3 Carbonate Rock/Brine interactions

2.3.1 Impacts of Ca^{2+} , Mg^{2+} , and SO_4^{2-} in seawater on improved oil recovery in Chalk

Seawater has been identified as being able to increase the water wetness of carbonate reservoirs. Much of that body of research has been conducted through spontaneous imbibition studies on outcrop chalk cores at the University of Stavenger. Their laboratory studies showed that seawater acted as a wettability modifier towards weakly water-wet chalk, especially at high temperature [12, 22, 23]. This has been attributed to the presence of Ca^{2+} , Mg^{2+} , and SO_4^{2-} ions in seawater. These three divalent ions which are naturally present in seawater have been identified as important ions in changing the surface charge of chalk and are more effective when present in favourable ratios. Ca^{2+} , Mg^{2+} , and SO_4^{2-} have been confirmed as potential determining ions of the chalk carbonate surface, as

they were able to change the zeta potential of chalk drastically (figures 1 and 2) [16,24,25].

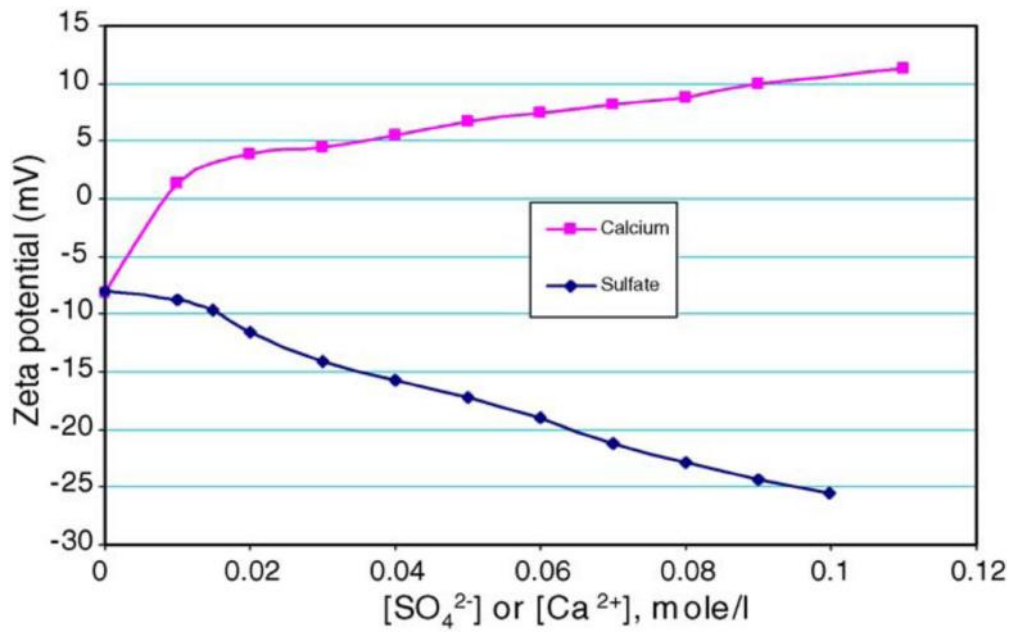


Figure 1: Zeta potential measurements on an aqueous chalk suspension system by adding Sulfate and Calcium ions [24]

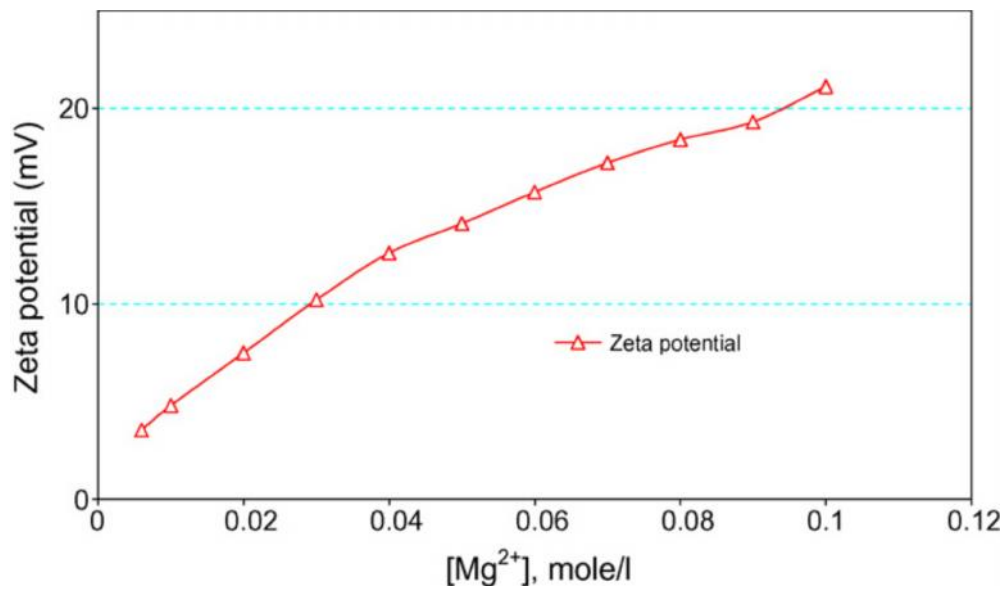


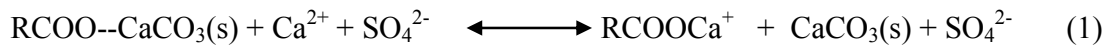
Figure 2: Zeta potential measurements on an aqueous chalk suspension system by adding Magnesium ion [25]

Through spontaneous imbibition experiments, oil recovery improved by increasing the sulfate ion concentration in the imbibing fluid, and the efficiency of the wettability alteration process in the presence of sulfate increased as the temperature increased due to increase in adsorption of SO_4^{2-} . Increased oil recovery was also observed with increasing concentration of Ca^{2+} in the brine but this impact was less significant as the concentration of sulfate ion in the imbibing fluid decreased [26]. Some of the experimental facts obtained by Austad and co-workers have been summarized by Zhang et al. [25] as follows;

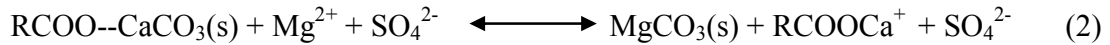
- The adsorption of SO_4^{2-} onto the chalk surface increases as the temperature increases.
- Co-adsorption of Ca^{2+} onto the chalk surface increases as the adsorption of SO_4^{2-} increases.
- At high temperature, Mg^{2+} substitutes Ca^{2+} at the chalk surface, and the degree of substitution increases as the temperature increases.
- Adsorption of SO_4^{2-} onto the chalk surface will increase the concentration of Mg^{2+} close to the surface.
- Spontaneous imbibition of water into weakly-water wet chalk increases as the concentration of SO_4^{2-} , Ca^{2+} and Mg^{2+} in the imbibing fluid increases.
- Neither Ca^{2+} nor Mg^{2+} will increase spontaneous imbibition of water without the presence of SO_4^{2-} in the imbibing fluid, and SO_4^{2-} is inactive without the presence of either Ca^{2+} or Mg^{2+} .

- Ca^{2+} is able to modify the wetting conditions both at low and high temperature but Mg^{2+} is only active at high temperatures.

The chemical mechanism proposed for wettability alteration involves initially the adsorption of sulfate onto the positively charged chalk surface which will lower the positive charge. Due to less electrostatic repulsion, more Ca^{2+} can adsorb onto the chalk surface, and this will facilitate some desorption/displacement of the carboxylic material from the surface as illustrated by reaction (1) [27] below;



At high temperature, Mg^{2+} is able to substitute/displace Ca^{2+} linked to the carboxylic groups on the chalk surface, and this degree of substitution increased as the temperature increased because Mg^{2+} becomes more reactive because of dehydration. The displacement reaction is illustrated by reaction (2) [27] below;



The role of SO_4^{2-} in the two reactions is to act as catalyst. The suggested surface charge alteration mechanism is presented in Figure 3 below;

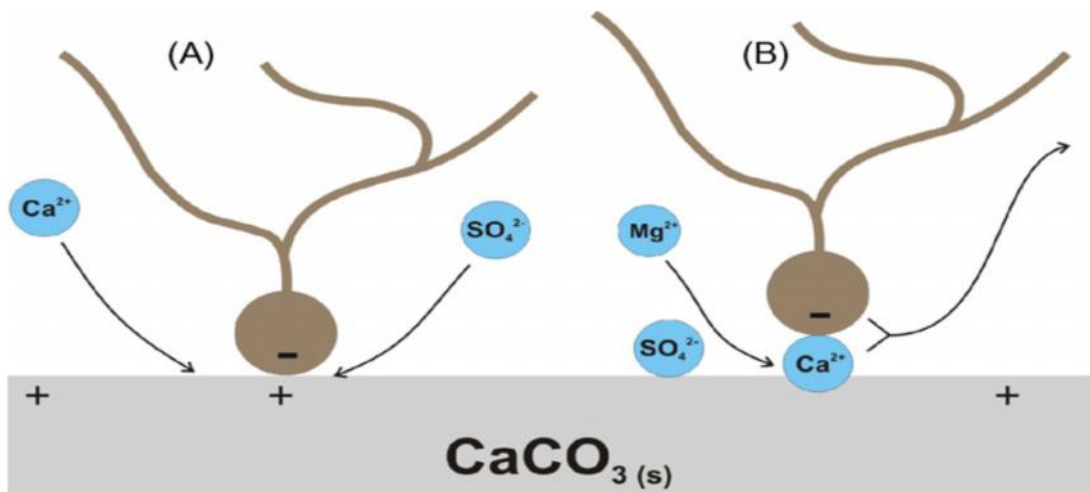


Figure 3: Schematic model of the suggested mechanism for the wettability alteration induced by seawater. (A) Proposed mechanism when Ca^{2+} and SO_4^{2-} are active at lower and high temperature. (B) Proposed mechanism when Mg^{2+} and SO_4^{2-} are active at higher temperatures [27]

This surface charge alteration mechanism proposed by Austad and Co-workers [25, 27] was challenged by Hiorth et al. [28] who investigated how water chemistry affects surface charge and rock dissolution in a pure calcium carbonate rock similar to the Stevns Klint chalk. They constructed and applied a chemical model that couples bulk aqueous and surface chemistry and also addresses mineral precipitation and dissolution. They observed that the surface potential changes are not able to explain the observed changes in oil recovery caused by seawater imbibitions or temperature but the precipitation/dissolution model was able to. As a result, mineral dissolution was proposed as the wettability alteration controlling factor.

Ferno et al. [29] casted some doubt on the wettability alteration effect of sulfate ion on chalk by investigating the effect of increased sulfate concentrations in imbibing fluids at 130°C using different outcrop chalks from three different quarries. They observed

increased oil recovery in only one chalk type, indicating the dependence of the sulfate effect on the chalk type. Mineral depositions and compositional differences are the key features believed to be responsible.

Despite all the large body of experimental work proving that the improved oil recovery from chalk was as a result of wettability alteration, Zahid et al. [30] questioned the proposed chemical mechanism after flooding completely water-wet chalk cores with brines with different sulfate concentrations. Surprisingly, oil recovery was improved with the cores at this strongly water wet conditions, indicating that there are other factors apart from wettability alteration that contribute to increased oil recovery. The recovery increased as the sulfate concentration and temperature increased. Other factors suggested are oil composition and temperature.

2.3.2 Impacts of Ca^{2+} , Mg^{2+} , and SO_4^{2-} in seawater on improved oil recovery in Limestone

Probably due to different biological origin, limestone is believed to have a less reactive surface to chalk [1]. Strand et al. [1] performed similar experimental studies to that of chalk and concluded that a reservoir limestone rock reacts chemically in the same way as chalk towards the potential determining ions, although the reactivity was lower than for chalk. 15% higher recovery was obtained with seawater containing SO_4^{2-} compared to seawater without SO_4^{2-} , indicating that the relative interaction between Ca^{2+} and Mg^{2+} towards the limestone is dictated by the presence of SO_4^{2-} .

Further studies on limestone and dolomite have also demonstrated the important role of SO_4^{2-} in the wettability modification process [31, 32]. Gupta et al. [31] obtained

incremental oil recoveries over formation waterflood recoveries of 5-9% using seawater containing 4 times sulfate ions ($4 \times \text{SO}_4^{2-}$) via coreflood experiments on dolomite and limestone cores, while Ligthelm et al. [32] obtained higher recoveries on a micro-crystalline limestone by increasing sulfate concentration in spontaneously imbibing brine. Other salts like borate and phosphate are also able to give additional recovery even better than sulfate ions [31]. Adding borate and phosphate salts individually into the seawater (without sulfate) gave 15% and 20% OOIP incremental recovery respectively on limestone cores. Contrary to the findings of Strand et al. [1], Gupta et.al. [31] reported an additional 11.4% OOIP oil recovery when softened water (formation water with Ca^{2+} and Mg^{2+} selectively removed) was flooded into a limestone core. They have cited rock dissolution and surface ion exchange as the mechanisms responsible for the wettability alteration process.

2.3.3 Impacts of NaCl in seawater on improved oil recovery in Chalk and Limestone

The impact of non-active salt like NaCl which is abundantly present in seawater on oil recovery from chalk and limestone has been investigated, revealing that seawater depleted in NaCl appears to be a better wettability modifier [33-35]. Spontaneous imbibition experiments on chalk cores showed that seawater depleted in NaCl increased oil recovery by 10% OOIP [33], while a further increase of 5 to 18% OOIP was obtained when the NaCl depleted seawater was spiked with sulfate ion [34]. Shariatpanahi et al. [35] also confirmed experimentally similar effect of NaCl on limestone after recovering additional 13% OOIP from limestone cores by imbibing seawater depleted in NaCl. Both Na^+ and Cl^- are not regarded as potential determining ions towards the chalk surface, and

so are not part of the inner stern layer [33]. The presence of high concentrations of NaCl indicates that a lot of Na^+ and Cl^- will be present in the double layer thus decreasing the ability of the active ions Ca^{2+} , Mg^{2+} , and SO_4^{2-} to come in contact with the positively charged carbonate surface to release the carboxylic material. A decrease in the non-active ions in the ionic double layer will therefore allow better access of the active ions to the carbonate surface. These ions will then interact with the surface, improve the water wetness and ultimately increase the oil recovery. This confirmed that not only is the concentration of the active ions Ca^{2+} , Mg^{2+} and SO_4^{2-} important for wettability alteration to take place, but also the amount of non-active salt, such as NaCl, has an impact on the wettability alteration process.

2.3.4 Impact of Low Saline Brines on Oil Recovery in Sandstones

Improvement of oil recovery from sandstone cores containing clays by low salinity waterflooding was reported as far back as 1959, when Martin [36] observed increased recovery of heavy oil through injection of fresh water into cores. Bernard [37] also through core flooding experiments showed that a fresh floodwater will produce more oil than a brine in sandstone cores containing hydratable clays. The increased oil recovery was attributed to clay dispersion into fine particles, and consequent plugging of flow channels and increase in pressure drop. Much attention was not paid to these discoveries until in the 1990s. Numerous laboratory imbibition and coreflood experiments have demonstrated the benefits of low saline brines in sandstone cores [4, 38-49]. Successful field tests have also confirmed the existence of the low salinity effect (LSE) [50-55]. Although the mechanism is still a subject of debate, it is generally accepted that it is caused by wettability alteration to a more favourable state.

Berg et al. [56] provided direct experimental evidence with montmorillonite clay particles that wettability modification of clay surfaces is the microscopic mechanism for low salinity flooding ruling out other proposed mechanisms such as emulsification [51], pH-induced in-situ surfactant generation and interfacial tension reduction [51], fines migration [42], and selective plugging of water-bearing pores via clay swelling [44] as the most relevant mechanisms. Other proposed mechanisms are multi-component ionic exchange between the rock minerals and injected brine [51], expansion of electrical double layers [32, 57], anhydrite cement dissolution [58, 59], and salting-in mechanism [60].

Morrow and Buckley [4] listed significant clay fraction, presence of connate water and mixed wet state of rock material as necessary conditions for low salinity effect (LSE) in Berea sandstone cores. However, LSE was not observed in some of the cases where these conditions were met. For instance, Zekri et al. [61] flooded sandstone cores without clay using low saline brines and observed significant improvement in the recovery, which proves that low salinity flooding can be effective without the presence of clay. The brine's salinity is usually between 1,000-2,000 ppm but effects have been observed up to 5,000 ppm [62].

2.3.5 Impact of Low Saline Brines on Oil Recovery in Carbonates

Low saline brines were not expected to improve oil recovery from carbonate reservoirs and so seldomly received attention. This is because the LSE has been attributed to the presence of high clay content which is very minimal if present at all in carbonates [53]. However, scientific interest in this research area was stimulated by the recent research work of Yousef et al. [5], in which they investigated the effect of injecting diluted

seawater in Middle Eastern carbonate cores through coreflood experiments. They reported 18 to 19% incremental recovery over conventional waterflooding as a result of stepwise dilution of the seawater up to 20-times dilution, and they attributed the improved oil recovery to the alteration of the rock wettability towards a more water-wet state. Alotaibi et al. [63] also performed several wettability studies on Middle Eastern limestone cores, using formation, aquifer and seawater synthetic brines, with concentrations of 230,000 ppm, 5,436 ppm, and 54,680 ppm respectively. They showed that seawater or formation water made calcium carbonate substrates oil-wet but it became water -wet when aquifer or deionized water was used. They also obtained an additional oil recovery of 8.6% from their coreflood experiments when aquifer water was injected after formation brine. Romanuka et al. [64] through Amott spontaneous imbibition tests observed increased oil recovery in limestone and dolostone cores by lowering the brine's ionic strength and attributed it to wettability change. Austad et al. [65] through coreflooding experiments obtained tertiary low-salinity EOR effects through wettability alteration in limestone cores and concluded that it is due to the presence of anhydrite. The microscopic dissolution of anhydrite through NMR studies was also shown to significantly enhance the connectivity between macropore and micropore systems [66]. Sulfate ion which is created from the dissolution of anhydrite is believed to be the catalyst in the wettability alteration process [65, 66].

Zahid et al. [67] sequentially flooded various diluted seawater into reservoir carbonate cores and observed no low salinity effect at ambient temperature but significant increase in oil recovery at 90°C were observed. The decrease in salinity at 90°C was observed to increase pressure drop significantly, making fines migration and rock dissolution possible

mechanisms of the low salinity flooding. Anhydrite dissolution was however ruled out as a mechanism since no anhydrite was present in the rock.

Surface charge alteration is believed to be another wettability alteration approach [5, 68, 69], and so the impact of diluted seawater on carbonate rock surface charge was investigated using the Zeta Potential (ZP) technique. Diluted seawater was found to alter the carbonate rock surface charges to more negative state, which will trigger the release of adsorbed carboxylic oil components from rock surface, improve the water wetness and eventually improve/enhance oil recovery [66]. However, flooding of low saline brines was not observed to improve oil recovery in chalk [64, 65, 67, 61], and was even reported to have decreased the oil recovery drastically [34]. The decrease in oil recovery is attributed to the decrease in the concentration of the active ions which have been found to be able to alter wettability in chalk.

CHAPTER 3

EXPERIMENTAL METHODOLOGY

The complex nature of limestone rock necessitated a brief experimental study on reagent grade precipitated calcium carbonate (PCC). This was done to help in acquiring a fundamental understanding of the interactions of Ca^{2+} , Mg^{2+} , and SO_4^{2-} with the carbonate surface. The study on PCC served as a guideline for the experimental studies that was carried out on reservoir limestone rock.

3.1 Materials

3.1.1 Limestone sample

Eight limestone core plugs obtained from a Saudi-Arabian carbonate reservoir were crushed to about 10 mm and then subjected to a soxhlet extraction involving toluene followed by methanol until clear/transparent effluent solution was detected. This was necessary in order to extract the crude oil, and clean the crushed sample of water and any form of salt. It was cleaned for a total of 22 hours. The sample free of organic impurities was dried in a laboratory oven at 60°C for 16 hours. It was thereafter ground to minus 100 μm by an automatic mortar-pestle system. Mineralogical and petrophysical properties of the limestone powder were then determined through X-Ray Diffraction

(XRD), X-Ray Fluorescence (XRF), and Scanning Electron Microscope-Energy Dispersive X-Ray (SEM-EDX) methods. Results of the characterization are presented in Table 1 and Figure 4. A major limitation of the XRF technique is that it cannot detect Oxygen. However, the elements detected by all techniques have to be normalized to 100%. This limitation must be responsible for the big variation in the percentage of calcium ion in the XRF and SEM-EDX limestone analysis as can be seen in Table 1. While the XRF technique takes into account the whole sample, the SEM-EDX technique utilizes very small portions of the sample. XRD results (figure 4) revealed that the limestone powder is composed of 25% calcite, 73 % dolomite and 2 % anhydrite. This reflects that the rock samples are dolomitic limestone. Figure A1 in the appendix also shows the SEM image of the limestone.

3.1.2 Precipitated Calcium carbonate (PCC) and other analytical grade reagents

The PCC used in this study was purchased from Fluka. It is in the form of fine powder, with purity greater than 99 %. Its chemical analysis as provided on the bottle label is presented in Table 1. Other analytical grade reagents utilized for the brine preparations in this study are listed in Table 2.

Table 1: Chemical composition of carbonate samples used in this study

	Uthmaniyah Arab-D limestone		PCC
Item	XRF Wt. %	SEM-EDX At. %	Wt. %
Mg	1.05	3.29	
Ca	97.29	31.25	
Si	0.18	0.15	
P	0.16		
Fe	0.87		≤0.005
S	0.46	0.35	
C		12.44	
O		52.48	
SO ₄			≤0.02
Cl			≤0.02
CaCO ₃			> 99

Table 2: Analytical grade reagents used in brine preparations

REAGENT	MANUFACTURER
Na ₂ SO ₄ (Anhydrous)	Scharlau
CaSO ₄ · $\frac{1}{2}$ H ₂ O	BDH Chemicals
NaHCO ₃	BDH Chemicals
Na ₂ CO ₃	Merck
NaCl	Panreac
MgCl ₂ · 6H ₂ O	Loba Chemie
CaCl ₂ · 2H ₂ O	Scharlau

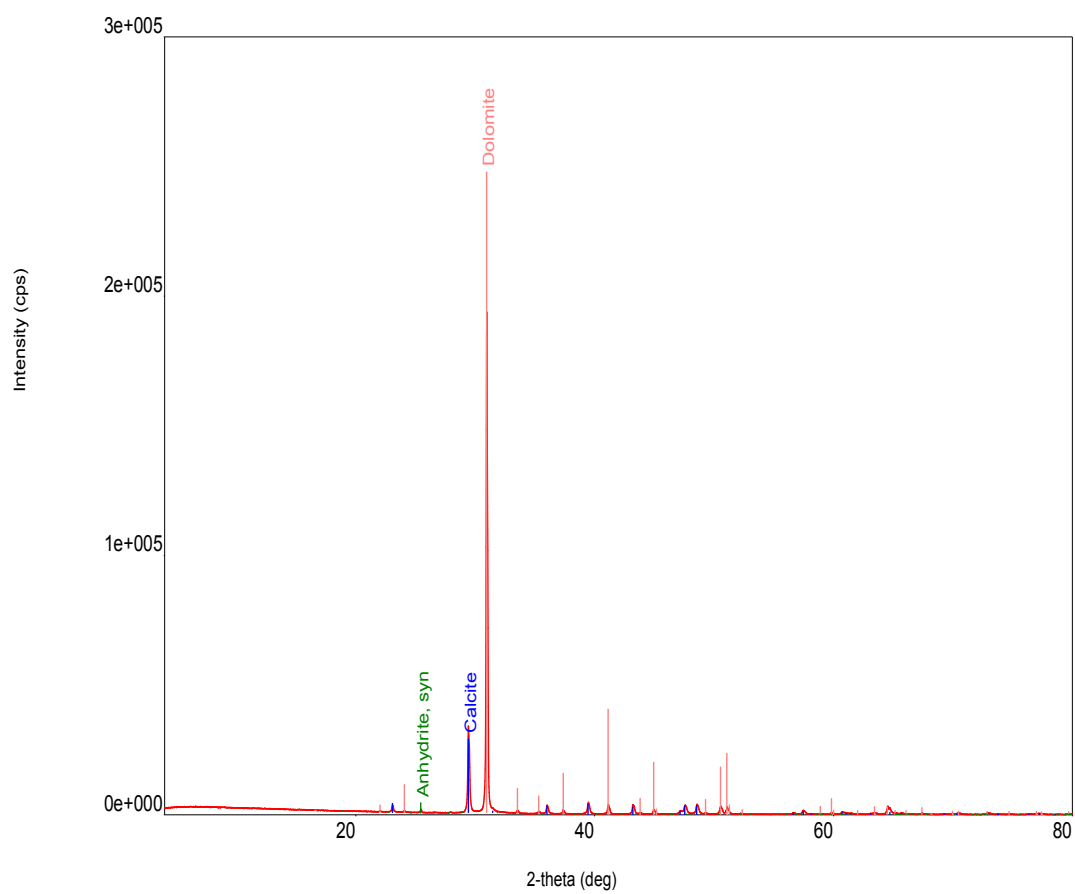


Figure 4: XRD pattern of Arab-D limestone powder

3.1.3 Brines

All brines used for this study were synthetically prepared from analytical grade salts and de-ionized (DI) water. The ultra-pure DI water utilized was produced with a Millipore Milli-Q lab water system, and it had a conductivity of $0.055 \mu\text{S.cm}^{-1}$ (resistivity of $18.2 \text{ M}\Omega.\text{cm}$) at 25°C .

For the limestone adsorption studies, 16 brines were utilized. The injection Arabian Gulf seawater with a salinity of 57,600 ppm was initially prepared, after which 2 times dilution was made. This twice diluted Arabian Gulf seawater was called 50% SW. Ionic compositions of the injection sea water and the 50% SW are presented in Table 3. Sixteen brine combinations were thus prepared by adjusting the ionic compositions of Ca^{2+} , Mg^{2+} , SO_4^{2-} , and Cl^- of the 50% SW. The compositions of the 16 brines are given in Table 4.

Table 3: Ionic Composition of injection Arabian Gulf seawater and 50% SW

	Brine Compositions (ppm)							
	Ca^{2+}	Mg^{2+}	Na^+	Cl^-	SO_4^{2-}	HCO_3^-	TDS	Ionic Strength(M)
Seawater	650	2110	18300	32200	4290	120	57670	1.1484
50% SW	325	1055	9150	16100	2145	60	28835	0.5742

Table 4: Initial brine compositions

Brines	Ionic Concentrations (ppm)							Ionic Strength(M)
	Ca ²⁺	Mg ²⁺	Na ⁺	Cl ⁻	SO ₄ ²⁻	HCO ₃ ⁻	TDS	
Brine 1	325	1055	10764	17006	4290	60	33500	0.6667
Brine 2	650	1055	9644	17006	2145	60	30560	0.6140
Brine 3	650	1055	10391	17006	4290	60	33452	0.6749
Brine 4	325	1055	9737	17006	2145	60	30328	0.5997
Brine 5	325	2100	9243	17006	2145	60	30879	0.6750
Brine 6	650	2100	9150	17006	2145	60	31111	0.6892
Brine 7	325	2100	10271	17006	4290	60	34052	0.7420
Brine 8	650	2100	10177	17006	4290	60	34283	0.7562
Brine 9	325	1055	14918	25000	2145	60	43503	0.8251
Brine 10	650	1055	14825	25000	2145	60	43735	0.8394
Brine 11	325	1055	15946	25000	4290	60	46676	0.8921
Brine 12	650	1055	15852	25000	4290	60	46907	0.9063
Brine 13	650	2100	15359	25000	4290	60	47459	0.9816
Brine 14	325	2100	14424	25000	2145	60	44054	0.9004
Brine 15	650	2100	14331	25000	2145	60	44286	0.9146
Brine 16	325	2100	15452	25000	4290	60	47227	0.9674

3.1.4 Crude Oil

Crude oil (dead) from the same Saudi Arabian carbonate reservoir where the limestone was obtained was used in this study. The oil was filtered through a 5µm filter paper with a vacuum pump to remove any suspended particles and water. Before usage of the oil, it was vacuumed overnight to remove light ends to minimize the possibility of gas evolution during experiments at high temperatures.

3.2 Experimental Procedures and Equipments

3.2.1 Adsorption Experiments in the Absence of Crude Oil

Determination of Solid/Liquid (S/L) ratio: In order to eliminate the effects of S/L ratio, an equilibrium S/L ratio was experimentally determined. This was conducted by increasing the S/L ratio of PCC/sulfate brine up to 20% and measuring the adsorption of SO_4^{2-} from a 72 ppm (0.00075M) sulfate brine at different solids concentration. As observed from the results presented in Figure 5, the adsorption density of sulfate ion onto the PCC decreased rapidly with an increase in solid/liquid ratio up to about 4%. Afterwards, the reduction in the adsorption density was very minimal, and it became relatively constant at slightly above 5% solids concentration. All adsorption experiments were thus conducted at S/L ratio of 6.7%, which is slightly above 5%.

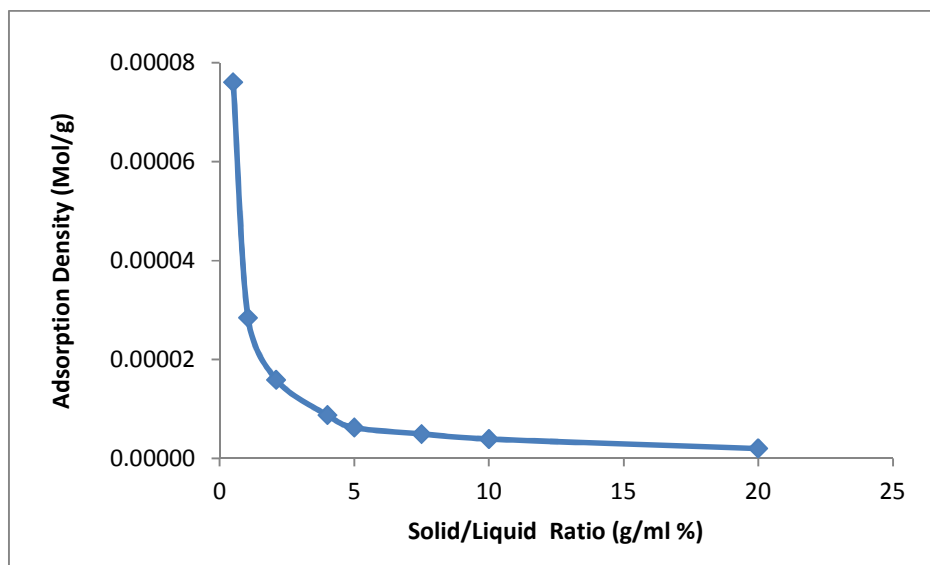


Figure 5: Effect of Solid/Liquid ratio on sulfate ion adsorption onto PCC

Determination of Equilibrium Time: The minimum conditioning time required for the samples to reach equilibrium in the absence of crude oil was experimentally determined. The equilibrium time (conditioning time) was experimentally verified by conditioning several limestone samples in Arabian Gulf seawater with S/L ratio of 6.7% (2g of limestone in 30 ml seawater) at 25°C and 90°C for different times, up to a maximum of 24 hours. The samples were then analyzed for the desired ions. Although, the maximum time required for the samples to reach equilibrium was determined to be around 8.3 hours (Figure 6a), the samples were conditioned for 24 hours using a wrist-arm shaker at 25°C and shaking hot water bath at 90°C, and then left for at least another 24 hours without shaking at the same conditioning temperature to be very certain equilibrium has been achieved. This was necessary in order eliminate time-dependent errors in all adsorption experiments.

Samples Preparation: The following steps were taken in preparing the samples for adsorption experiments on PCC and Limestone in the absence of crude oil:

1. 2g of solid (PCC or limestone) was weighed and carefully transferred into 40 ml glass screw-cap vials containing 30ml of synthetic brine of known ionic concentrations. The brines used for the limestone adsorption experiments are the 16 synthetically prepared brines presented in Table 4, while clean brines (brines containing only one ion) of varying SO_4^{2-} , Ca^{2+} , and Mg^{2+} concentrations were utilized for adsorption studies on PCC.
2. The vials were teflon sealed and properly capped to avoid contamination and prevent any form of leakage especially at elevated temperatures.

3. The Teflon sealed screw-cap vials containing the samples were conditioned at the desired temperature for 24 hours and left for at least another 24 hours at the same temperature to ensure that the samples have reached equilibrium. Conditioning of the samples at 25°C was done with a multi-wrist arm shaker, while those at 90°C was conducted in a shaking hot-water bath.
4. Following equilibration, the supernatant brines were carefully extracted with a 10 ml syringe and filtered through a 0.45 micron membrane syringe filter into properly labelled clean glass vials.
5. The supernatant brines, along with their initial brines were then analysed for ionic concentrations of Ca^{2+} , Mg^{2+} , SO_4^{2-} , and Cl^-

3.2.2 Adsorption Experiments in the Presence of Crude Oil

Determination of Equilibrium Time: The minimum conditioning time required for the samples to reach equilibrium in the presence of crude oil was experimentally verified by conditioning several limestone samples of 2g in glass vials containing 15 ml of seawater and 15 ml of crude oil for several hours. The samples were then analyzed for the desired ions. Even though the maximum time required for the samples to reach equilibrium was determined to be around 12 hours (Figure 6d), the samples were conditioned for 24 hours, and then left for at least another 24 hours at the same conditioning temperature without shaking to be very certain equilibrium has been achieved.

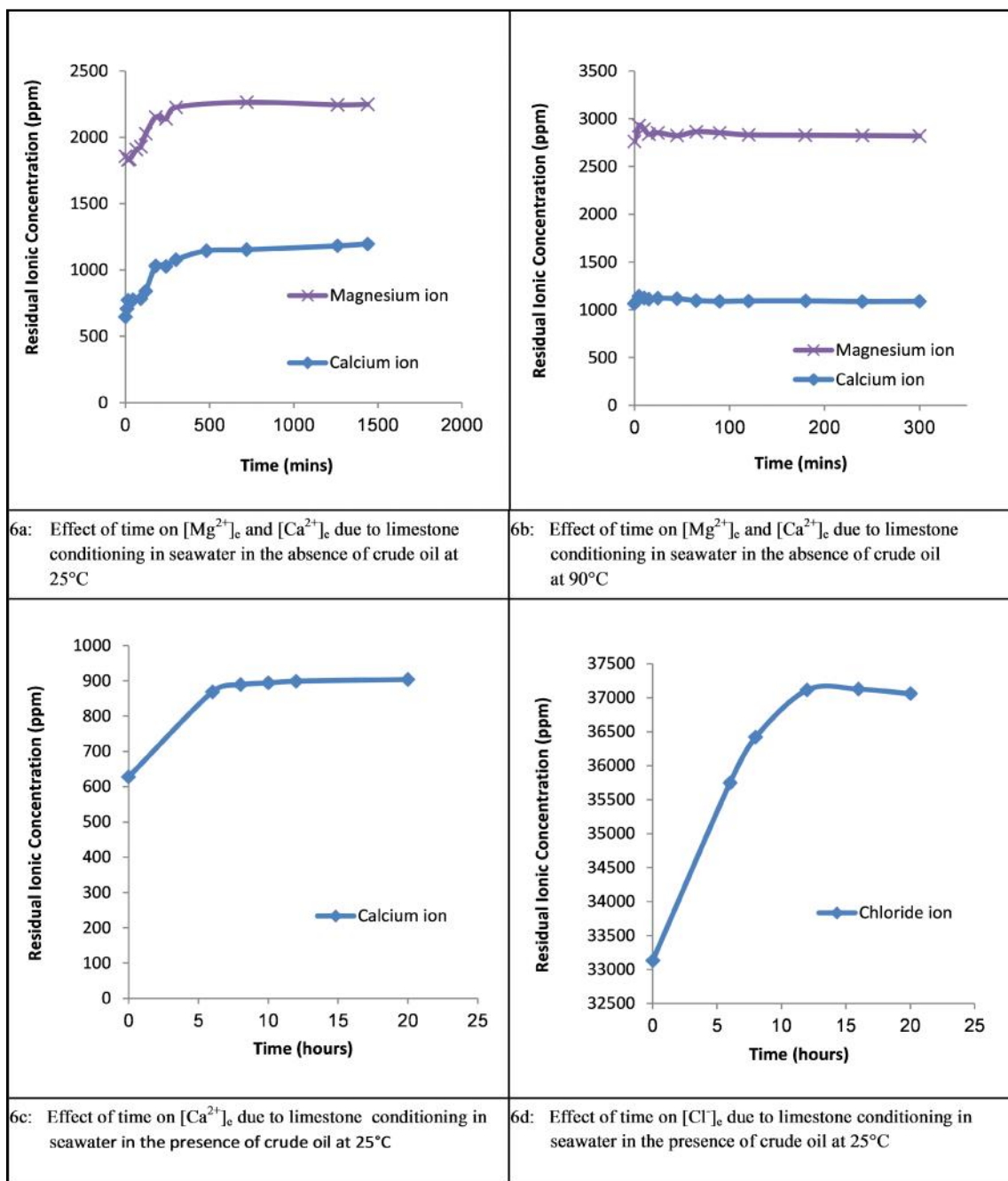


Figure 6: Equilibrium time for adsorption of ions onto limestone

Samples Preparation: The following steps were taken in preparing the samples for adsorption experiments on limestone in the presence of crude oil:

1. 2g of limestone powder was weighed and carefully transferred into 40 ml glass screw-cap vials containing 15 ml of synthetic brine of known ionic concentrations and 15 ml of crude oil.
2. The vials were teflon sealed and properly capped to avoid contamination and prevent any form of leakage especially at elevated temperatures.
3. The Teflon sealed screw-cap vials containing the samples were conditioned at 25°C and 90°C for 24 hours, and left for at least another 24 hours at the same temperature to ensure equilibration.
6. Following equilibration, crude oil was carefully pipetted with an automatic 5 ml pipette, while the supernatant brines were carefully extracted with a 10 ml syringe and filtered through a 0.45 micron membrane syringe filter into properly labelled clean glass vials.
4. The supernatant brines, along with their initial brines were then analyzed for ionic concentrations of Ca^{2+} , Mg^{2+} , SO_4^{2-} , and Cl^- .

3.2.3 Chemical Analysis of Brines

The ionic concentrations of Ca^{2+} , and Mg^{2+} in brines were analyzed by an Inductive Coupled Plasma (ICP-OES), model Spectro Ciros Vision, manufactured by Spectro, Germany, and an Atomic Absorption Spectrophotometer (AAS), while SO_4^{2-} and Cl^- were analyzed by an Ion-Exchange Chromatograph, ICS-3000, produced by Dionex corporation, Sunnyvale, CA.

The ICP-OES is a type of emission spectroscopy that uses the inductively coupled plasma to produce excited atoms and ions that emit electromagnetic radiation at wavelengths characteristic of a particular element. The intensity of this emission is indicative of the concentration of the element within the sample. The AAS utilizes the phenomenon that ground state metals absorb light at particular wavelengths. Metal ions in a solution are converted to atomic state by means of a flame. Light of the appropriate wavelength is supplied and the amount of light absorbed can be measured against a standard curve. The ionic concentrations of the brines were very high, and so there was need to dilute the samples in order to be within a suitable concentration range for both Ca^{2+} and Mg^{2+} of the equipment. Therefore, the brines were diluted 100 times with deionized water, and preserved by acidifying with 5% HNO_3 . 1% Lanthanum was also added to the final dilution to overcome potential chemical interferences which may affect the accuracy of the analysis.

The Ion Chromatograph (IC) measures concentrations of ions by separating them based on their interaction with a resin. Sample solutions pass through a pressurized chromatographic column where ions are absorbed by column constituents. As an ion extraction liquid, known as eluent, runs through the column, the absorbed ions begin separating from the column. Each ion is identified by its retention time within the separation column. The sample ions are detected in the detector and the signals produced are measured against standard calibration curves, for the ionic concentrations. The very high concentrations of Cl^- in the brines necessitated a 500 times dilution of our samples with deionized water before analyzing.

All diluted samples were kept in properly capped plastic tubes at room temperature for at least 16 hours before analyzing. This was just a necessary precaution taken to ensure homogeneity is achieved after dilution.

3.2.4 Adsorption density calculations

The adsorption densities of Ca^{2+} , Mg^{2+} , SO_4^{2-} , and Cl^- on our limestone and PCC samples were calculated from the differences in concentrations of the ions between the initial and equilibrated brine solutions. The equation for the adsorption density calculation is [70]

$$\Gamma = \frac{(C_i - C_e)V}{m} \quad (3)$$

Where;

Γ = adsorption density (mg/g or mol/g)

C_i = Initial brine concentration (mg/l or mol/l)

C_e = Residual brine concentration (mg/l or mol/l)

V = Volume of the initial solution (l)

m = Mass of solid added(in g).

3.2.5 Adsorption Results Analysis on Limestone

Studying the interactions of more than one ion in brine necessitated the statistical analysis of our experimental adsorption results by the Analysis of Variance (ANOVA) method. The ANOVA is an efficient statistical technique for analyzing the effect of categorical factors on a response. It can be used to determine: (a) which factors have a significant effect on the response, and/or (b) how much of the variability in the response variable is attributable to each factor.

In this research, the effects of 4 factors, which are Ca^{2+} , Mg^{2+} , SO_4^{2-} , and Cl^- on adsorption/desorption of these ions have been experimentally investigated. The 4 factors in our ANOVA were labelled as factors A, B, C, and D respectively. Table 5 presents the factors and concentration levels that have been used.

Table 5: Factors and levels used in adsorption ANOVA

Factors	Ions	Level 1 (ppm) minimum	Level 2 (ppm) maximum
A	Ca^{2+}	325	650
B	Mg^{2+}	1055	2100
C	SO_4^{2-}	2145	4290
D	Cl^-	17006	25000

3.2.6 Zeta Potential Measurements

Alteration of surface charges is one of the proposed underlying mechanisms governing wettability alteration in carbonates. The zeta potential (ZP) technique is one way of measuring the surface charge of a particle dispersed in a liquid. In this research, zeta potential (ZP) measurements have been conducted with the Zeta Potential Analyzer (Zetapals) by Brookhaven Instruments Corporation, and the Zeta Meter 3.0. The Zetapals instrument utilizes phase-analysis light-scattering technique for the determination of the electrophoretic mobility (measure of speed) of charged colloidal suspensions and calculates the zeta potential (in mV) with the Smoluchowsky and Huckel models. Since all the measurements were in aqueous systems, the Smoluchowsky equation was used to calculate the ZP. Equation 4 below shows the Smoluchowsky equation [21];

$$ZP = 113000 \frac{V_t}{D_t} \times EM \quad (4)$$

Where;

ZP = Zeta potential, millivolts (mV)

V_t = Viscosity of the suspending liquid in poises at temperature “t”

D_t = Dielectric constant of the suspending liquid at temperature

EM = Electrophoretic mobility at actual temperature

The Zetapals is equipped with electrodes which consist of palladium mounted on a machined support, a temperature sensor to measure the temperature near the sample and a He-Ne laser which is used as a light source. The laser beam passes through the sample in a cell which carries two electrodes that generates an electric field. Light is scattered by

the particles in the cell and is Doppler shifted because the scattered particles are moving in the electric field. The frequency of light scattered into the detector is Doppler shifted by an amount proportional to the velocity of the particles. The Zeta meter 3.0 has a microprocessor unit that calculates either time, EM or ZP, a microscope module with which colloidal particles are viewed and tracked, and an electrophoresis cell that contains the sample, and in which electrodes are inserted. A particle is tracked between two traverses under an applied voltage, and then combines the tracking time with the tracking voltage and the ocular micrometer tracking distance to compute the EM, which is then converted into ZP with the Smoluchowsky equation.

Samples for ZP measurements on the Zetapals were conditioned for 2 days before analyzing. For ZP measurements in seawater, the high conductance (due to high salt concentration) of our modified seawater necessitated the need to condition the Zeta pals electrode in 1M NaCl salt before taking each measurement. One or two drops of the limestone-seawater suspension was diluted into about 2 ml of its initial brine in a disposable polystyrene cuvette in order to reduce the particle number concentration. A top is placed on the cuvette, and the suspension is then rocked back and forth several times to ensure it becomes homogeneous. Before putting the sample into the equipment, the capped cuvette is sonicated in an ultrasonic bath for at least 30 seconds, as this will help dislodge any dust stuck to cell walls and cap. Inside the equipment, the sample is allowed to equilibrate to the set temperature for a period of 5 minutes prior to beginning of analysis. Due to the need to achieve good reproducibility, at least 4 measurements of a single run each of 90 cycles were made, and then the average zeta potential obtained for each sample. The sample was changed after each measurement to prevent degradation of

sample. This measurement method (several measurements of 1 run of 90 cycles) was not applied to brines with low salinities, whose ZP values were directly measured by making several runs of shorter cycles depending on the ionic strength of the brine. Very good reproducibilities were obtained for all ZP measurements.

For measurements on Zeta Meter 3.0., the carbonate powder-brine suspension was conditioned for 2 hours at $23 \pm 2^\circ\text{C}$. The samples were centrifuged for 3 min at 5000 rpm to let particles settle. An aliquot taken from the supernatant and a small amount of sample taken from the mineral bed were used to measure the zeta potentials. An average of ten measurements was taken to represent the measured potential.

CHAPTER 4

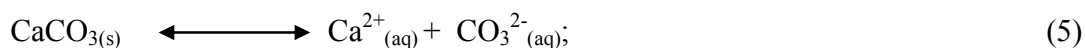
RESULTS AND DISCUSSION

4.1 Experimental Results on Precipitated Calcium Carbonate (PCC)

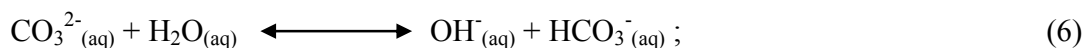
4.1.1 Adsorption Results on PCC

4.1.1.1 Calcium ion adsorption onto PCC

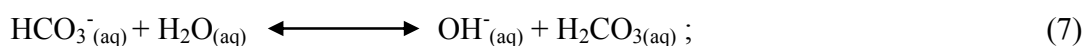
CaCO_3 is a slightly soluble salt, with its solubility highly pH and temperature dependent. Products of the interaction of CaCO_3 with water are Ca^{2+} , CO_3^{2-} , HCO_3^- and H_2CO_3 . The adsorption of Ca^{2+} onto PCC must be evaluated together with the solubility constants (K_{sp}) and base dissociation constants (K_{b}) of all the involving reactions at the desired temperature. The following chemical reactions and their equilibrium constants have been considered in the adsorption data analysis;



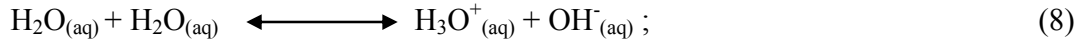
$$K_{\text{sp}} = 4.96 \times 10^{-9} \text{ M}^2 \text{ and } 7.64 \times 10^{-10} \text{ M}^2 \text{ at } 25^\circ\text{C and } 90^\circ\text{C respectively}$$



$$K_{\text{b},1} = 2.25 \times 10^{-4} \text{ M and } 1.45 \times 10^{-6} \text{ M at } 25^\circ\text{C and } 90^\circ\text{C respectively}$$



$$K_{\text{b},2} = 2.13 \times 10^{-8} \text{ M and } 7.21 \times 10^{-3} \text{ M at } 25^\circ\text{C and } 90^\circ\text{C respectively}$$



$K_w = 1.00 \times 10^{-14} \text{ M}^2$ and $5.30 \times 10^{-13} \text{ M}^2$ at 25°C and 90°C respectively

The equilibrium constants at 25°C were obtained from Huang et al. [71], while the equations utilized in estimating them at 90°C have been obtained from different sources [72-75], and described in the appendix.

The Ca^{2+} adsorption experimental data have been analyzed with the same method described and utilized by Huang et al. [71]. The adsorbed Ca^{2+} concentration, $[\text{Ca}^{2+}]_{\text{ads}}$ is estimated from;

$$[\text{Ca}^{2+}]_{\text{ads}} = [\text{Ca}^{2+}]_{\text{ini}} + [\text{Ca}^{2+}]_{\text{diss}} - [\text{Ca}^{2+}]_{\text{eq}} \quad (9)$$

Where;

$$[\text{Ca}^{2+}]_{\text{diss}} = \frac{K_{sp}}{[\text{Ca}^{2+}]_{\text{eq}}} + \frac{K_{sp}K_{b,1}}{[\text{Ca}^{2+}]_{\text{eq}}[\text{OH}^-]_{\text{eq}}} + \frac{K_{sp}K_{b,1}K_{b,2}}{[\text{Ca}^{2+}]_{\text{eq}}[\text{OH}^-]_{\text{eq}}^2} \quad (10)$$

Subscripts “ini”, “diss”, and “eq” represents initial, dissociation and equilibrium respectively.

The Ca^{2+} adsorption experimental results are presented in Figure 7. It shows that increasing the Ca^{2+} concentration in the brine resulted in an increase in the Ca^{2+} adsorbed onto the PCC. This increase gradually stabilizes after a certain concentration. Temperature also plays a key role in the adsorption of Ca^{2+} , as an increase in the temperature from 25°C to 90°C resulted into a significant increase in the Ca^{2+} adsorbed onto the PCC. This result conforms with the experimental observations of Zhang et al. [16].

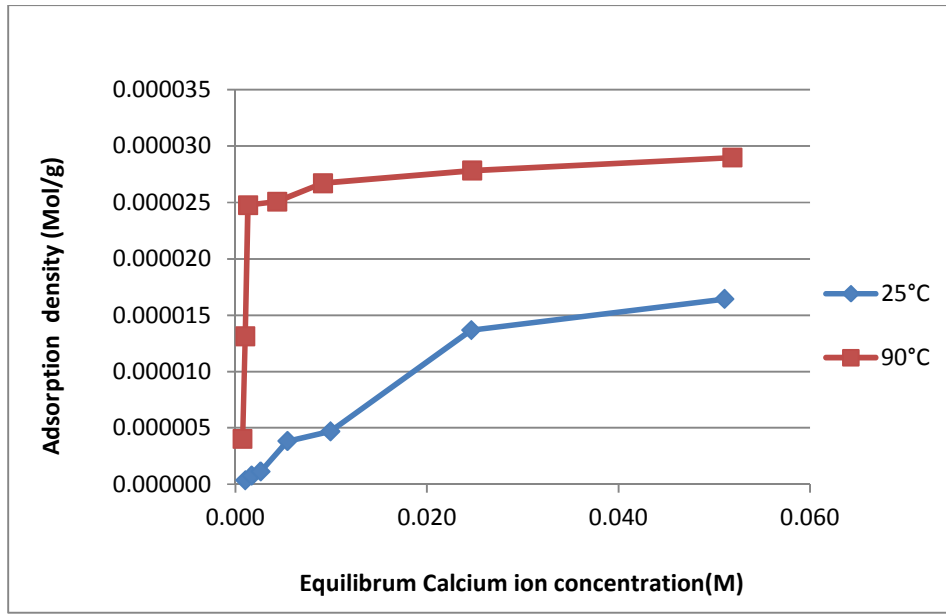
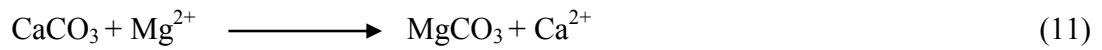


Figure 7: Adsorption isotherms of Ca^{2+} onto PCC at 25°C and 90°C.

4.1.1.2 Magnesium ion adsorption onto PCC

Magnesium ion is a dominant ion in most carbonate reservoirs because dolomite $\text{CaMg}(\text{CO}_3)_2$ always accompanies calcite. Mg^{2+} has been found to be favourable to oil recovery when adsorbed. As can be seen from Figure 8a, the experimental results on PCC revealed that Mg^{2+} adsorption increases with increasing $[\text{Mg}^{2+}]$ in brine. It also shows that Mg^{2+} adsorbs more strongly at 90°C than at 25°C. This is because Mg^{2+} becomes more reactive as the temperature increases due to partial dehydration of the ion [1]. The substitution of Ca^{2+} in the crystal lattice of chalk and limestone by Mg^{2+} occurs at high temperature, and this degree of this substitution increases as the temperature increases [1, 25]. Interestingly, this experimental observation has also been confirmed by the results on PCC, as presented in Figure 8b. The $[\text{Ca}^{2+}]$ in the supernatant MgCl_2 brine is observed to increase as the concentration of Mg^{2+} in the initial MgCl_2 brine increased. This increase became more significant at 90°C. The adsorption trend of Mg^{2+} in Figure 8a and the

desorption trend of Ca^{2+} in Figure 8b helps in confirming a sort of substitution or displacement reaction taking place. This substitution reaction (Equation 11) between Mg^{2+} and Ca^{2+} at the PCC surface is very slow at 25°C but increases significantly at 90°C . It is a reaction that has been found to increase the water wetness of carbonate reservoirs. This finding is in line with previous findings on chalk and limestone [1, 25].



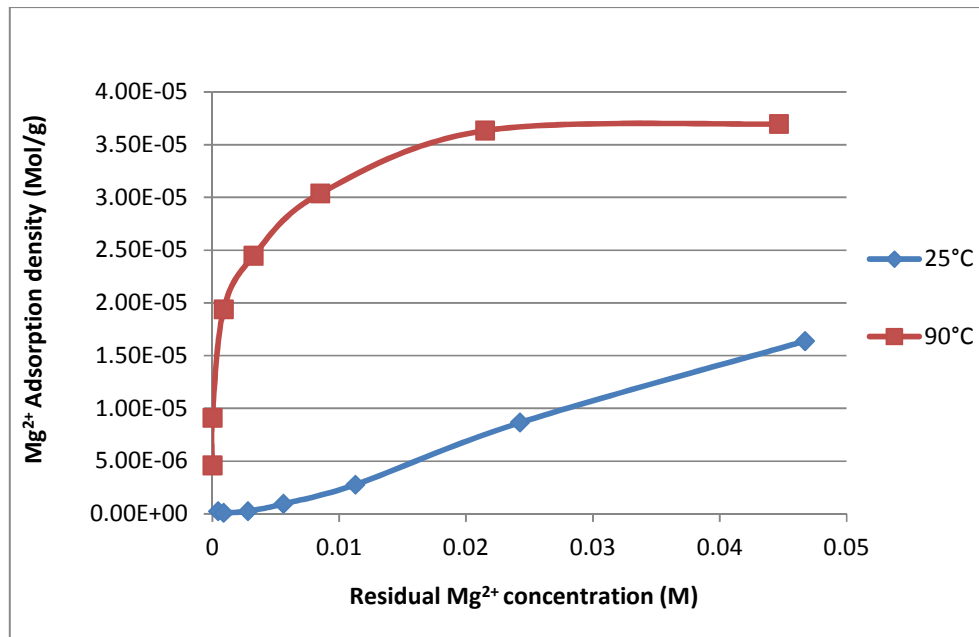


Figure 8a: Adsorption isotherms of Mg^{2+} onto PCC at 25°C and 90°C.

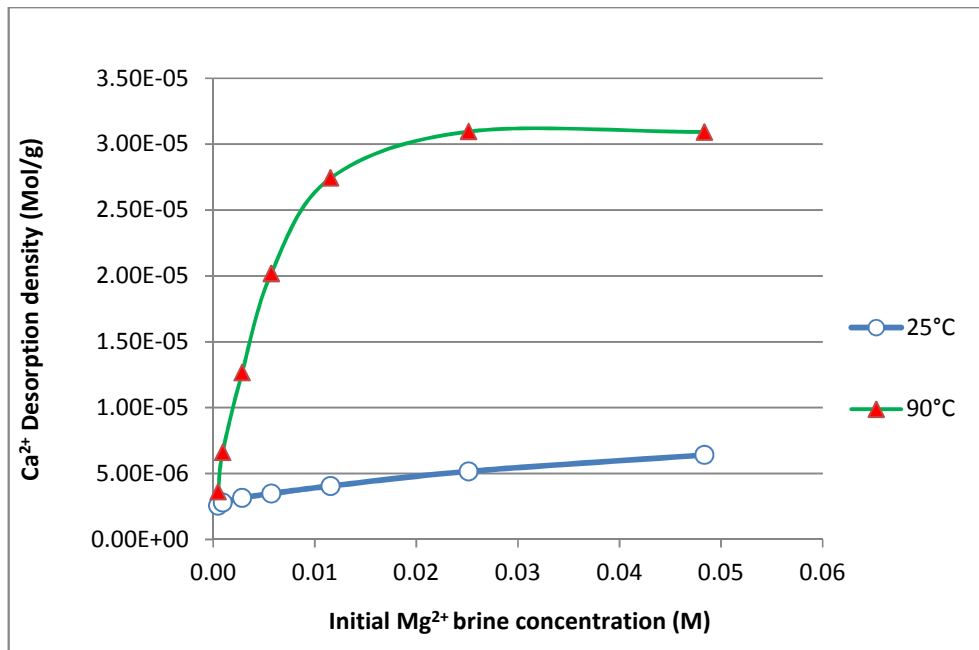


Figure 8b: Desorption of Ca^{2+} in PCC- Mg^{2+} brine interactions at 25°C and 90°C.

4.1.1.3 Sulfate ion adsorption onto PCC

Figure 9 presents adsorption results of sulfate ion onto PCC at 25°C and 90°C. The results show that the adsorption of sulfate ion increases as the concentration of sulfate ion in brine is increased. Sulfate ion adsorption however decreased with an increase in temperature. This is against the findings in chalk that sulfate ion adsorption increases with an increase in temperature [12, 24, 25, and 76]. The ionic interaction of Ca^{2+} and SO_4^{2-} in brine could lead to precipitation of CaSO_4 at temperatures $>100^\circ\text{C}$ or 130°C [16, 25, 77]. However, slight precipitations of CaSO_4 were observed in our samples at 90°C , which might be a factor in the scattering of the experimental data points at 90°C . A limitation of the data analysis was the inability to estimate the sulfate ionic concentrations coming into solution from the PCC at the different sulfate brine concentrations, which might have affected the accuracy of the adsorption data.

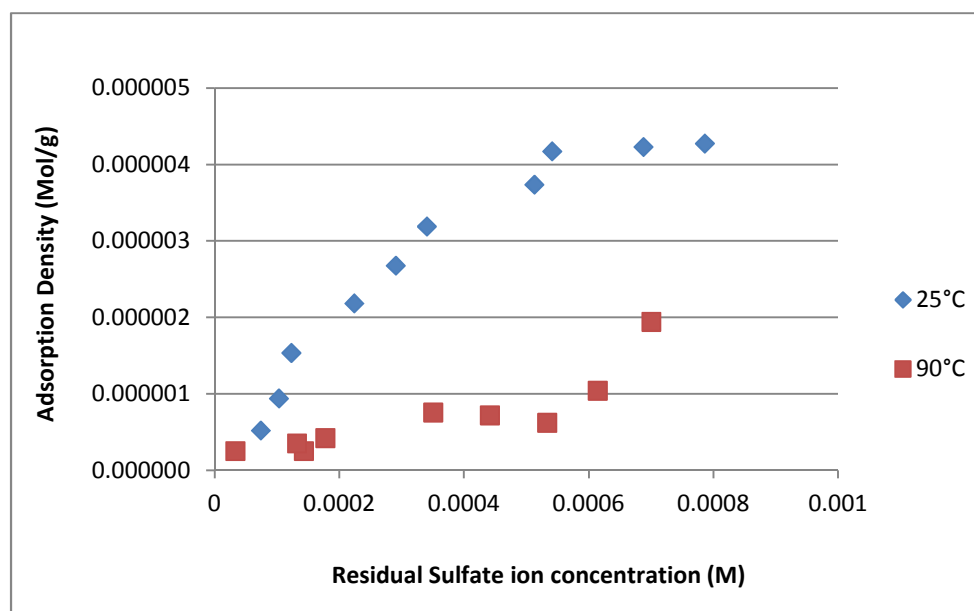


Figure 9: Adsorption isotherms of SO_4^{2-} onto PCC at 25°C and 90°C .

4.1.2 Zeta Potential Results on PCC

4.1.2.1 Iso-Electric Point (IEP) of PCC

The electrokinetic properties of CaCO_3 in aqueous media has been widely studied but with varying results. Much of this variation is due to the complex behaviour of calcite under different conditions. CaCO_3 dissolves in water to produce the following chemical species which are in equilibrium: Ca^{2+} , H^+ , HCO_3^- , CO_3^{2-} , OH^- , and H_2CO_3 . The electrokinetic potential of the calcite surface will depend on the redistribution of these chemical ionic species between the surface and solution resulting into the formation of either positive or negative charges [78]. Many authors agree that the potential-determining ions of the calcite surface are Ca^{2+} , CO_3^{2-} , HCO_3^- , H^+ , OH^- . The potential determining role of H^+ , and OH^- infers that the surface charge of calcite, like many other solids is pH dependent. The pH, at which the surface is electrically neutral, pH_{PZC} , is known as the point of zero charge (PZC). Electrokinetic properties of solids are studied by making zeta potential measurements, and therefore the pH at which the zeta potential is zero, pH_{IEP} , is defined as the isoelectric point (IEP). Although, these two terms (PZC and IEP) are often used interchangeably, they are actually different. The IEP is used to represent the zero point of charge in systems in which ions other than the lattice ions of the solid get adsorbed onto the solid, while the PZC represents the zero point of charge in the absence of specific ionic adsorption from solution onto the solid (other than the crystal's lattice ions) [79]. In the present system, the PZC and IEP are equal since we have studied the electrokinetic properties of PCC in deionized water.

Figure 10 illustrates the zeta potential profile of PCC as a function of pH. An IEP value of 6.45 is obtained at equilibrium. This value is in agreement with the literature value range of 4 to 10.8 for calcite [80]. Generally, when the pH is higher than the IEP, an excess concentration of negative species (CO_3^{2-} , HCO_3^-) will predominate at the interface, and the surface will be negatively charged. Similarly, a lower pH than the IEP will favour an excess concentration of positive species (Ca^{2+}) at the interface, which will result into the surface being positively charged.

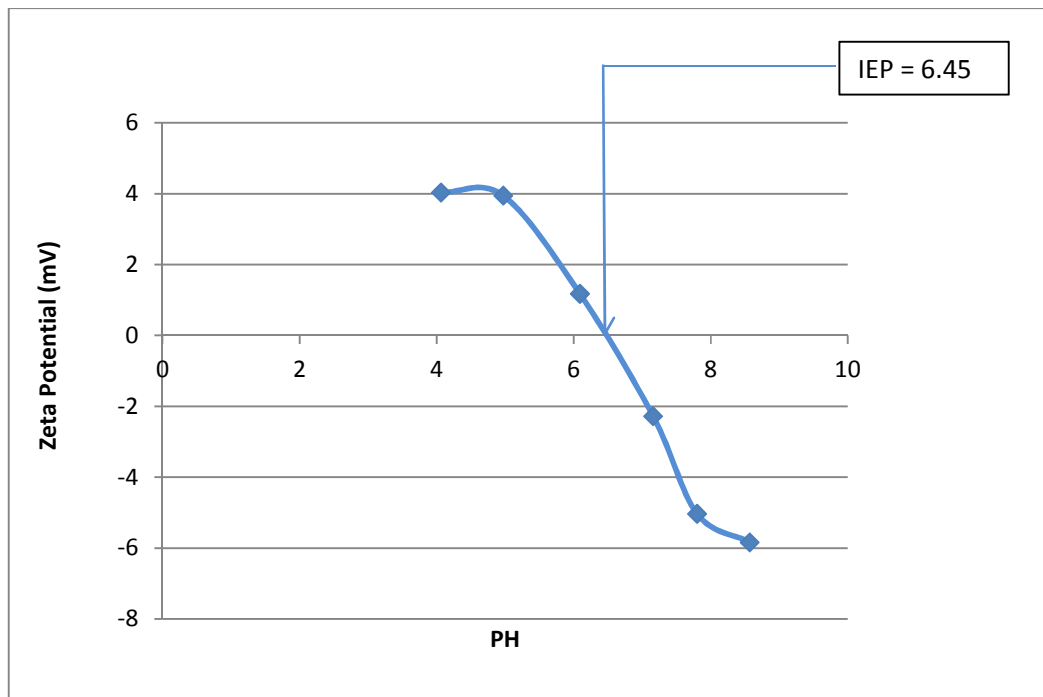


Figure 10: Zeta Potential profile of PCC as a function of pH at 25°C.

4.1.2.2 Impact of Sulfate, Calcium, and Magnesium ions on the Zeta Potential of PCC

In addition to Ca^{2+} , which is part of the crystal lattice of CaCO_3 , Mg^{2+} and SO_4^{2-} have also been identified as potential determining ions of CaCO_3 [16, 25, 81, 82]. The present study has been able to confirm the potential determining status of these ions on PCC, as presented in Figure 11. Figures 11a, 11b and 11c show that the value of the zeta potential of PCC increases when Ca^{2+} or Mg^{2+} concentrations are increased in brine, while it decreases when SO_4^{2-} concentration is increased in brine. Similar effects of these ions on the surface charge of CaCO_3 were also observed on chalk [16, 25].

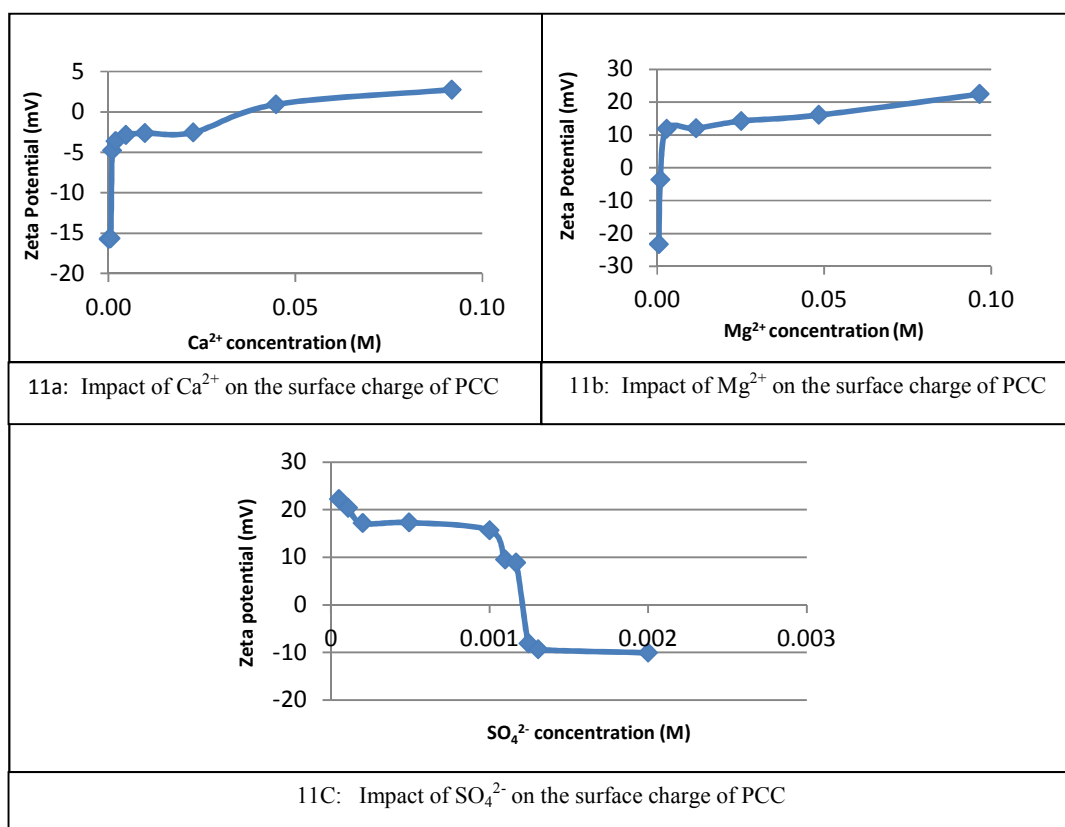


Figure 11: Impact of Ca^{2+} , Mg^{2+} , and SO_4^{2-} on the zeta potential of PCC

4.1.2.3 Impact of Temperature on the Zeta Potential of PCC

Reservoir temperatures are usually higher than 25°C, and so the impact of temperature on the zeta potential of PCC was investigated. Zeta potential results of PCC at 25°C and 90°C are presented in Figure 12. Results indicate that the zeta potential of PCC decreases with an increase in temperature. This is expected because an increase in temperature will increase the solubility of Ca^{2+} , and so more Ca^{2+} will leave the carbonate crystal lattice and come into solution [69], hence reducing the positivity of the surface charge of the PCC. This observation is consistent with the previous findings of Alotaibi et al. [69], Yousef et al. [66], and Rodriguez and Araujo [83].

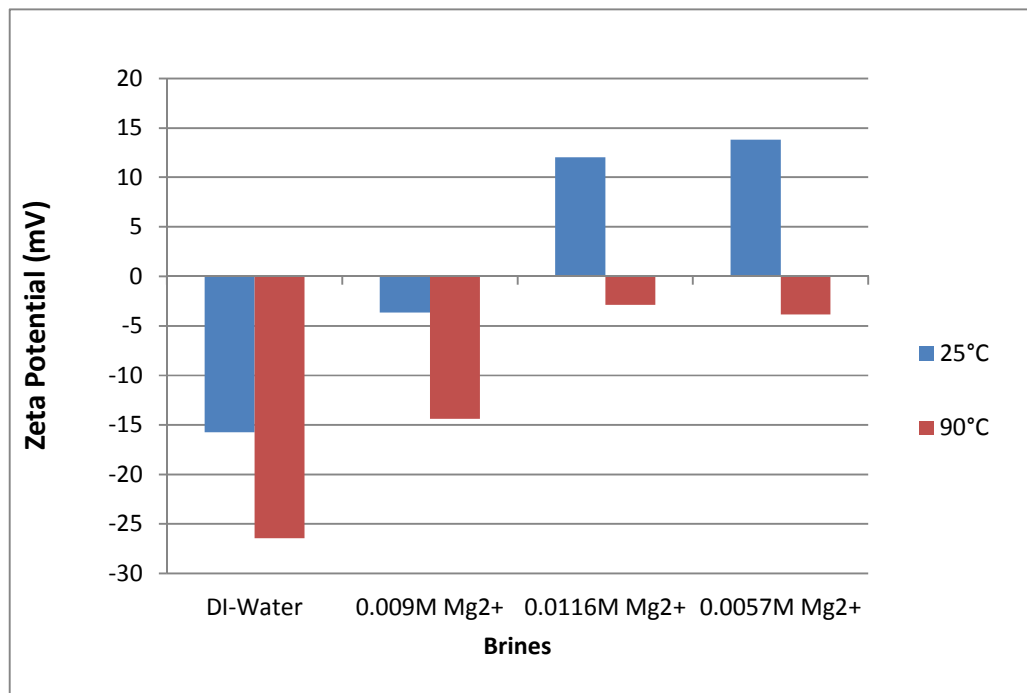


Figure 12: Effect of temperature on the zeta potential of PCC

4.2 Experimental Results on Limestone

As explained in section 3.2, all adsorption studies on limestone have been conducted in modified seawater at 25°C and 90°C, and the results have been statistically analyzed by the analysis of variance (ANOVA) technique. The statistical analysis has been done with the raw experimental adsorption data for limestone presented in Tables A1 to A4 in the appendix. The results of the statistical analysis are presented in form of adsorption response graphs. The interpretation of the response graphs is for the purpose of selecting the best levels for significant factors. The plots depict the average value for the outcome being measured for the corresponding factor at a particular level setting. The graphs are presented first by main effect and the interaction effects. Interactions take precedence over a single effect taken alone because it represents the combined effects of two factors. However, both the interactions and main effects are utilized in the interpretation of the results. Zeta potential results of limestone in seawater are also presented. Table 6 presents all factors and their respective ionic concentrations considered in the ANOVA .

Table 6: Ionic concentrations of all factors considered in ANOVA

Factors	Ionic Concentrations (ppm)			
	Ca ²⁺	Mg ²⁺	SO ₄ ²⁻	Cl ⁻
A1	325			
A2	650			
B1		1055		
B2		2100		
C1			2145	
C2			4290	
D1				17006
D2				25000
A1-B1	325	1055		
A1-B2	325	2100		
A2-B1	650	1055		
A2-B2	650	2100		
A1-C1	325		2145	
A1-C2	325		4290	
A2-C1	650		2145	
A2-C2	650		4290	
A1-D1	325			17006
A1-D2	325			25000
A2-D1	650			17006
A2-D2	650			25000
B1-C1		1055	2145	
B1-C2		1055	4290	
B2-C1		2100	2145	
B2-C2		2100	4290	
B1-D1		1055		17006
B1-D2		1055		25000
B2-D1		2100		17006
B2-D2		2100		25000
C1-D1			2145	17006
C1-D2			2145	25000
C2-D1			4290	17006
C2-D2			4290	25000

4.2.1 Static Adsorption studies on Limestone

4.2.1.1 Adsorption of Ca^{2+} , Mg^{2+} , SO_4^{2-} , and Cl^- on Limestone in the absence of crude oil at 25°C

Figures 13 to 20 present the adsorption response graphs of parametric study conducted using limestone rock samples in the absence of crude oil at 25°C.

Calcium Ion Interactions

Rather than seeing adsorption, all levels of interaction between Ca^{2+} , Mg^{2+} , SO_4^{2-} , and Cl^- in seawater showed desorption of calcium ion from the limestone surface (Figures 13 and 14). This can be due to the mineral dissolution of calcite, anhydrite and dolomite from the limestone sample. Main effect results of Ca^{2+} present in seawater on the adsorption of Ca^{2+} onto the limestone rock sample is presented in Figure 13. It shows that decreasing the concentrations of either calcium or sulfate ions in seawater will increase the calcium ion desorption from the limestone surface. In other words, increasing calcium and sulfate ion concentrations could trigger adsorption of calcium ion. Conversely, increase of either magnesium or chloride ions (or simultaneously) in seawater will inhibit Ca^{2+} adsorption. Figure 14 shows that interactions of A2 with B1, and A2 with D1 shows the least desorption of calcium ion from the limestone surface, which means that in order to trigger adsorption of calcium ion, it is required to increase the concentration of calcium ion in Arabian Gulf seawater, while decreasing magnesium or chloride ion concentrations or both.

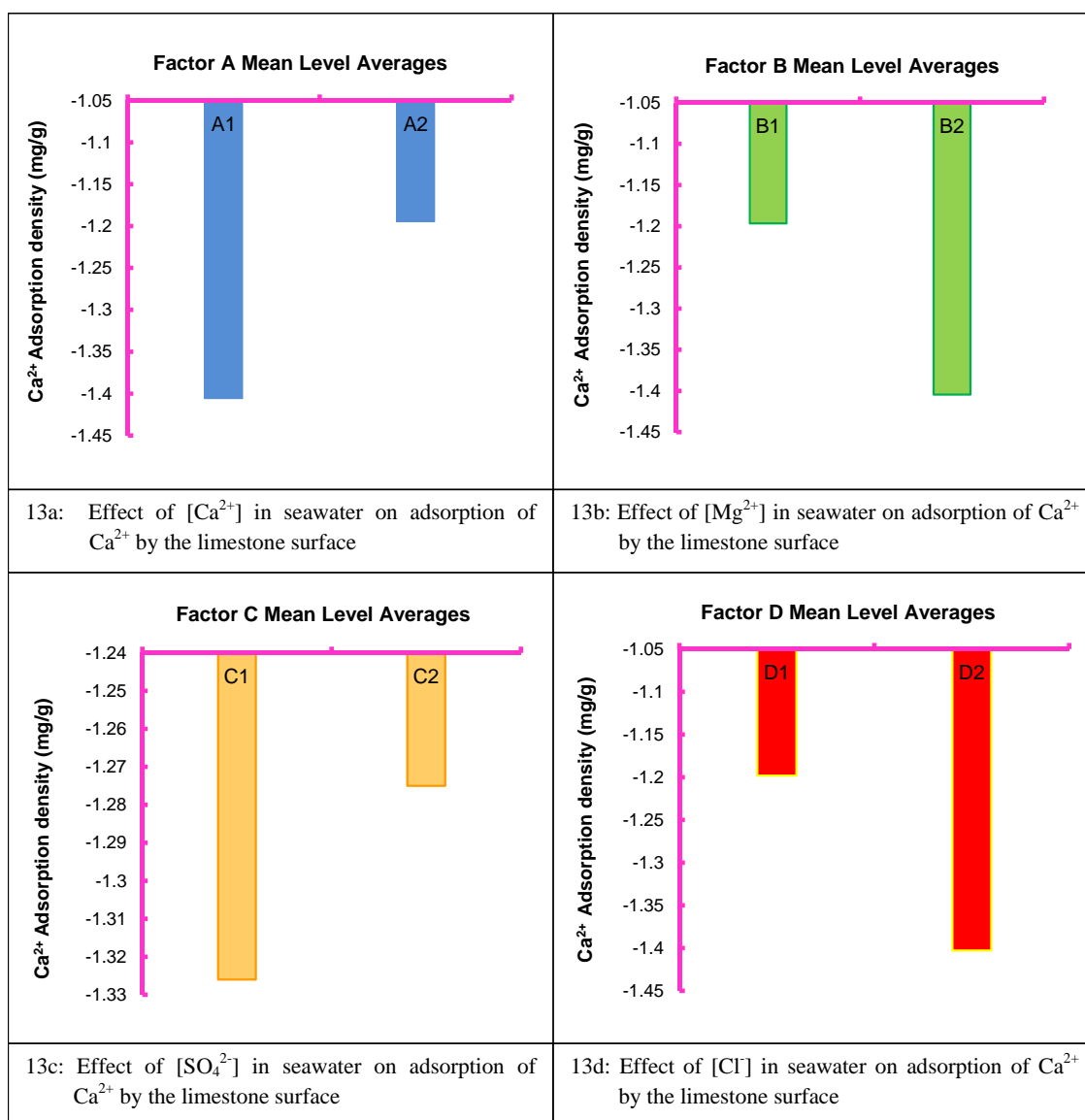


Figure 13: Main effects of [Ca²⁺], [Mg²⁺], [SO₄²⁻], and [Cl⁻] on the adsorption of Ca²⁺ by limestone at 25°C in the absence of crude-oil

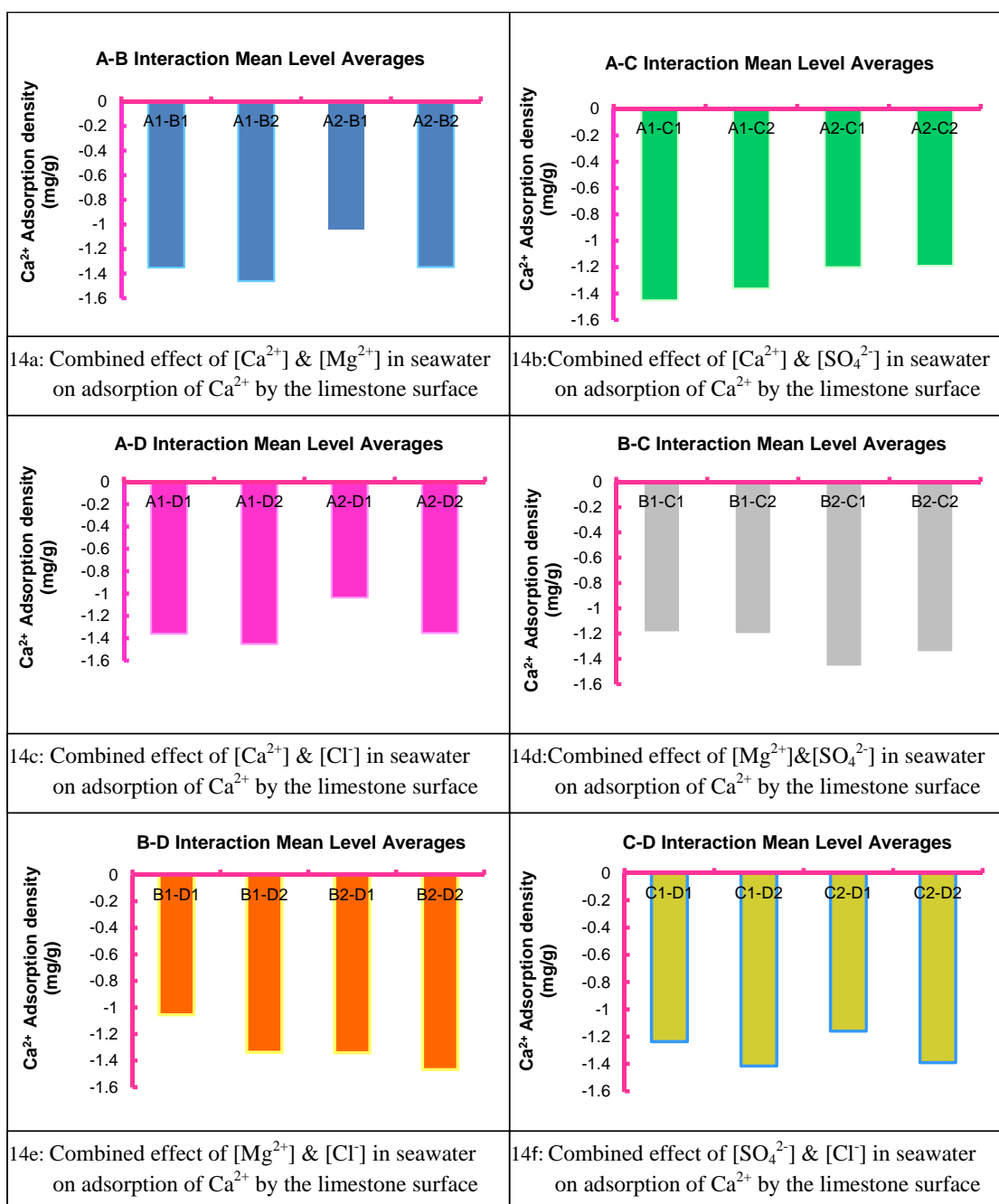


Figure 14: Two-way interactions of [Ca²⁺], [Mg²⁺], [SO₄²⁻], and [Cl⁻] on the adsorption of Ca²⁺ by limestone at 25°C in the absence of crude-oil

Magnesium Ion Interactions

Figure 15 shows the main effect results of Mg^{2+} present in seawater on the adsorption of Ca^{2+} onto the limestone rock sample. It can be observed from this figure that decreasing the concentrations of Ca^{2+} , Mg^{2+} , and Cl^- ions resulted into adsorption of magnesium ion onto the limestone surface, with sulfate ion showing opposite effect. Chloride ion seems to be very influential on magnesium adsorption as Figure 15d shows that the highest adsorption and desorption of magnesium ion is obtained at low and high chloride ion concentrations respectively. Two-way interactions presented in Figure 16 indicates that all interactions that occurred at the lower level of calcium, magnesium, and chloride ions (A1-B1, A1-B2, A2-B1, A1-C1, A1-C2, A1-D1, A1-D2, B1-C1, B1-C2, and B1-D1, A2-D1, B2-D1, C1-D1, and C2-D1) amazingly resulted into adsorption of magnesium ions. Interestingly, the highest adsorption and desorption was obtained from interactions C2-D1 (Figure 16f), and A2-D2 (Figure 16c). This confirms again that reducing chloride ion concentration in seawater seems to be the optimum way to trigger Mg^{2+} adsorption onto limestone at 25°C, in the absence of crude oil. Decreasing calcium ion concentration in seawater will also enhance magnesium ion adsorption.

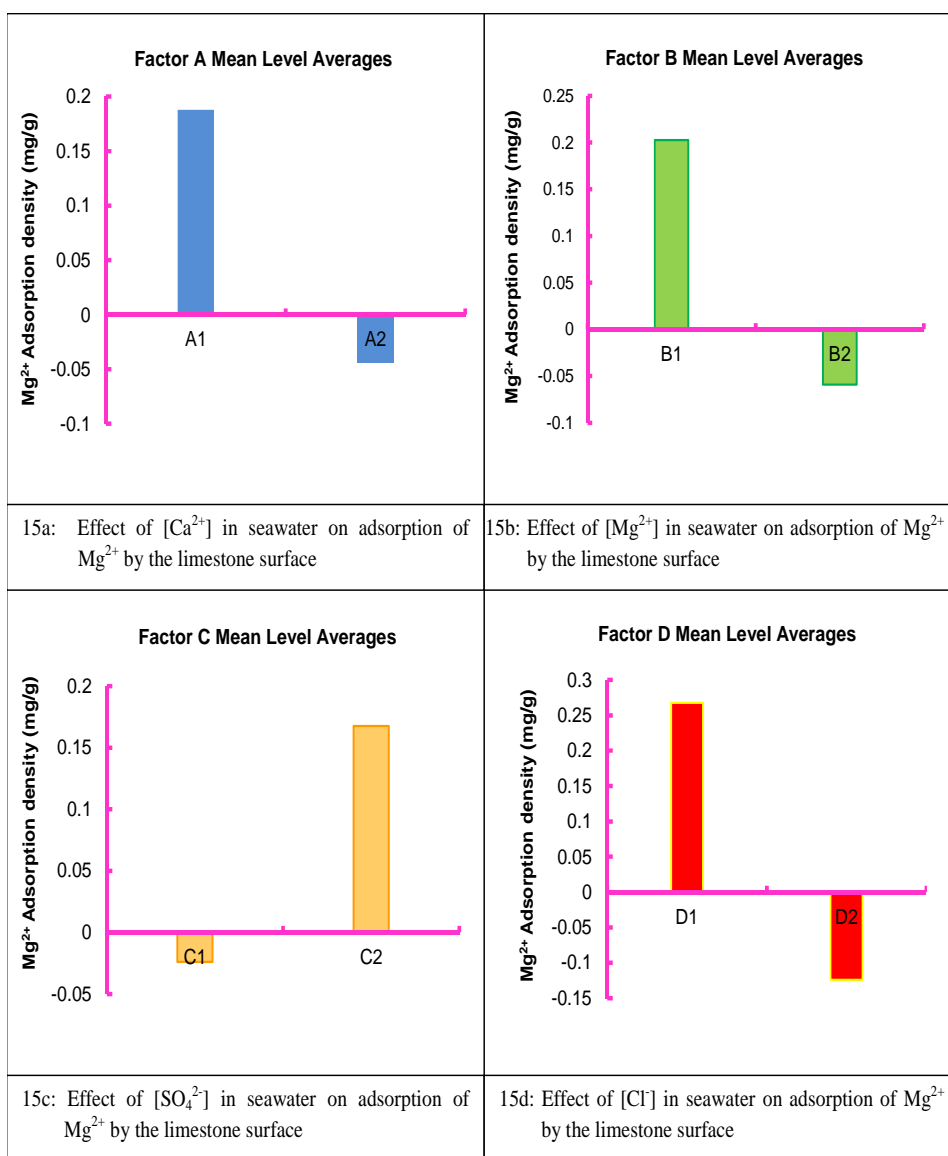


Figure 15: Main effects of [Ca²⁺], [Mg²⁺], [SO₄²⁻], and [Cl⁻] on the adsorption of Mg²⁺ by limestone at 25°C in the absence of crude-oil

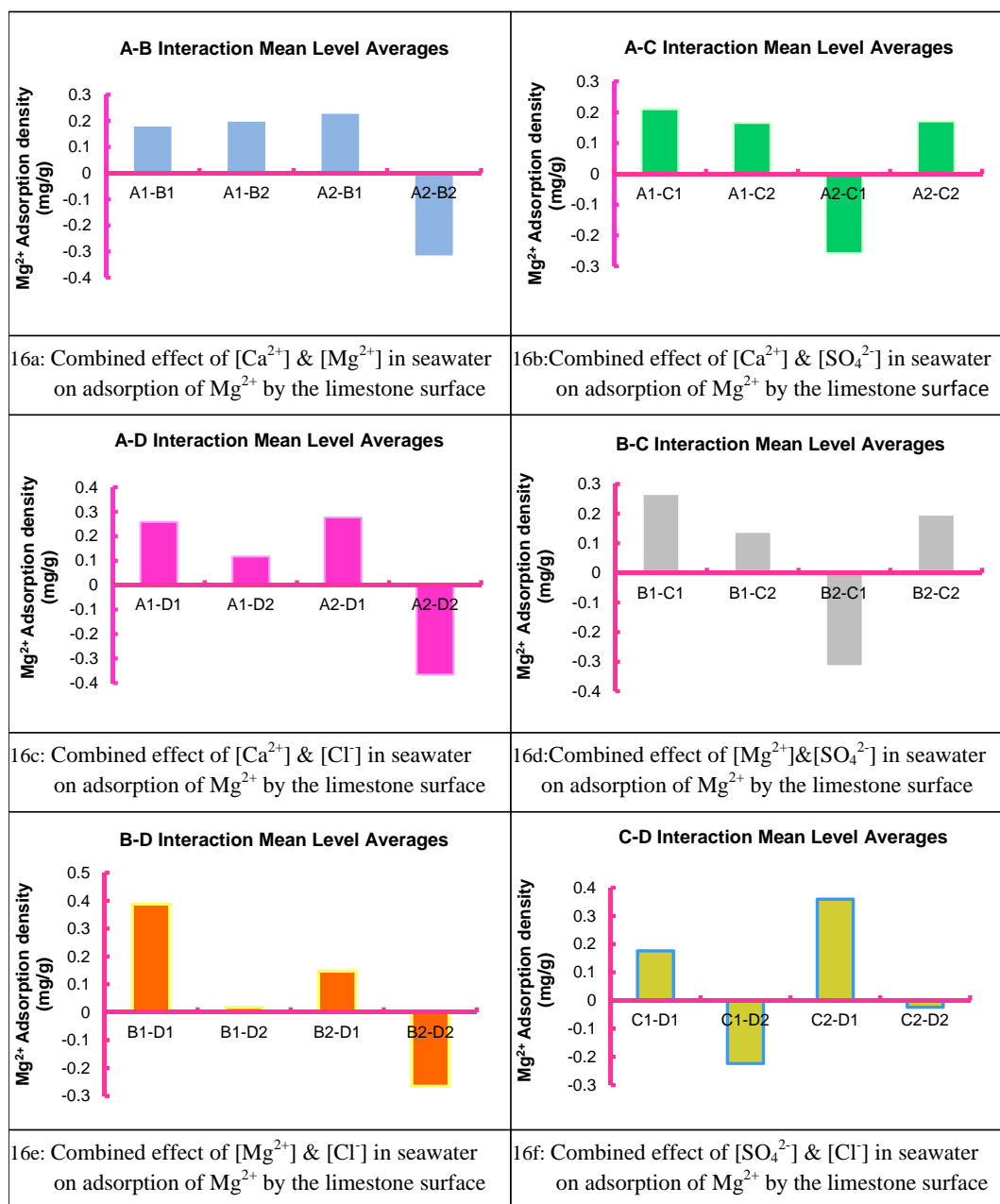


Figure 16: Two-way interactions of [Ca²⁺], [Mg²⁺], [SO₄²⁻], and [Cl⁻] on the adsorption of Mg²⁺ by limestone at 25°C in the absence of crude-oil

Sulfate Ion Interactions

Figures 17 and 18 show the main effects and two-way interactions of Ca^{2+} , Mg^{2+} , SO_4^{2-} , and Cl^- concentrations in seawater on the adsorption of SO_4^{2-} onto limestone respectively. It can be seen from these figures that all levels of interaction between Ca^{2+} , Mg^{2+} , SO_4^{2-} , and Cl^- in seawater showed desorption of SO_4^{2-} from the limestone surface. This could be due to the mineral dissolution of anhydrite from the limestone sample. The main effect results (Figure 17) revealed that decreasing chloride, magnesium and calcium ions in seawater will increase sulfate ion desorption from limestone. Conversely, increasing sulfate ion concentration in seawater will result into decreasing desorption of sulfate ion and vice-versa. The highest and lowest desorptions are obtained with effects A1 and A2 respectively, meaning that increasing calcium ion concentration can trigger sulfate ion adsorption at an optimum concentration. The two-factor interaction effects presented in Figure 18 indicates that interaction A2-B2 and A1-B2 yielded the lowest and highest levels of desorption of sulfate ion respectively. The facts that a high level of magnesium ion (B2) is involved in both interactions confirm that their effect on sulfate adsorption is actually due to the domineering effect of calcium ion. This calcium ion effect is also observed with all other interactions of A1 and A2. These interactions coupled with the main effects confirm that the most important and most effective ion in ensuring sulfate ion adsorption is the calcium ion. Decreasing Ca^{2+} concentration in seawater will seriously impede adsorption of SO_4^{2-} onto limestone at 25°C in the absence of crude oil.

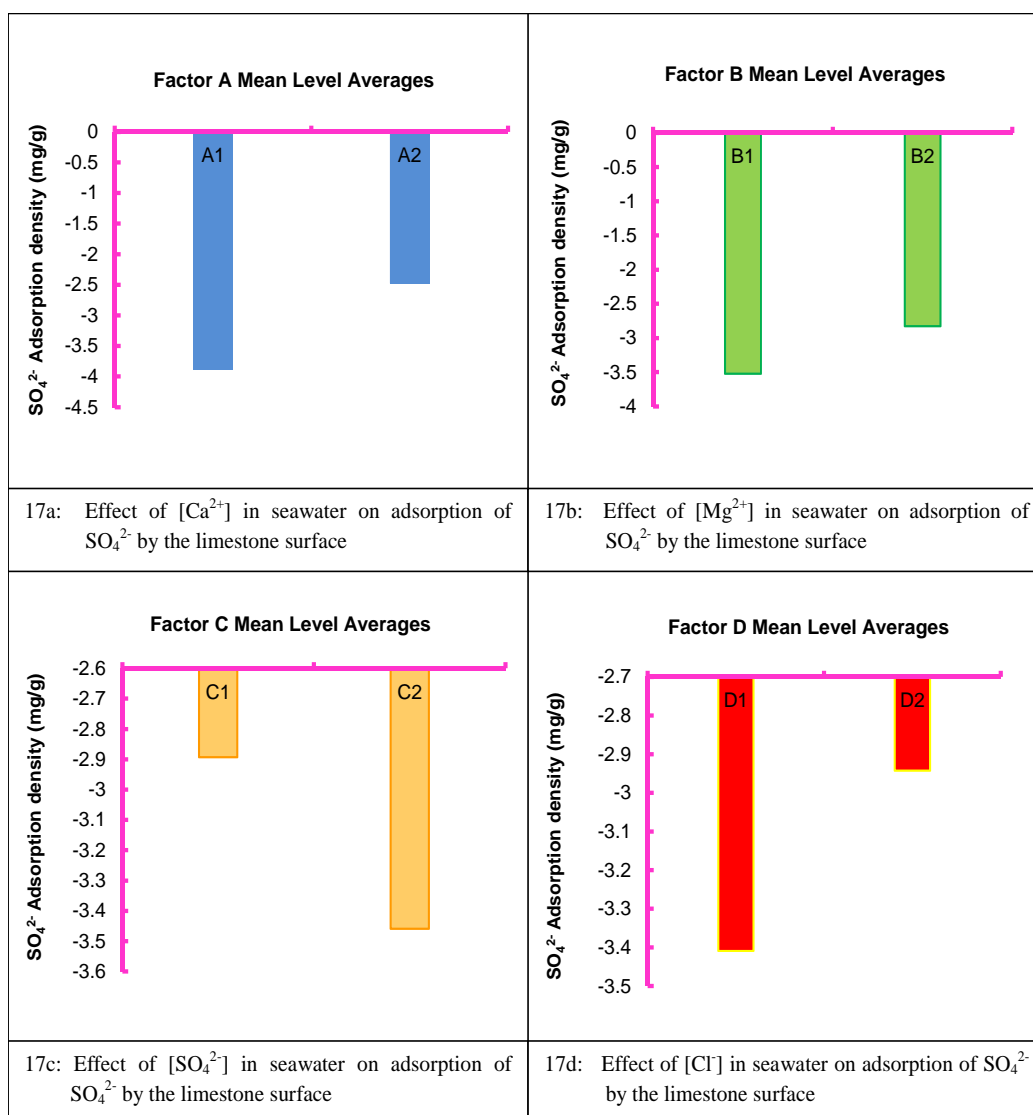


Figure 17: Main effects of [Ca²⁺], [Mg²⁺], [SO₄²⁻], and [Cl⁻] on the adsorption of SO₄²⁻ by limestone at 25°C in the absence of crude-oil

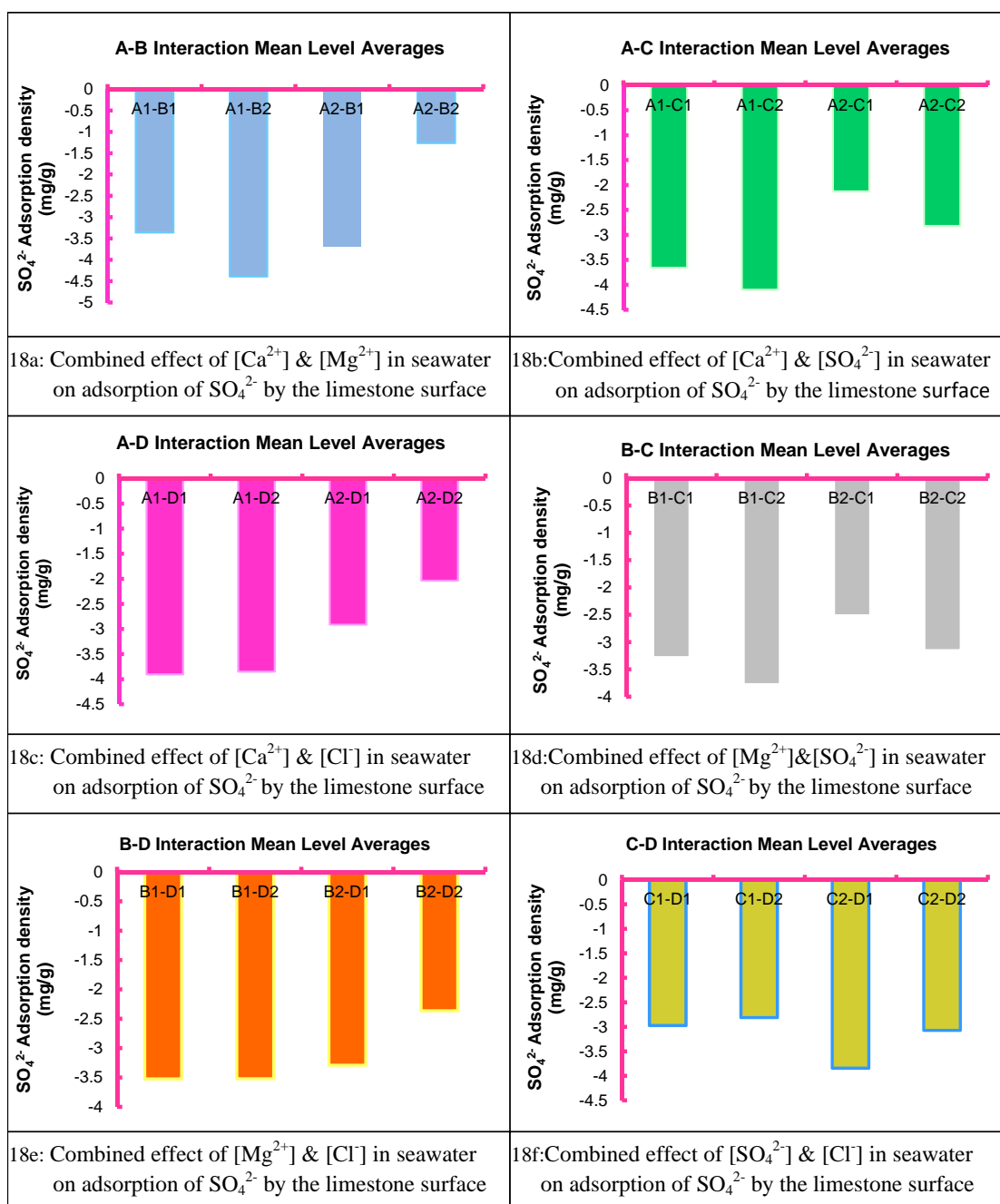


Figure 18: Two-way interactions of [Ca²⁺], [Mg²⁺], [SO₄²⁻], and [Cl⁻] on the adsorption of SO₄²⁻ by limestone at 25°C in the absence of crude-oil

Chloride Ion Interactions

Figure 19 presents the main effects of Ca^{2+} , Mg^{2+} , SO_4^{2-} , and Cl^- concentrations in seawater on chloride ion adsorption. It is observed that decreasing the concentration of all ions in seawater will increase the amount of chloride ion desorption into solution and vice-versa. The chloride ion desorption can be attributed to the dissolution of halite or any other Cl^- containing compound from the rock. Although Cl^- was not detected by the XRD, SEM, and XRF characterization methods utilized for the rock analysis, it was observed that Cl^- was coming into solution when the rock was conditioned in deionized water, thus confirming that Cl^- is contained in the rock. It was probably not detected by the characterization methods as a result of its minute amount, which was below the detection limits of the characterization equipments. The highest desorption of chloride ion is obtained at low concentration of calcium ion, while the only adsorption of chloride ion onto the limestone rock surface is at high calcium ion concentration (Figure 19a). Increasing the chloride ion concentration in seawater is also seen to significantly reduce its desorption from the rock (Figure 19d). Two-way interactions of Ca^{2+} , Mg^{2+} , SO_4^{2-} , and Cl^- concentrations in seawater on chloride ion adsorption is presented in Figure 20. It shows that adsorption of chloride ions onto limestone is observed with interactions A2-B2, A2-C2, A2-D2, B2-D2, and C2-D2. This means that increasing simultaneously the concentrations of calcium and magnesium ions, calcium and chloride ions, calcium and sulfate ions, magnesium and chloride ions, and sulfate and chloride ions in seawater will promote adsorption of chloride ions. The highest adsorption is however observed with interaction A2-B2 (high $[\text{Ca}^{2+}]$ -high $[\text{Mg}^{2+}]$), with the lowest adsorption (highest desorption) being A1-D1 (low $[\text{Ca}^{2+}]$ -low $[\text{Cl}^-]$) as can be seen in Figures 20a and 20c

respectively. It is also obvious from Figure 20 that all interactions involving low seawater concentrations of calcium and chloride show relatively high level of chloride ion desorption (Figures 20a, 20b, 20c, 20e, 20f). It can therefore be confirmed that increasing the concentrations of calcium ions followed by chloride ions in seawater are the optimum ways to enhance chloride ion adsorption onto limestone at 25°C in the absence of crude oil.

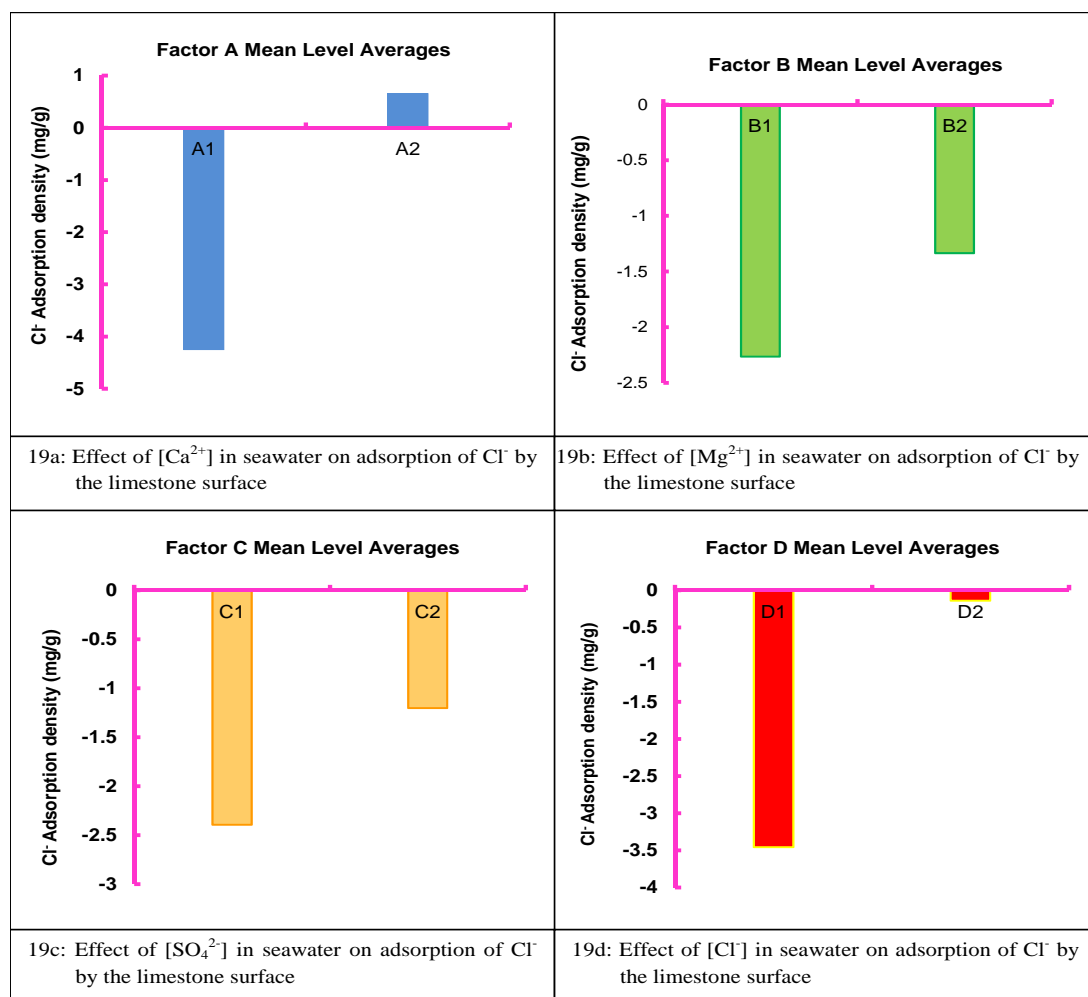


Figure 19: Main effects of [Ca²⁺], [Mg²⁺], [SO₄²⁻], and [Cl⁻] on the adsorption of Cl⁻ by limestone at 25°C in the absence of crude-oil

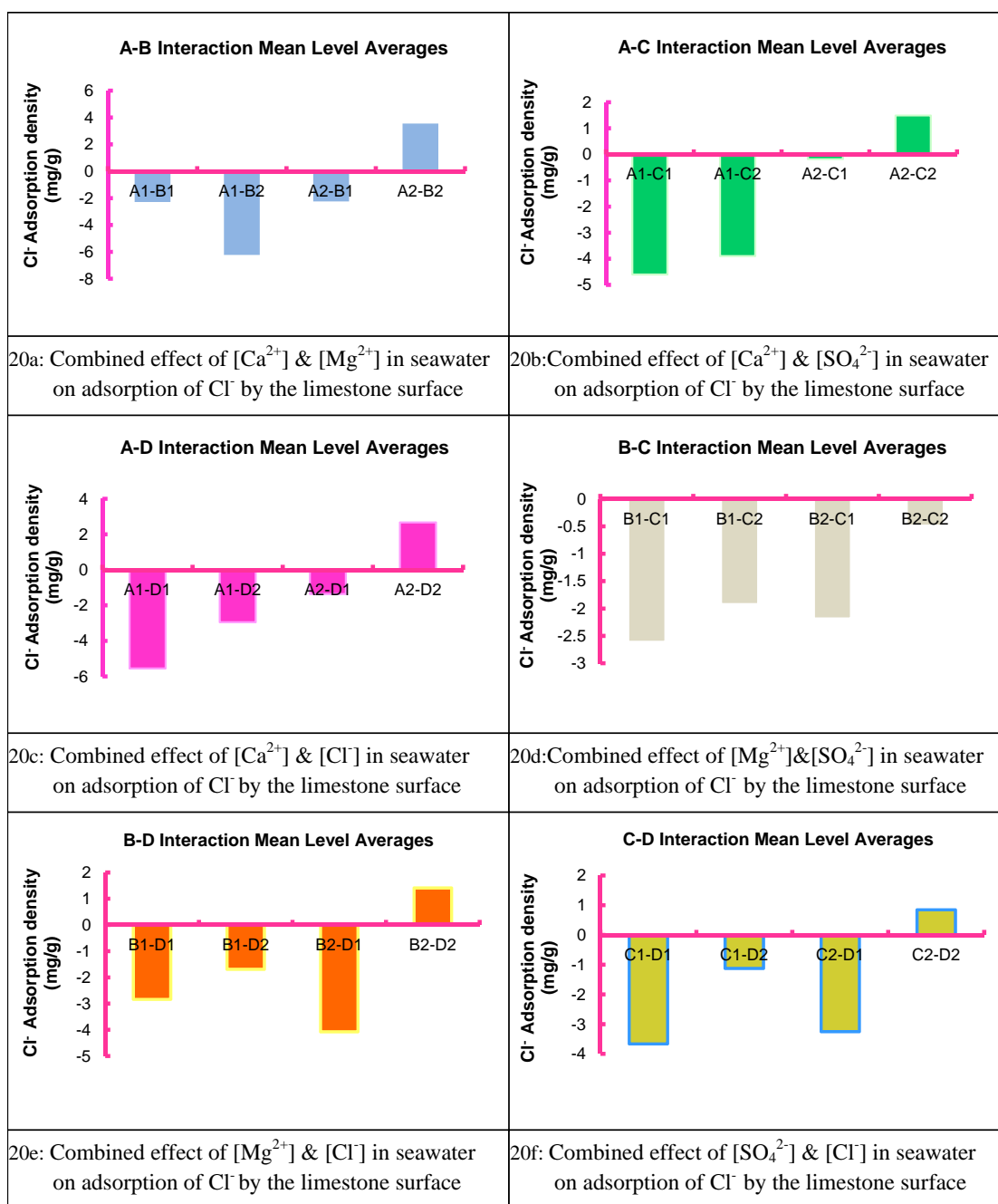


Figure 20: Two-way interactions of $[\text{Ca}^{2+}]$, $[\text{Mg}^{2+}]$, $[\text{SO}_4^{2-}]$, and $[\text{Cl}^-]$ on the adsorption of Cl^- by limestone at 25°C in the absence of crude-oil

4.2.1.2 Adsorption of Ca^{2+} , Mg^{2+} , SO_4^{2-} , and Cl^- on Limestone in the presence of crude oil at 25°C

Calcium Ion Interactions

Figures 21 and 22 present the main effects and two-way interactions of Ca^{2+} , Mg^{2+} , SO_4^{2-} , and Cl^- concentrations in seawater on the adsorption of Ca^{2+} onto limestone respectively in the presence of crude oil at 25°C. It can be seen from these figures that all levels of interaction between Ca^{2+} , Mg^{2+} , SO_4^{2-} , and Cl^- in seawater showed desorption of calcium ion from the limestone surface. The main effect results presented in Figure 21 showed that the highest desorption of calcium ion from the rock is obtained at low calcium ion concentration, while the lowest desorption is observed at high calcium ion concentration. It is also observed that all two-factor Interactions (Figure 22) involving A1 (A1-B1, A1-B2, A1-C1, A1-C2, A1-D1, and A1 - D2) all showed relatively high desorption of calcium ion from the limestone surface, while those involving A2 (A2-B1, A2-B2, A2-C1, A2-C2, A2-D1, A2-D2) yielded the lowest desorptions. It is interesting to see from Figure 22 that the highest and lowest desorptions of calcium ion are observed with interactions A1-D2, and A2-D2 respectively (Figure 22c). The presence of high chloride ion in these two peak interactions eliminates chloride effect, and confirms a domineering effect of calcium ion. All these calcium interactions support the main effect from Figure 21 that decreasing the calcium ion concentration in seawater will significantly increase the amount of calcium ion that will desorb from the rock. Although, only desorption of calcium ion has been observed under the present conditions, it is obvious that in order to trigger any sort of calcium ion adsorption onto the limestone, the optimum way is to continually increase the calcium ion concentration in the injected seawater.

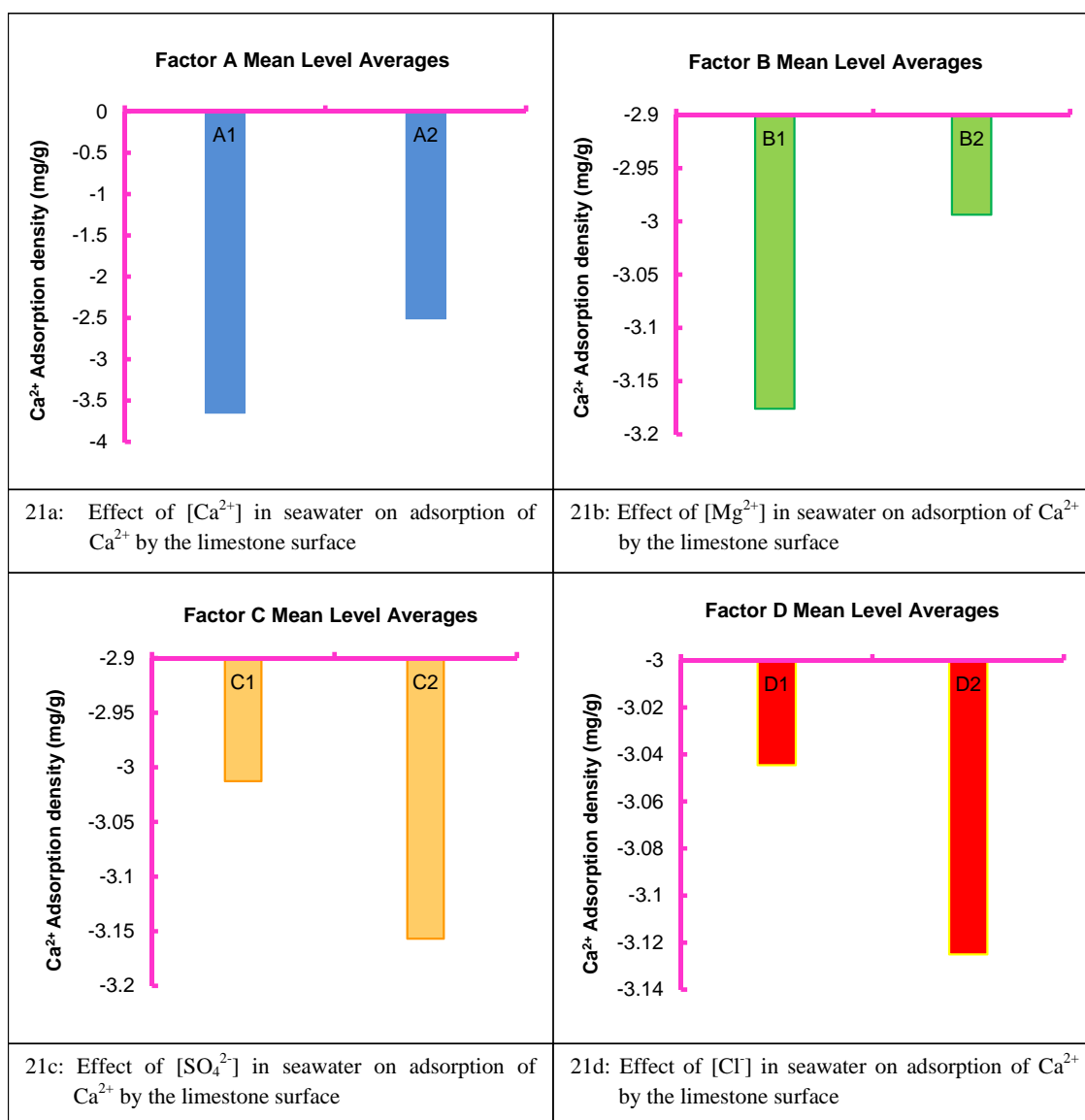


Figure 21: Main effects of [Ca²⁺], [Mg²⁺], [SO₄²⁻], and [Cl⁻] on the adsorption of Ca²⁺ by limestone at 25°C in the presence of crude-oil

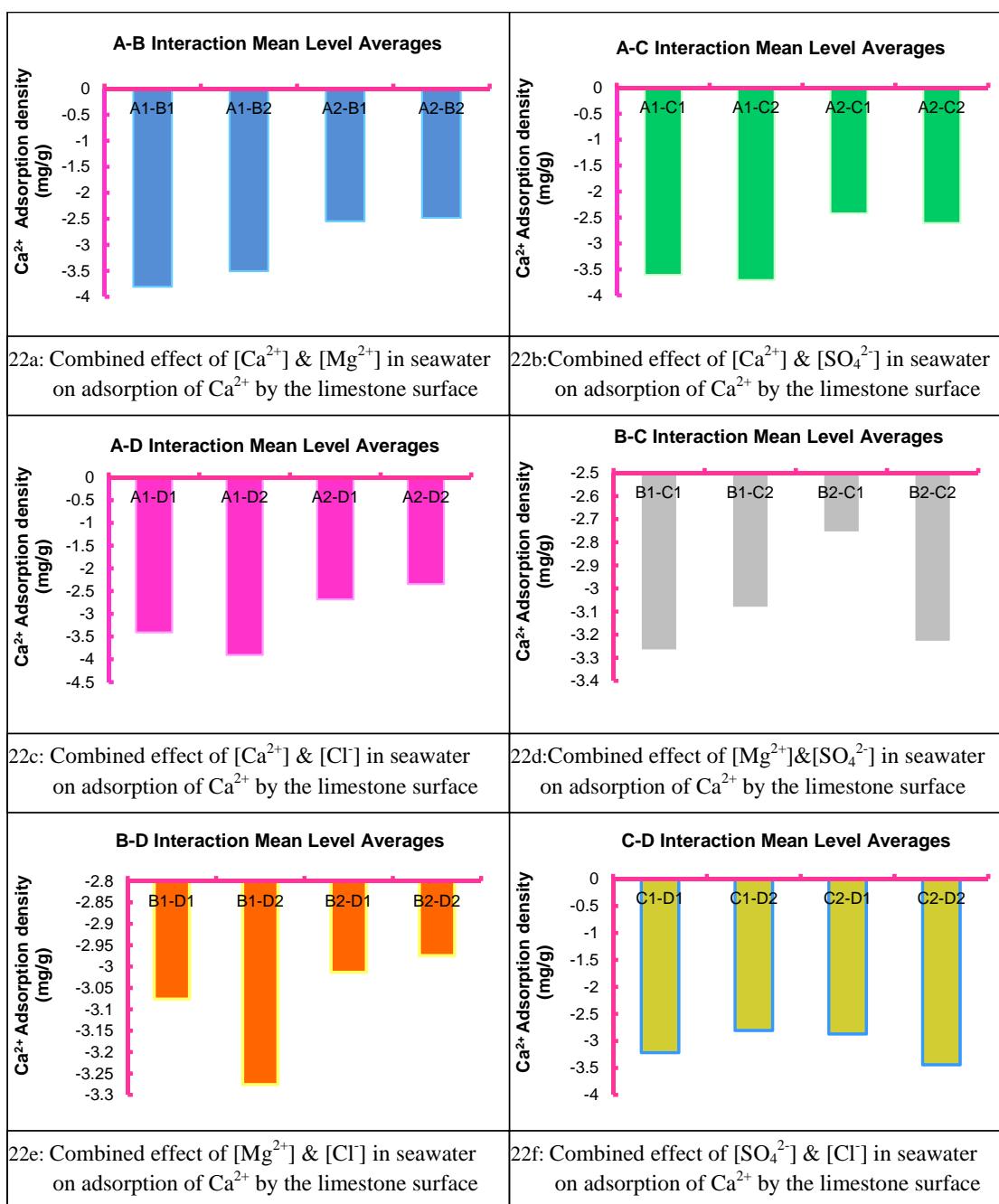


Figure 22: Two-way interactions of [Ca²⁺], [Mg²⁺], [SO₄²⁻], and [Cl⁻] on the adsorption of Ca²⁺ by limestone at 25°C in the presence of crude-oil

Magnesium Ion Interactions

The main effects of Ca^{2+} , Mg^{2+} , SO_4^{2-} , and Cl^- concentrations in seawater on Mg^{2+} adsorption onto limestone is presented in Figure 23. This figure showed desorption of Mg^{2+} from the limestone rock at all levels of concentrations of all ions. This can be explained by dolomite dissolution from the rock. An increase in magnesium, sulfate and chloride ions in seawater significantly increased the desorption of magnesium ion, while calcium ion showed an opposite effect. From Figure 23c, the highest amount of desorption of magnesium ion was observed at high sulfate concentration (C2), while the lowest desorption was obtained at low sulfate concentration (C1). The two-factor interactions presented in Figure 24 indicates that adsorption of Mg^{2+} occurs from interactions A2-B1, A1-C1, B1-C1, B1-D1, and C1-D1, which shows the highest adsorption. The highest desorptions of magnesium ion was however observed from interactions A1-C2, and B2-C2. All the interactions and the main effects point to the significance of SO_4^{2-} in Mg^{2+} adsorption, with Chloride ion also playing a major role. It can also be seen that the optimum way to enhance Mg^{2+} adsorption onto the limestone at 25°C in the presence of crude oil is to reduce the concentrations of both SO_4^{2-} and Cl^- simultaneously in the injected seawater.

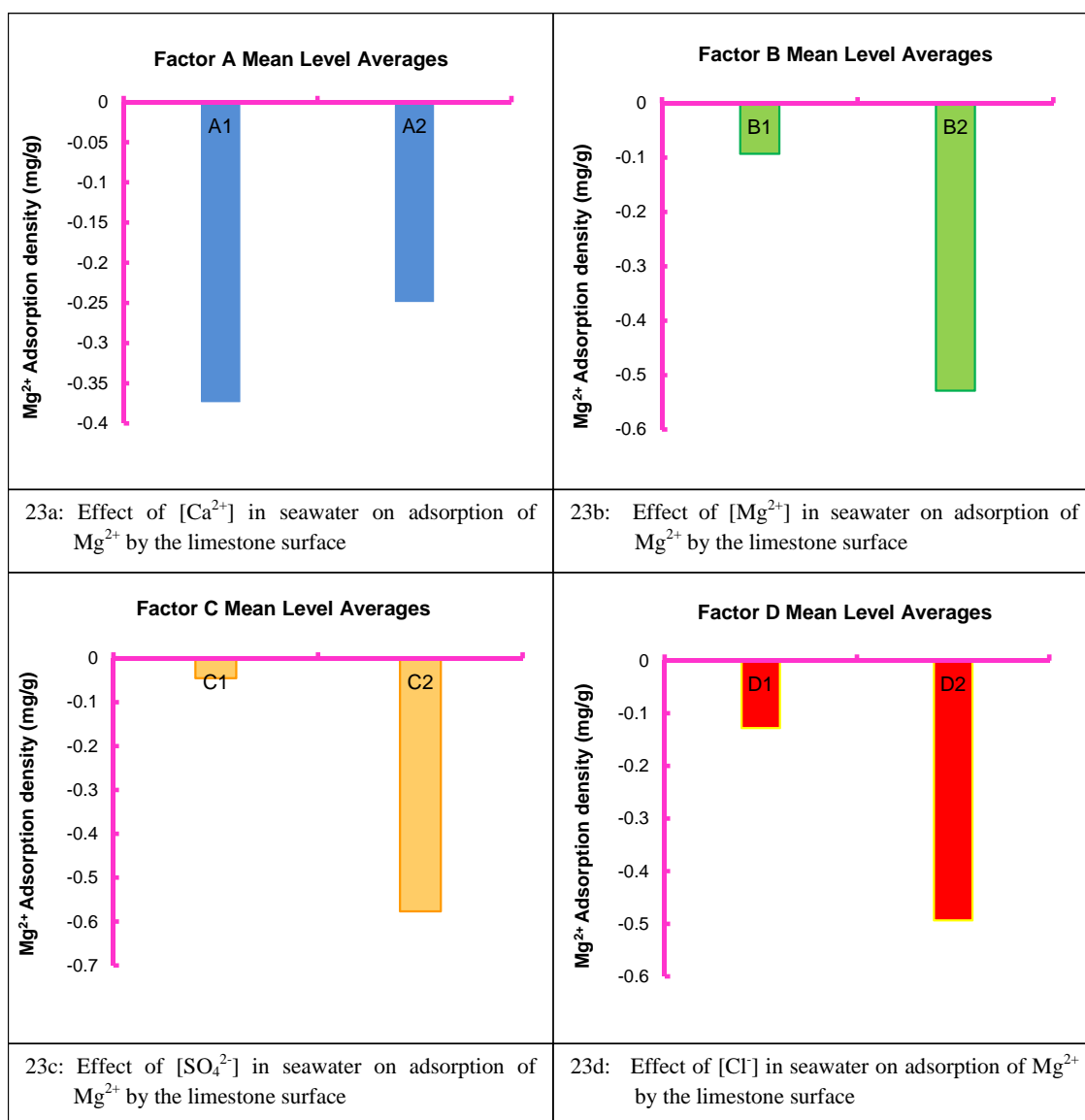


Figure 23: Main effects of $[\text{Ca}^{2+}]$, $[\text{Mg}^{2+}]$, $[\text{SO}_4^{2-}]$, and $[\text{Cl}^-]$ on the adsorption of Mg^{2+} by limestone at 25°C in the presence of crude-oil

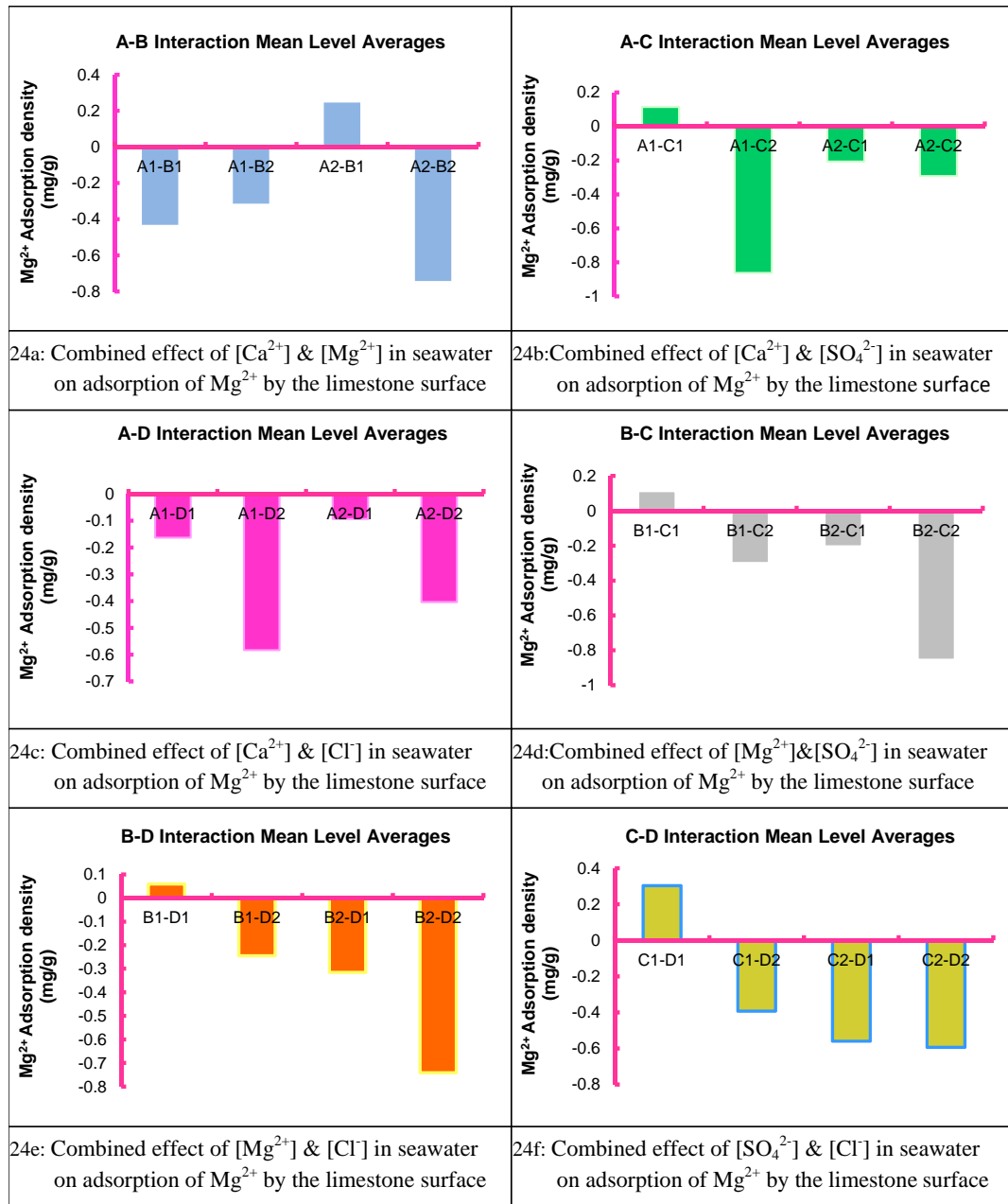


Figure 24: Two-way interactions of [Ca²⁺], [Mg²⁺], [SO₄²⁻], and [Cl⁻] on the adsorption of Mg²⁺ by limestone at 25°C in the presence of crude-oil

Sulfate Ion Interactions

Figures 25 and 26 present the main effects and two-way interactions respectively of Ca^{2+} , Mg^{2+} , SO_4^{2-} , and Cl^- concentrations in seawater on the adsorption of SO_4^{2-} onto limestone in the presence of crude oil at 25°C. It can be seen from these figures that all levels of interaction between Ca^{2+} , Mg^{2+} , SO_4^{2-} , and Cl^- in seawater showed desorption of SO_4^{2-} from the limestone surface. This can be due to the mineral dissolution of anhydrite from the limestone sample. Main effect results presented in Figure 25 show that the highest and lowest desorptions of SO_4^{2-} ion from the rock is obtained at low calcium and high calcium concentration (A1 and A2) respectively. Interactions A1-B1, A1-C2, and A1-D2 all show the highest desorptions of sulfate ion, while the lowest desorption is observed at interaction A2-B1 (Figure 26). These two-factor interactions coupled with the main effects suggest that decreasing Ca^{2+} concentration in seawater will significantly increase desorption of sulfate ion and consequently hinder its adsorption onto limestone at 25°C, in the presence of crude oil.

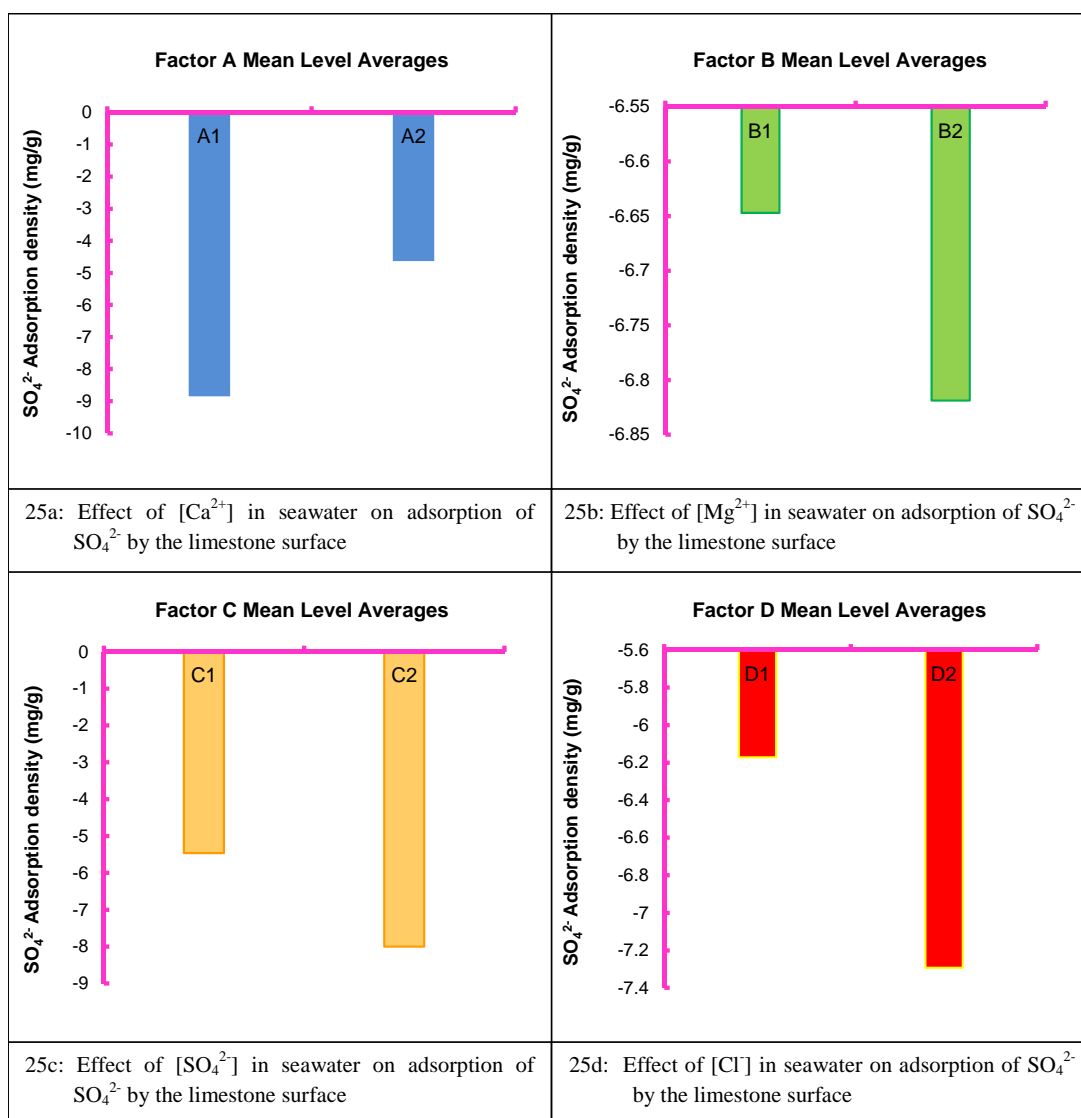


Figure 25: Main effects of $[\text{Ca}^{2+}]$, $[\text{Mg}^{2+}]$, $[\text{SO}_4^{2-}]$, and $[\text{Cl}^-]$ on the adsorption of SO_4^{2-} by limestone at 25°C in the presence of crude-oil

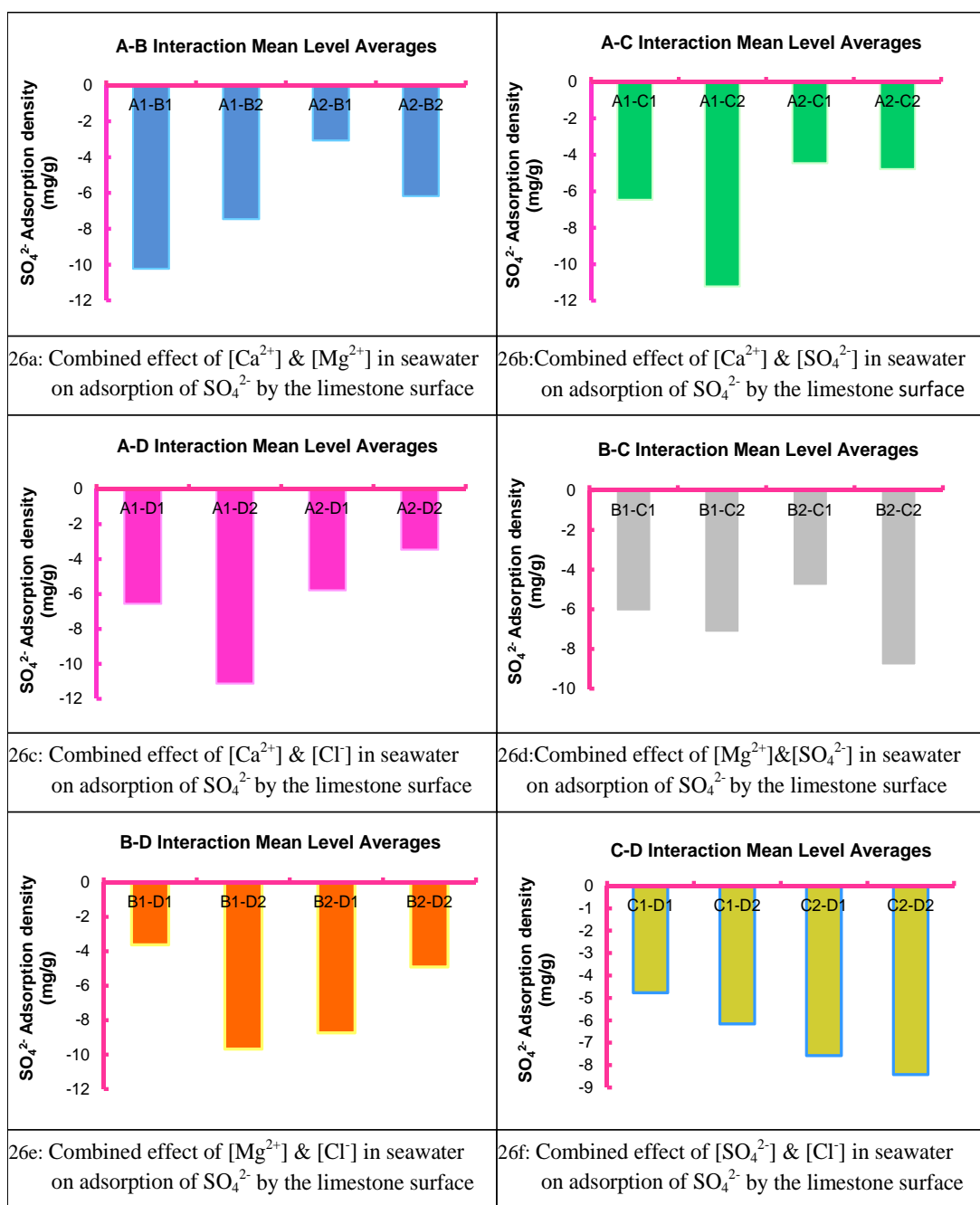


Figure 26: Two-way interactions of [Ca²⁺], [Mg²⁺], [SO₄²⁻], and [Cl⁻] on the adsorption of SO₄²⁻ by limestone at 25°C in the presence of crude-oil

Chloride Ion Interactions

The main effect results of chloride ion concentration in seawater on calcium, magnesium, sulfate, and chloride ion adsorption onto limestone is presented in Figure 27. It indicates that increasing sulfate, chloride, and magnesium ions, and decreasing calcium ions in seawater will increase chloride ion desorption from the rock. The highest and lowest desorptions of chloride ion are obtained from the effects A1 (low calcium) and A2 (high calcium) respectively. The significant effect of calcium ion is also seen in the two-factor interactions which are presented in Figure 28. It is observed that the highest desorptions of chloride ion are obtained from interactions A1-B1, A1-C2 and A1-D2. Contrary to this, the highest adsorptions are produced from interactions A2-B1, and A2-D2. All interactions confirm that a reduction in calcium ion's concentration in seawater will significantly reduce the possibility of chloride's adsorption onto the limestone rock surface at 25°C, in the presence of crude-oil.

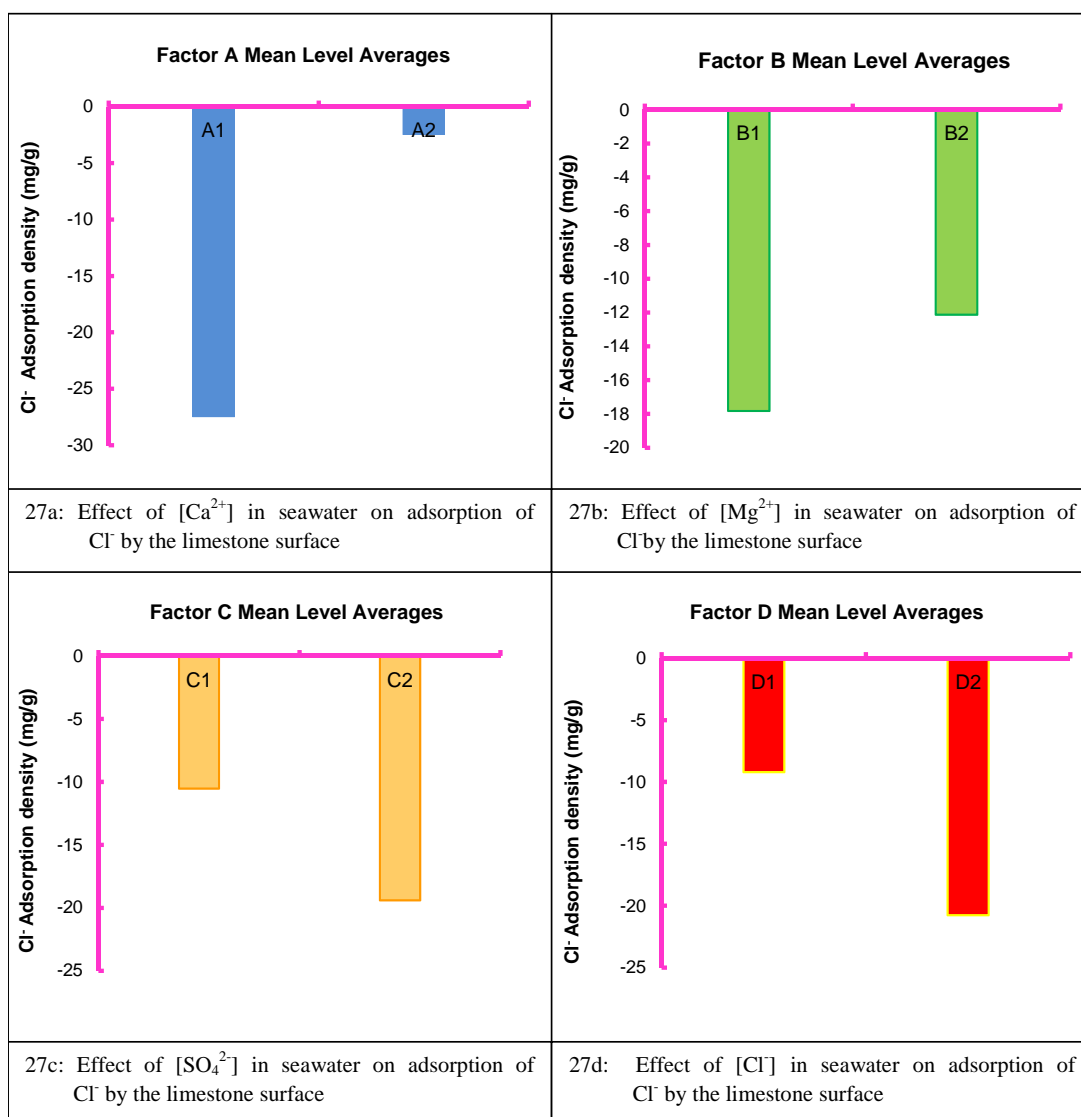


Figure 27: Main effects of [Ca²⁺], [Mg²⁺], [SO₄²⁻], and [Cl⁻] on the adsorption of Cl⁻ by limestone at 25°C in the presence of crude-oil

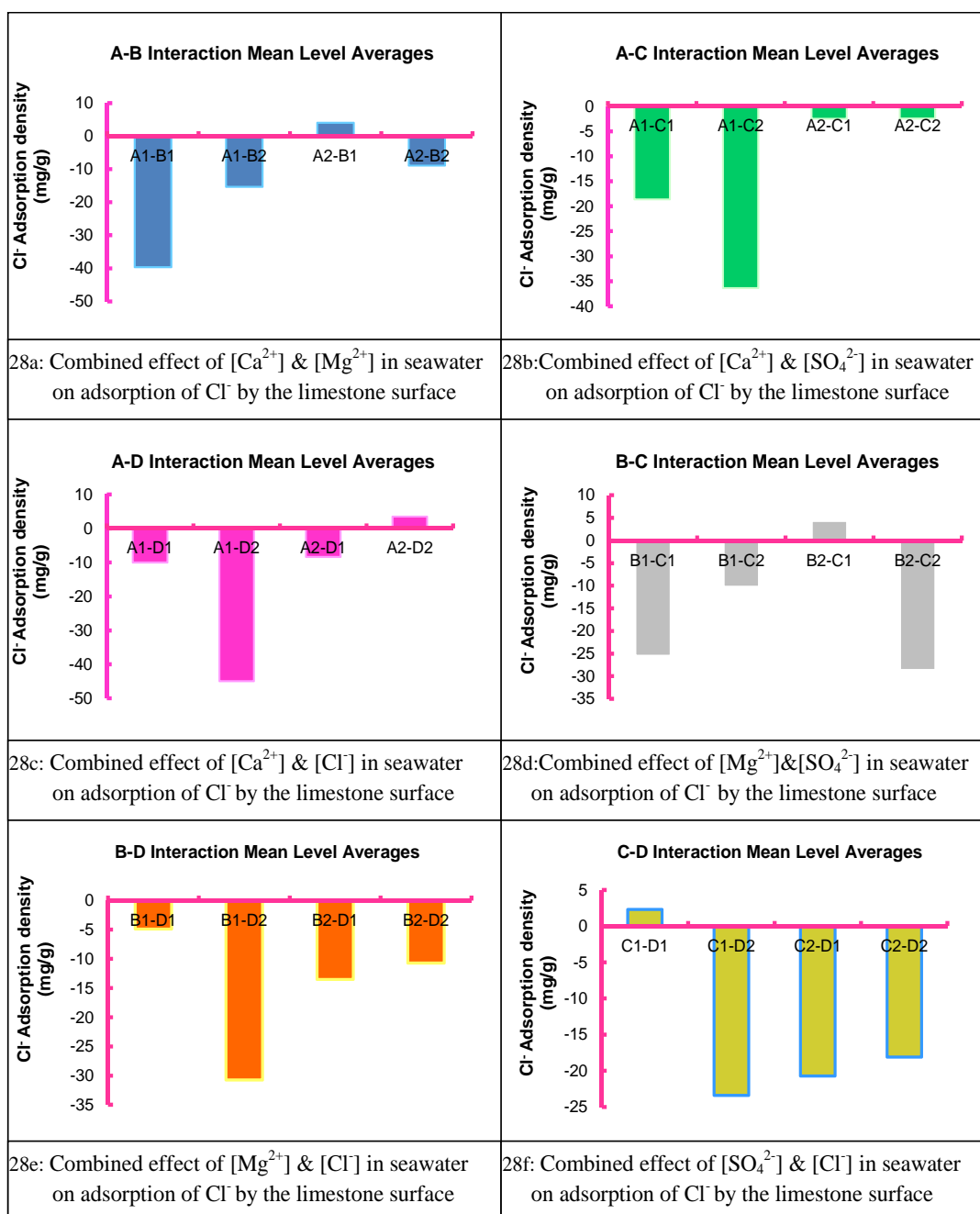


Figure 28: Two-way interactions of [Ca²⁺], [Mg²⁺], [SO₄²⁻], and [Cl⁻] on the adsorption of Cl⁻ by limestone at 25°C in the presence of crude-oil

4.2.1.3 Adsorption of Ca^{2+} , Mg^{2+} , SO_4^{2-} , and Cl^- on Limestone in the absence of crude oil at 90°C

Calcium Ion Interactions

Figures 29 and 30 indicate that all levels of interaction between Ca^{2+} , Mg^{2+} , SO_4^{2-} , and Cl^- in seawater yielded desorption of calcium ion from the limestone surface at 90°C. This can be due to mineral dissolution of calcite, anhydrite and dolomite from the limestone sample. The main effect results of Ca^{2+} (Figure 29) showed that decreasing the concentrations of either calcium or sulfate ions in seawater will increase the calcium ion desorption from the limestone surface and vice-versa. On the contrary, a decrease in either magnesium or chloride ions in seawater resulted in less desorption of calcium ion. Interestingly, effect A1 and A2 yielded the highest and lowest desorptions of calcium ion respectively. It is also observed from the two-factor interactions presented in Figure 30 that all interactions of A1 (A1-B1, A1-B2, A1-C1, A1-C2, A1-D1, and A1-D2) gave relatively the highest desorptions while interactions of A2 yielded much lower desorptions. The highest and lowest desorptions are obtained from interactions A1-B2, and A2-B2 respectively. However, the presence of B2 in both peak interactions eliminates high magnesium effect, and confirms calcium ion as the dominant factor. From the foregoing discussion, it is reasonable to conclude that in order to assure the occurrence or promotion of adsorption of calcium ions onto limestone at 90°C in the absence of crude oil, calcium ion concentration in the injected or surrounding seawater should be increased.

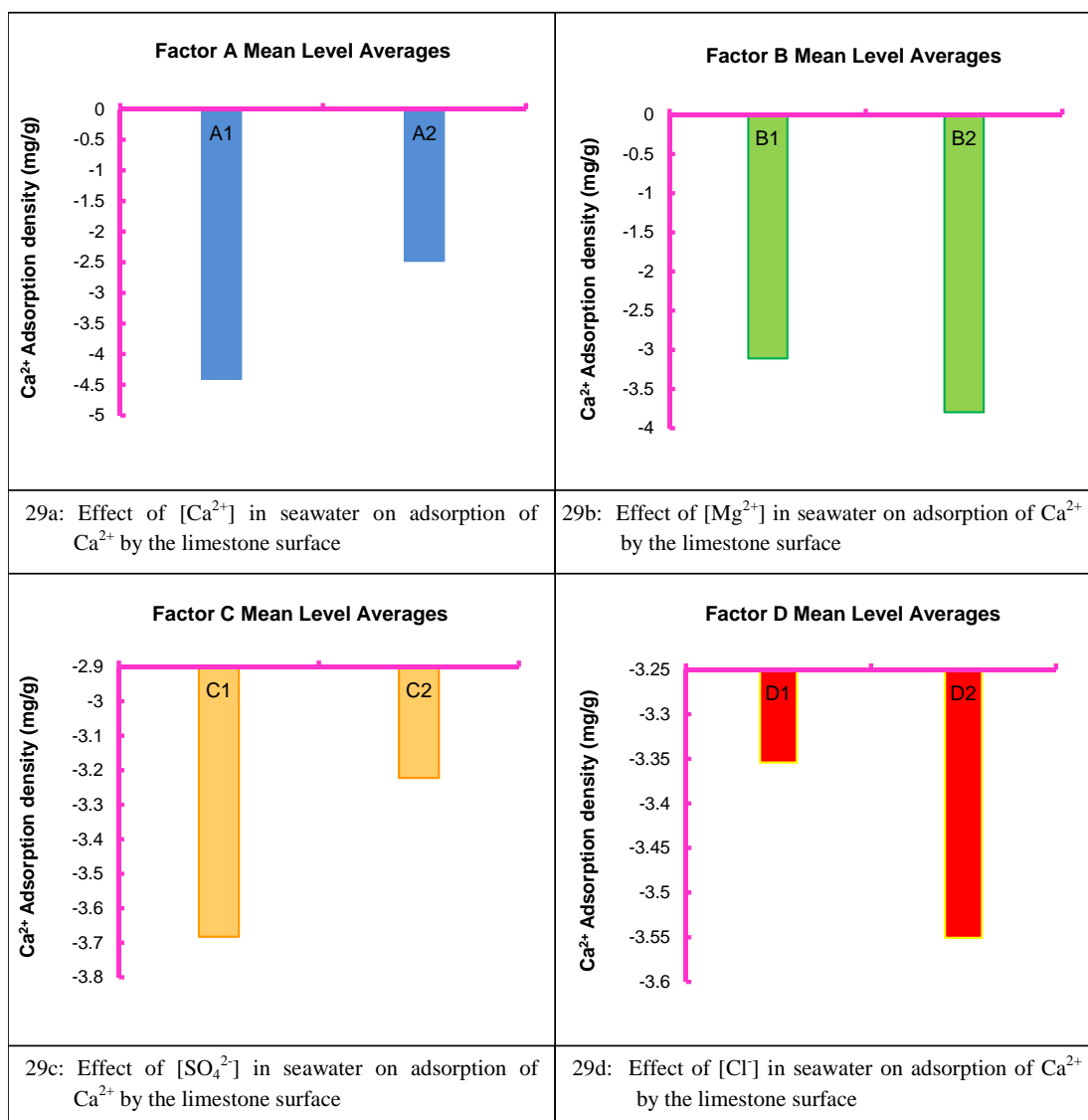


Figure 29: Main effects of [Ca²⁺], [Mg²⁺], [SO₄²⁻], and [Cl⁻] on the adsorption of Ca²⁺ by limestone at 90°C in the absence of crude-oil

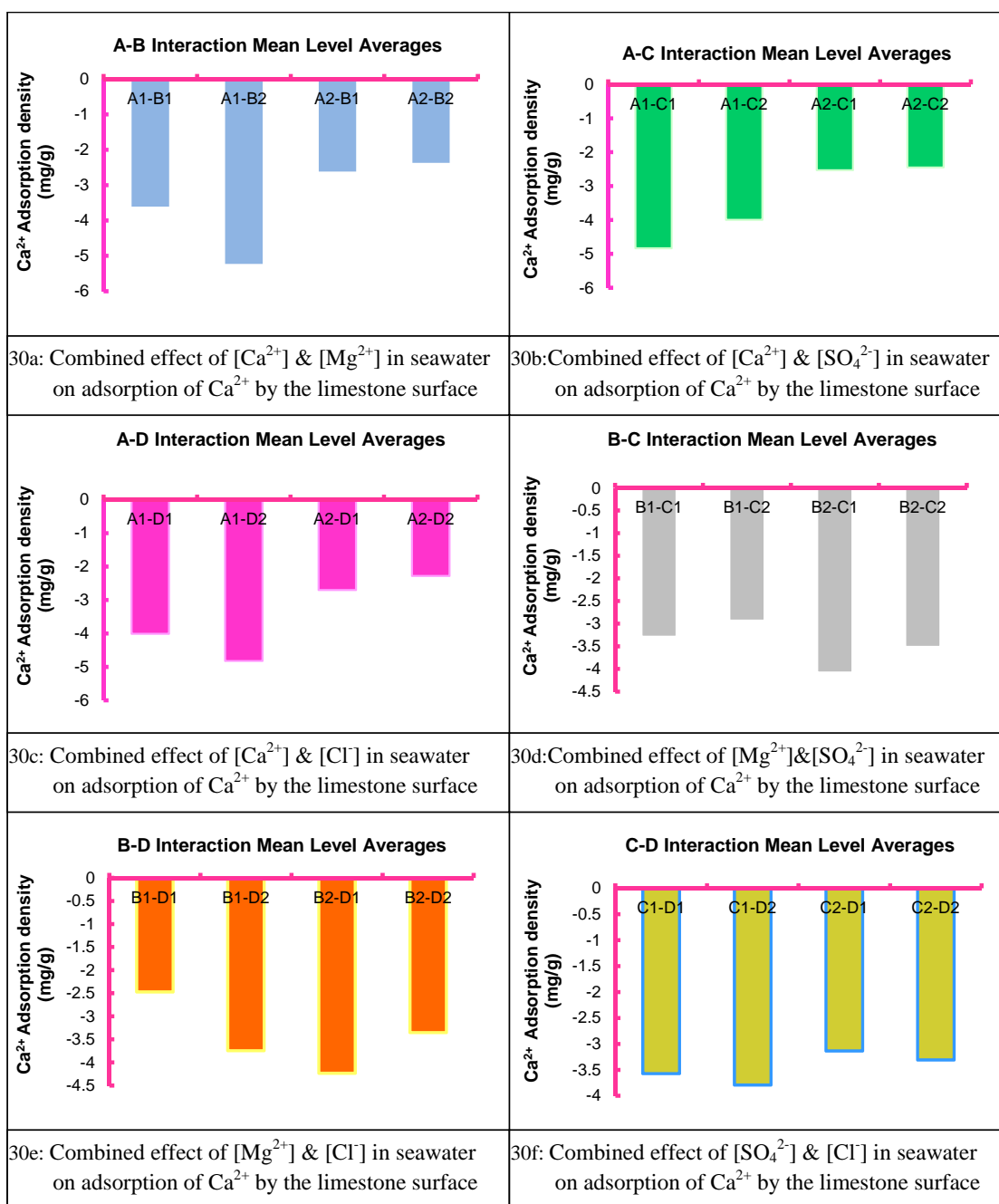


Figure 30: Two-way interactions of [Ca²⁺], [Mg²⁺], [SO₄²⁻], and [Cl⁻] on the adsorption of Ca²⁺ by limestone at 90°C in the absence of crude-oil

Magnesium Ion Interactions

Figures 31 and 32 present the main effects and two-way interactions respectively of Ca^{2+} , Mg^{2+} , SO_4^{2-} , and Cl^- concentrations in seawater on the adsorption of Mg^{2+} onto limestone in the absence of crude oil at 90°C . Main effects results (Figure 31) indicates that magnesium adsorption is enhanced by either increasing magnesium, sulfate and chloride ions or decreasing calcium ions in seawater. Sulfate ions seem to have a significant impact as it is observed that the highest and lowest adsorptions of magnesium ions occurred with effects C2 and C1 respectively. The two-factor interactions B2-C2, and C2-D2 yielded the highest adsorptions of magnesium ion (Figure 32), while the only desorption (very slight) is seen at interaction A2-C1. These interactions coupled with the main effects confirm the important role of sulfate ion concentration in magnesium ion adsorption. Since high magnesium and chloride ions are also observed to be influential, it is reasonable to conclude that the optimum way to promote magnesium ion adsorption onto limestone at 90°C in the absence of crude oil is to increase simultaneously either the concentrations of sulfate and magnesium ions or sulfate and chloride ions in the injected seawater.

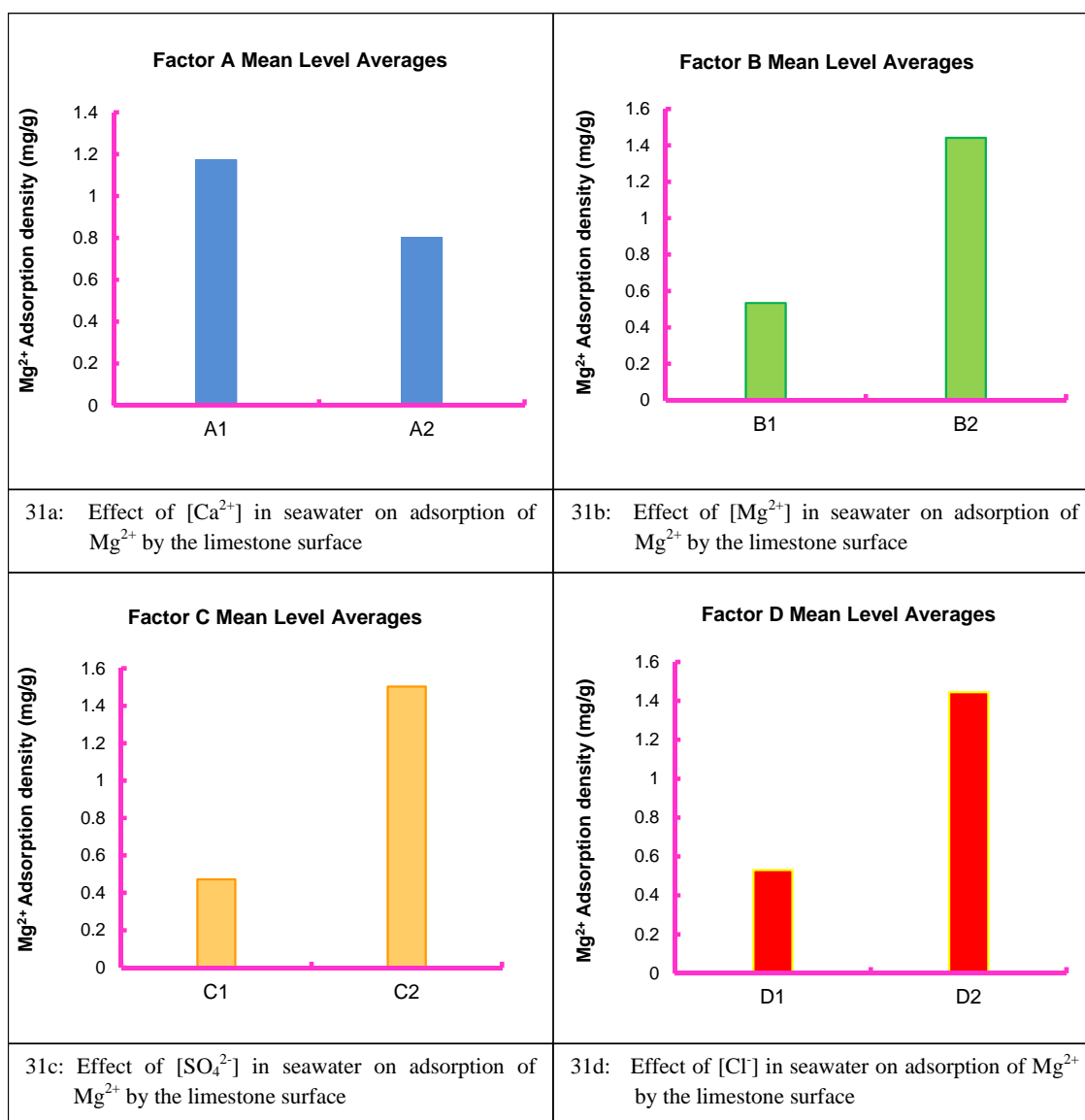


Figure 31: Main effects of $[Ca^{2+}]$, $[Mg^{2+}]$, $[SO_4^{2-}]$, and $[Cl^-]$ on the adsorption of Mg^{2+} by limestone at 90°C in the absence of crude-oil

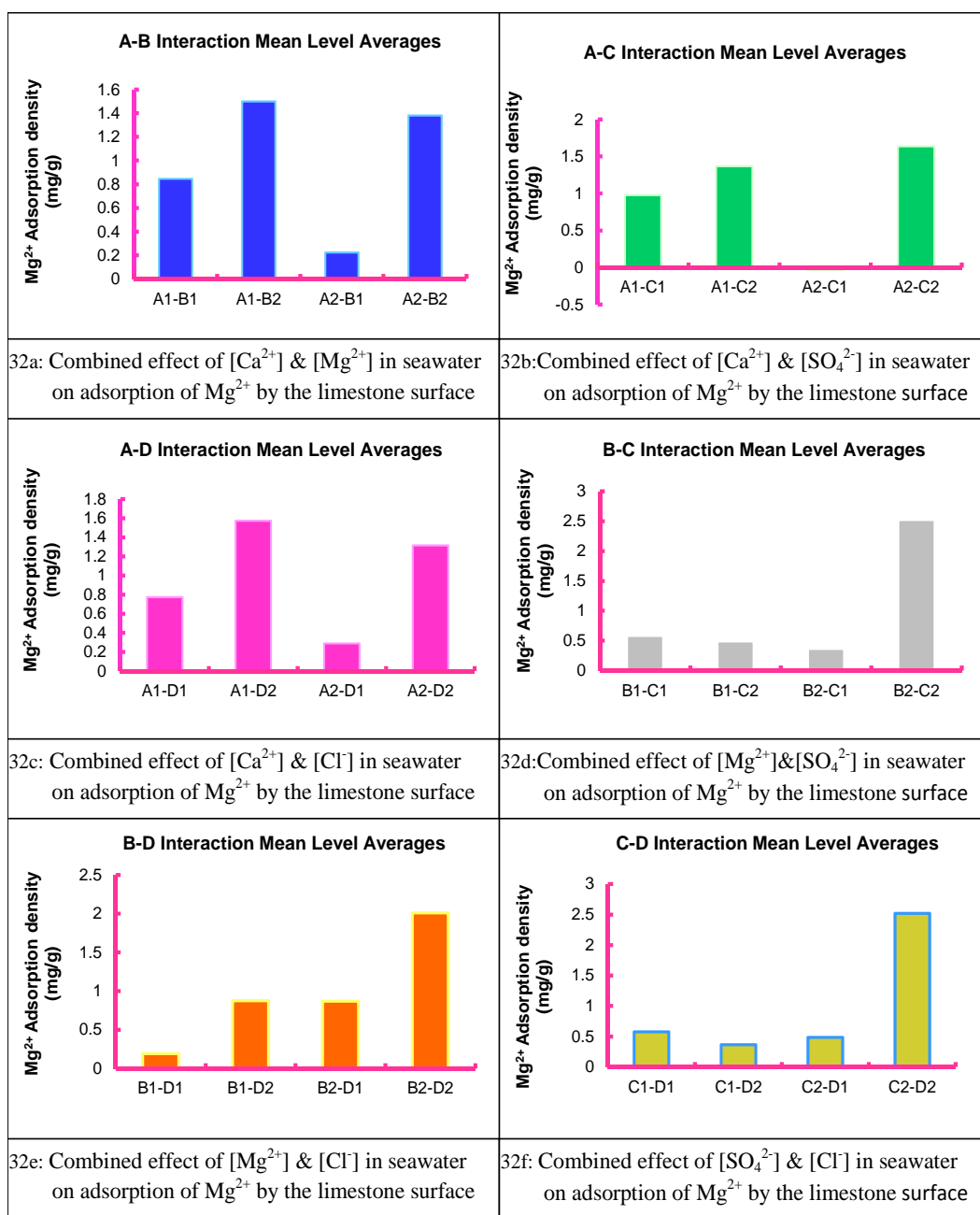


Figure 32: Two-way interactions of [Ca²⁺], [Mg²⁺], [SO₄²⁻], and [Cl⁻] on the adsorption of Mg²⁺ by limestone at 90°C in the absence of crude-oil

Sulfate Ion Interactions

Figure 33 presents the main effects of calcium, magnesium, sulfate and chloride ion concentrations in seawater on sulfate adsorption at 90°C in the absence of crude-oil. Reducing calcium, magnesium and sulfate ion's concentrations increased desorption of sulfate ion, while the opposite effect is observed with the chloride ion as can be seen from Figure 33. It is interesting to note that the highest and lowest desorptions are observed at effects A1 and A2 respectively, meaning that increasing calcium ion concentration will significantly reduce sulfate desorption and may trigger its adsorption. The two-factor interaction (Figure 34) seems to confirm this. In fact, all adsorptions of sulfate ion are observed to involve high calcium concentration (A2-B2, A2-C2, and A2-D1). Conversely, all interactions of A1 show relatively high desorptions of sulfate ion. Moreover, the highest adsorption and desorption of sulfate ions are obtained at interactions A2-B2, and A1-B1 respectively. All the interactions coupled with the main effects prove that the optimum way to enhance sulfate adsorption onto limestone at 90°C in the absence of crude oil is to increase calcium ion concentration in seawater.

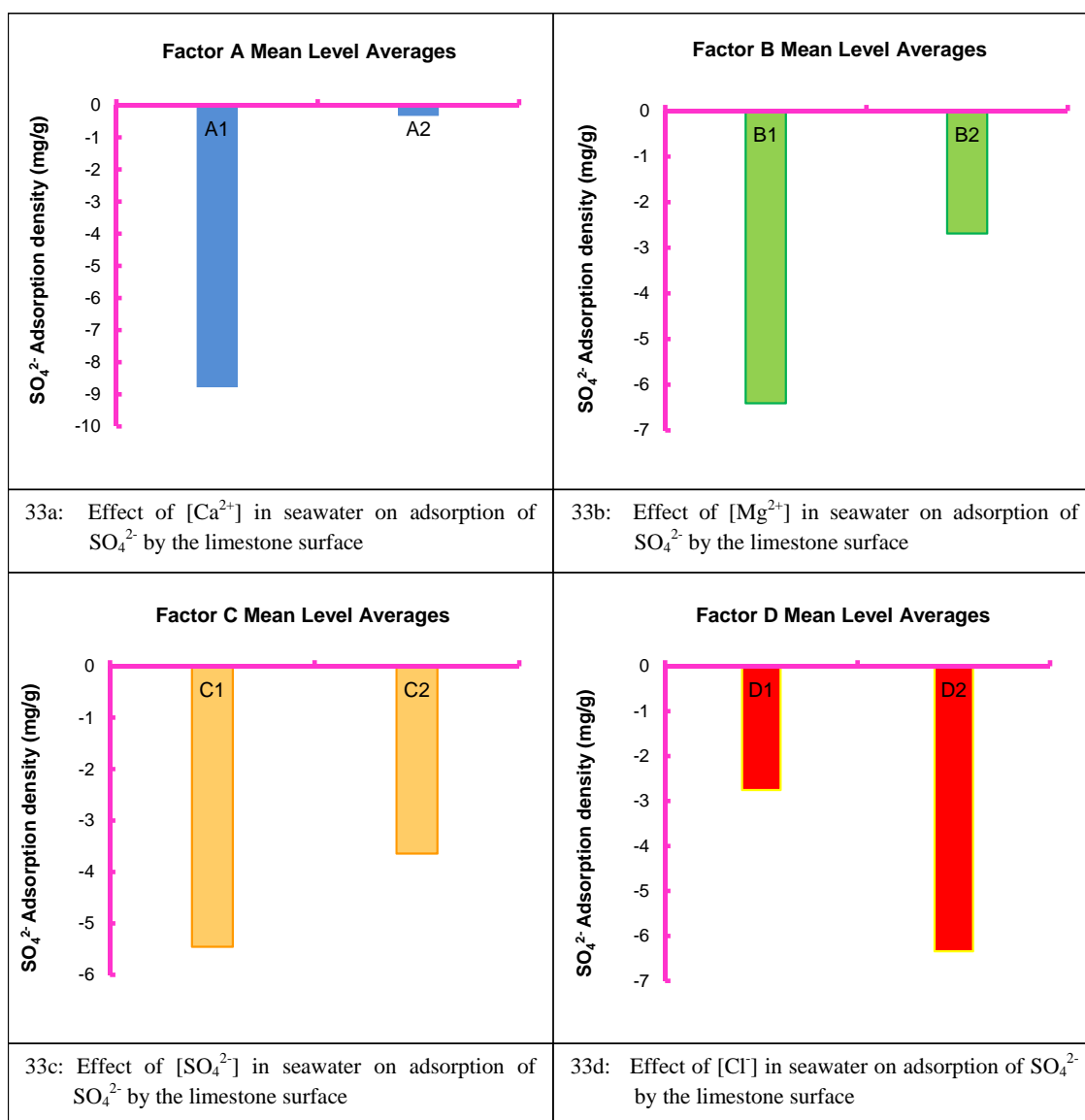


Figure 33: Main effects of [Ca²⁺], [Mg²⁺], [SO₄²⁻], and [Cl⁻] on the adsorption of SO₄²⁻ by limestone at 90°C in the absence of crude-oil

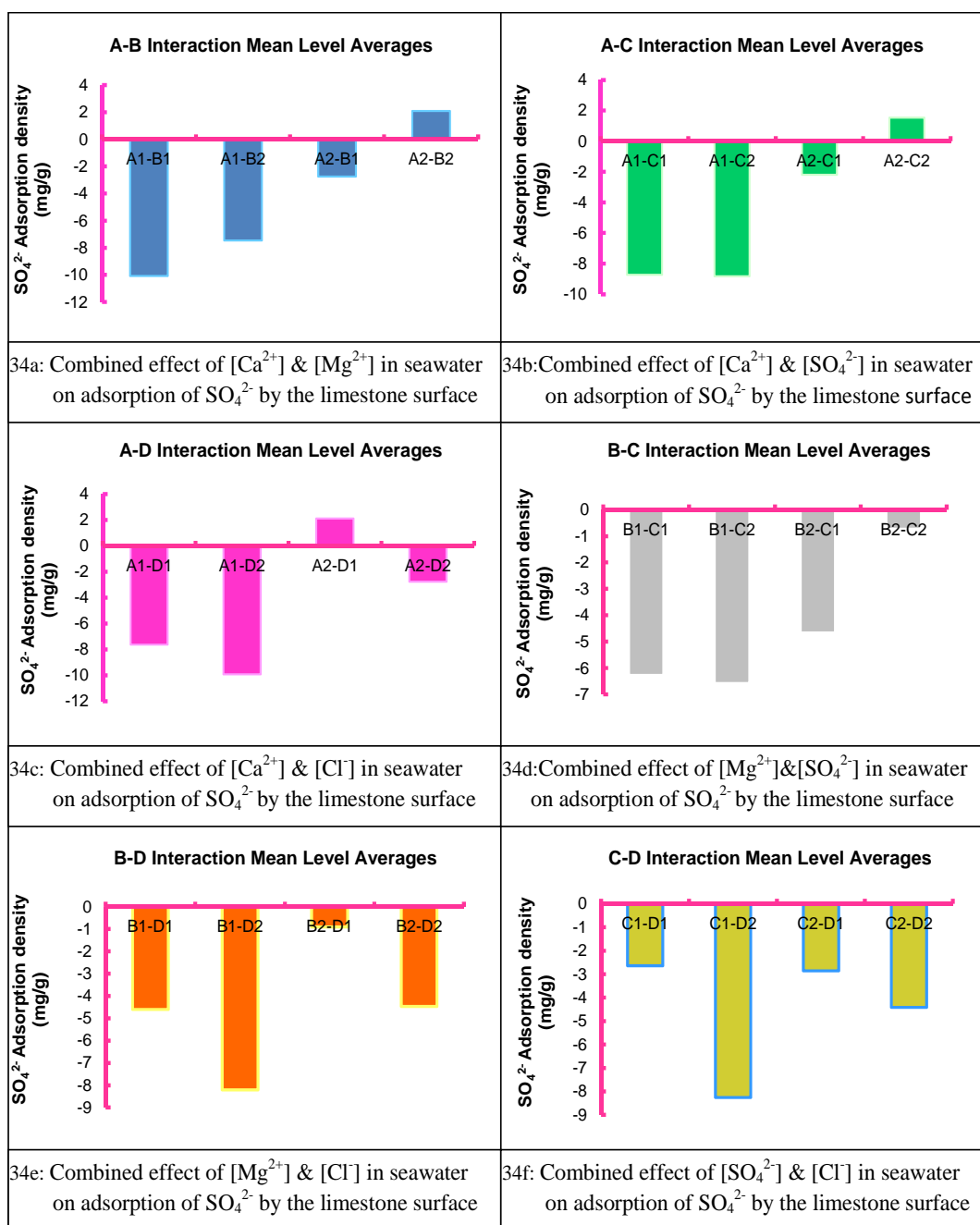


Figure 34: Two-way interactions of [Ca²⁺], [Mg²⁺], [SO₄²⁻], and [Cl⁻] on the adsorption of SO₄²⁻ by limestone at 90°C in the absence of crude-oil

Chloride Ion Interactions

The main effects of ions on chloride ion adsorption presented in Figure 35 indicate that decreasing calcium, magnesium, and sulfate ions will increase chloride desorption, while a decrease in chloride concentration will decrease its desorption. Chloride ion desorption can be attributed to the dissolution of halite or any other Cl⁻ containing compound from the rock. The highest and lowest desorptions are obtained at effects A1 and A2 respectively. The two-factor interactions presented in Figure 36 show that highest adsorptions of chloride ion occurred at interactions A2-B2, A2-C2, and A2-D1, while the highest desorptions are observed at interactions C1-D2, A1-D2, and B1-D2. All interactions show that simultaneously increasing calcium and decreasing chloride ion concentrations in seawater is the optimum way to enhance chloride ion adsorption onto limestone at 90°C in the absence of crude oil.

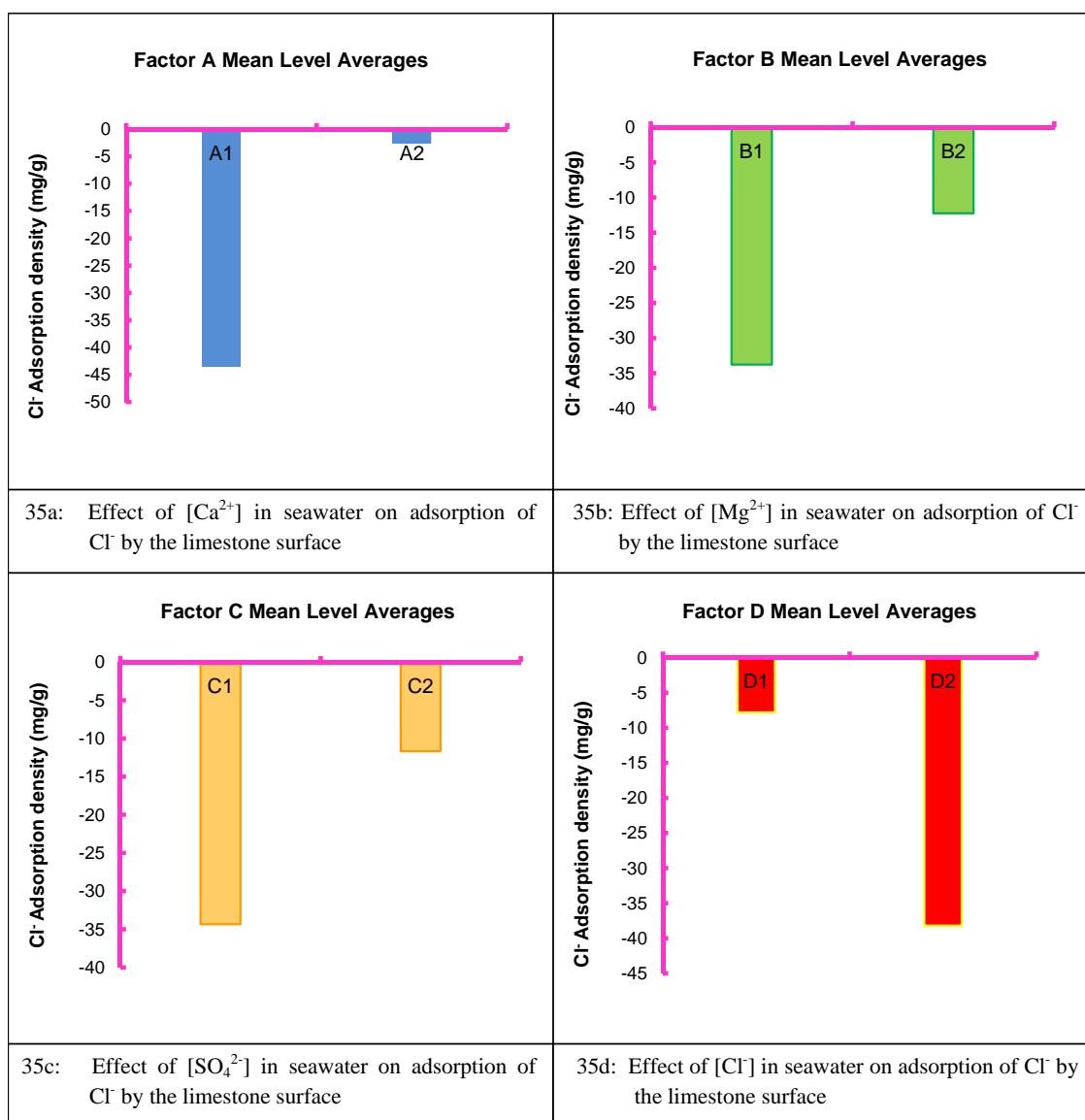


Figure 35: Main effects of $[\text{Ca}^{2+}]$, $[\text{Mg}^{2+}]$, $[\text{SO}_4^{2-}]$, and $[\text{Cl}^-]$ on the adsorption of Cl^- by limestone at 90°C in the absence of crude-oil

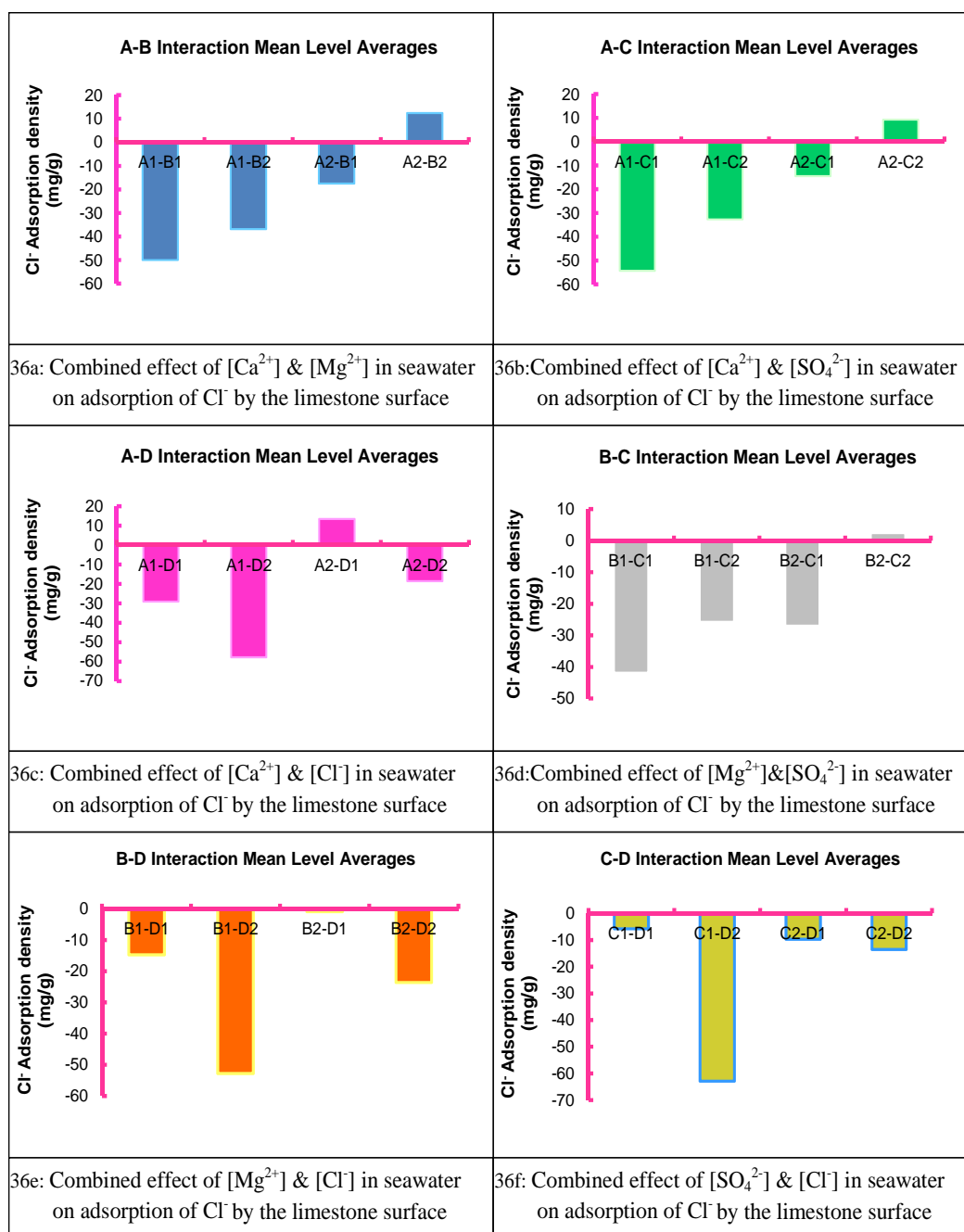


Figure 36: Two-way interactions of [Ca²⁺], [Mg²⁺], [SO₄²⁻], and [Cl⁻] on the adsorption of Cl⁻ by limestone at 90°C in the absence of crude-oil

4.2.1.4 Adsorption of Ca^{2+} , Mg^{2+} , SO_4^{2-} , and Cl^- on Limestone in the presence of crude oil at 90°C

Calcium Ion Interactions

Desorption of calcium ion occurred at all levels of interactions between the ions as Figures 37 and 38 shows. Main effect results in Figure 37 shows that the amount of desorption can be decreased by either increasing the concentrations of calcium and sulfate ions individually or decrease the concentrations of magnesium and chloride ions individually in seawater. The highest desorption of calcium ion from the limestone rock is obtained at low calcium concentration, while the lowest desorption is observed at high calcium concentration as evidenced by effects A1 and A2 respectively. It is observed from the two-factor interactions (Figure 38) that all interactions involving the low concentration of calcium (A1-B1, A1-B2, A1-C1, A1-C2, A1-D1, and A1 - D2) showed relatively high calcium ion desorption, while those involving A2 showed the lowest calcium desorptions. Magnesium ion is also seen to be very influential on calcium ion adsorption by observing that all B1 and B2 interactions demonstrated a relatively low and high calcium ion desorption respectively. Interestingly, the highest and lowest desorptions in the two-factor interactions occurred at A1-B2 and A2-B1 respectively. All evidences confirm that the optimum way to reduce calcium ion desorption and enhance its adsorption onto the limestone at 90°C in the presence of crude oil is to simultaneously increase the calcium ion and decrease the magnesium ions in the injected or surrounding seawater.

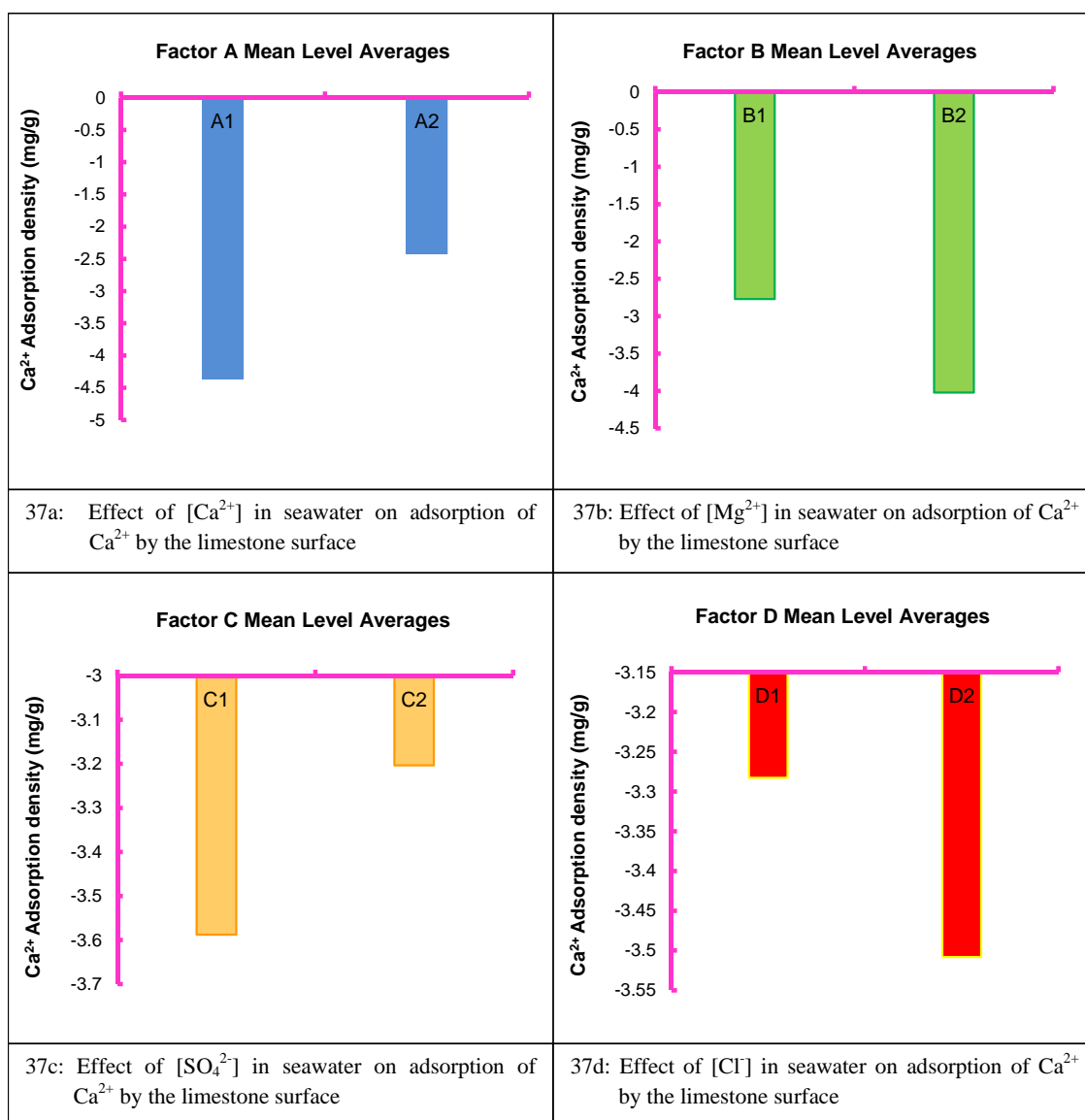


Figure 37: Main effects of [Ca²⁺], [Mg²⁺], [SO₄²⁻], and [Cl⁻] on the adsorption of Ca²⁺ by limestone at 90°C in the presence of crude-oil

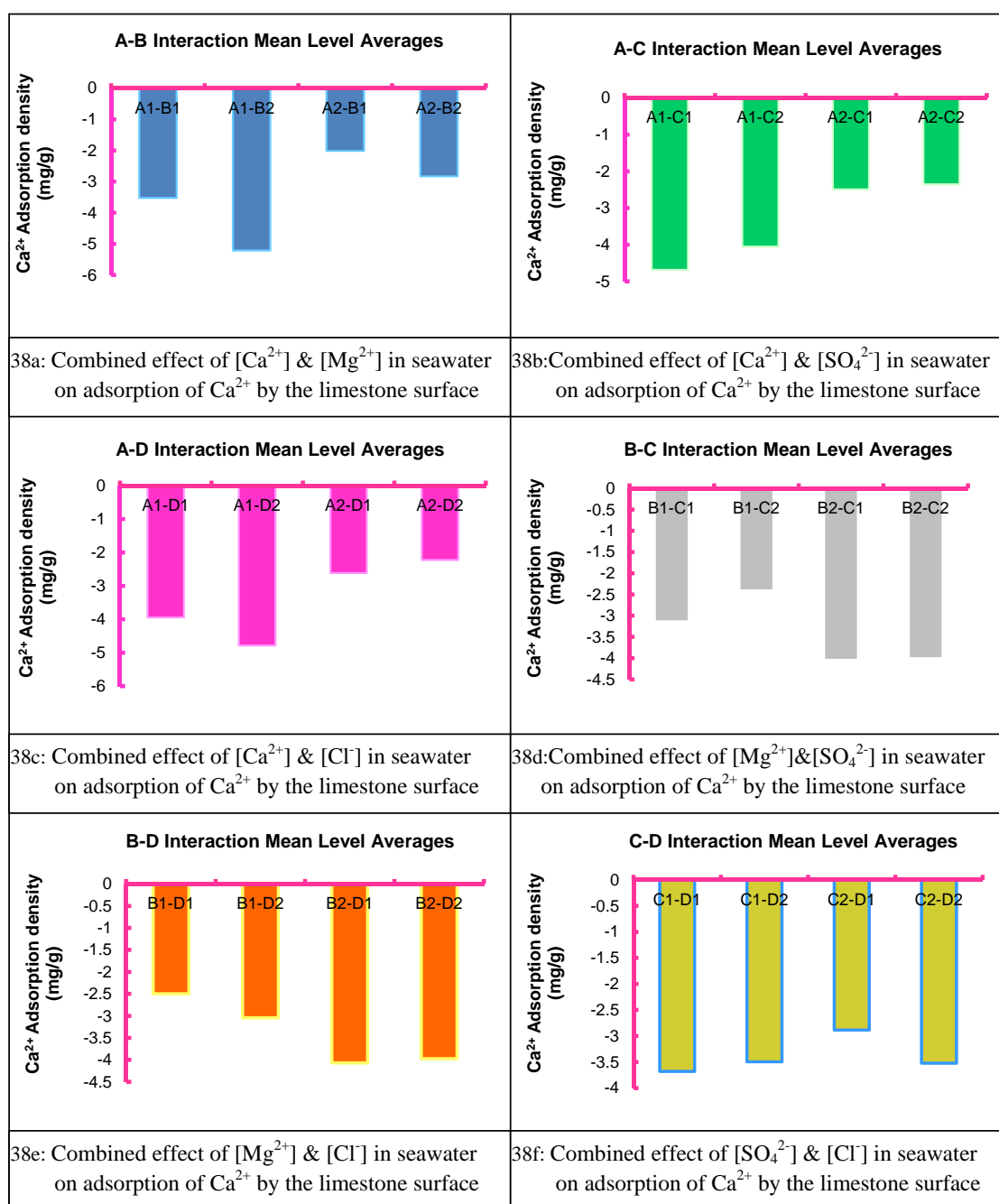


Figure 38: Two-way interactions of [Ca²⁺], [Mg²⁺], [SO₄²⁻], and [Cl⁻] on the adsorption of Ca²⁺ by limestone at 90°C in the presence of crude-oil

Magnesium Ion Interactions

Figures 39 and 40 indicate that all levels of interactions ensured adsorption of magnesium ion onto the limestone powder. It is observed from figure 39 that either a decrease in the individual concentrations of calcium or chloride ions or an increase in the individual concentrations of sulfate or magnesium ions is needed to enhance magnesium adsorption. It is also seen that the highest adsorption of magnesium ion onto the rock is obtained at low calcium concentration, while the lowest adsorption is observed at high calcium concentration as evidenced by effects A1 and A2 respectively, which means that calcium ion concentration in seawater is very important for magnesium ion adsorption. This is also supported by Figure 40, which shows that all the interactions involving A1 and A2 gave the highest and lowest adsorptions of magnesium ions respectively. Increasing the magnesium and sulfate ions in seawater is also seen to promote magnesium ion adsorption, which is reflected in the highest and lowest amounts of magnesium adsorption obtained from interactions A1-B2, and A2-C1 respectively. All these two-factor interactions coupled with the main effects prove that a decrease in calcium ion concentration is very important for promotion of magnesium ion adsorption. The optimum way to enhance magnesium ion adsorption onto limestone at 90°C in the presence of crude oil is to simultaneously decrease the calcium ions and increase either magnesium or sulfate ions in the injected seawater.

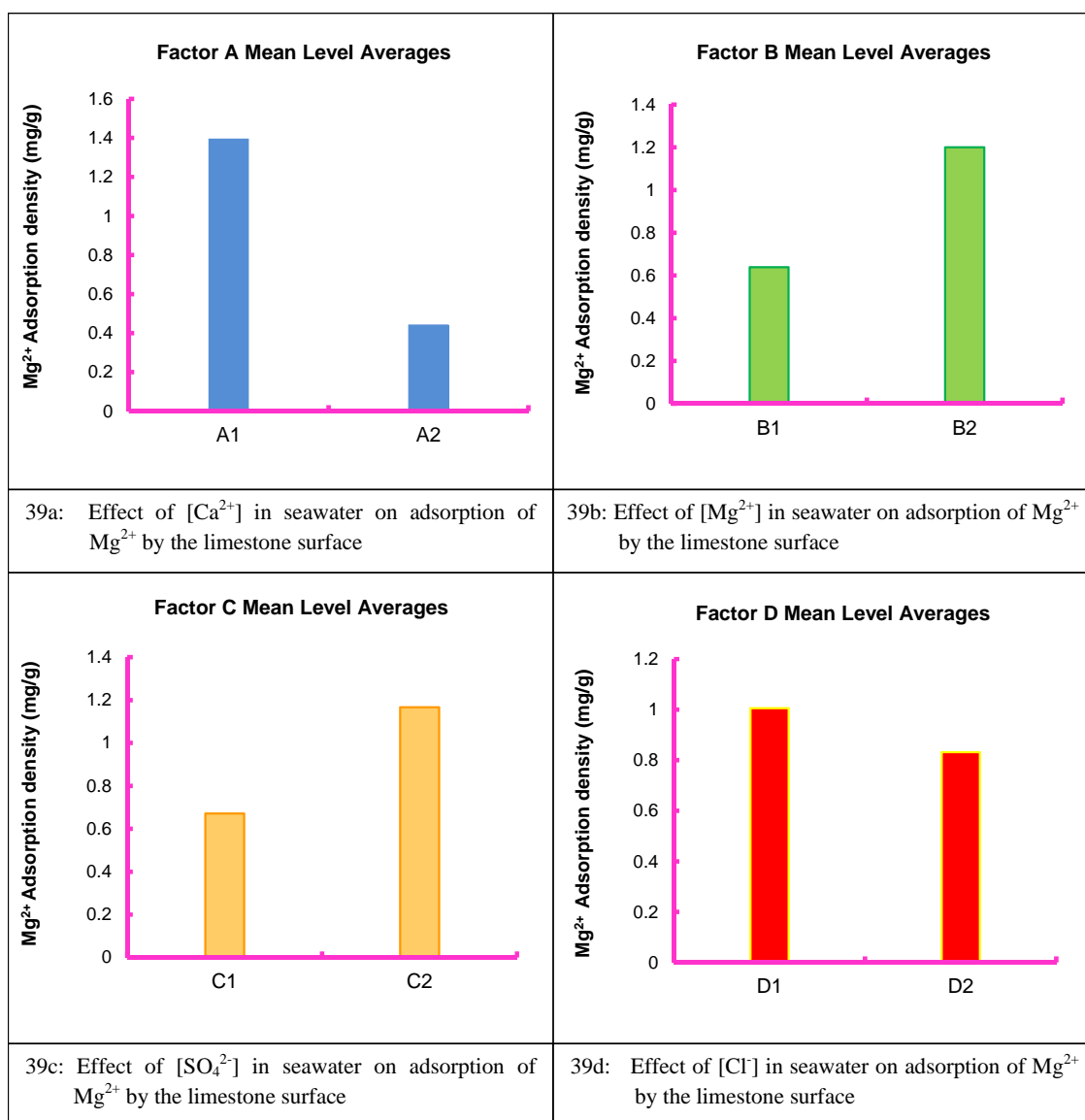


Figure 39: Main effects of $[Ca^{2+}]$, $[Mg^{2+}]$, $[SO_4^{2-}]$, and $[Cl^-]$ on the adsorption of Mg^{2+} by limestone at 90°C in the presence of crude-oil

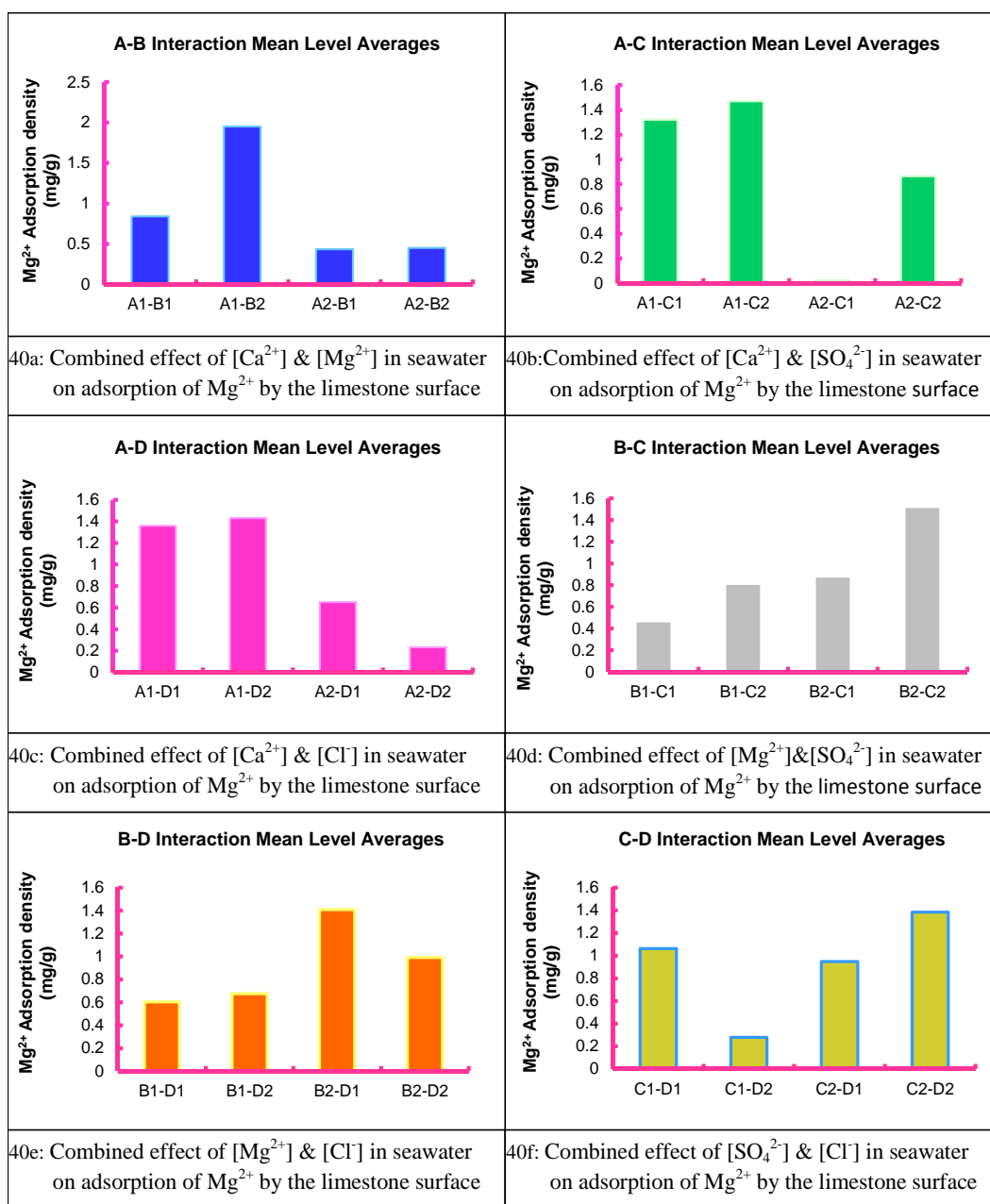


Figure 40: Two-way interactions of [Ca²⁺], [Mg²⁺], [SO₄²⁻], and [Cl⁻] on the adsorption of Mg²⁺ by limestone at 90°C in the presence of crude-oil

Sulfate Ion Interactions

The main effect results presented in Figure 41 shows that decreasing the concentrations of either sulfate or calcium ions in seawater will increase sulfate ion desorption from the limestone, while magnesium and chloride ions show the opposite effect. The two-factor interactions presented in Figure 42 highlights the significance of calcium and sulfate ions in seawater. It is observed that all interactions of C2 (A1-C2, A2-C2, B2-C2, B1-C2, C2-D1, and C2-D2) and A2 (A2-B1, A2-B2, A2-C1, A2-C2, A2-D1, A2-D2) showed relatively the lowest desorptions of sulfate ion, while the highest desorption is observed at interaction A1-C1. Adsorption of sulfate ions are observed at interactions A2-D1, and A2-B2, which means an increase in calcium ions will significantly enhance sulfate adsorption. However, the impact of calcium and sulfate ions appears to be very similar from both the main effects and interactions A1-C2, and A2-C1. A decrease in chloride ion concentration in the seawater will also assure sulfate adsorption as seen from interaction A2-D1 (Figure 42c), which showed the highest adsorption. From the foregoing discussion, we can conclude that the optimum way to enhance sulfate ion adsorption onto limestone at 90°C in the presence of crude oil is to increase both calcium and sulfate ions, and decrease chloride ions in the injected seawater.

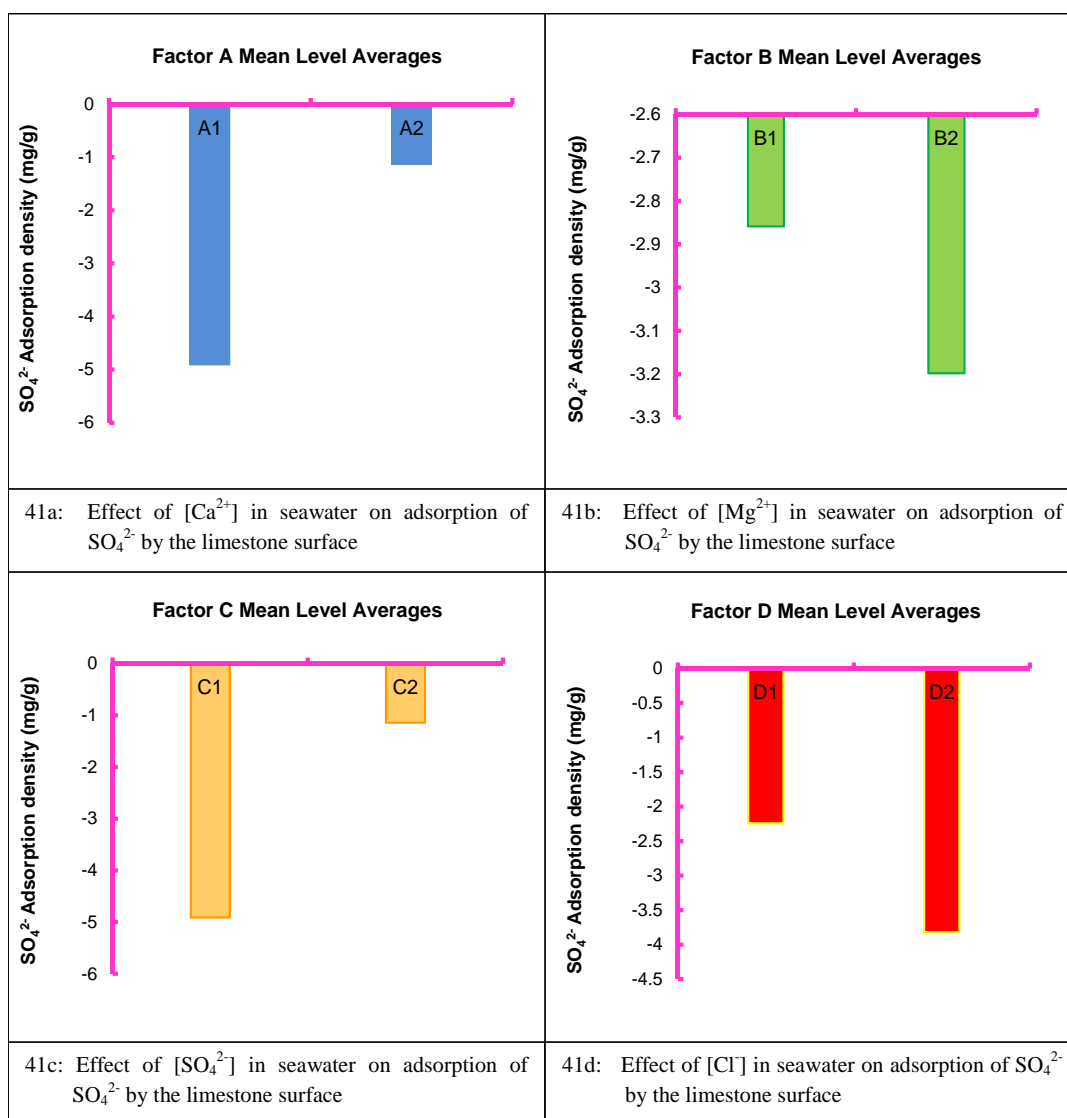


Figure 41: Main effects of [Ca²⁺], [Mg²⁺], [SO₄²⁻], and [Cl⁻] on the adsorption of SO₄²⁻ by limestone at 90°C in the presence of crude-oil

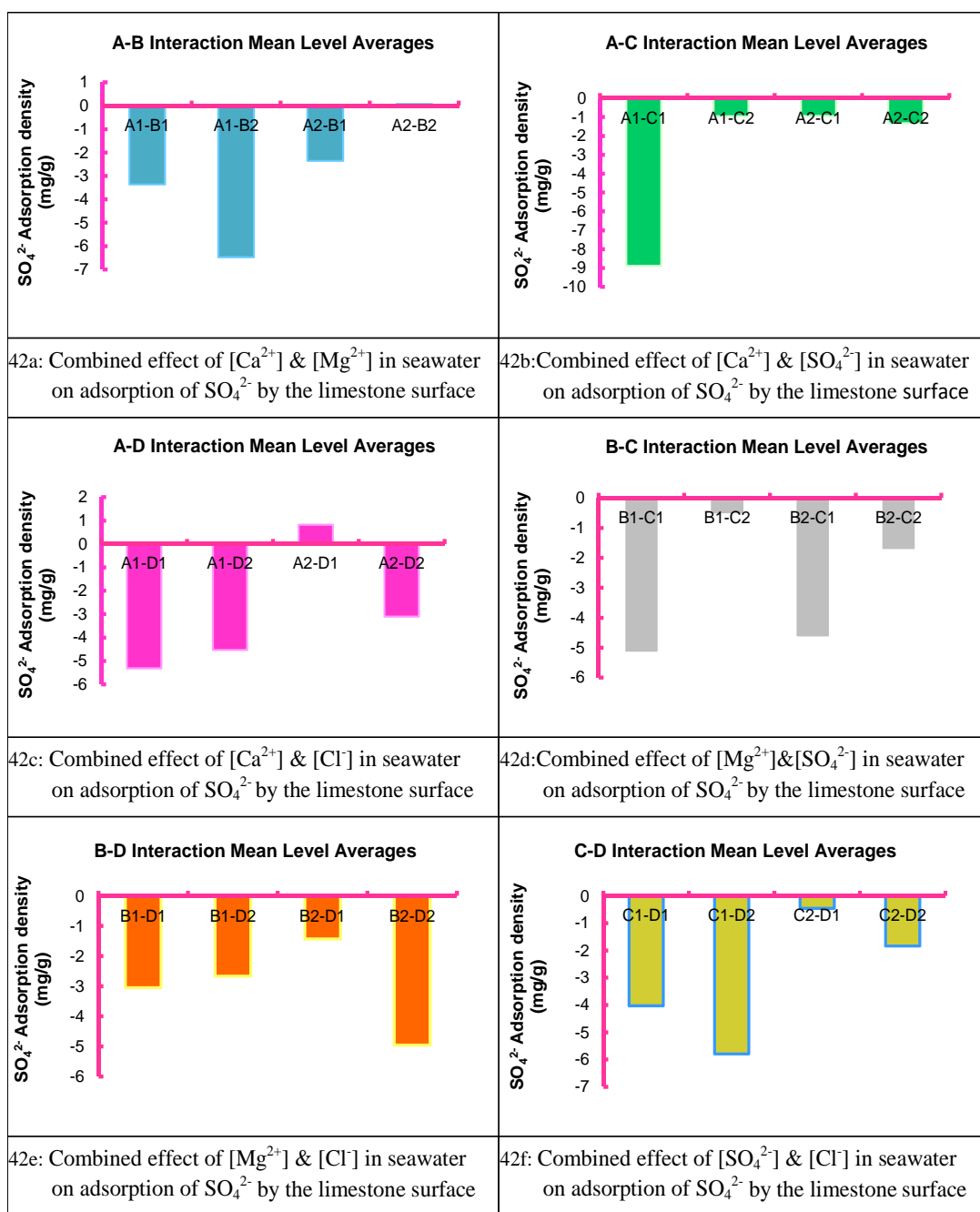


Figure 42: Two-way interactions of [Ca²⁺], [Mg²⁺], [SO₄²⁻], and [Cl⁻] on the adsorption of SO₄²⁻ by limestone at 90°C in the presence of crude-oil

Chloride Ion Interactions

The main effects results presented in Figure 43 indicate that chloride ion desorption can be decreased by either increasing individually the concentrations of calcium, magnesium, and sulfate ions or decreasing chloride ion concentration in seawater. The observed desorptions of Cl^- can be related to the dissolution of halite or any other Cl^- containing compound from the rock. The highest desorption of chloride ion is obtained at low concentration of sulfate ion (C1), while the lowest desorption of chloride ion from the limestone rock surface is at high sulfate ion concentration (C2), indicating that sulfate ion could play a significant role in chloride ion adsorption. Figure 44 which shows the two-factor interactions indicates that the highest desorptions of chloride ion are obtained from interactions involving A1 and C1 (A1-B1, A1-B2, A1-C1, A1-D1, B1-C1, and C1-D2), the highest being A1-C1. Conversely, all interactions with the highest adsorptions of chloride ion involve A2 and C2 (A2-B2, A1-C2, A2-C1, A2-D1, and B1-C2). Thus, we can conclude that chloride ion adsorption onto limestone at 90°C in the presence of crude oil can be enhanced by increasing both sulfate and calcium ions in the injected seawater.

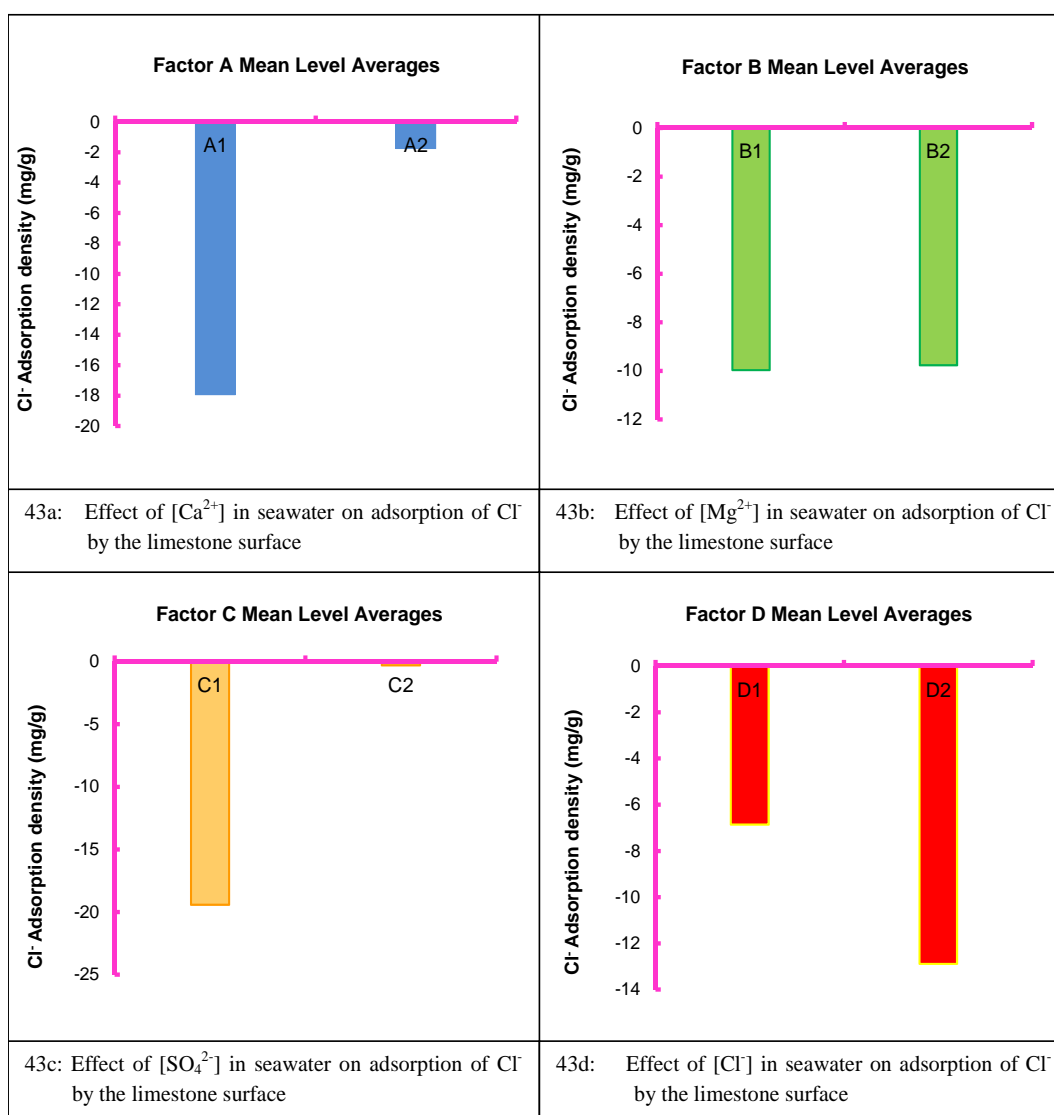


Figure 43: Main effects of $[Ca^{2+}]$, $[Mg^{2+}]$, $[SO_4^{2-}]$, and $[Cl^-]$ on the adsorption of Cl^- by limestone at $90^{\circ}C$ in the presence of crude-oil

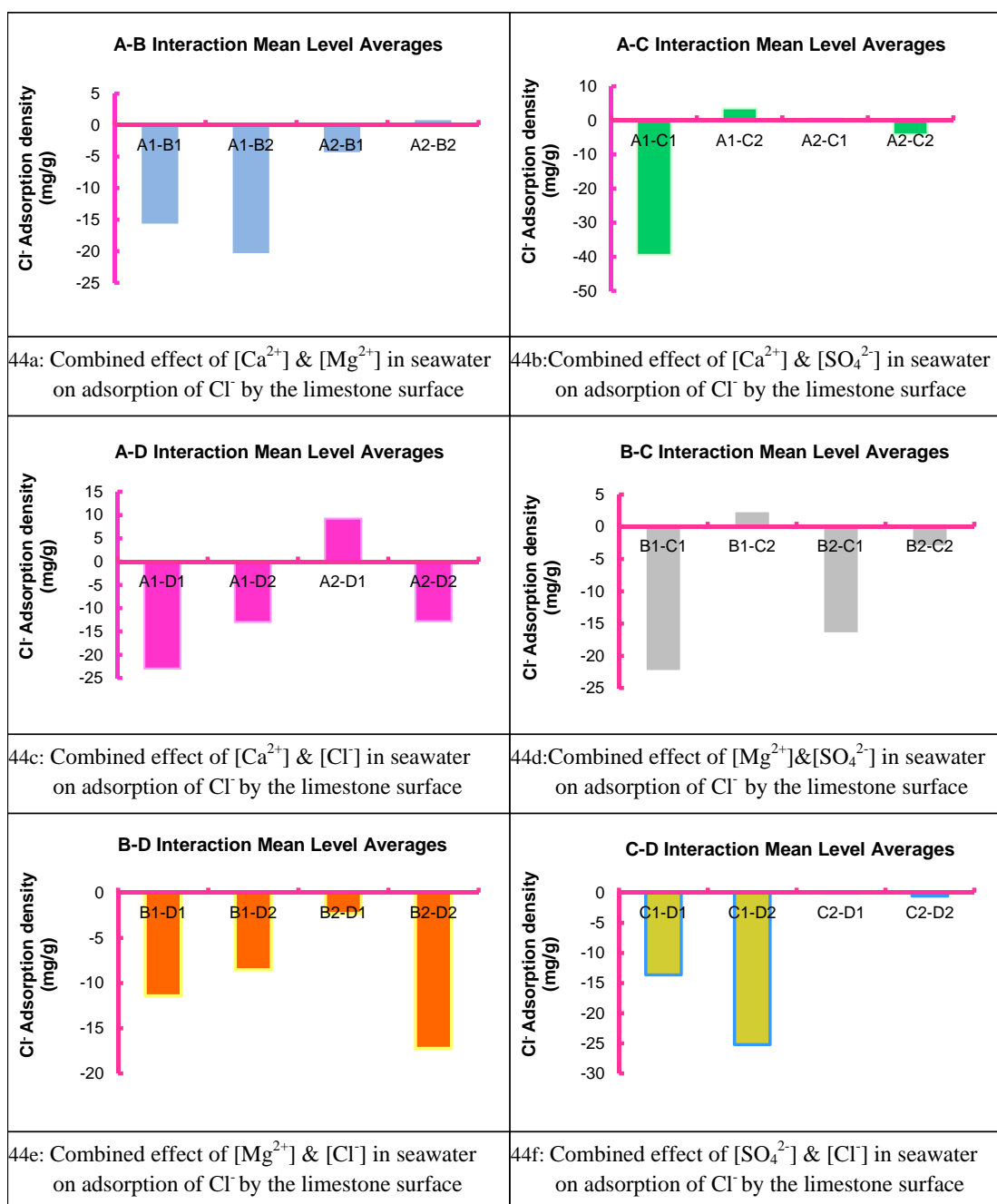


Figure 44: Two-way interactions of $[Ca^{2+}]$, $[Mg^{2+}]$, $[SO_4^{2-}]$, and $[Cl^-]$ on the adsorption of Cl^- by limestone at 90°C in the presence of crude-oil

4.2.1.5 Impact of crude oil on the adsorption of Ca^{2+} , Mg^{2+} , SO_4^{2-} , and Cl^- on Limestone at 25°C

Having presented adsorption results in the presence and absence of crude oil at 25°C and 90°C, it is imperative to identify the effect of crude oil on the ionic interactions at these temperatures, taking the interactions in the absence of crude oil as a base case.

Calcium Ion Interactions

Figures 45 and 46 compares the main effects and two-way interactions respectively of Ca^{2+} , Mg^{2+} , SO_4^{2-} , and Cl^- concentrations in seawater on the adsorption of Ca^{2+} onto limestone in the absence and presence of crude oil at 25°C. It can be observed from both figures that more calcium goes into solution in the presence of oil than in its absence in all interactions. In otherwords, it can imply that there is less adsorption of calcium ion when crude oil is present than in its absence. This is probably due to less access of the calcium ion to the limestone in the presence of oil. Increase of calcium ion concentration in seawater will significantly trigger the adsorption of calcium ions onto limestone both in the absence and presence of crude oil at 25°C.

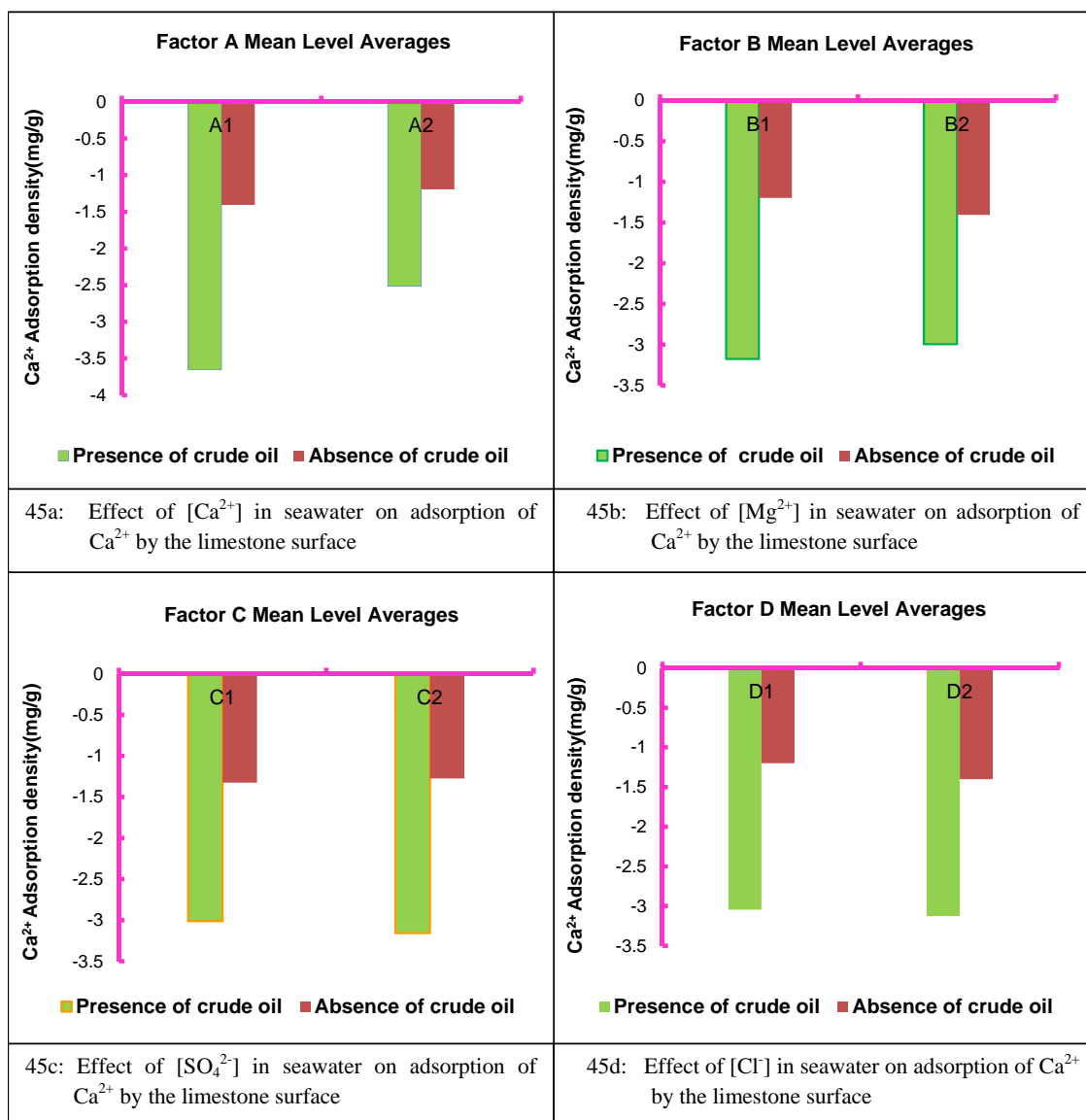


Figure 45: Main effects of $[Ca^{2+}]$, $[Mg^{2+}]$, $[SO_4^{2-}]$, and $[Cl^-]$ on the adsorption of Ca^{2+} by limestone at 25°C in the absence and presence of crude-oil

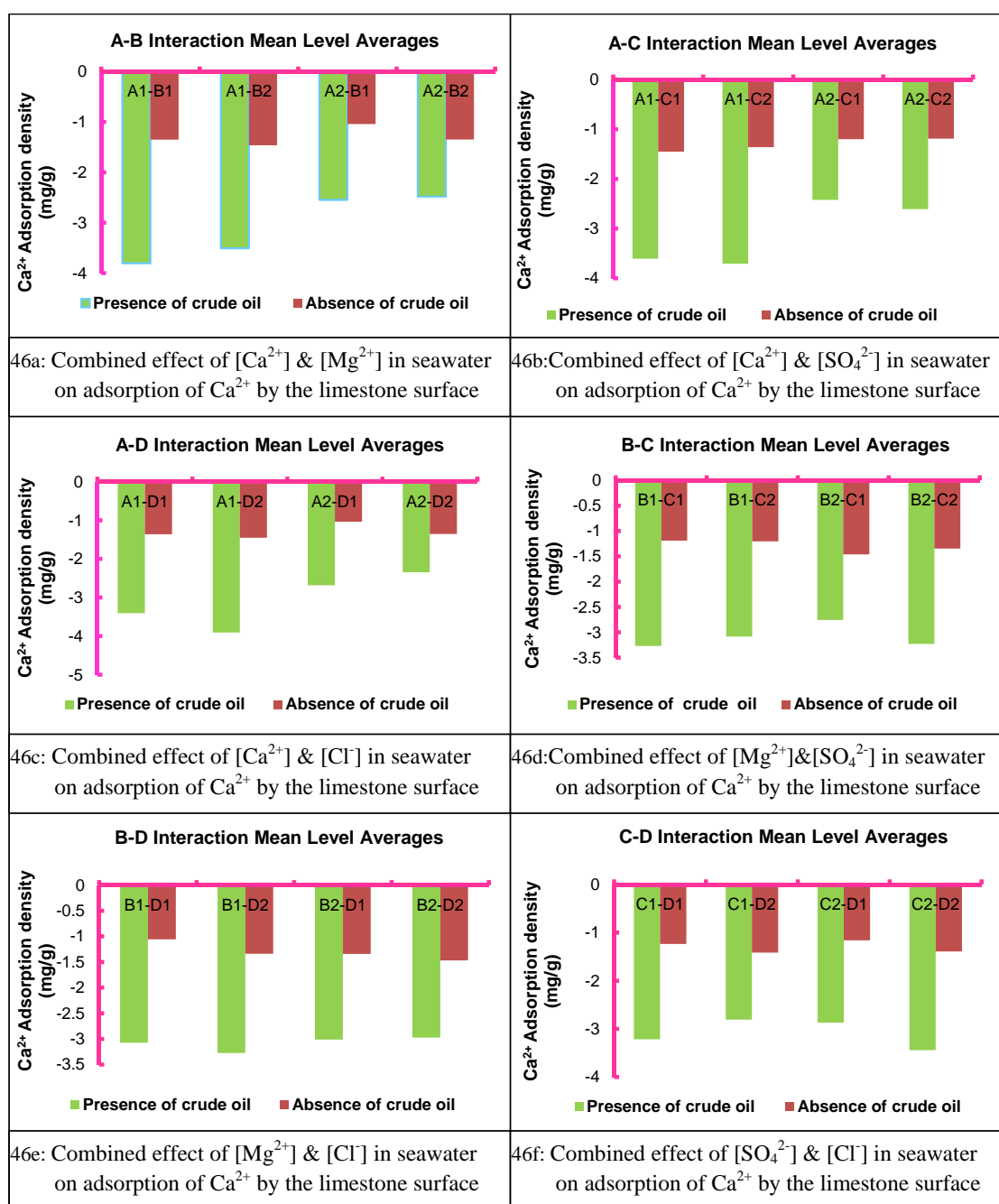


Figure 46: Two-way interactions of [Ca²⁺], [Mg²⁺], [SO₄²⁻], and [Cl⁻] on the adsorption of Ca²⁺ by limestone at 25°C in the absence and presence of crude-oil

Magnesium Ion Interactions

Figures 47 and 48 generally show that there is more adsorption of magnesium ions onto limestone in the absence of crude-oil than in its presence. This is again due to the fact that the ions have better access to the rock when crude-oil is not present. The presence of crude oil will prevent direct contact of magnesium ions with the limestone rock, thereby reducing its adsorption rate. While magnesium adsorption onto limestone in the absence of crude oil can be enhanced by decreasing chloride and calcium ion concentrations, decreasing chloride and sulfate ions in seawater seem to be the optimum condition for magnesium adsorption in the presence of crude oil. Chloride ion is a common factor to both cases.

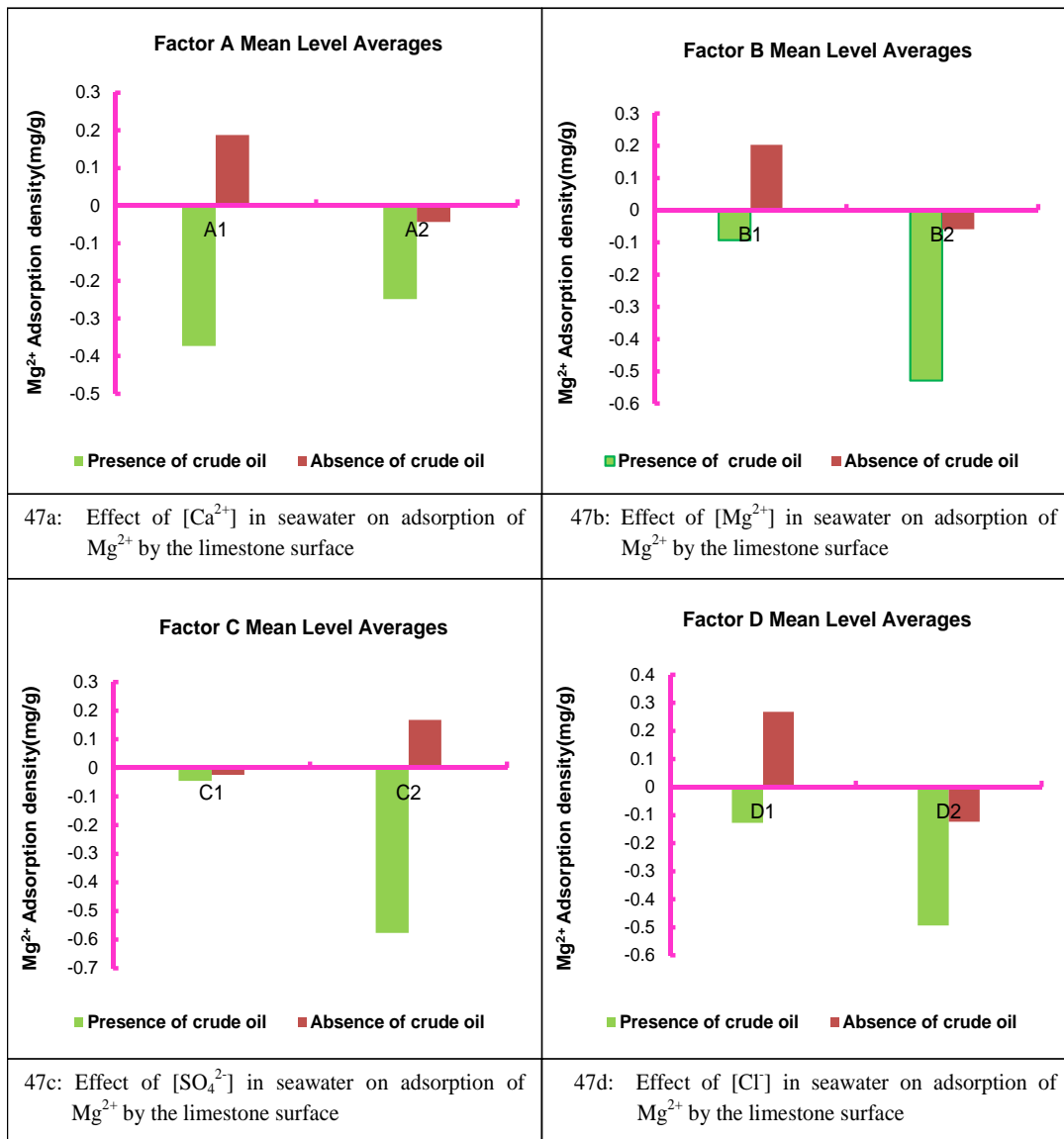


Figure 47: Main effects of $[Ca^{2+}]$, $[Mg^{2+}]$, $[SO_4^{2-}]$, and $[Cl^-]$ on the adsorption of Mg^{2+} by limestone at 25°C in the absence and presence of crude-oil

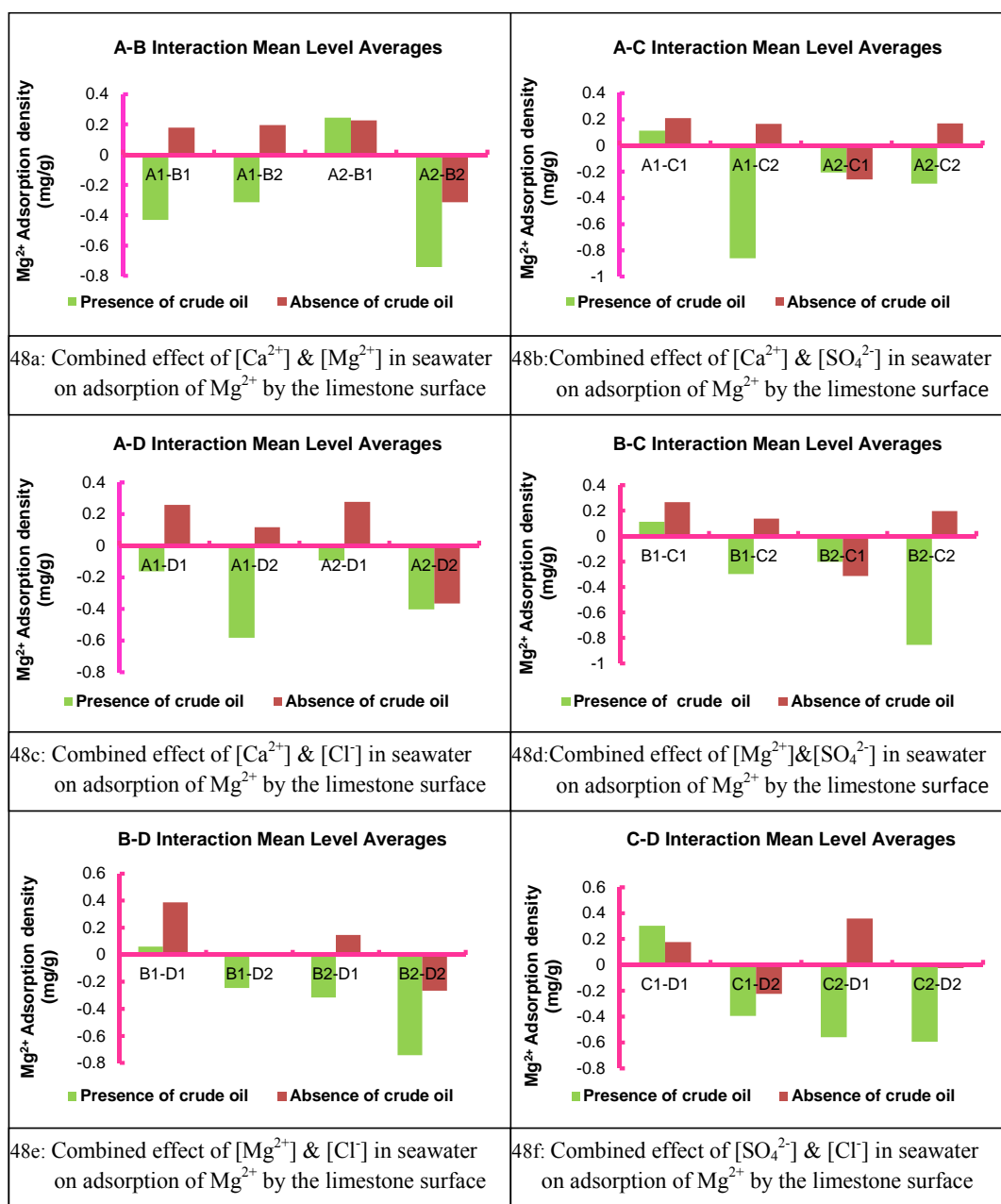


Figure 48: Two-way interactions of [Ca²⁺], [Mg²⁺], [SO₄²⁻], and [Cl⁻] on the adsorption of Mg²⁺ by limestone at 25°C in the absence and presence of crude-oil

Sulfate Ion Interactions

Figures 49 and 50 shows the effect of crude oil on sulfate adsorption onto limestone at 25°C in the presence and absence of crude oil. While all the interactions show desorption of sulfate ion, it is generally observed that the desorption is much higher in the presence of crude oil than in its absence. This means that the possibility of adsorption of sulfate ion would be much higher in the absence of crude oil than in its presence. This is due to less access of the sulfate ion to the limestone rock in the presence of crude-oil. The crude oil forms a thick coat around the limestone, thereby inhibiting direct contact of ions with the powder. However, both cases commonly identify calcium ion as the most significant ion for sulfate ion adsorption. Decreasing Ca^{2+} concentration in seawater will seriously impede adsorption of SO_4^{2-} onto limestone at 25°C in the absence and presence of crude oil.

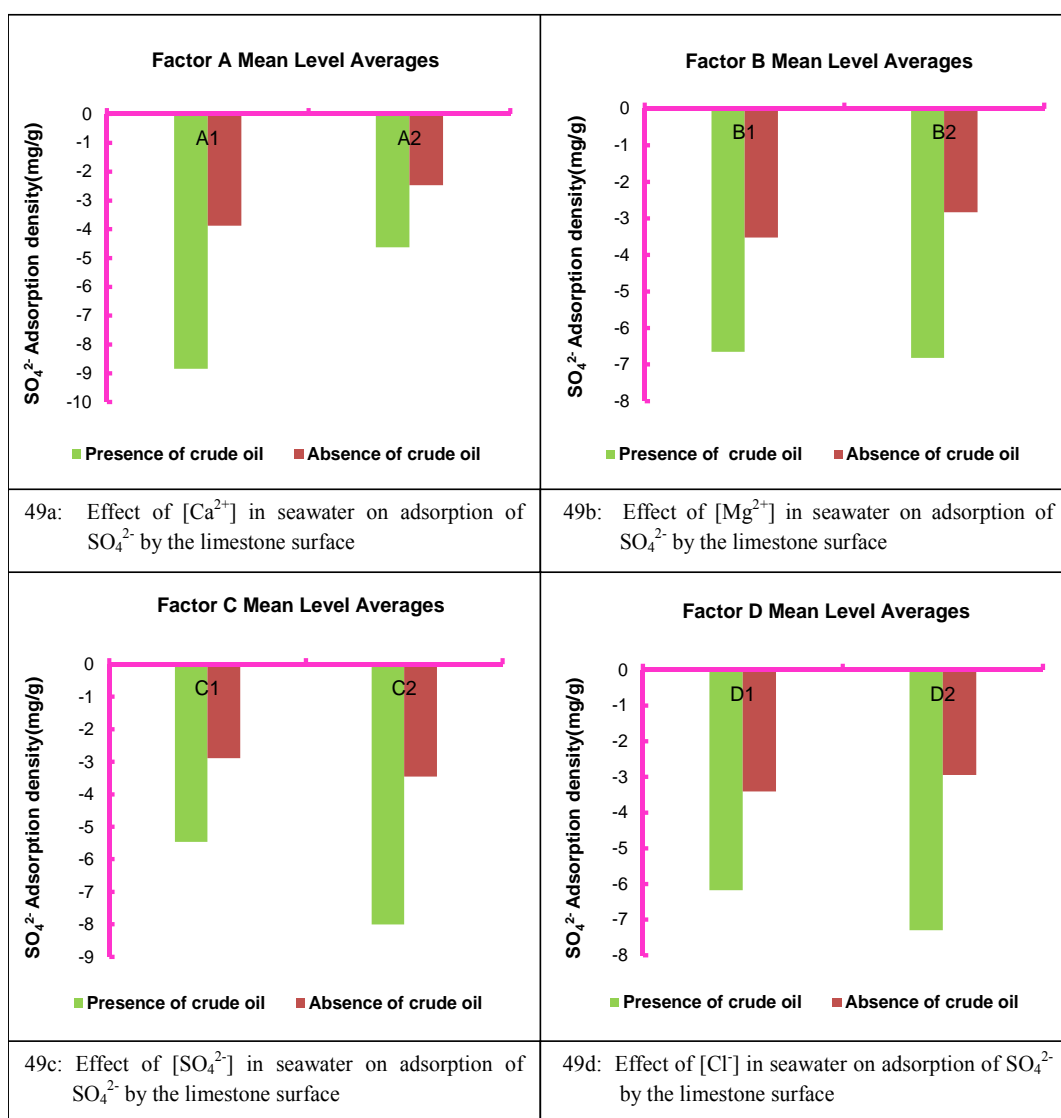


Figure 49: Main effects of $[\text{Ca}^{2+}]$, $[\text{Mg}^{2+}]$, $[\text{SO}_4^{2-}]$, and $[\text{Cl}^-]$ on the adsorption of SO_4^{2-} by limestone at 25°C in the absence and presence of crude-oil

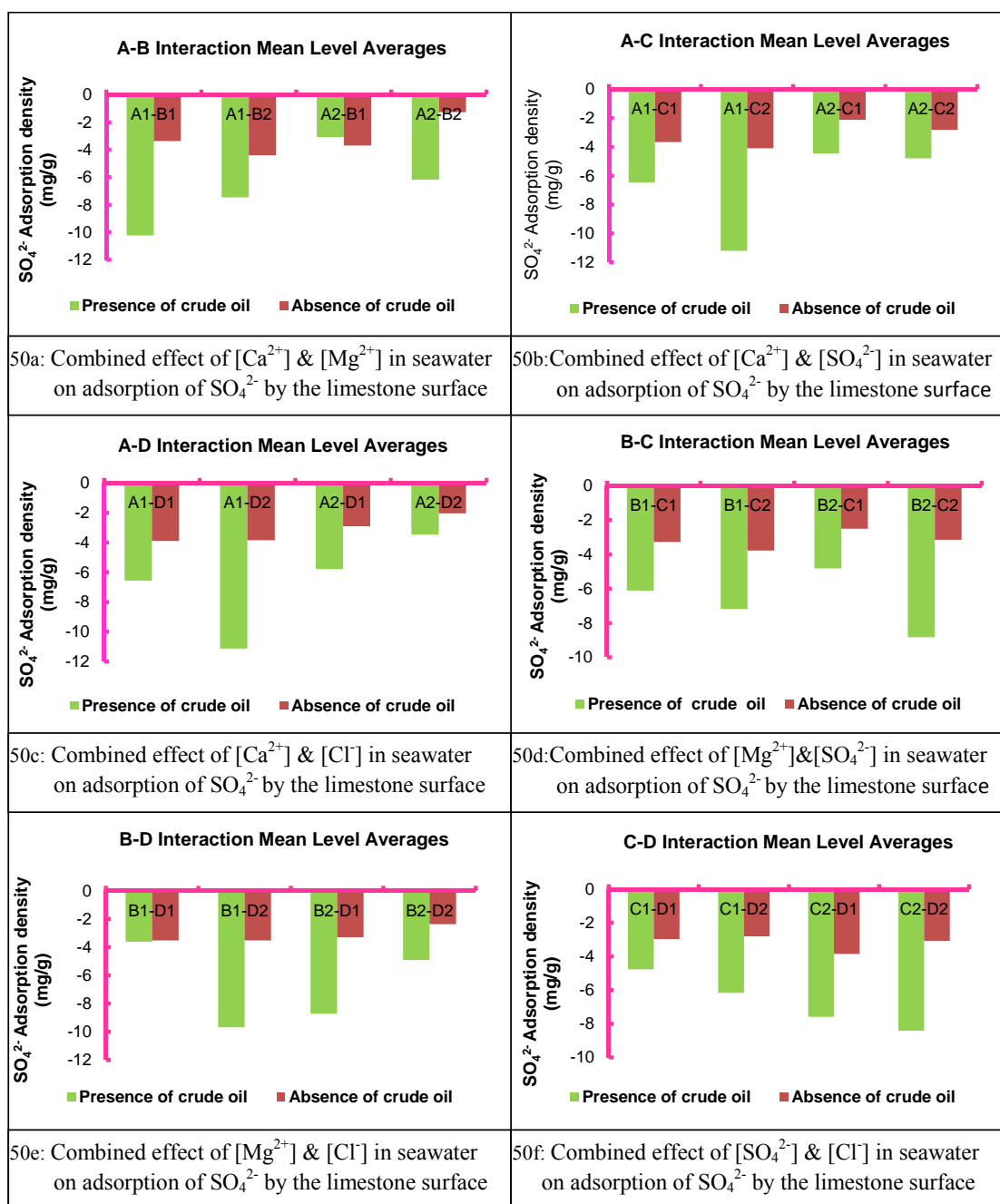


Figure 50: Two-way interactions of [Ca²⁺], [Mg²⁺], [SO₄²⁻], and [Cl⁻] on the adsorption of SO₄²⁻ by limestone at 25°C in the absence and presence of crude-oil

Chloride Ion Interactions

Figures 51 and 52 show that there is a significant difference in the amount of chloride desorbed from the limestone surface in the absence and presence of crude oil. More desorption in the presence of crude oil means that adsorption of chloride ion will be more in the absence of crude oil. This is the same observation with calcium, magnesium, and sulfate ions. It is due to less access of the chloride ion to the limestone powder in the presence of crude-oil. While chloride adsorption onto limestone in the absence of crude oil can be enhanced by increasing chloride and calcium ion concentrations, increasing calcium ions only in seawater seem to be the optimum condition for chloride adsorption in the presence of crude oil. Calcium ion is a common factor to both cases.

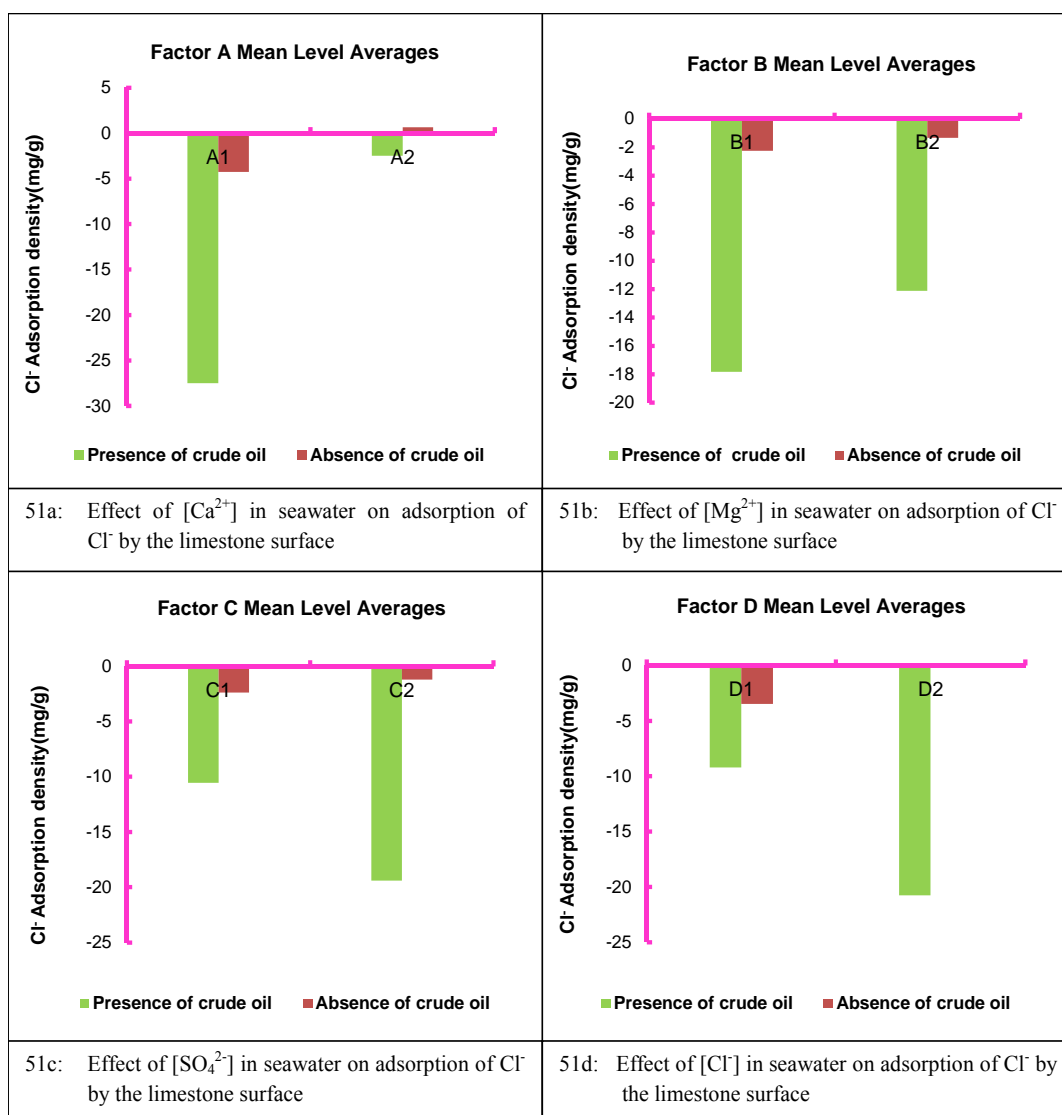


Figure 51: Main effects of [Ca²⁺], [Mg²⁺], [SO₄²⁻], and [Cl⁻] on the adsorption of Cl⁻ by limestone at 25°C in the absence and presence of crude-oil

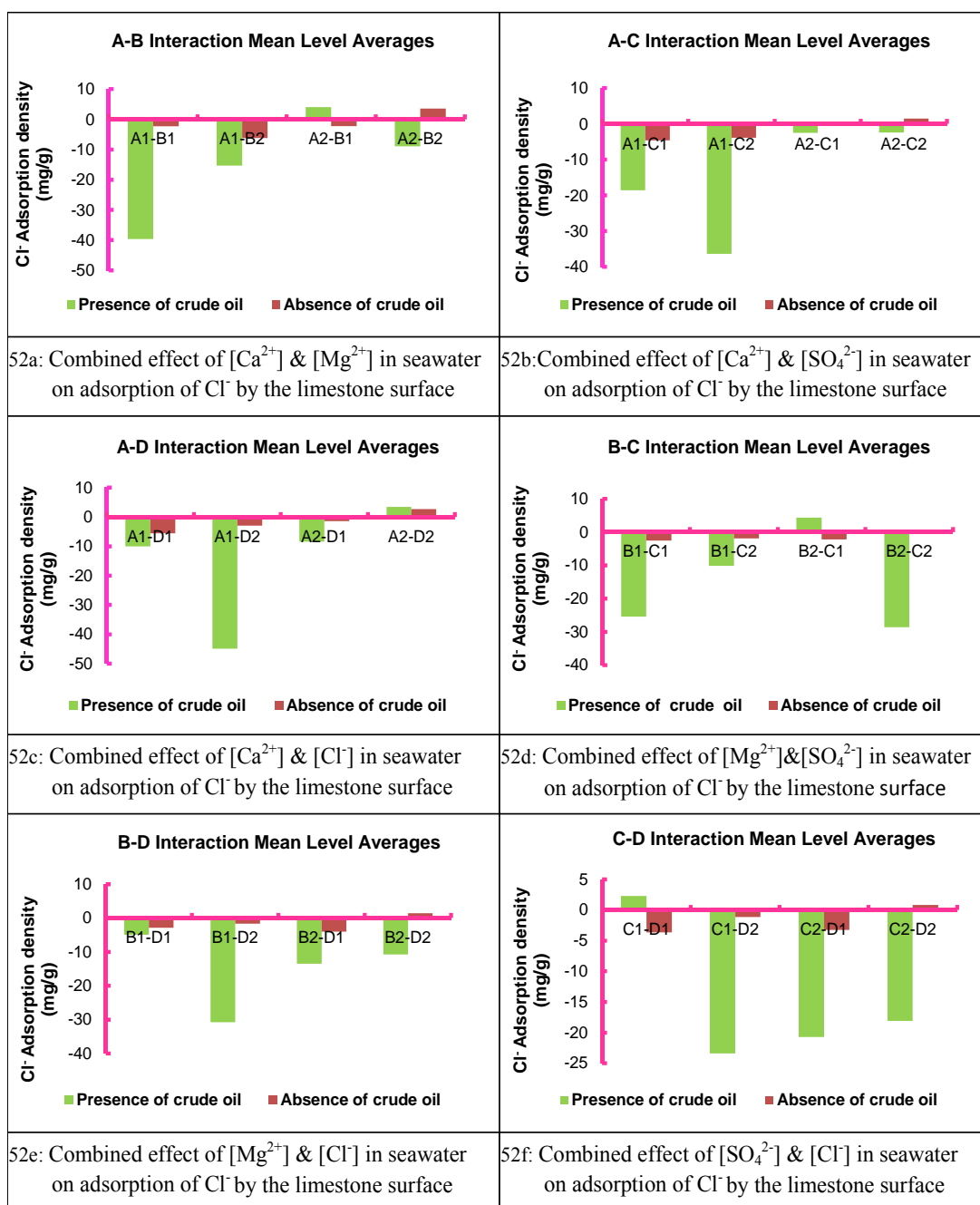


Figure 52: Two-way interactions of [Ca²⁺], [Mg²⁺], [SO₄²⁻], and [Cl⁻] on the adsorption of Cl⁻ by limestone at 25°C in the absence and presence of crude-oil

4.2.1.6 Impact of crude oil on the adsorption of Ca^{2+} , Mg^{2+} , SO_4^{2-} , and Cl^- on Limestone at 90°C

Calcium Ion Interactions

Although all interactions in the absence and presence of crude oil at 90°C show desorption of calcium ions, no significant difference is observed, as can be seen from Figures 53 and 54. This might be due to the impact of high temperature which increased the access of the ions to the limestone powder in the presence of crude oil. Unlike at 25°C, it was actually observed that the crude oil coating of the limestone powder was significantly reduced or even eliminated in some samples after conditioning at 90°C. While calcium ion adsorption onto limestone in the absence of crude oil can be significantly enhanced by increasing calcium ion concentrations alone, increasing calcium ions while reducing magnesium ions in seawater is the optimum condition for calcium adsorption in the presence of crude oil. Calcium ion concentration is commonly important in both the absence and presence of crude oil.

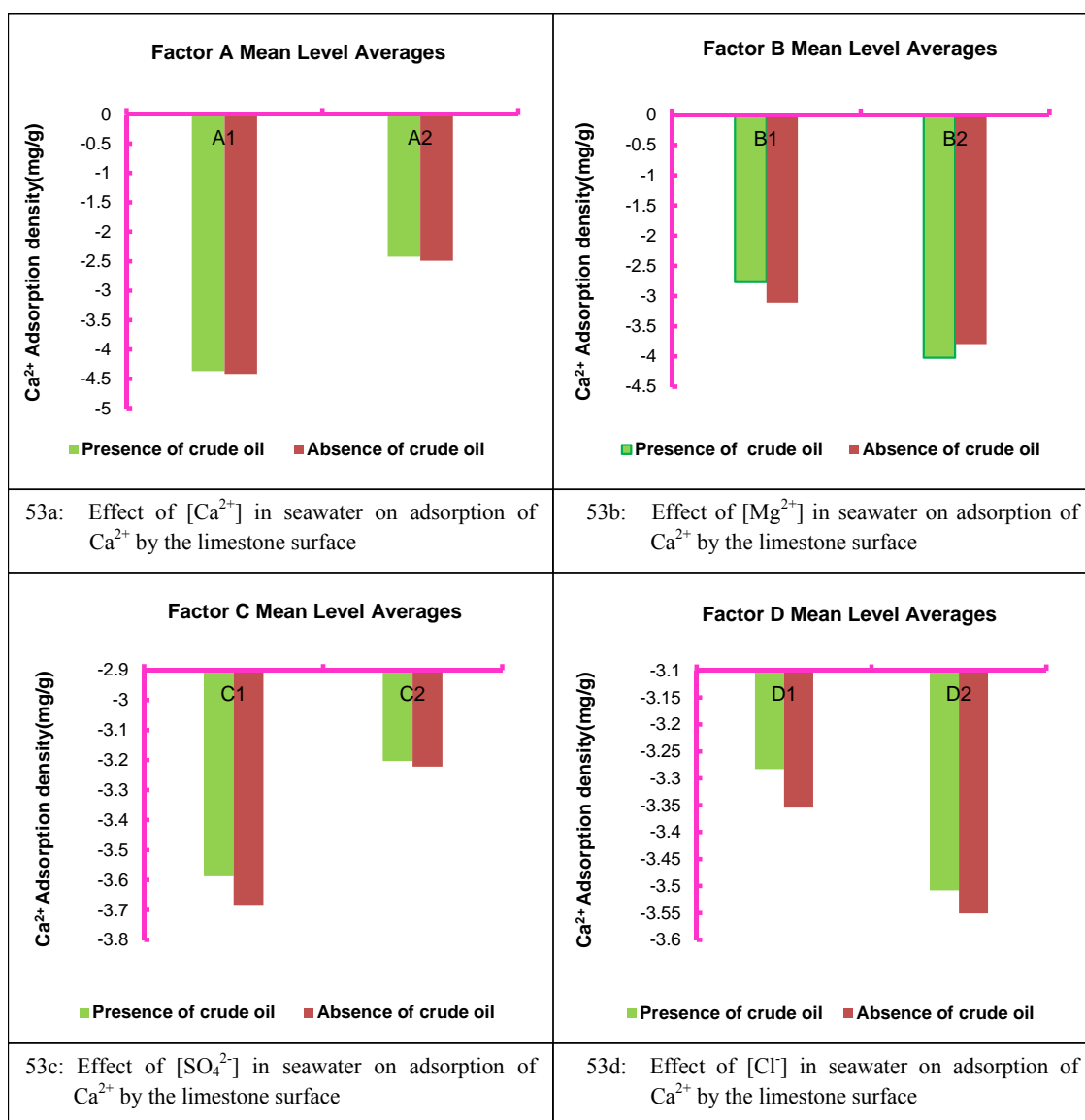


Figure 53: Main effects of $[Ca^{2+}]$, $[Mg^{2+}]$, $[SO_4^{2-}]$, and $[Cl^-]$ on the adsorption of Ca^{2+} by limestone at $90^{\circ}C$ in the absence and presence of crude-oil

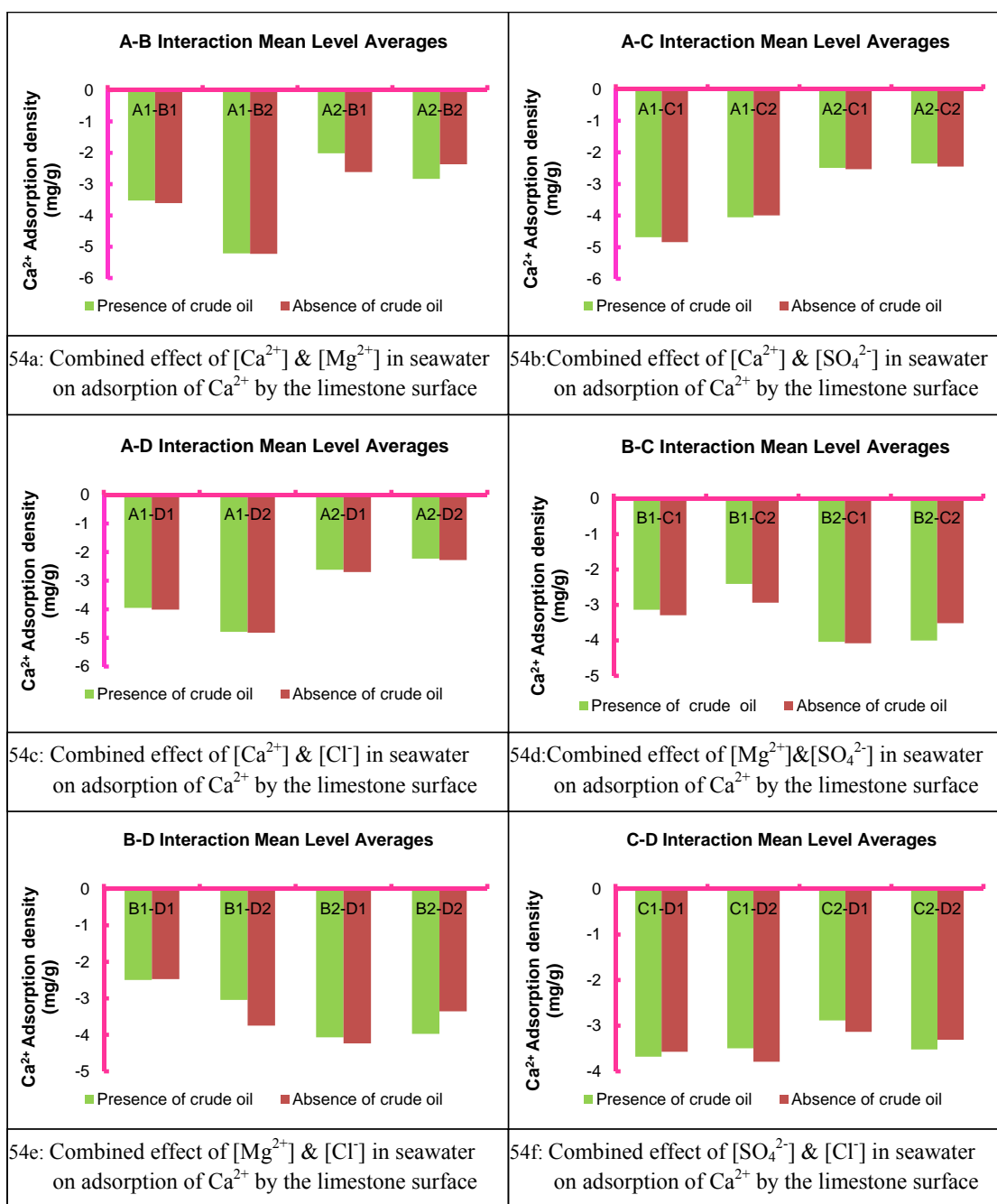


Figure 54: Two-way interactions of [Ca²⁺], [Mg²⁺], [SO₄²⁻], and [Cl⁻] on the adsorption of Ca²⁺ by limestone at 90°C in the absence and presence of crude-oil

Magnesium Ion Interactions

Although only adsorption of magnesium ions is observed in the absence and presence of crude oil, comparing magnesium ion interactions at 90°C seems to be very complex, with significant differences, as observed in Figures 55 and 56. However, a closer look at these figures show a particular trend. The main effects in Figure 55 seems to indicate that at low concentrations of all the ions, more magnesium ions are adsorbed in the presence of crude-oil. Contrary to this, high concentrations of ions ensure a higher adsorption of magnesium ions in the absence of crude oil. The two-factor interactions of A1-C1, A2-C2, A1-D1, A2-D2, B1-D1, B2-D2, C1-D1, and C2-D2 also confirm the same trend, that is, at low concentrations of ions, more magnesium ion is adsorbed in the presence of crude-oil, while at high concentrations, less magnesium ion is adsorbed in the presence of crude-oil. The reason for this behaviour is not known and may require further investigation if deemed necessary. While sulfate ions seem to be the catalyst for magnesium adsorption in the absence of oil, calcium ion is the most important ion to ensure magnesium ion adsorption in the presence of crude oil.

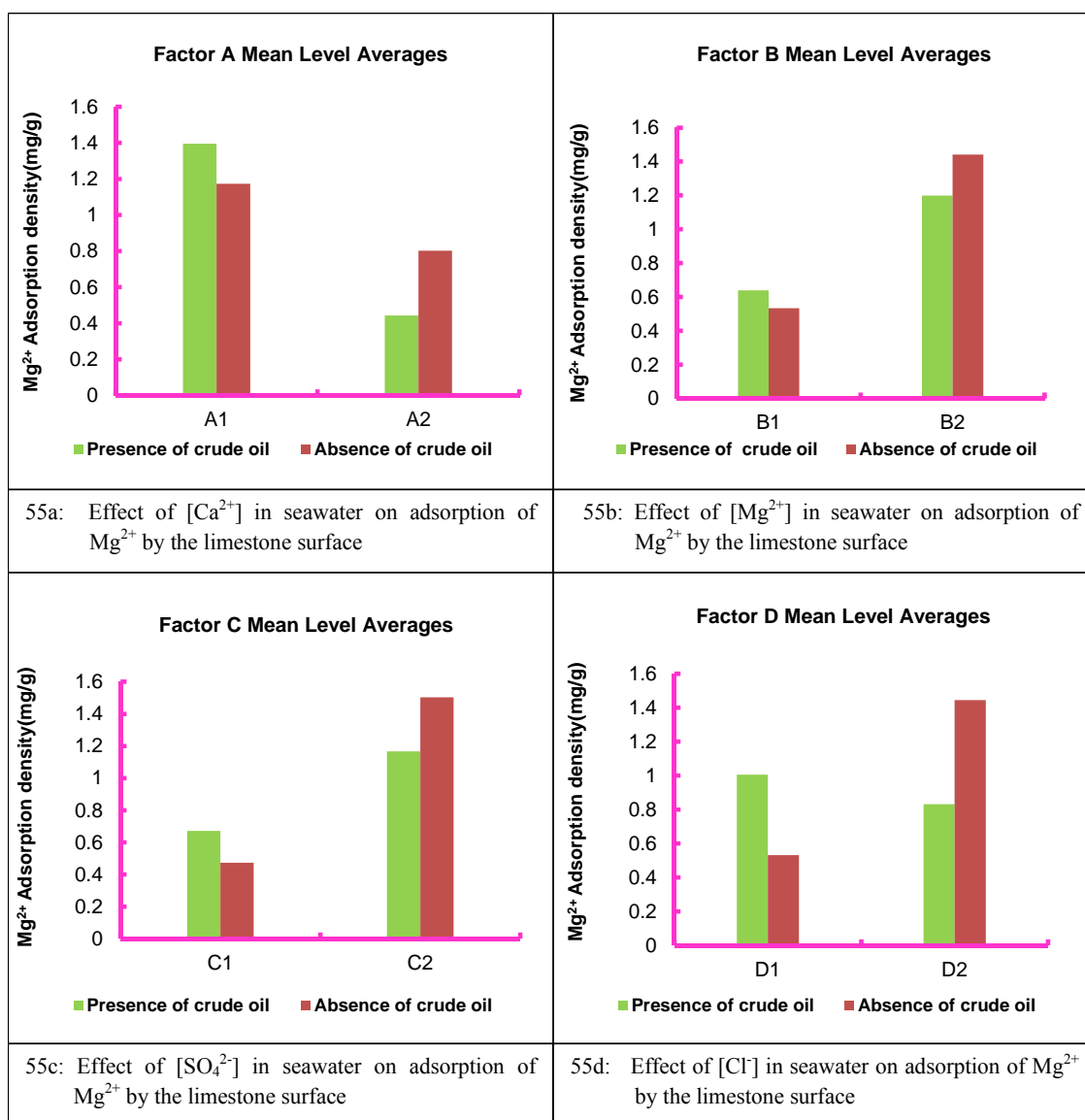


Figure 55: Main effects of [Ca²⁺], [Mg²⁺], [SO₄²⁻], and [Cl⁻] on the adsorption of Mg²⁺ by limestone at 90°C in the absence and presence of crude-oil

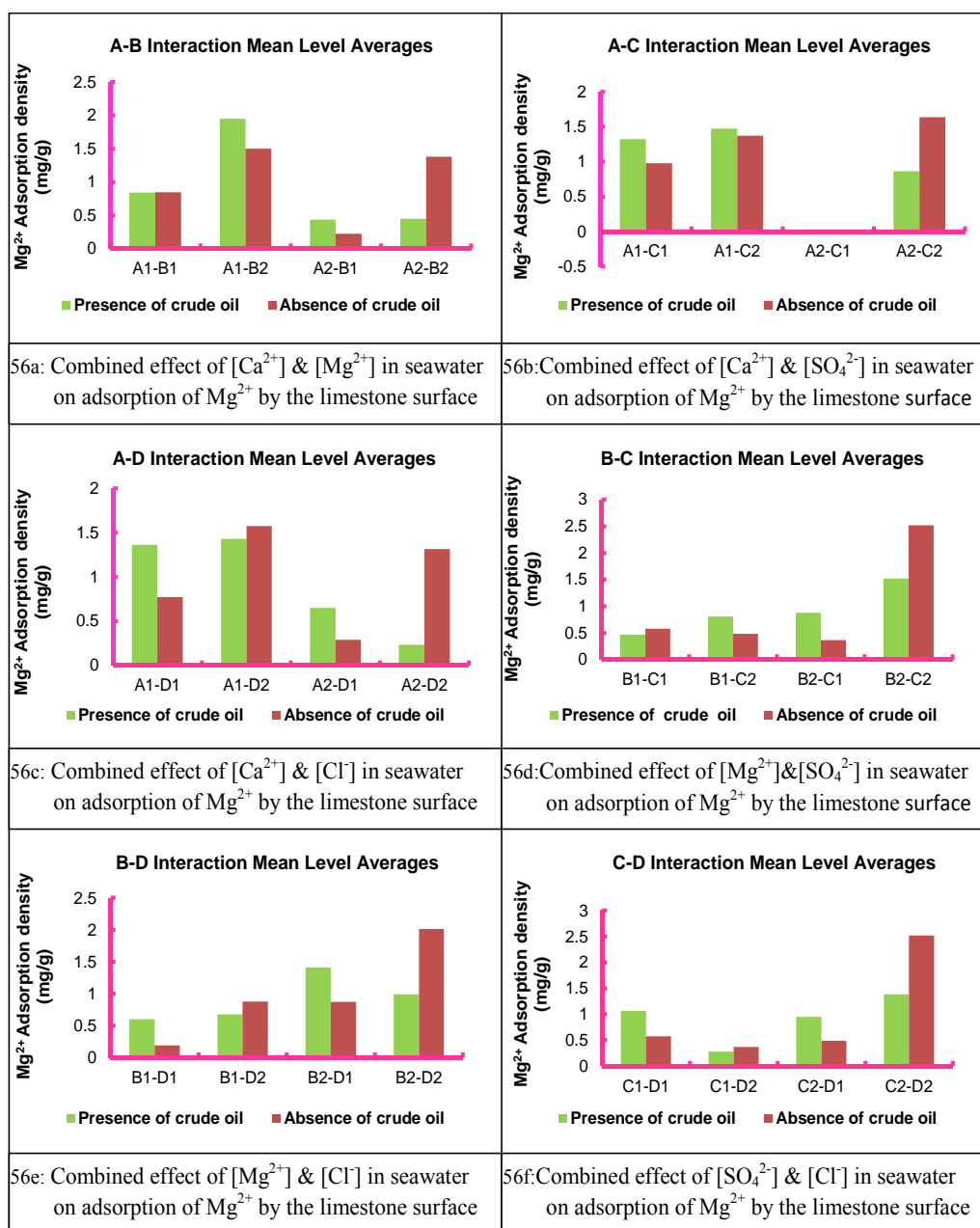


Figure 56: Two-way interactions of [Ca²⁺], [Mg²⁺], [SO₄²⁻], and [Cl⁻] on the adsorption of Mg²⁺ by limestone at 90°C in the absence and presence of crude-oil

Sulfate Ion Interactions

Figures 57 and 58 compares the main effects and two-way interactions respectively of Ca^{2+} , Mg^{2+} , SO_4^{2-} , and Cl^- concentrations in seawater on the adsorption of SO_4^{2-} onto limestone in the absence and presence of crude oil at 90°C. The sulfate ion interactions in the presence and absence of crude oil are slightly different, and more interactions show more desorption of sulfate ion in the absence of crude oil. However, the same conclusions can be drawn from them. Increasing calcium and sulfate ions, while decreasing chloride ions in the injected seawater will enhance sulfate ion adsorption in both cases.

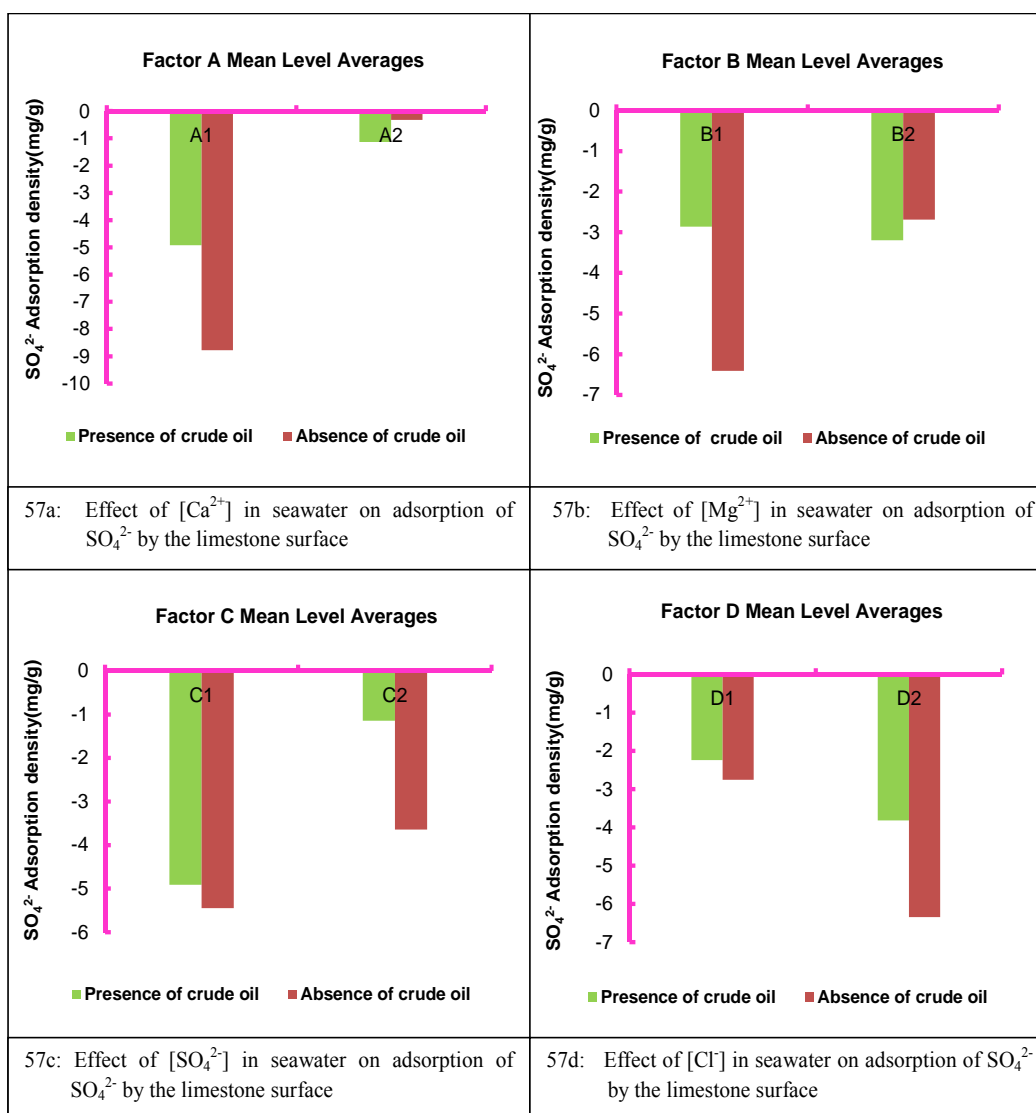


Figure 57: Main effects of $[Ca^{2+}]$, $[Mg^{2+}]$, $[SO_4^{2-}]$, and $[Cl^-]$ on the adsorption of SO_4^{2-} by limestone at $90^\circ C$ in the absence and presence of crude-oil

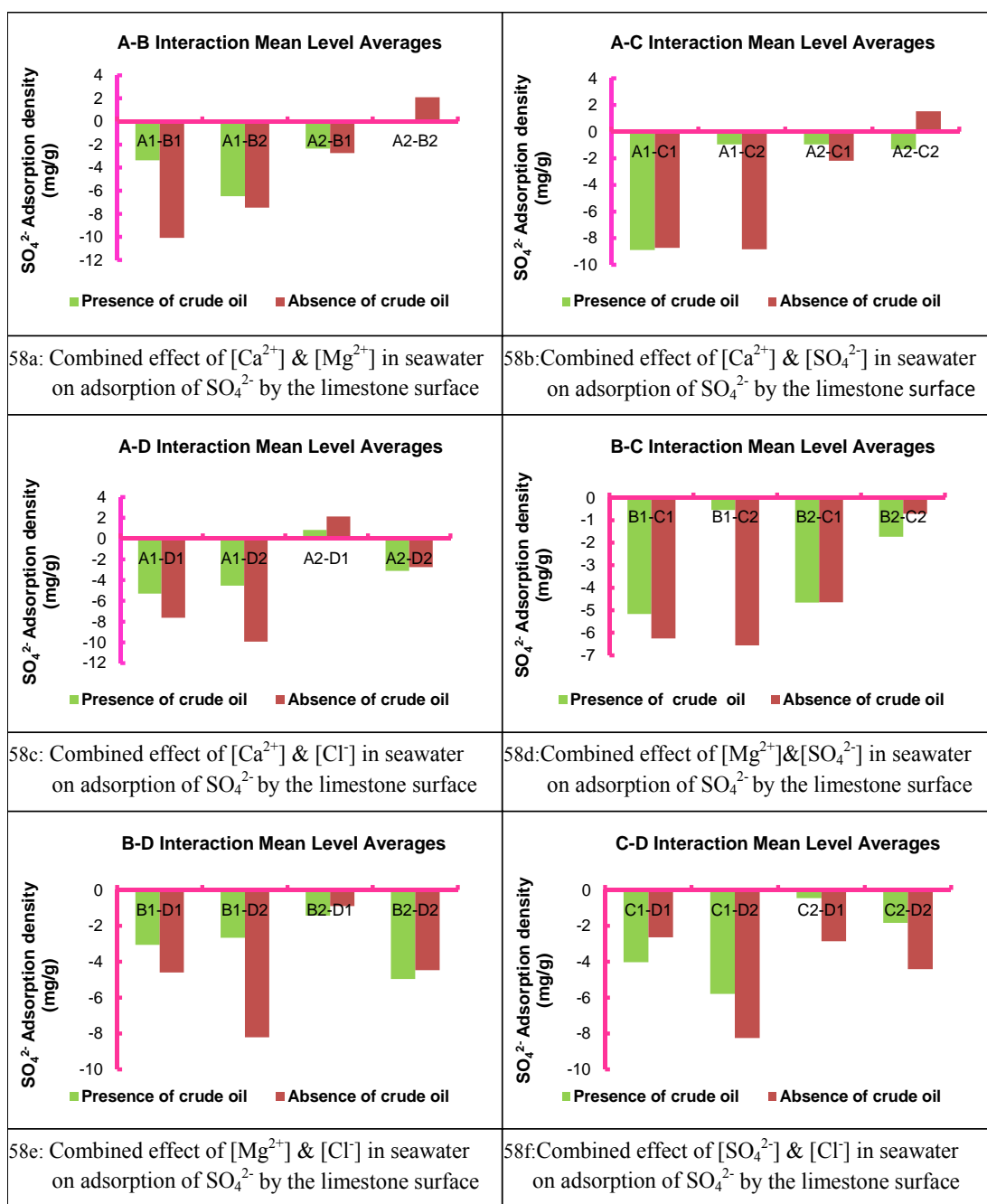


Figure 58: Two-way interactions of [Ca²⁺], [Mg²⁺], [SO₄²⁻], and [Cl⁻] on the adsorption of SO₄²⁻ by limestone at 90°C in the absence and presence of crude-oil

Chloride Ion Interactions

It is generally observed from Figures 59 and 60 that more desorption of chloride ion occurred from the limestone rock in the absence of crude oil. The reason for this behaviour is not known but it must be related to the high temperature. While chloride adsorption can be mostly enhanced in the absence of crude oil by simultaneously increasing calcium and decreasing chloride ionic concentrations in seawater, the increase of sulfate and calcium ions will promote chloride ion adsorption in the presence of crude oil. Calcium ion will thus enhance adsorption in both cases.

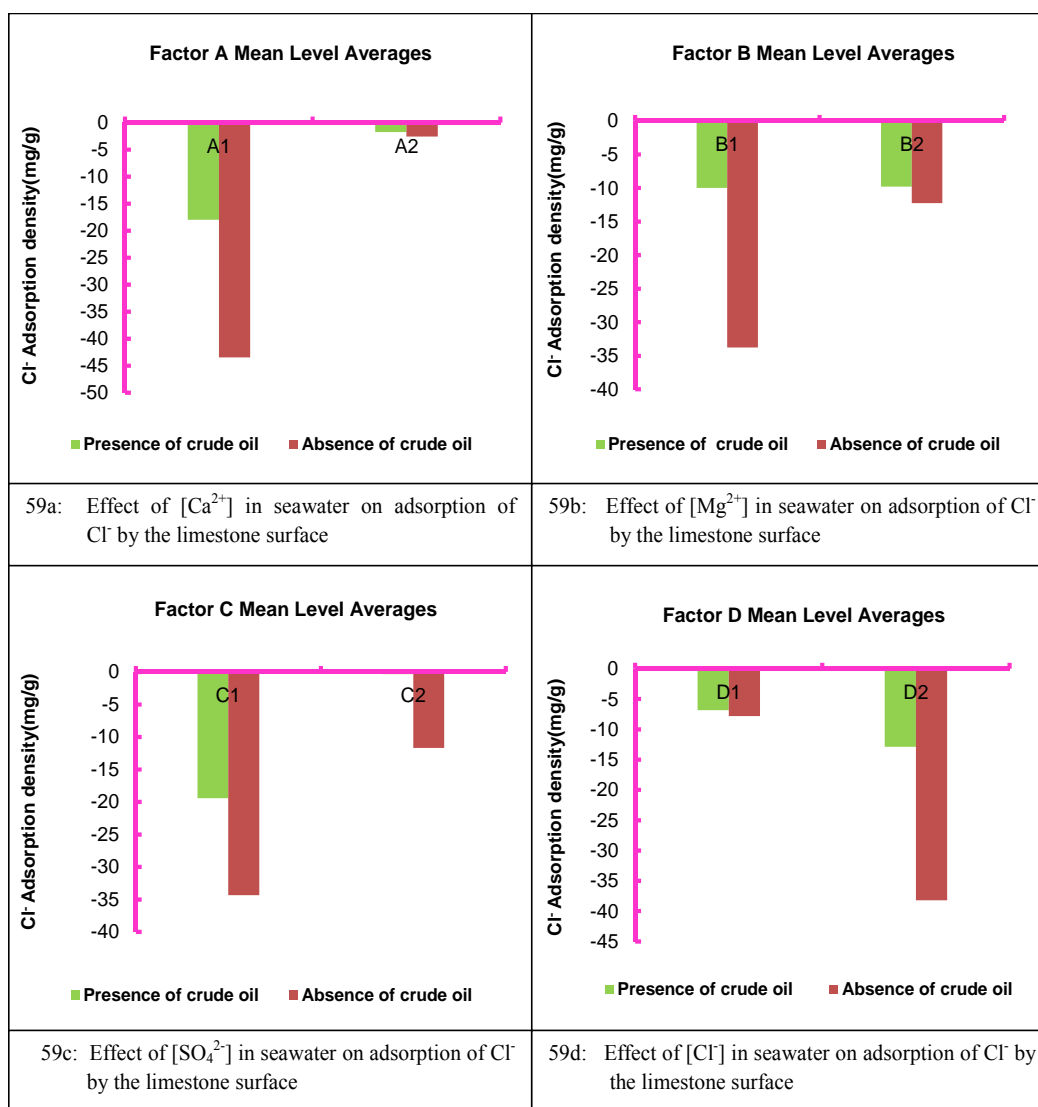


Figure 59: Main effects of $[Ca^{2+}]$, $[Mg^{2+}]$, $[SO_4^{2-}]$, and $[Cl^-]$ on the adsorption of Cl^- by limestone at $90^\circ C$ in the absence and presence of crude-oil

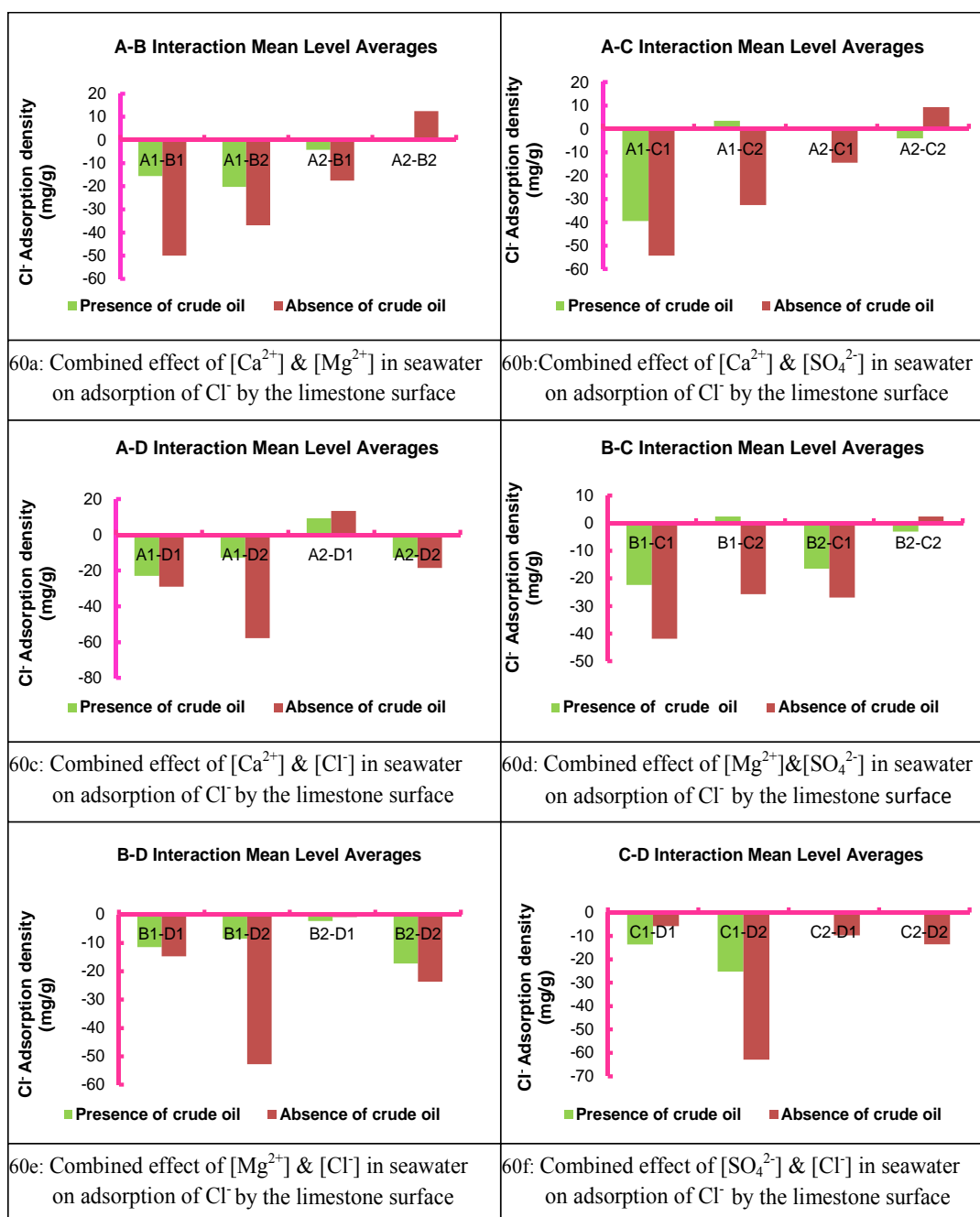


Figure 60: Two-way interactions of [Ca²⁺], [Mg²⁺], [SO₄²⁻], and [Cl⁻] on the adsorption of Cl⁻ by limestone at 90°C in the absence and presence of crude-oil

4.2.1.7 Temperature effect on the adsorption of Ca^{2+} , Mg^{2+} , SO_4^{2-} , and Cl^- on Limestone in the absence of crude oil

Calcium Ion Interactions

Although, desorption is observed at both temperatures, Figures 61 and 62 obviously show that more calcium ions go into solution at 90°C than at 25°C. This must be related to substitution reaction of magnesium ions. Magnesium ion gets highly reactive at high temperatures and then it substitutes or displaces calcium ions from the crystal lattice of carbonates. This fact has also been experimentally proven with the PCC, which is shown in Figure 8b. Both temperatures however show that increasing calcium ions in seawater is the optimum way to enhance calcium ion adsorption onto limestone in the absence of crude oil.

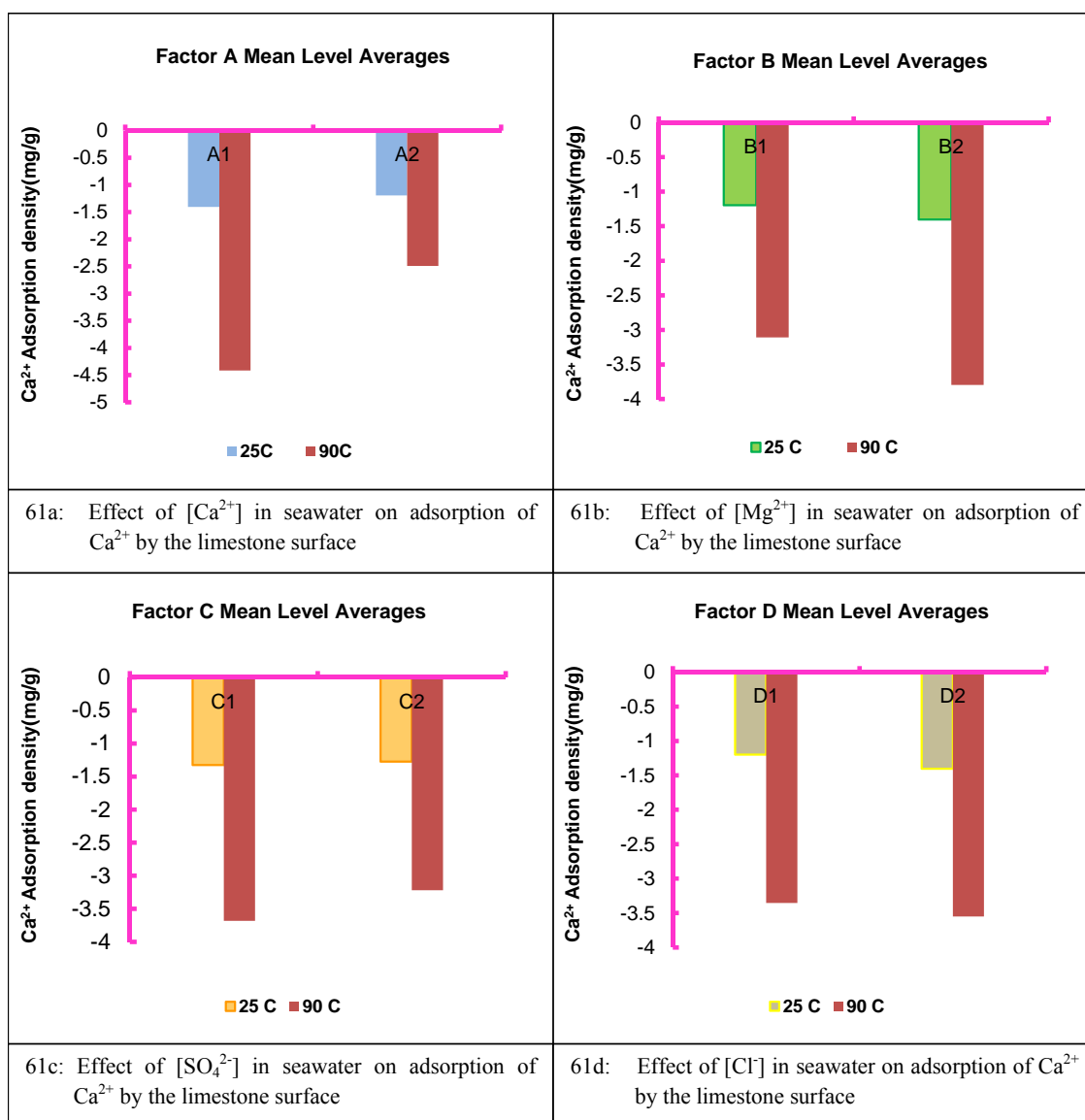


Figure 61: Main effects of $[Ca^{2+}]$, $[Mg^{2+}]$, $[SO_4^{2-}]$, and $[Cl^-]$ on the adsorption of Ca^{2+} by limestone at 25°C and 90°C in the absence of crude-oil

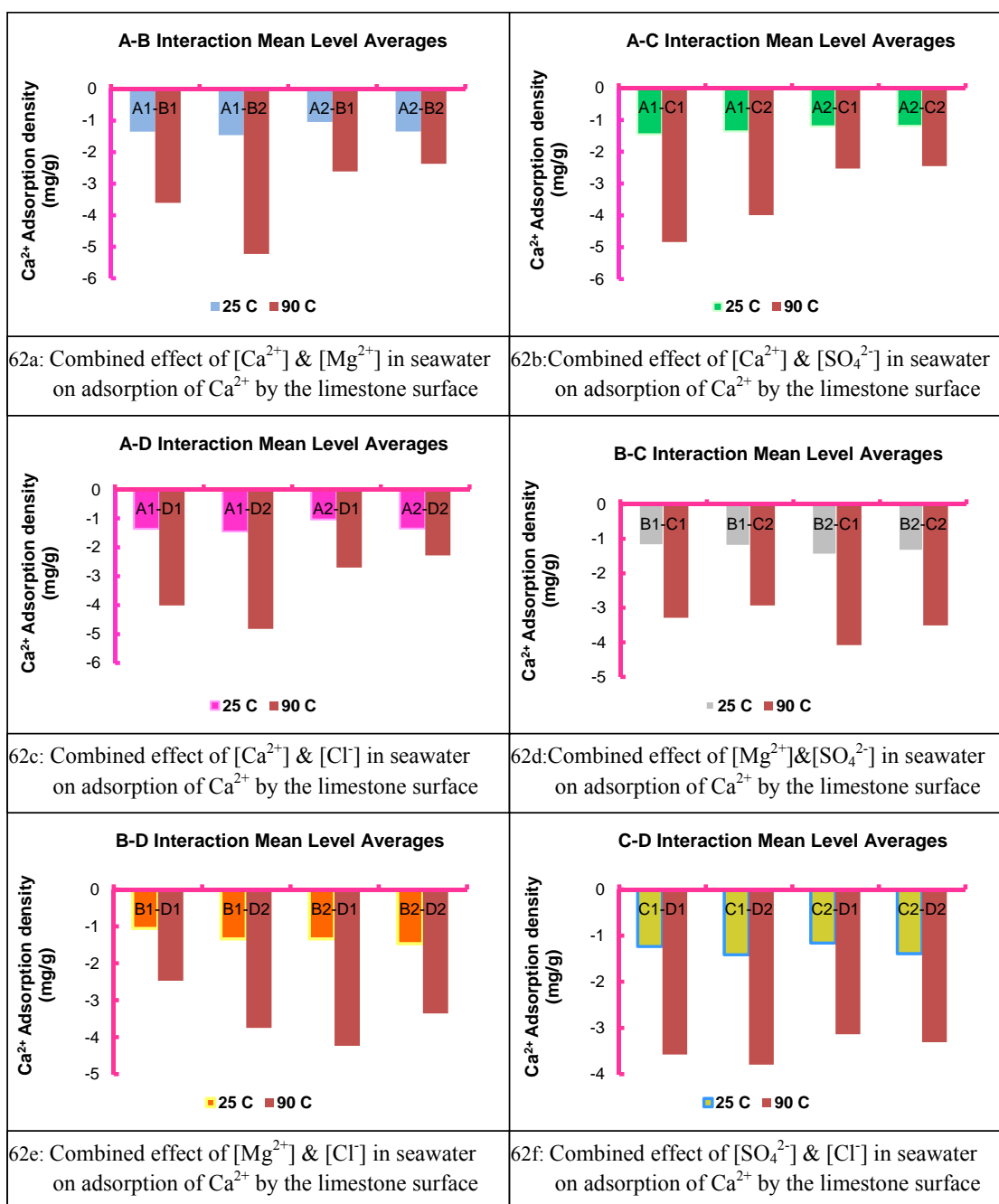


Figure 62: Two-way interactions of [Ca²⁺], [Mg²⁺], [SO₄²⁻], and [Cl⁻] on the adsorption of Ca²⁺ by limestone at 25°C and 90°C in the absence of crude-oil

Magnesium Ion Interactions

Significant differences are observed in the amount of magnesium adsorbed onto limestone at the two temperatures, as shown in Figures 63 and 64. More magnesium ion is adsorbed onto limestone at 90°C than at 25°C because magnesium ion gets more reactive at high temperatures due to dehydration of the ion [1]. At 25°C, it was observed that a decrease in chloride and calcium ions will enhance magnesium adsorption, while an increase in both sulfate and magnesium ions will enhance magnesium ion adsorption at 90°C.

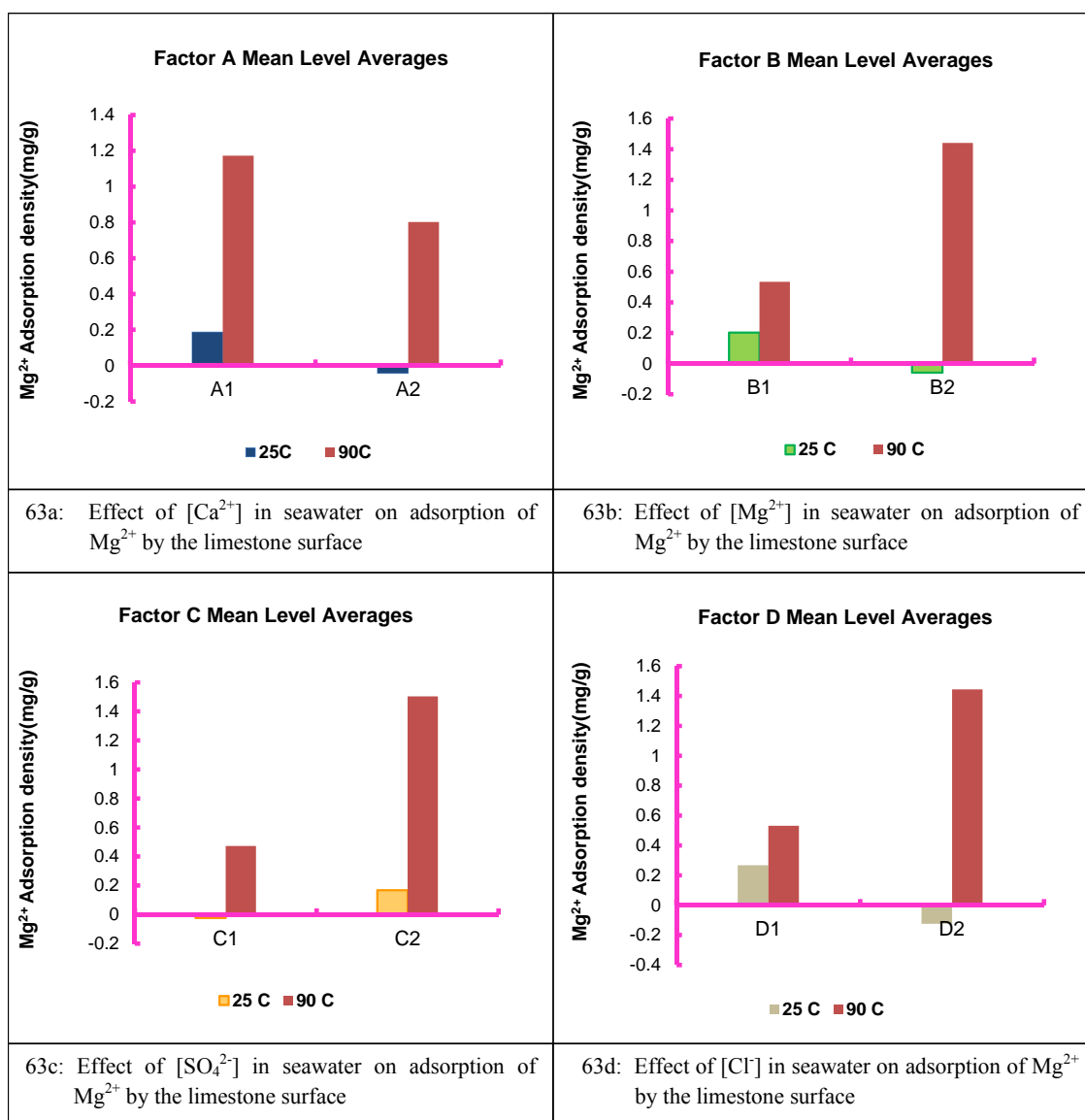


Figure 63: Main effects of $[Ca^{2+}]$, $[Mg^{2+}]$, $[SO_4^{2-}]$, and $[Cl^-]$ on the adsorption of Mg^{2+} by limestone at 25°C and 90°C in the absence of crude-oil

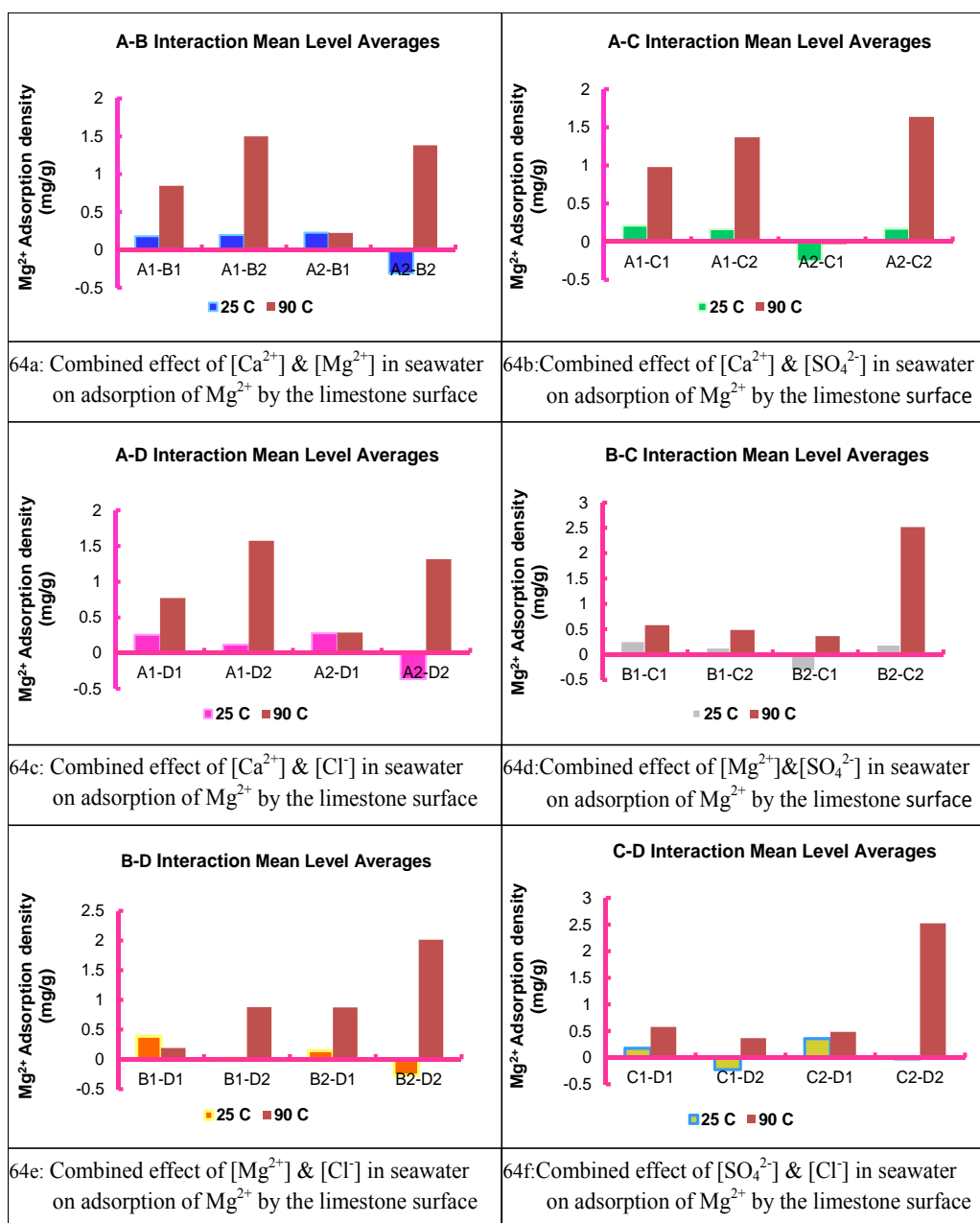


Figure 64: Two-way interactions of [Ca²⁺], [Mg²⁺], [SO₄²⁻], and [Cl⁻] on the adsorption of Mg²⁺ by limestone at 25°C and 90°C in the absence of crude-oil

Sulfate Ion Interactions

The interactions of sulfate ion at room temperature and 90°C are different, as Figures 65 and 66 indicate. While all interactions at 25°C show desorption of sulfate ion, interactions A2-B2, A2-C2, and A2-D1 at 90°C yielded adsorption of sulfate ion. Interactions at both temperatures reveal that a decrease in both calcium and sulfate ion concentrations in seawater will seriously impede sulfate ion adsorption onto limestone.

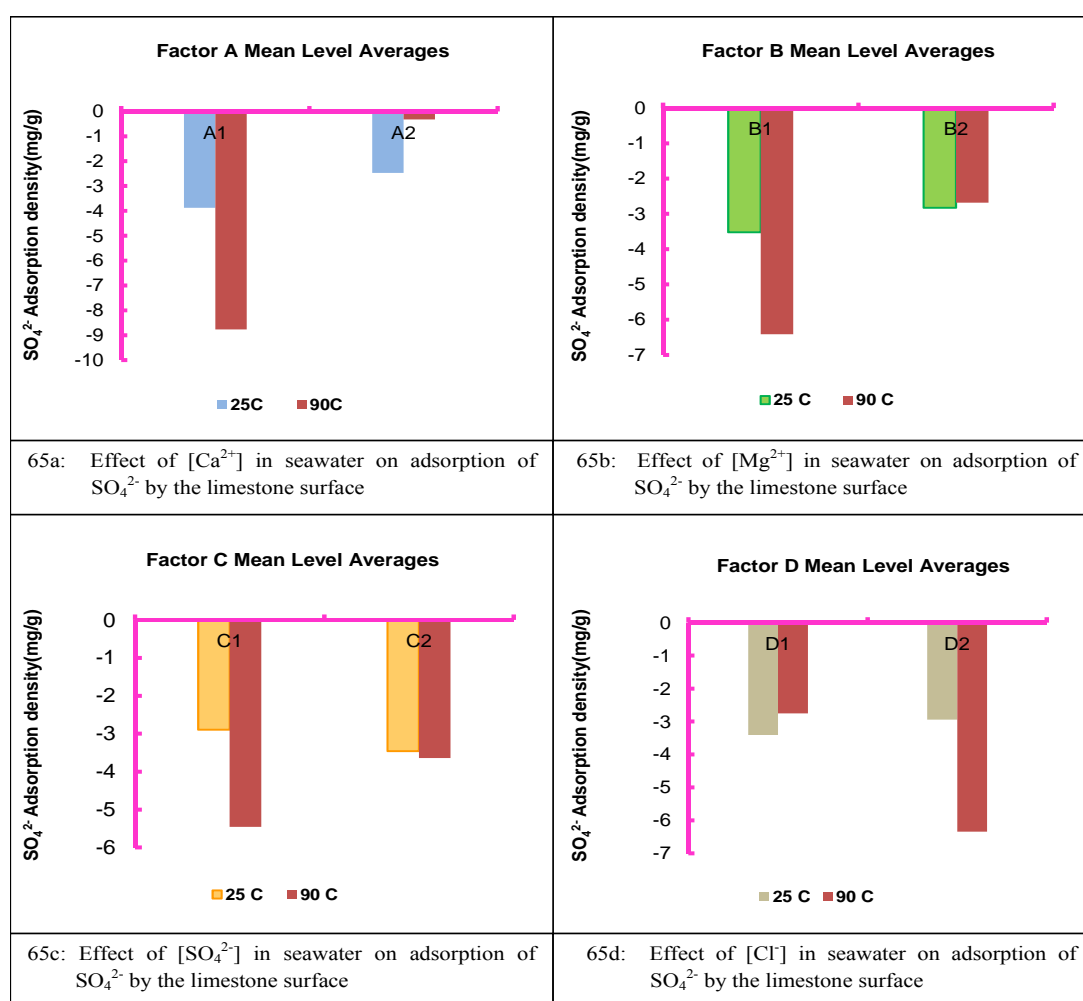


Figure 65: Main effects of [Ca²⁺], [Mg²⁺], [SO₄²⁻], and [Cl⁻] on the adsorption of SO₄²⁻ by limestone at 25°C and 90°C in the absence of crude-oil

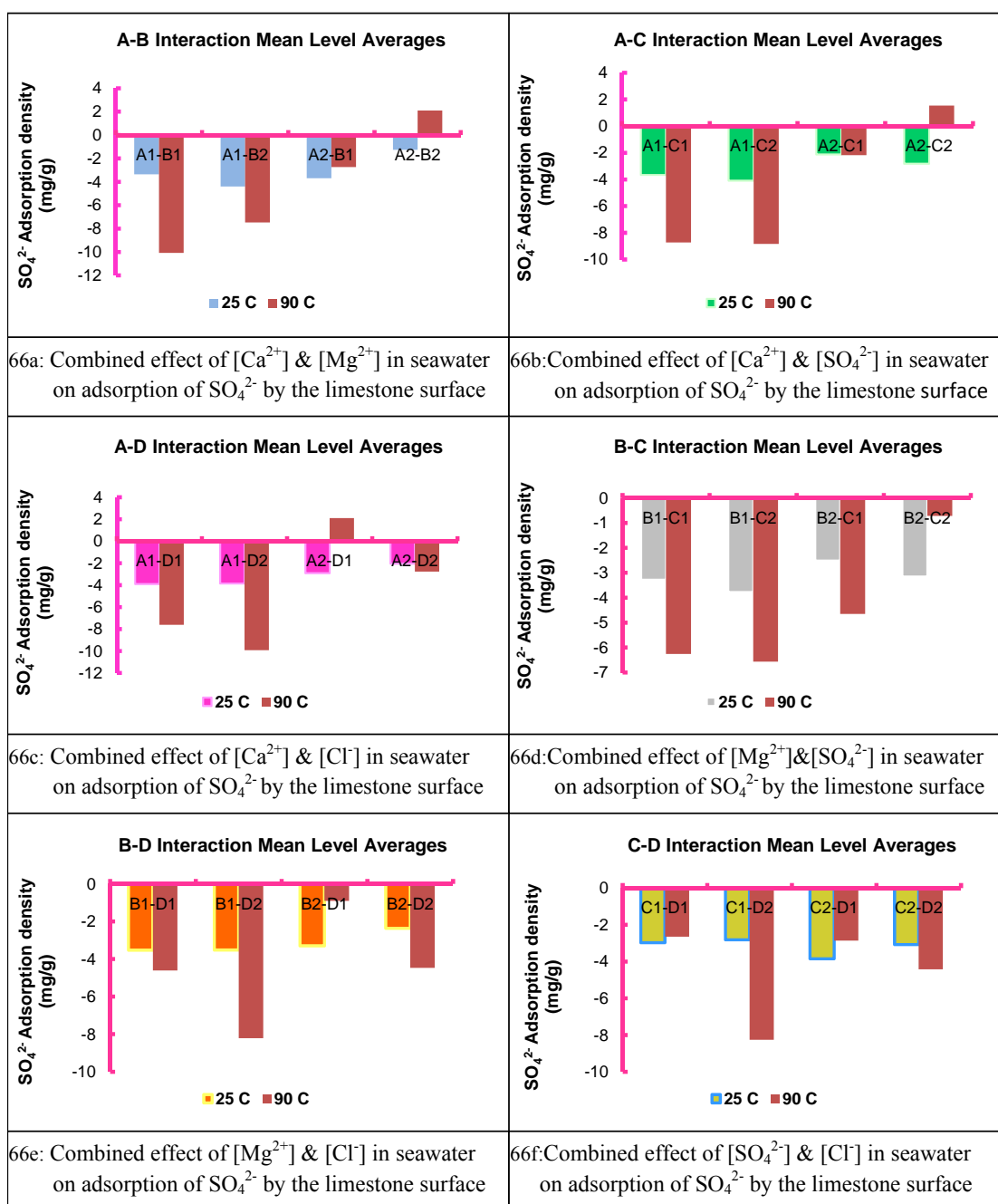


Figure 66: Two-way interactions of [Ca²⁺], [Mg²⁺], [SO₄²⁻], and [Cl⁻] on the adsorption of SO₄²⁻ by limestone at 25°C and 90°C in the absence of crude-oil

Chloride Ion Interactions

More chloride ions go into solution at 90°C than at 25°C, as Figures 67 and 68 generally show. At 25°C, chloride adsorption can be promoted mostly by increasing calcium and chloride ions in seawater, while an increase in calcium and rather a decrease in chloride ions in seawater seems to be the optimum way to promote chloride adsorption at 90°C.

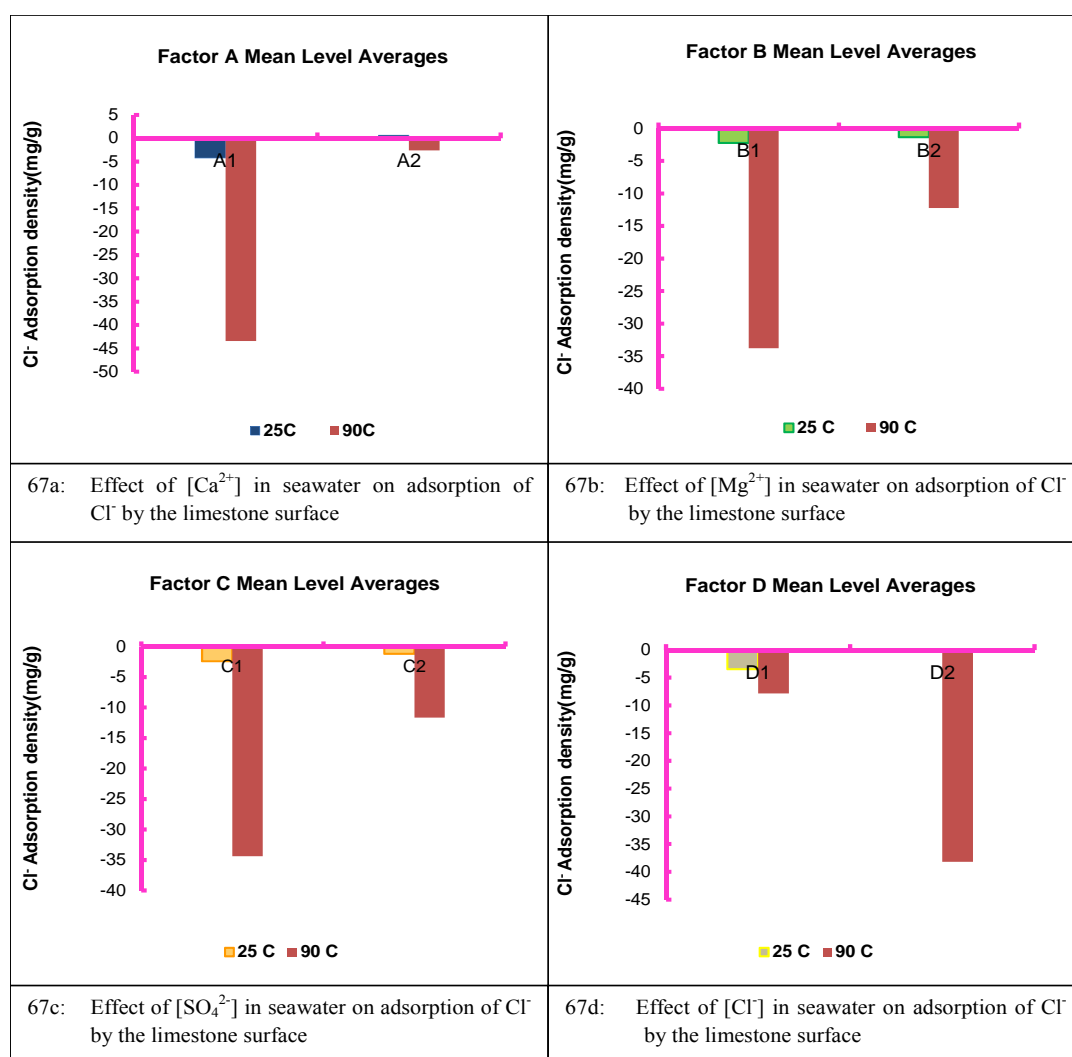


Figure 67: Main effects of [Ca²⁺], [Mg²⁺], [SO₄²⁻], and [Cl⁻] on the adsorption of Cl⁻ by limestone at 25°C and 90°C in the absence of crude-oil

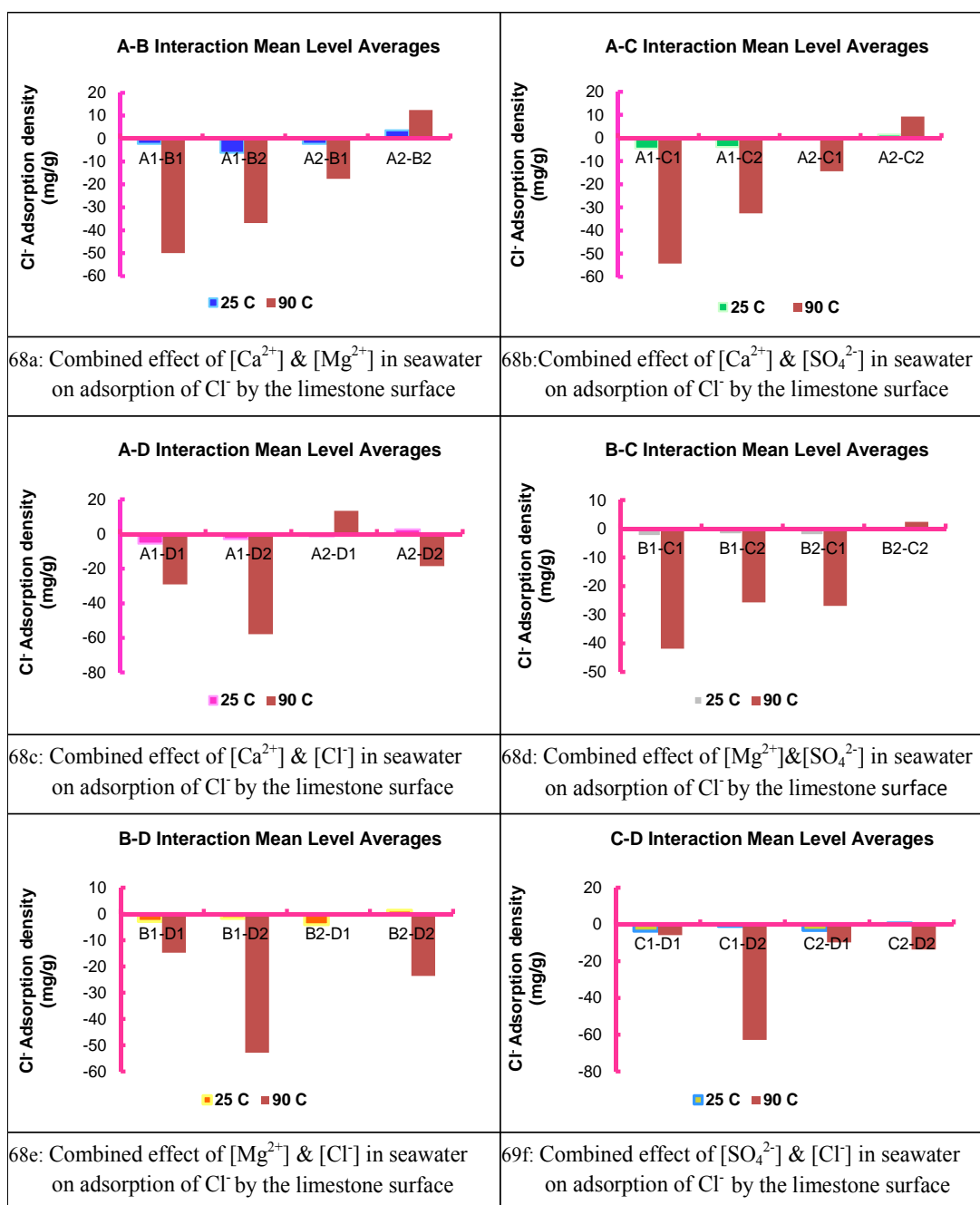


Figure 68: Two-way interactions of [Ca²⁺], [Mg²⁺], [SO₄²⁻], and [Cl⁻] on the adsorption of Cl⁻ by limestone at 25°C and 90°C in the absence of crude-oil

4.2.1.8 Temperature effect on the adsorption of Ca^{2+} , Mg^{2+} , SO_4^{2-} , and Cl^- on Limestone in the presence of crude oil

Calcium Ion Interactions

It can be generally observed from Figures 69 and 70 that more calcium ions go into solution at 90°C than 25°C. This can be related to the substitution reaction of magnesium ion at 90°C, which can be seen from Figure 71. The substitution of calcium ion on the carbonate matrix by magnesium ion increases with temperature. While increasing calcium ion concentration alone in seawater is enough to significantly trigger calcium ion adsorption at 25°C, simultaneously increasing calcium and decreasing magnesium ions in seawater is what is needed to enhance calcium adsorption at 90°C. Decreasing magnesium ions in seawater will decrease the amount of calcium ions that will go into solution at 90°C as can be seen from Figures 69b, 70a, 70d, and 70e.

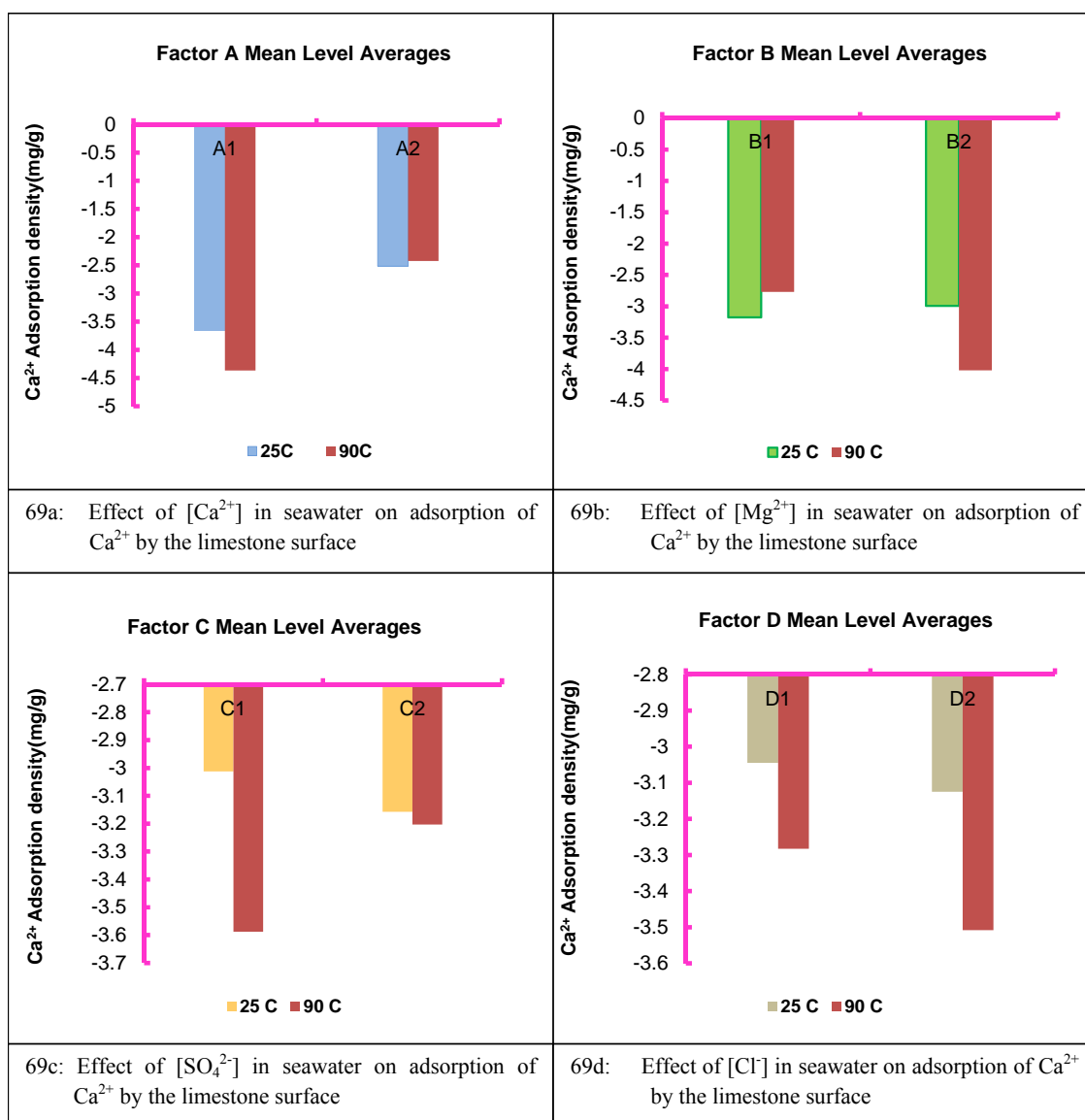


Figure 69: Main effects of $[Ca^{2+}]$, $[Mg^{2+}]$, $[SO_4^{2-}]$, and $[Cl^-]$ on the adsorption of Ca^{2+} by limestone at 25°C and 90°C in the presence of crude-oil

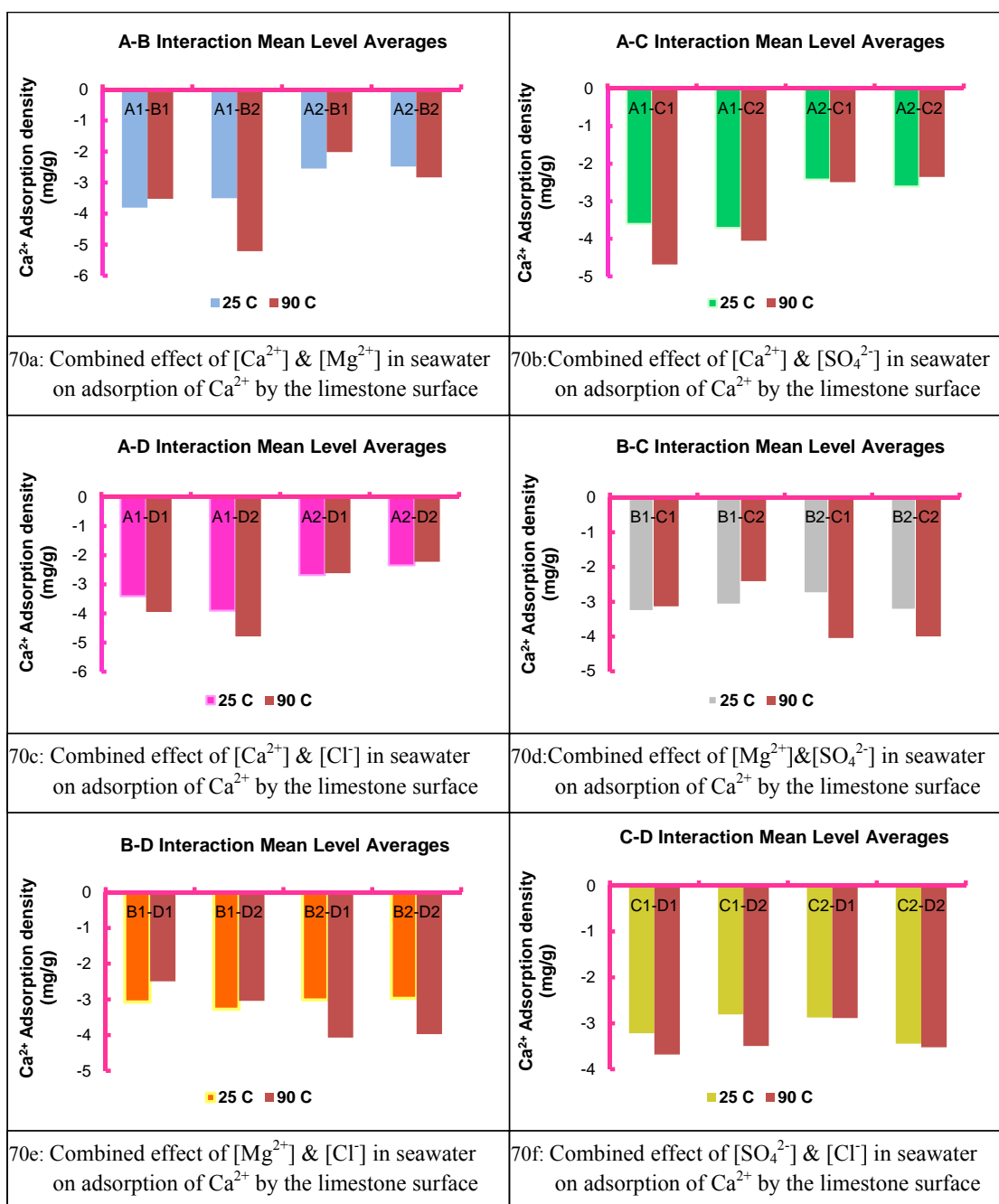


Figure 70: Two-way interactions of [Ca²⁺], [Mg²⁺], [SO₄²⁻], and [Cl⁻] on the adsorption of Ca²⁺ by limestone at 25°C and 90°C in the presence of crude-oil

Magnesium Ion Interactions

Figures 71 and 72 show that adsorption of magnesium ions increases with temperature. Magnesium ion gets highly reactive at high temperature due to its partial dehydration. Unlike at 25°C, the high temperature ensured direct contact of the ions with the rock, as was observed from the samples after conditioning at 90°C. At 25°C, magnesium ion adsorption onto limestone can be promoted by reducing the concentrations of both SO_4^{2-} and Cl^- simultaneously in the injected seawater. This is completely different from the interactions at 90°C, wherein magnesium adsorption onto limestone can be enhanced by simultaneously decreasing the calcium ions and increasing either magnesium or sulfate ions in the injected or surrounding seawater.

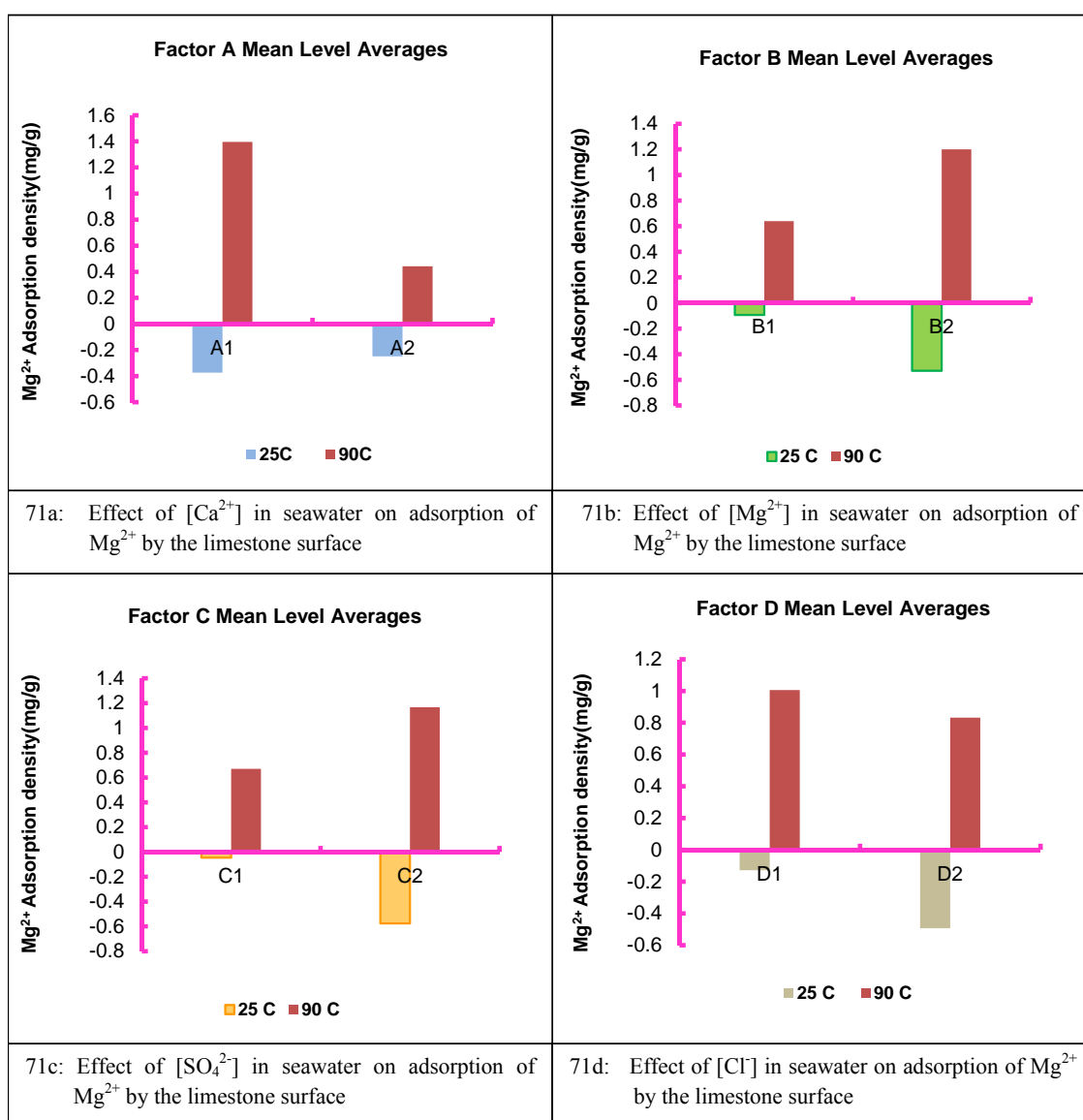


Figure 71: Main effects of $[Ca^{2+}]$, $[Mg^{2+}]$, $[SO_4^{2-}]$, and $[Cl^-]$ on the adsorption of Mg^{2+} by limestone at 25°C and 90°C in the presence of crude-oil

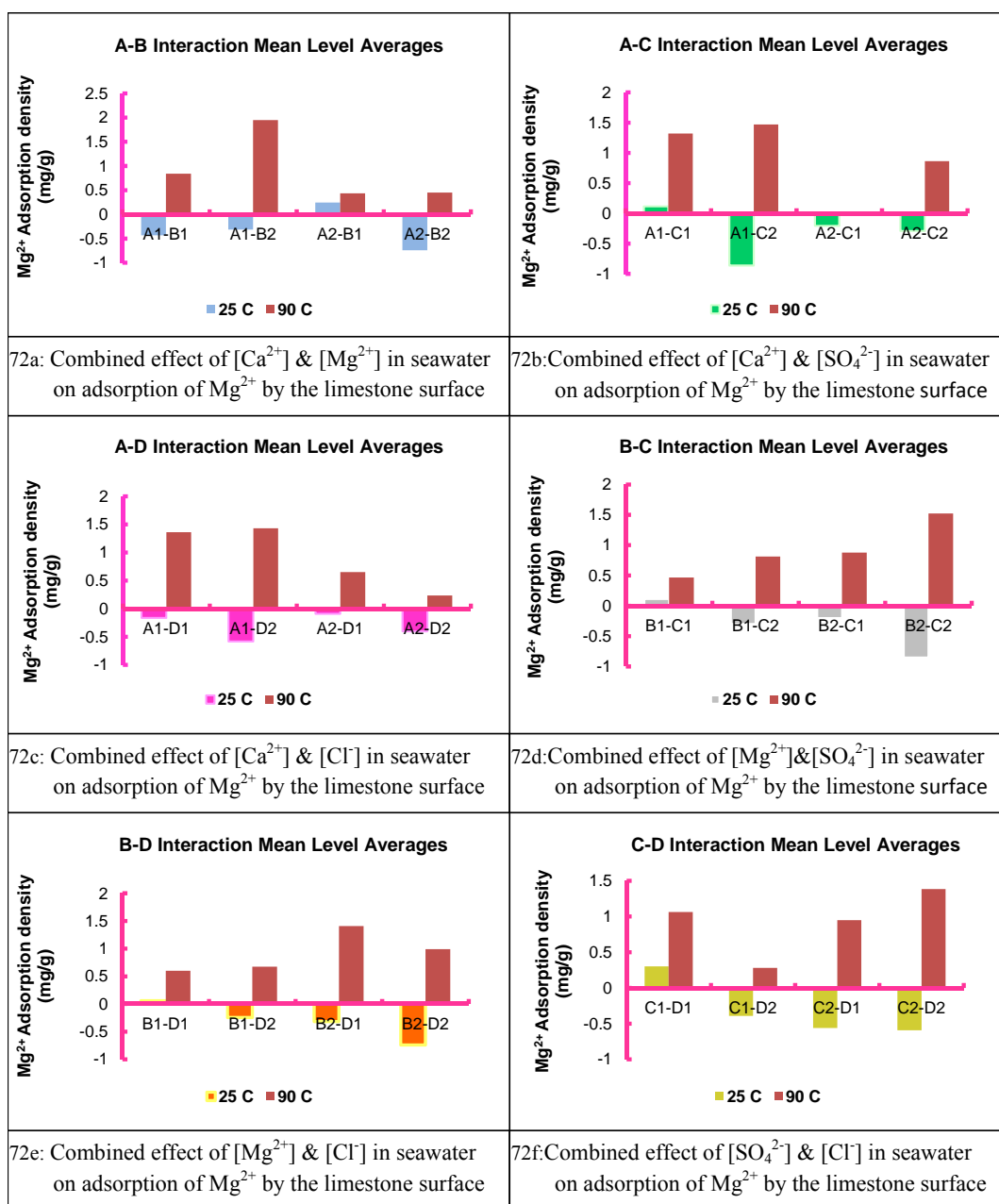


Figure 72: Two-way interactions of [Ca²⁺], [Mg²⁺], [SO₄²⁻], and [Cl⁻] on the adsorption of Mg²⁺ by limestone at 25°C and 90°C in the presence of crude-oil

Sulfate Ion Interactions

It can be generally observed from Figures 73 and 74 that there is more desorption of sulfate ion at 25°C than 90°C. In other words, there is less adsorption of sulfate ions at 25°C. This indicates that adsorption of sulfate ion onto limestone will increase with temperature. Calcium ion was found to be the most influential ion on sulfate adsorption at 25°C, as an increase in calcium ion in seawater will enhance it. In addition to an increase in calcium ion, an increase in sulfate ion was found to equally promote sulfate adsorption onto limestone at 90°C. Decreasing the chloride ion concentration in the injected or surrounding seawater also enhanced sulfate adsorption at 90°C.

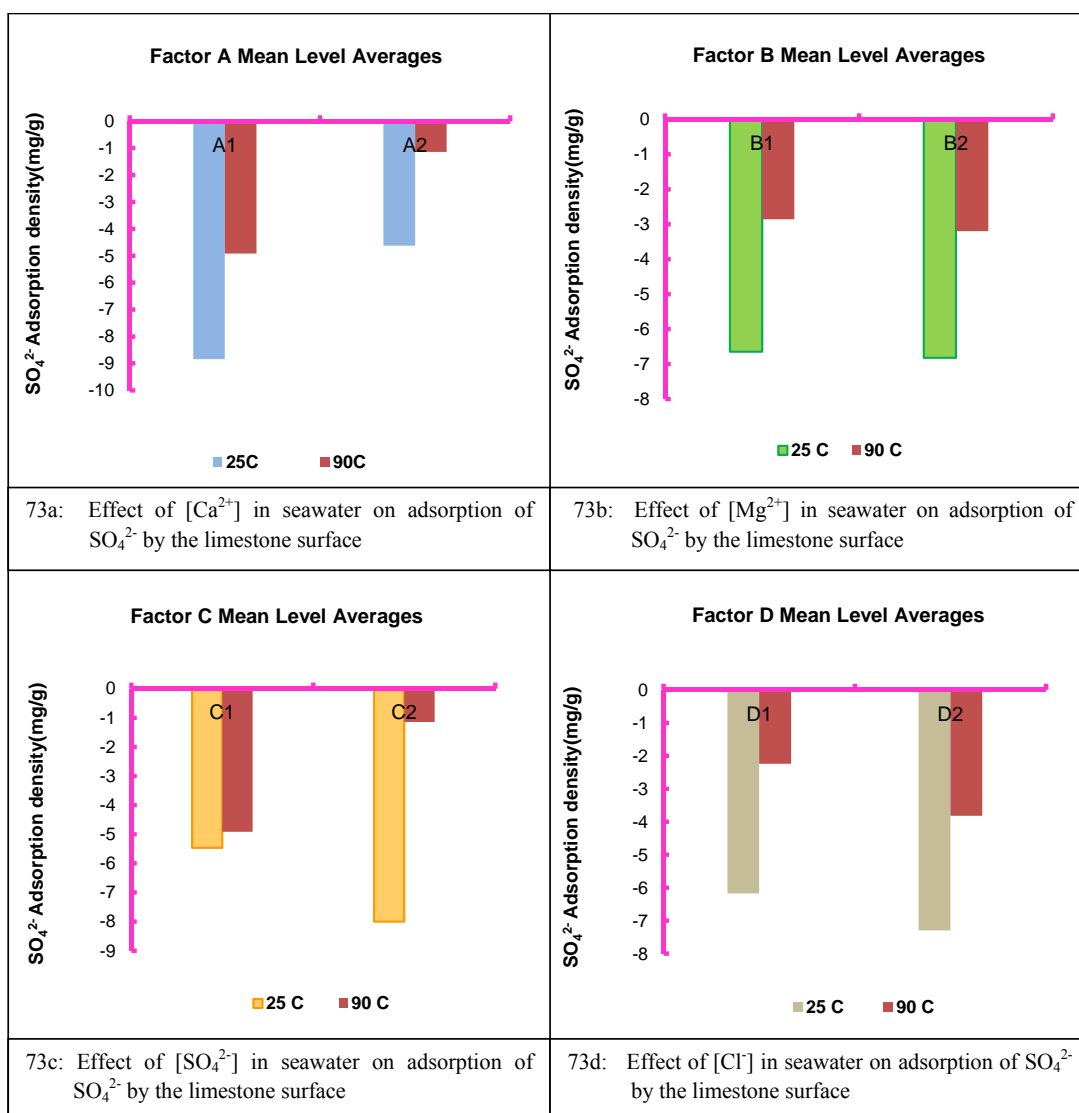


Figure 73: Main effects of $[Ca^{2+}]$, $[Mg^{2+}]$, $[SO_4^{2-}]$, and $[Cl^-]$ on the adsorption of SO_4^{2-} by limestone at 25°C and 90°C in the presence of crude-oil

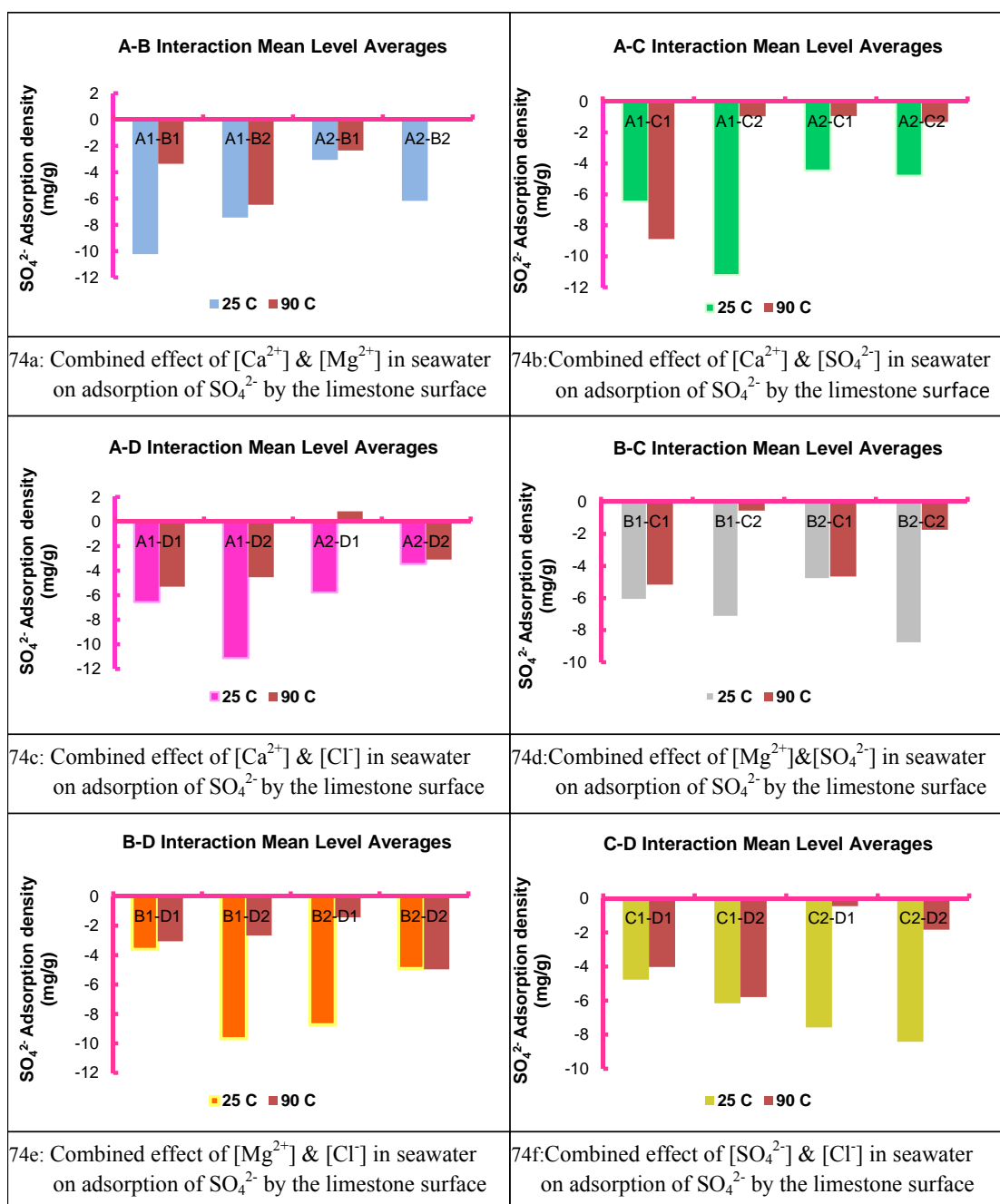


Figure 74: Two-way interactions of [Ca²⁺], [Mg²⁺], [SO₄²⁻], and [Cl⁻] on the adsorption of SO₄²⁻ by limestone at 25°C and 90°C in the presence of crude-oil

Chloride Ion Interactions

More interactions in Figures 75 and 76 seems to indicate higher chloride desorption from limestone at 25°C than 90°C. Thus, it can be safely agreed upon that chloride ion adsorption will increase with temperature. Interactions at 25°C confirm that a reduction in calcium ion's concentration in seawater will significantly reduce the possibility of chloride's adsorption onto the limestone rock surface, while it was concluded from experiments at 90°C that chloride adsorption onto limestone can be enhanced by increasing both sulfate and calcium ions. Calcium ion is commonly influential on chloride adsorption at both temperatures.

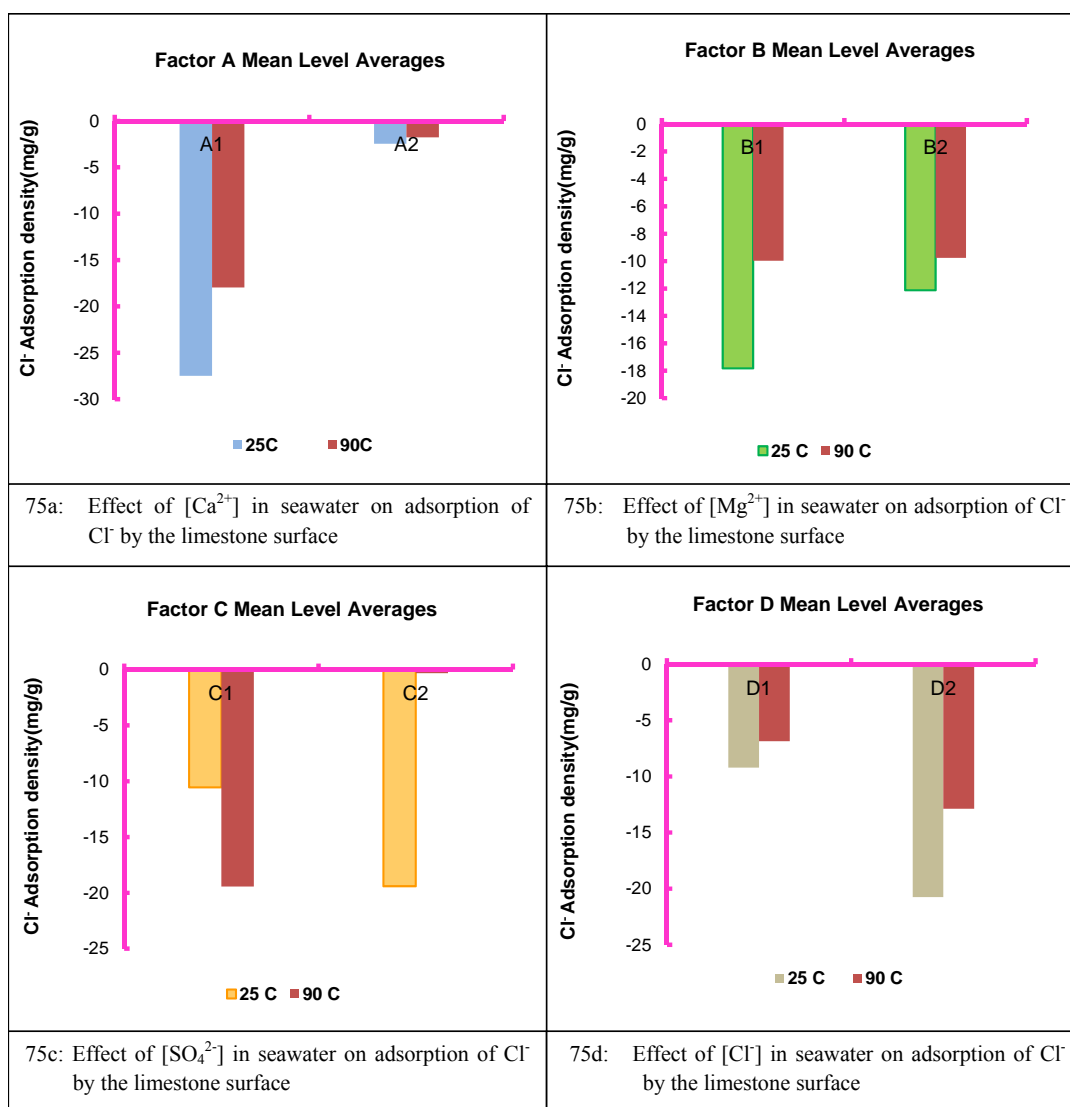


Figure 75: Main effects of $[Ca^{2+}]$, $[Mg^{2+}]$, $[SO_4^{2-}]$, and $[Cl^-]$ on the adsorption of Cl^- by limestone at 25°C and 90°C in the presence of crude-oil

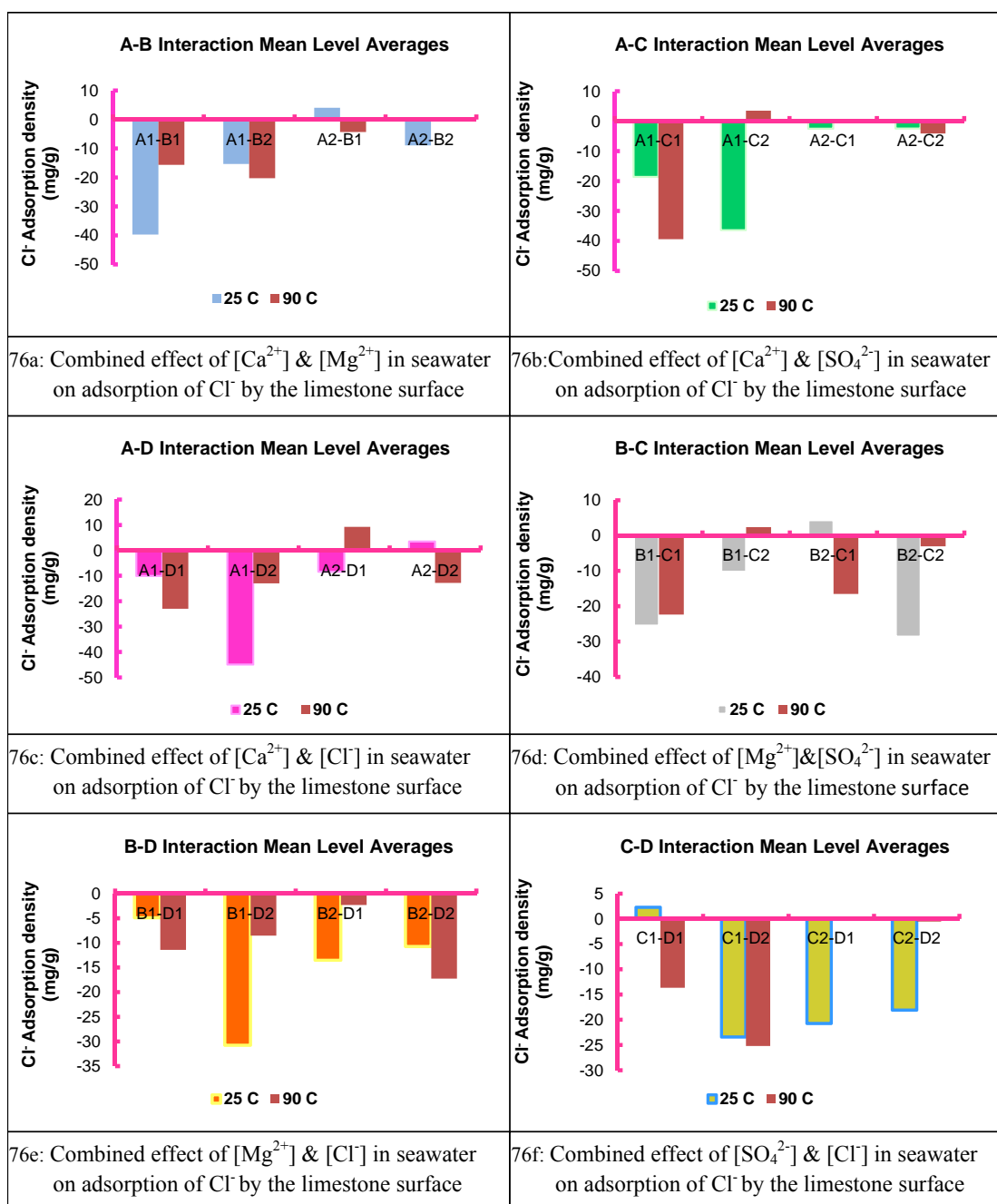


Figure 76: Two-way interactions of [Ca²⁺], [Mg²⁺], [SO₄²⁻], and [Cl⁻] on the adsorption of Cl⁻ by limestone at 25°C and 90°C in the presence of crude-oil

4.2.1.9 Summary of adsorption results of Ca^{2+} , Mg^{2+} , SO_4^{2-} , and Cl^- on Limestone

From the foregoing discussions, it is obvious that the rock-fluid interactions of Ca^{2+} , Mg^{2+} , SO_4^{2-} , and Cl^- with limestone under the different conditions are complex, which means that utilizing just any of them without determining the best that suits the reservoir conditions will be ineffective. For ease of understanding, a summary of the major observations are discussed.

The rock-fluid interactions at 25°C, in the absence of crude oil has shown that Calcium ion adsorption onto limestone can be enhanced by most importantly increasing calcium ion concentration in seawater, and decreasing magnesium or chloride ion concentrations or both. Magnesium ion adsorption will be promoted mostly by decreasing chloride ion concentrations in seawater. A decrease in calcium ion will also favour magnesium ion adsorption, but will seriously impede adsorption of SO_4^{2-} onto limestone. Increasing the concentrations of calcium and chloride ions in seawater will enhance chloride ion adsorption. Anhydrite (CaSO_4) dissolution will be promoted at this condition by decreasing calcium ions in the injected or surrounding seawater.

Interactions at 25°C, in the presence of crude oil showed that increasing the calcium ion concentration in the injected seawater will significantly promote calcium ion adsorption, while Mg^{2+} adsorption onto the limestone can be enhanced by mostly reducing the concentrations of both SO_4^{2-} and Cl^- simultaneously in seawater. Decreasing Ca^{2+} concentration in seawater will significantly hinder sulfate and chloride ion's adsorption onto limestone. It is again seen here that anhydrite (CaSO_4) dissolution will be

significantly promoted by decreasing calcium ions in the injected or surrounding seawater.

At 90°C, in the absence of crude oil, rock-fluid interactions confirmed that increasing of calcium ion in seawater is the optimum way to enhance calcium ion adsorption onto the rock. Magnesium ion adsorption can be enhanced by simultaneously increasing either the concentrations of sulfate and magnesium ions or sulfate and chloride ions in the injected seawater. Sulfate ion adsorption can mostly be promoted by increasing calcium ions in seawater, while simultaneously increasing calcium and decreasing chloride ion concentrations in seawater is the optimum way to enhance chloride ion adsorption onto limestone. Anhydrite dissolution can be enhanced by decreasing both calcium and magnesium ions, decreasing both calcium and sulfate ions, and decreasing and increasing calcium and chloride ions respectively simultaneously in seawater.

The rock-fluid interactions at 90°C, in the presence of crude oil showed that the optimum way to enhance calcium ion adsorption onto limestone is to simultaneously increase and decrease the calcium and magnesium ions respectively in seawater. Magnesium ion adsorption can be significantly promoted by simultaneously decreasing the calcium ions with an increase in either magnesium or sulfate ions. Increasing both calcium and sulfate ions, and decreasing chloride ions in the injected seawater will significantly promote sulfate ion adsorption onto limestone, while chloride ion adsorption can be enhanced by increasing both sulfate and calcium ions in the injected seawater. Anhydrite dissolution in this case will be significantly promoted by decreasing both calcium and sulfate ions, while also increasing both magnesium and chloride ions.

Increasing the temperature altered the interactions of our ions. More calcium ion go into solution as a result of the high reactivity of magnesium ions at high temperature. This high reactivity ensured high magnesium adsorption, thereby substituting or displacing calcium ions in the limestone crystal lattice. Thus, the substitution reaction which has been reported to increase the water wetness of carbonate reservoirs [1, 25, 27, 66] has been confirmed. Sulfate ion desorption from the limestone rock significantly decreased at high temperature, which means that the dissolution of anhydrite is also a function of temperature. The desorption of sulfate ion was found to significantly decrease as the temperature increased from 25°C to 90°C. This finding is in line with the recent observation of Yousef et al. [66].

4.2.2 Zeta Potential Results on Limestone

4.2.2.1 Iso-Electric Point (IEP) of Limestone

Figure 77 illustrates the zeta potential profile of limestone in deionized water as a function of pH. An IEP value of 7.03 is obtained at equilibrium. The literature IEP values of calcite ranges from 4 to 10.8, while that of dolomite is generally reported as ≤ 7 [80]. Since 73% of our limestone sample is dolomite, it is logical that our limestone IEP should be close to 7, which is in agreement with the literature values. At $\text{pH} > \text{IEP}$, an excess concentration of negative species will predominate at the interface, and the surface will be negatively charged, while at $\text{pH} < \text{IEP}$, there will be an excess concentration of positive species at the interface, which will result into the surface being positively charged.

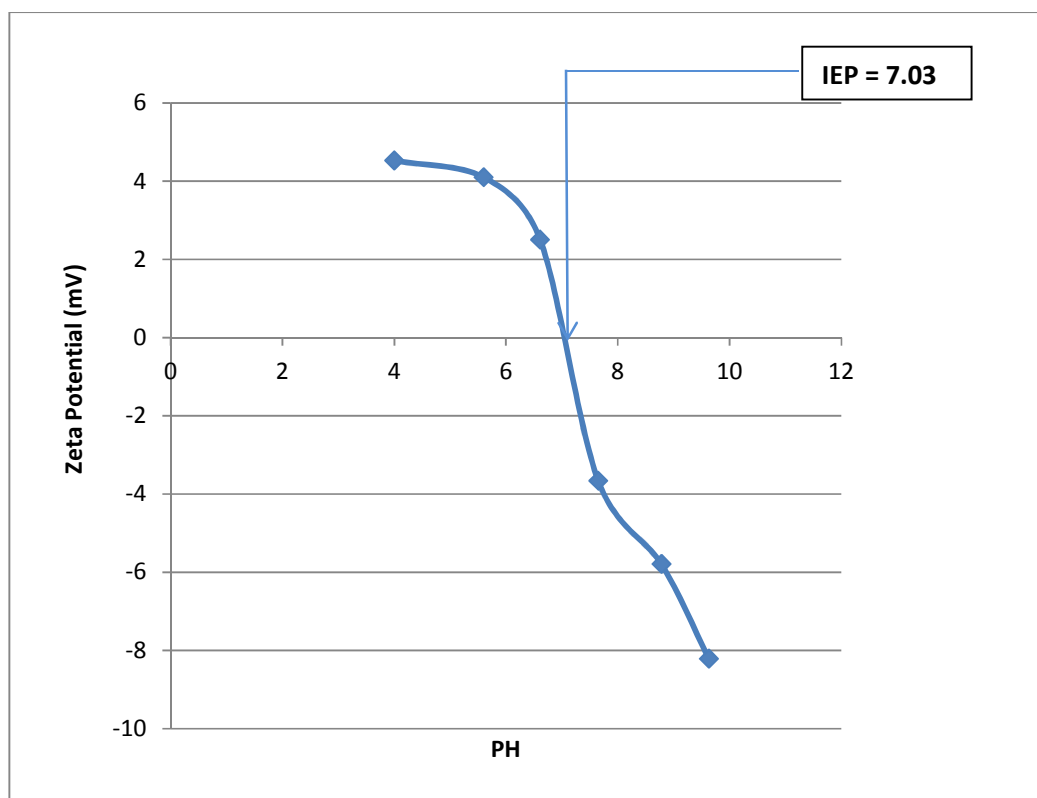


Figure 77: Zeta Potential profile of limestone in deionized water as a function of pH at 25°C.

4.2.2.2 Impact of Calcium, Magnesium, Sulfate, Carbonate, and Bi-Carbonate ions on the Zeta Potential of limestone

The effects of increasing the concentrations of calcium, magnesium, sulfate, carbonate and bi-carbonate ions in clean brines (brines containing only one ion) on the zeta potential of limestone are presented in Figure 78. It is observed that increases in the ionic concentrations of calcium and magnesium ions increased the positivity of the surface charge of limestone as can be seen from Figures 78a and 78b. Conversely, increasing the ionic concentrations of sulfate, carbonate and bi-carbonate ions decreased the zeta potential of limestone, thus confirming all these ions as potential determining ions of limestone. It is interesting to see from Figure 78d that the effect of carbonate ion overweighs that of bi-carbonate ion, which means that the carbonate ion is a stronger potential determining ion for limestone than bi-carbonate ion.

Sulfate ion effect on carbonate charges has been identified to be very crucial for improved oil recovery [1, 12, 22, 23, 25], and so further evaluation was carried out on the relative strength of SO_4^{2-} in the presence of Ca^{2+} and Mg^{2+} on the Zeta Potential of limestone. The results, which are presented in Figure 79, indicate that as the SO_4^{2-} to Ca^{2+} and SO_4^{2-} to Mg^{2+} ratios increase, the zeta potential of limestone decreases. It is also interesting to observe the trends in this figure which generally emphasizes again that the higher the sulfate concentration in the brine, the higher the reduction of the surface charge of limestone.

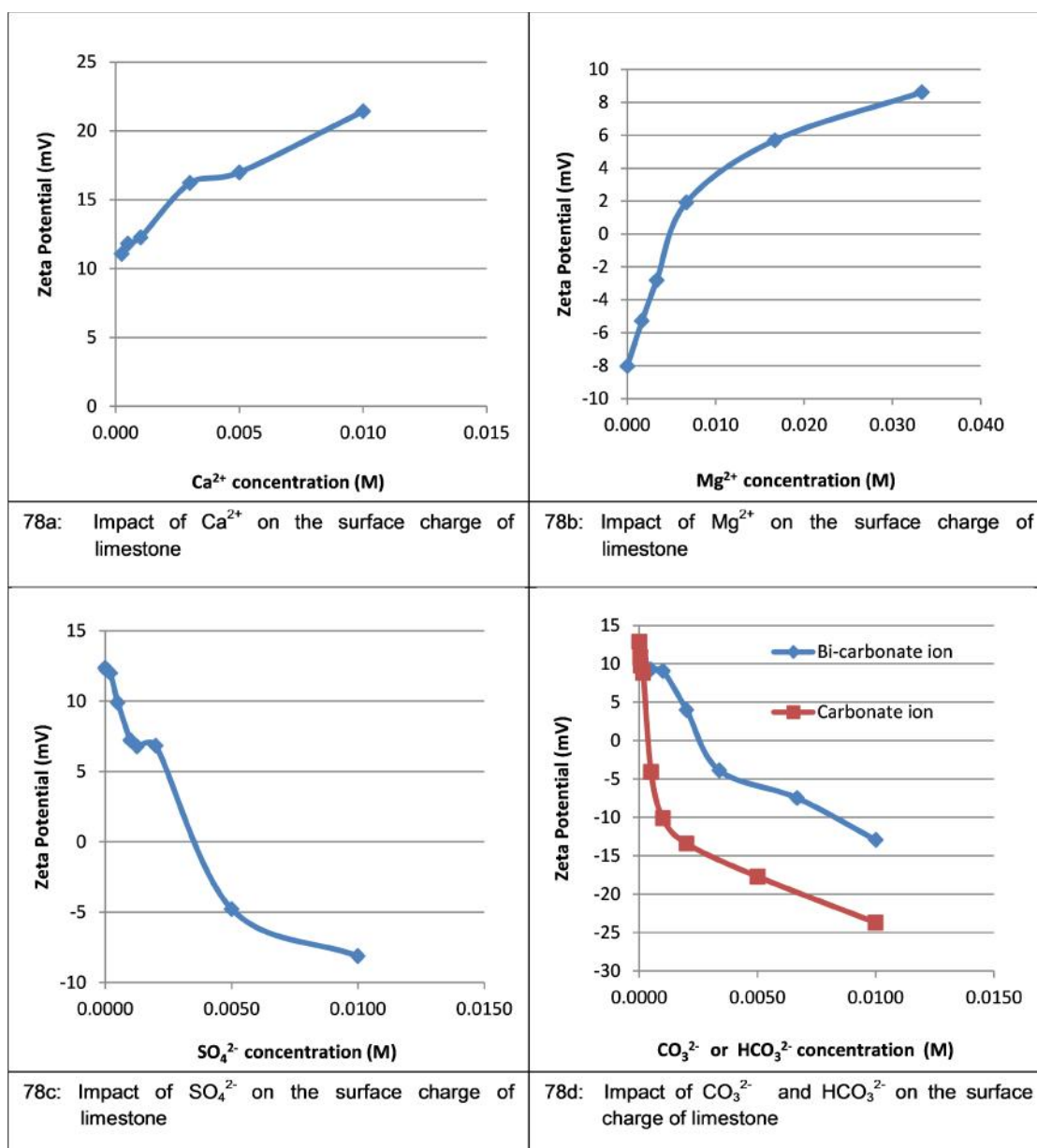
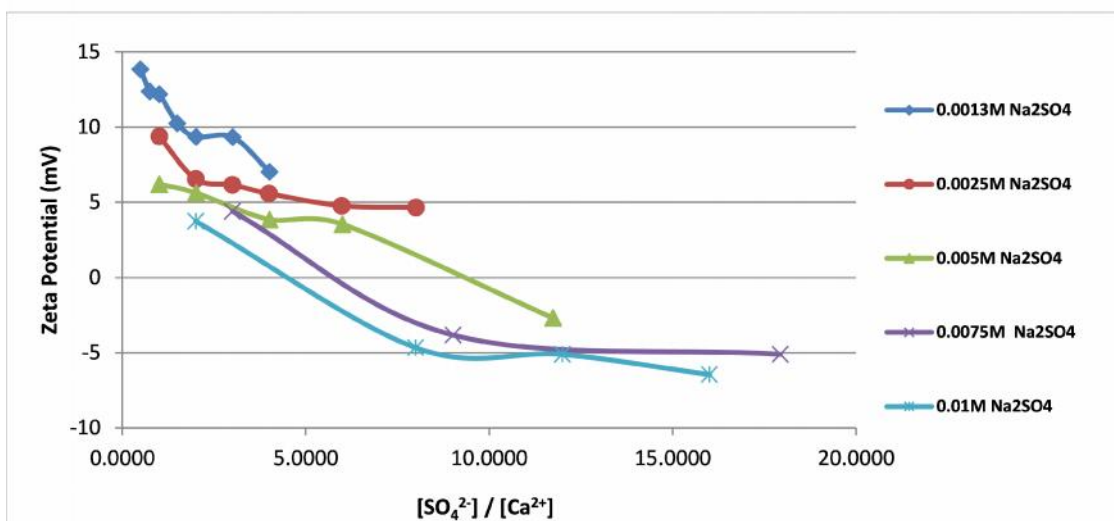
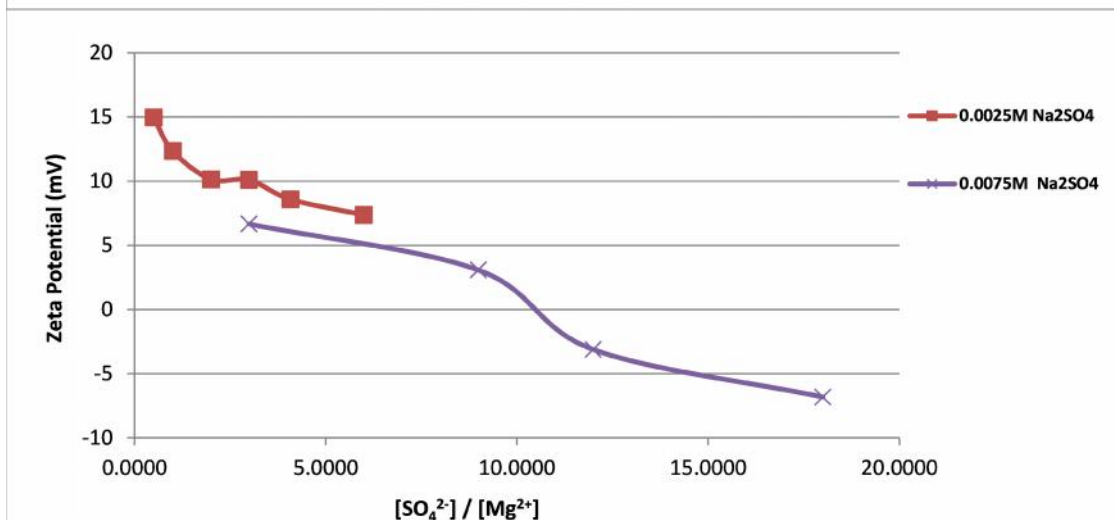


Figure 78: Impact of Ca^{2+} , Mg^{2+} , SO_4^{2-} , CO_3^{2-} , and HCO_3^- on the zeta potential of limestone at 25°C



79a: Impact of $[\text{SO}_4^{2-}] / [\text{Ca}^{2+}]$ on the surface charge of limestone



79b: Impact of $[\text{SO}_4^{2-}] / [\text{Mg}^{2+}]$ on the surface charge of limestone

Figure 79: Effect of varying $\text{SO}_4^{2-} / \text{Ca}^{2+}$ and $\text{SO}_4^{2-} / \text{Mg}^{2+}$ ratios on the zeta potential of limestone

4.2.2.3 Zeta potential of limestone in seawater

Zeta potential of limestone particles were measured after conditioning in seawater in the absence and presence of crude oil at 25 °C. Table 4 presents the compositions of the 16 brines used in this study. Because most carbonate reservoirs have pH values of 7-8 [84], all our zeta potential measurements were made at pH ranging from 7.4 to 7.5. Results presented in Figure 80 indicate a negative zeta potential between 0 and -12 mV for the limestone particles in all the 16 brines. Alotaibi et al. [85] reported negative zeta potential values of -12.72 mV and -4.65 mV for oil-wet and intermediately-wet limestone particles respectively in seawater at pH 8. A value of -8.3mV has been reported for dolomite particles in 10% diluted seawater [69]. Yousef et al. [66] reported recently about -2.5mV and -10mV for carbonate particles in twice diluted seawater at 40°C and 60°C respectively at pH 7-8. Reduction in the ionic strength of seawater by dilution was also shown to change the zeta potential of carbonate rock towards more negative, and eventually alter rock wettability [66]. Even though wettability tests are beyond the scope of this thesis, it has been confirmed that limestone particles will interact differently in different fluid environments. Figure 80 also shows that the presence of crude oil made the surface charge of limestone particles more negative than in the absence of oil. This can be attributed to the fact that more calcium ions were able to leave the carbonate lattice in the presence of oil, thus creating more negative charges [69]. This zeta potential result thus confirms the adsorption results presented earlier in Figures 45 and 46. Ca^{2+} raw adsorption experimental results for limestone presented in Figure 81 also confirms this result.

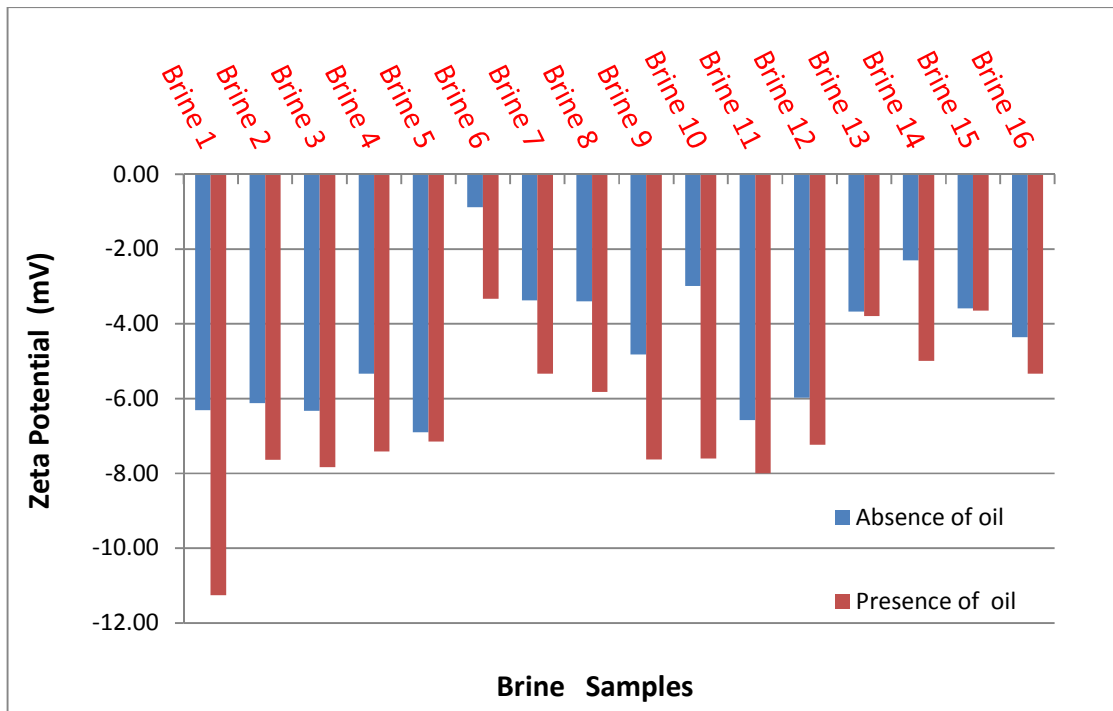


Figure 80: Zeta potential of limestone in modified seawater brines in the presence and absence of crude oil at 25°C

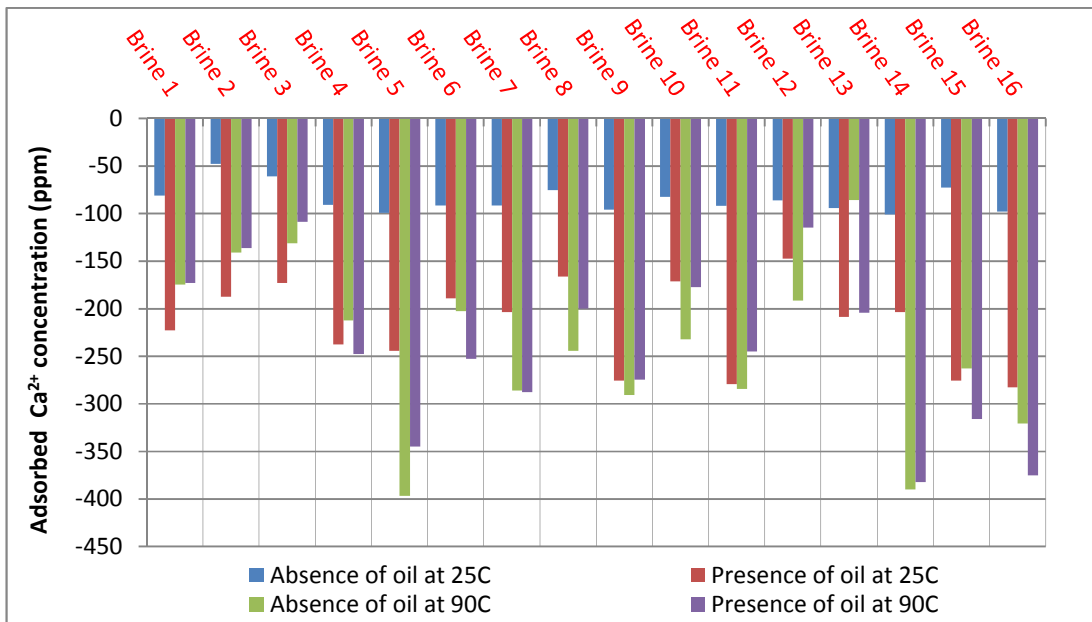


Figure 81: Ca^{2+} raw experimental adsorption result on limestone

Figures 82, 83, and 84 also present respectively Mg^{2+} , SO_4^{2-} , and Cl^- raw adsorption experimental results for limestone in the presence and absence of crude oil at 25°C and 90°C. It is generally observed from figure 82 that Mg^{2+} adsorption onto limestone occurred mostly in the absence and presence of crude oil at 90°C, while most desorptions of Mg^{2+} occurred in the absence and presence of crude oil at 25°C. Figure 83 shows mostly desorption of SO_4^{2-} from the limestone at all conditions, with Cl^- showing both adsorptions and desorptions at all conditions as can be seen from figure 84.

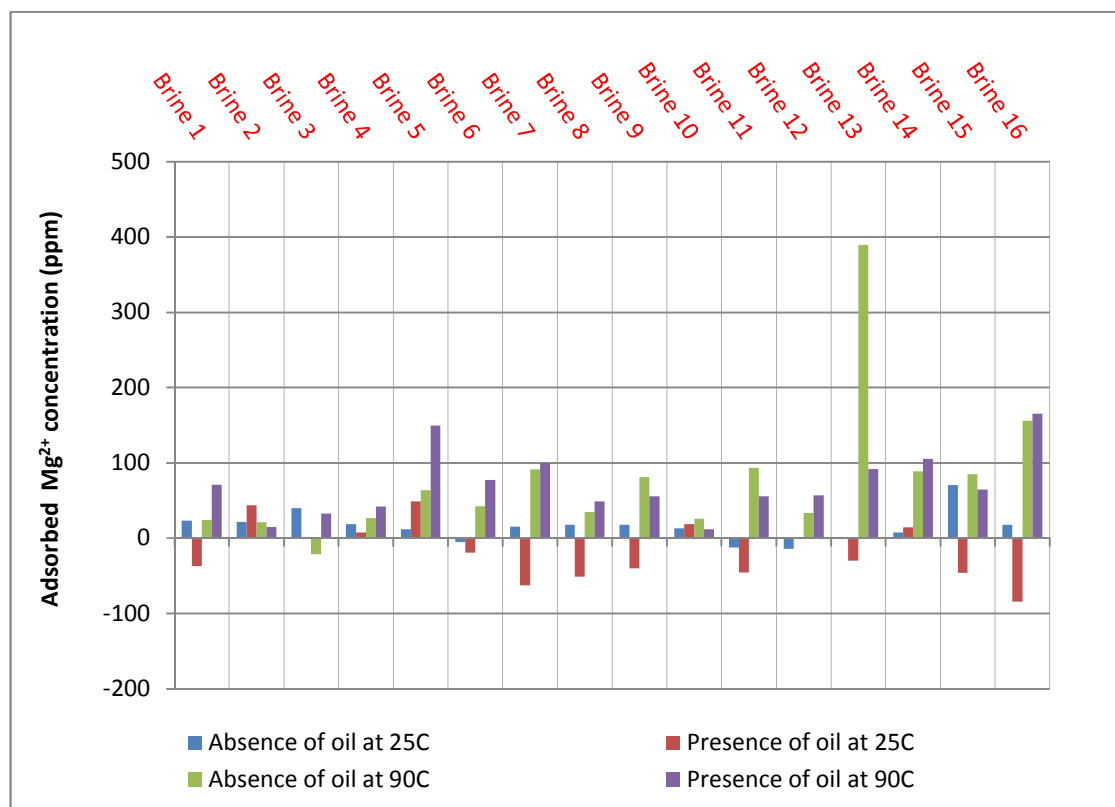


Figure 82: Mg^{2+} raw experimental adsorption result on limestone

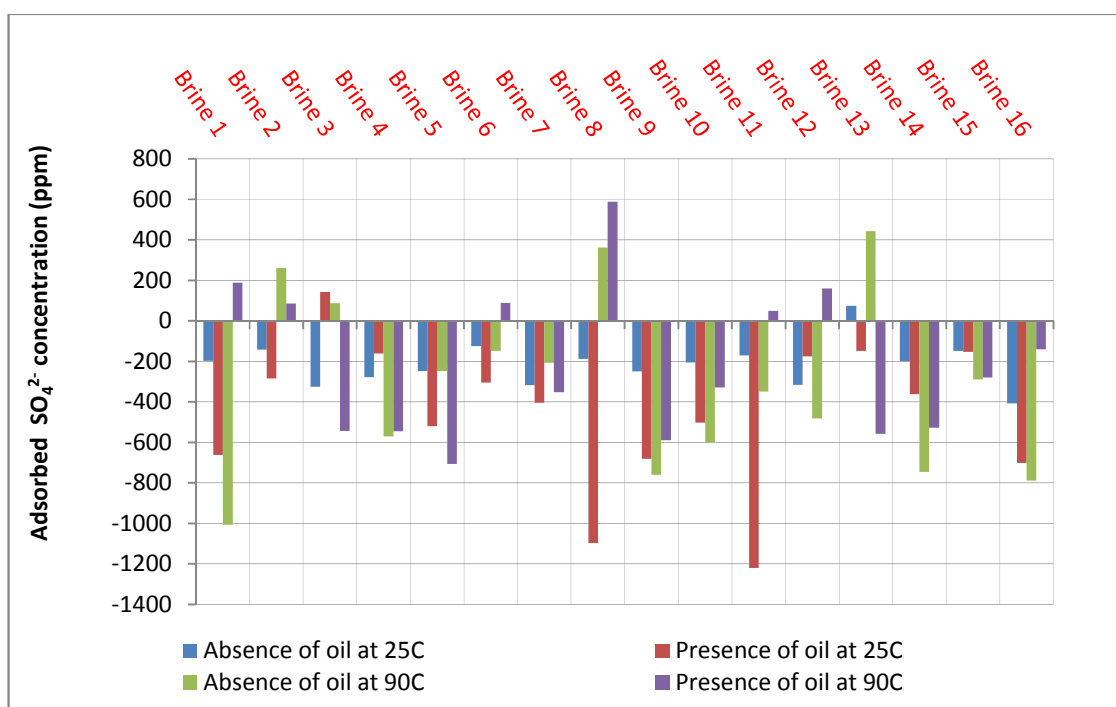


Figure 83: SO_4^{2-} raw experimental adsorption result on limestone

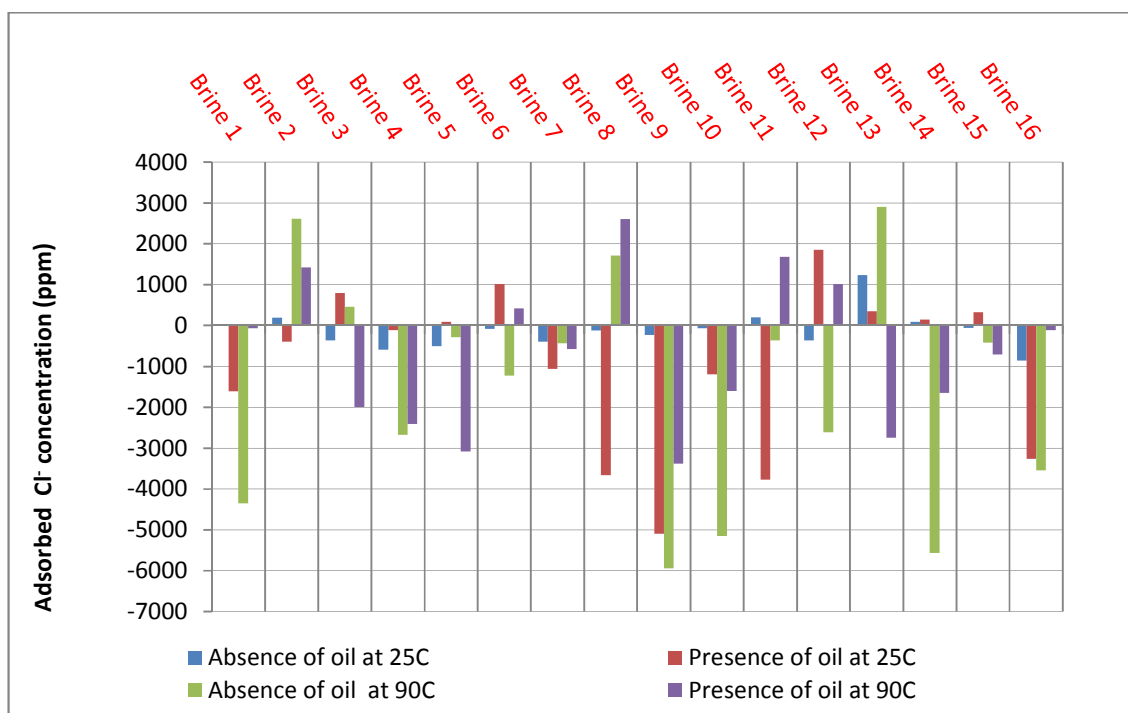


Figure 84: Cl^- raw experimental adsorption result on limestone

4.2.2.4 Impact of Temperature on the Zeta Potential of Limestone

The effect of temperature on the zeta potential of limestone was evaluated using deionized water and 25% SW (4 times diluted seawater) at three different temperatures, specifically 40°C, 55°C and 70°C. The results, which are presented in Figure 85 show that the zeta potential values decrease with an increase in temperature. The solubility of calcium ion increases with temperature, resulting into more Ca^{2+} leaving the carbonate crystal lattice, hence creating more negative charges [69]. This observation is consistent with results presented earlier in Figure 11 for the PCC and also with the findings of Alotaibi et al. [69], Yousef et al. [66], and Rodriguez and Araujo [83].

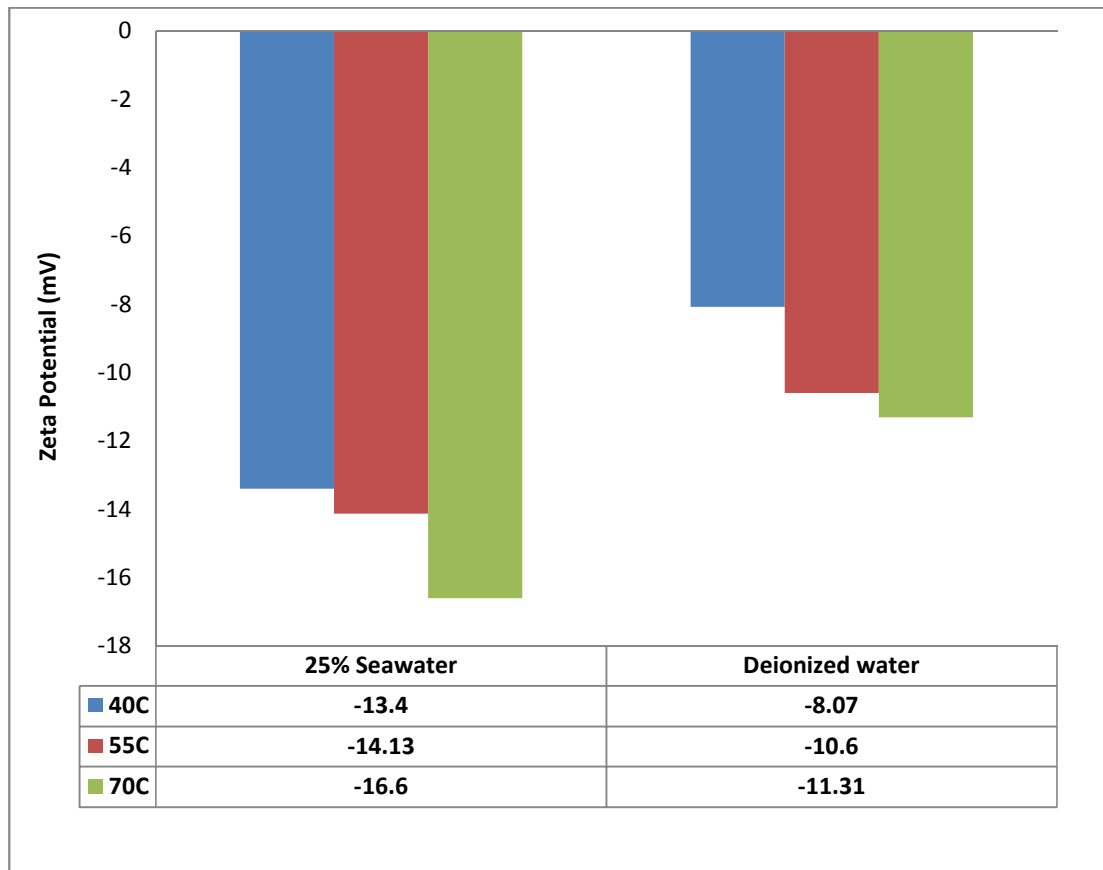


Figure 85: Effect of temperature on the zeta potential of limestone

CHAPTER 5

CONCLUSIONS AND RECOMMENDATIONS

5.1 CONCLUSIONS

Based on the results of this study, the following main conclusions can be drawn:

- The rock-fluid interactions of Ca^{2+} , Mg^{2+} , SO_4^{2-} , and Cl^- in seawater with carbonate rocks are dependent on the rock type and constituents, brine composition, presence of crude oil, and reservoir temperature.
- Fundamental adsorption studies on precipitated calcium carbonate (PCC) showed that calcium, magnesium, and sulfate ions will adsorb onto PCC from brine, and the magnitude of adsorption is directly proportional to the concentration of these ions in brine.
- Adsorption of calcium and magnesium ions onto PCC increased with temperature, and substitution of calcium ion on the PCC crystal lattice by magnesium ion increased significantly with temperature.
- Zeta potential results on PCC confirm that calcium, magnesium, and sulfate ions are potential determining ions for PCC by altering the surface charge of PCC.

- Adsorption results on limestone in the absence of crude oil at 25°C showed that calcium ion adsorption onto limestone can be enhanced by increasing calcium ion concentration in seawater, and decreasing magnesium or chloride ion concentrations or both. Magnesium ion adsorption will be promoted mostly by decreasing either calcium or chloride ion's concentrations in seawater. Decrease of calcium ion in seawater will tremendously reduce adsorption of sulfate ion onto limestone. Increasing the concentrations of calcium and chloride ions in seawater will enhance chloride ion adsorption. Anhydrite (CaSO_4) dissolution will be promoted by decreasing calcium ions in the injected or surrounding seawater.
- Adsorption results on limestone in the presence of crude oil at 25°C showed that increasing the calcium ion concentration in the injected seawater will significantly promote calcium ion adsorption, while magnesium ion adsorption onto the limestone can be enhanced by mostly reducing the concentrations of both sulfate and chloride ions simultaneously in seawater. Decreasing Ca^{2+} concentration in seawater will significantly hinder sulfate and chloride ion's adsorption onto limestone under this condition. Anhydrite (CaSO_4) dissolution will be significantly promoted by decreasing calcium ions in the injected or surrounding seawater.
- Adsorption results on limestone in the absence of crude oil at 90°C showed that increasing calcium ion in injected seawater is the optimum way to enhance calcium ion adsorption onto the limestone rock. Magnesium ion adsorption can be optimally enhanced by simultaneously increasing either the concentrations of sulfate and magnesium ions or sulfate and chloride ions in the injected seawater. Sulfate ion adsorption can mostly be promoted by increasing calcium ions in seawater, while simultaneously increasing calcium and decreasing chloride ion concentrations in

seawater is the optimum way to enhance chloride ion adsorption onto limestone. Anhydrite dissolution can be enhanced by decreasing both calcium and magnesium ions, decreasing both calcium and sulfate ions, and decreasing and increasing calcium and chloride ions respectively simultaneously in seawater.

- Limestone rock-fluid interactions in the presence of crude oil at 90°C showed that calcium ion adsorption can be increased by simultaneously increasing and decreasing the calcium and magnesium ions respectively in the injected seawater, while magnesium ion adsorption can be promoted by simultaneously decreasing the calcium ions with an increase in either magnesium or sulfate ions. Increasing both calcium and sulfate ions, and decreasing chloride ions in the injected seawater will significantly promote sulfate ion adsorption onto limestone, while chloride ion adsorption can be significantly enhanced onto limestone by increasing both sulfate and calcium ions in the injected seawater. Anhydrite dissolution from limestone in the presence of crude oil at 90°C can be significantly enhanced by decreasing both calcium and sulfate ions, while also increasing both magnesium and chloride ions.
- Temperature increase altered the adsorption interactions of our ions with limestone, by mostly the substitution reaction of magnesium ion, and the decrease in sulfate desorption from the limestone.
- Zeta potential results on limestone confirm that calcium, magnesium, sulfate, carbonate and bi-carbonate ions are potential determining ions of limestone by altering its surface charge.
- Limestone is negatively charged in seawater at pH range of 7.4 to 7.5. This surface charge was found to vary with different brine compositions, and the presence of crude oil generally decreased the zeta potential of limestone in seawater at 25°C.

- Increasing temperature reduced the surface charge of PCC and limestone in brine.

5.2 RECOMMENDATIONS

Having established the fundamental ionic interactions of Ca^{2+} , Mg^{2+} , SO_4^{2-} , and Cl^- in seawater with limestone, the following suggestions are recommended for future studies:

- Spontaneous imbibition and core-flooding of limestone cores should be done with the 16 brines utilized in the adsorption studies in order to assess their oil recovery potential.
- After assessing the oil recovery potential of the 16 brines, reference should be made back to the individual ionic adsorption raw results of the high potential brines to assess the kind of interactions taking place. Optimization of the interactions should then be done with the conclusions derived from the ANOVA adsorption studies.
- Zeta potential studies on limestone in diluted seawater, supported by wettability studies should be carried out to shed light on the relationship between zeta potential and wettability

APPENDIX

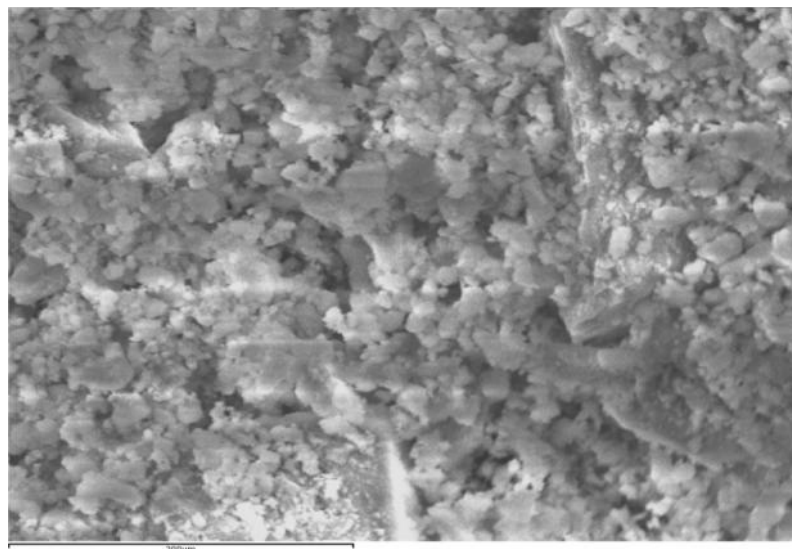


Figure A1: SEM image of Limestone

Table A1: Ca^{2+} raw experimental adsorption data on limestone

	Absence of oil at 25°C	Presence of oil at 25°C	Absence of oil at 90°C	Presence of oil at 90°C
Brines	$C_o - C_e$ (ppm)	$C_o - C_e$ (ppm)	$C_o - C_e$ (ppm)	$C_o - C_e$ (ppm)
Brine 1	-81.4	-222.6	-174.5	-173
Brine 2	-48	-187.2	-141.3	-136.4
Brine 3	-61.1	-172.8	-131.3	-108.8
Brine 4	-90.8	-237.4	-212.1	-247.4
Brine 5	-99.2	-244.4	-396.6	-344.7
Brine 6	-91.6	-188.8	-202.6	-252.7
Brine 7	-91.3	-203.8	-285.7	-287.6
Brine 8	-75.4	-166.3	-244.3	-199.7
Brine 9	-95.9	-275.4	-290.7	-274.5
Brine 10	-82.5	-171.3	-232.3	-177.2
Brine 11	-92.2	-279.2	-284.1	-244.8
Brine 12	-86.1	-147.4	-191.7	-114.6
Brine 13	-94.3	-208.6	-85.9	-204.3
Brine 14	-101	-203.8	-390	-382
Brine 15	-72.7	-275.3	-262.5	-316
Brine 16	-98	-282.5	-320.5	-375.1

Table A2: Mg^{2+} raw experimental adsorption data on limestone

	Absence of oil at 25°C	Presence of oil at 25°C	Absence of oil at 90°C	Presence of oil at 90°C
Brines	$C_o - C_e(\text{ppm})$	$C_o - C_e(\text{ppm})$	$C_o - C_e(\text{ppm})$	$C_o - C_e(\text{ppm})$
Brine 1	23.2	-37.2	24.3	71.1
Brine 2	21.7	43.7	21.4	14.7
Brine 3	39.8	1.9	-21.2	32.8
Brine 4	18.7	7.4	26.5	42
Brine 5	11.9	49.1	63.7	149.5
Brine 6	-5.4	-19.4	42.2	77.2
Brine 7	15	-62.8	91.4	99.9
Brine 8	17.8	-51.1	34.8	49.1
Brine 9	17.8	-39.8	81.4	55.5
Brine 10	13	18.8	25.7	11.9
Brine 11	-12.1	-45.5	93.1	55.8
Brine 12	-14	1.1	33.5	56.7
Brine 13	1.7	-29.5	389.3	91.6
Brine 14	7.5	14.1	88.9	105.1
Brine 15	70.7	-46.4	85.1	64.6
Brine 16	18	-84.3	156.1	165.1

Table A3: SO_4^{2-} raw experimental adsorption data on limestone

	Absence of oil at 25°C	Presence of oil at 25°C	Absence of oil at 90°C	Presence of oil at 90°C
Brines	$C_o-C_e(\text{ppm})$	$C_o-C_e(\text{ppm})$	$C_o-C_e(\text{ppm})$	$C_o-C_e(\text{ppm})$
Brine 1	-197	-661	-1006.9	187.85
Brine 2	-141	-285	262.5	86.5
Brine 3	-324	143	88.05	-543.8
Brine 4	-278	-161	-571.35	-544.15
Brine 5	-248	-520	-247.95	-705.95
Brine 6	-125	-304	-148	89.7
Brine 7	-317	-405	-205.55	-352.8
Brine 8	-188	-1098	361.45	587.6
Brine 9	-250	-682	-759.8	-590
Brine 10	-204	-503	-598.85	-329.9
Brine 11	-170	-1221	-350.05	49.55
Brine 12	-315	-175	-481.25	159.85
Brine 13	74	-148	442.65	-558.85
Brine 14	-198	-361	-745.9	-527.35
Brine 15	-148	-153	-289.55	-280.2
Brine 16	-408	-702	-790.05	-139.35

Table A4: Cl⁻ raw experimental adsorption data on limestone

	Absence of oil at 25°C	Presence of oil at 25°C	Absence of oil at 90°C	Presence of oil at 90°C
Brines	C _o -C _e (ppm)	C _o -C _e (ppm)	C _o -C _e (ppm)	C _o -C _e (ppm)
Brine 1	8	-1605	-4353.55	-62.5
Brine 2	193	-390	2624.25	1423.5
Brine 3	-364	799	465.1	-1995.65
Brine 4	-593	-111	-2674.25	-2407.6
Brine 5	-498	94	-285.6	-3080.3
Brine 6	-77	1020	-1224	426.95
Brine 7	-396	-1057	-432.3	-572.6
Brine 8	-115	-3663	1712	2612.75
Brine 9	-228	-5092	-5939.85	-3377.3
Brine 10	-67	-1195	-5156.8	-1598.85
Brine 11	205	-3771	-360.4	1681.95
Brine 12	-362	1857	-2612.35	1021.25
Brine 13	1238	355	2910.9	-2739.85
Brine 14	92	147	-5564.35	-1647.5
Brine 15	-59	332	-413.45	-705.75
Brine 16	-857	-3264	-3548	-110.1

**METHOD AND EQUATIONS USED IN THE ESTIMATION OF EQUILIBRUM
CONSTANTS AT 90°C FOR CALCIUM ION ADSORPTION DATA ANALYSIS
FOR PCC**

$$K_w \text{ at } 90^\circ\text{C} = 53 \times 10^{-14} [72]$$

$$K_{sp} = 9.237\text{E-}9 e^{-0.0277 T}, \text{ where } T \text{ is in } ^\circ\text{C} [76]$$

Acid dissociation constants for carbonic acid were calculated utilizing these two equations below [74];

$$pK_1 = 3404.71/T + 0.032786T - 14.8435$$

$$pK_2 = 2902.39/T + 0.02379T - 6.4980$$

where the absolute temperature $T = t(^{\circ}\text{C}) + 273.15 \text{ K}$.

$$\text{Then, } K_a = 10^{(-pK_a)}$$

$$K_b = \frac{K_w}{K_a} [75] \quad ;$$

K_b = Base dissociation constant

NOMENCLATURE

$[\text{Ca}^{2+}]$: Calcium ion concentration
$[\text{Mg}^{2+}]$: Magnesium ion concentration
$[\text{SO}_4^{2-}]$: Sulfate ion concentration
$[\text{Cl}^-]$: Chloride ion concentration
C_i	: Initial ionic concentration
C_e	: Equilibrium ionic concentration
$[\text{Ca}^{2+}]_e$: Calcium ion equilibrium concentration
$[\text{Mg}^{2+}]_e$: Magnesium ion equilibrium concentration
$[\text{SO}_4^{2-}]_e$: Sulfate ion equilibrium concentration
$[\text{Cl}^-]_e$: Chloride ion equilibrium concentration
$[\text{Ca}^{2+}]_{\text{ads}}$: Adsorbed calcium ion concentration
$[\text{Ca}^{2+}]_{\text{ini}}$: Initial calcium ion concentration
$[\text{Ca}^{2+}]_{\text{diss}}$: Dissociated calcium ion concentration
ppm	: parts per million
M	: Mole/Liter
PCC	: Precipitated Calcium Carbonate
K_{sp}	: Solubility Constant
K_b	: Base dissociation constant
K_w	: Water dissociation constant
OOIP	: Original oil in place
LSE	: Low Salinity Effect
Wt. %	: Weight Percent

At. %	: Atomic Percent
50% SW	: Twice-diluted seawater
25% SW	: 4 times-diluted seawater
ZP	: Zeta Potential
EM	: Electrophoretic Mobility
A1	: 325 ppm Ca^{2+}
A2	: 650 ppm Ca^{2+}
B1	: 1055 ppm Mg^{2+}
B2	: 2100 ppm Mg^{2+}
C1	: 2145 ppm SO_4^{2-}
C2	: 4290 ppm SO_4^{2-}
D1	: 17006 ppm Cl^-
D2	: 25000 ppm Cl^-
A1-B1	: 325 ppm Ca^{2+} , 1055 ppm Mg^{2+}
A1-B2	: 325 ppm Ca^{2+} , 2100 ppm Mg^{2+}
A2-B1	: 650 ppm Ca^{2+} , 1055 ppm Mg^{2+}
A2-B2	: 650 ppm Ca^{2+} , 2100 ppm Mg^{2+}
A1-C1	: 325 ppm Ca^{2+} , 2145 ppm SO_4^{2-}
A1-C2	: 325 ppm Ca^{2+} , 4290 ppm SO_4^{2-}
A2-C1	: 650 ppm Ca^{2+} , 2145 ppm SO_4^{2-}
A2-C2	: 650 ppm Ca^{2+} , 4290 ppm SO_4^{2-}
A1-D1	: 325 ppm Ca^{2+} , 17006 ppm Cl^-
A1-D2	: 325 ppm Ca^{2+} , 25000 ppm Cl^-
A2-D1	: 650 ppm Ca^{2+} , 17006 ppm Cl^-

A2-D2	: 650 ppm Ca^{2+} , 25000 ppm Cl^-
B1-C1	: 1055 ppm Mg^{2+} , 2145 ppm SO_4^{2-}
B1-C2	: 1055 ppm Mg^{2+} , 4290 ppm SO_4^{2-}
B2-C1	: 2100 ppm Mg^{2+} , 2145 ppm SO_4^{2-}
B2-C2	: 2100 ppm Mg^{2+} , 4290 ppm SO_4^{2-}
B1-D1	: 1055 ppm Mg^{2+} , 17006 ppm Cl^-
B1-D2	: 1055 ppm Mg^{2+} , 25000 ppm Cl^-
B2-D1	: 2100 ppm Mg^{2+} , 17006 ppm Cl^-
B2-D2	: 2100 ppm Mg^{2+} , 25000 ppm Cl^-
C1-D1	: 2145 ppm SO_4^{2-} , 17006 ppm Cl^-
C1-D2	: 2145 ppm SO_4^{2-} , 25000 ppm Cl^-
C2-D1	: 4290 ppm SO_4^{2-} , 17006 ppm Cl^-
C2-D2	: 4290 ppm SO_4^{2-} , 25000 ppm Cl^-

REFERENCES

- [1] Strand, S., Austad, T., Puntervold, T., Hognesen, E.J., Olsen, M., and Barstad, S.M.F., "Smart Water for oil recovery from fractured Limestone-A preliminary study". Energy & Fuels, 2008, 22, 3126–3133.
- [2] Austad, T., "Seawater in Chalk: An EOR and Compaction fluid". Paper presented at the 42nd US Rock mechanics symposium and 2nd US-Canada Rock mechanics symposium, San Francisco, USA, June 29-July 2, 2008.
- [3] Sharma, G., and Mohanty, K.K., "Wettability Alteration in High Temperature and High Salinity Carbonate Reservoirs". Paper SPE 147306 presented at the SPE Annual Technical Conference and Exhibition, Denver, Colorado, USA, October 30-November 2, 2011.
- [4] Morrow, N., and Buckley, J. "Improved oil recovery by low-salinity flooding". Distinguished Author Series, JPT, May, 2011, 106–112.
- [5] Yousef, A.A., Al-Saleh, S.H., Al-Kaabi, A.O., and Al-Jawfi, M.S., "Laboratory Investigation of Novel Oil Recovery Method for Carbonate Reservoirs". Paper CSUG/SPE 137634, presented at the Canadian Unconventional Resources & International Petroleum Conference, Calgary, Alberta, Canada, 19–21 October 2010.
- [6] Cossé, R. Basics of reservoir engineering. Oil and gas field development techniques. 1993 Éditions Technip, Paris. ISBN 2-7108-0630-4. Printed in France by Imprimerie Nouvelle, 45800 Saint-Jean-de-Braye.
- [7] Davies, S., and Kelkar, S., "Carbonate Stimulation". Middle East and Asia Reservoir Review. Number 8, 2011, 52-62.
- [8] http://en.wikipedia.org/wiki/Ghawar_Field.
- [9] http://en.wikipedia.org/wiki/South_Pars/North_Dome#cite_ref-0.
- [10] <http://geology.com/rocks/limestone.shtml>.
- [11] Puntervold, T., "Waterflooding of carbonate reservoirs, EOR by wetting alteration". PhD Thesis, University of Stavanger, Norway. 2008
- [12] Hognesen, E.J., Strand, S., and Austad, T., "Waterflooding of Preferential Oil-Wet carbonates: Oil Recovery Related to Reservoir Temperature and Brine Composition". Paper SPE 94166 presented at the SPE Europec/EAGE Annual Conference, Madrid, Spain, June 13-16, 2005.

- [13] Strand, S., Standnes, D.C., and Austad, T., “New Wettability test for chalk based on Chromatographic separation of SCN^- and SO_4^{2-} ”. *Journal of Petroleum Science and Engineering*, 2006, 52, 187–197.
- [14] Dubey, S.T., and Doe, P.H., “Base Number and Wetting Properties of Crude Oils”. *SPE Reservoir Engineering*, 1993, 195–200.
- [15] Hirasaki, G.J., “Wettability: Fundamentals and surface Forces”. *SPE Formation Evaluation*, 1991, 217–226.
- [16] Zhang, P., Tweheyo, M.T., and Austad, T., “Wettability Alteration and Improved Oil Recovery in Chalk: The Effect of calcium in the presence of Sulfate”. *Energy & Fuels*, 2006, 20, 2056–2062.
- [17] Standnes, D. C., Nogaret, L. A. D., Chen, H.-L., and Austad, T., “An evaluation of spontaneous imbibition of water into oil-wet carbonate reservoir cores using a non-ionic and a cationic surfactant”. *Energy & Fuels*, 2002, 16(6), 1557–1564.
- [18] Standnes, D.C., and Austad, T., “Wettability Alteration in chalk 2. Mechanism for Wettability alteration from oil-wet to water-wet using surfactants”. *Journal of Petroleum Science and Engineering*, 2000, 28, 123–143.
- [19] Gupta, R., and Mohanty, K.K., “Temperature effects on Surfactant-Aided Imbibition into fractured Carbonates”. Paper SPE 110204, September, 2010.
- [20] Kokal, S., and Al-Kaabi, A., “Enhanced oil recovery: Challenges and opportunities”. *World Petroleum Council, Official Publication* 2010, 64–69.
- [21] Zeta-meter 3.0 Manual, Zeta-Meter INC., 50-17 Fifth Street, Long Island City, N.Y. 11101. ZM 3+ Revision 2 May 1991.
- [22] Austad, T., Strand, S., Høgnesen, E.J., and Zhang, P., “Seawater as IOR fluid in fractured chalk”. Paper SPE 93000 presented at the 2005 SPE International Symposium on Oilfield Chemistry, Houston, TX, USA, February 2–4, 2005.
- [23] Webb, K.J., Black, C.J.J., and Tjetland, G., “A laboratory study investigating methods for improving oil recovery in carbonates”. Paper IPTC10506 presented at the International Petroleum Technology Conference, Doha, Qatar, November 21–23, 2005.
- [24] Zhang, P. and Austad, T., 2006. “Wettability and oil recovery from carbonates: Effects of temperature and potential determining ions”. *Colloids and Surfaces A: Physicochem. Eng. Aspects*, 279: 179–187.

- [25] Zhang, P., Tweheyo, M.T., and Austad, T., “Wettability alteration and improved oil recovery by spontaneous imbibition of seawater into chalk: Impact of the potential determining ions Ca^{2+} , Mg^{2+} , and SO_4^{2-} ”. Colloids and Surfaces A: Physicochem. Eng. Aspects, 2007, 301: 199-208.
- [26] Zhang, P. and Austad, T., 2004. “Waterflooding in chalk: Relationship between oil recovery, new wettability index, brine composition and cationic wettability modifier”, Paper SPE 94209 presented at the 14th Europec biennial conference. Society of petroleum engineers, Madrid, Spain
- [27] Austad, T., Strand, S., and Puntervold, T., “Is Wettability Alteration of carbonates by Seawater caused by Rock Dissolution”. Paper SCA2009-43 presented at the International Symposium of the Society of Core Analysts held in Noordwijk, The Netherlands, September 27-30, 2009.
- [28] Hiorth, A., Cathles, L.M and Madland, M.V., “The Impact of Pore Water Chemistry on Carbonate Surface Charge and Oil Wettability”. Transp Porous Med, 2010, 85, 1–21.
- [29] Ferno, M.A., Gronsdal, R., Asheim, J., Nyheim, A., Berge, M., and Graue, A., “Use of Sulfate for Water Based Enhanced Oil Recovery during Spontaneous Imbibition in chalk”. Article in Energy & Fuels, 2011.
- [30] Zahid, A., Stenby, E.H., and Shapiro, A.A., “Improved Oil Recovery in chalk: Wettability Alteration or something else?”. Paper SPE 131300 presented at the SPE Europec/EAGE Annual Conference and Exhibition, Barcelona, Spain, June 14-17, 2010.
- [31] Gupta, R., Griffin Smith, P.(Jr), Hu, L., Willingham, T.W., Cascio, M.L., Shyeh, J.J., and Harris, C.R., “Enhanced Waterflood for Middle East Carbonate Cores- Impact of Injection Water Composition”. Paper SPE 142668 presented at the SPE Middle East Oil and Gas Show and conference, Manama, Bahrain, September 25-28, 2011.
- [32] Ligthelm, D.J., Gronsveld, J., Hofman, J.P., Brussee, N.J., Marcelis, F. and Van Der Lind, H.A., “Novel Waterflooding Strategy by Manipulation of Injection Brine Composition”. Paper SPE 119835, presented at the SPE EUROPEC/EAGE Annual Conference and Exhibition, Amsterdam, The Netherlands, June 8-11, 2009.
- [33] Fathi, S.J., Austad, T., and Strand, S., “Smart Water as a Wettability Modifier in chalk: The Effect of Salinity and Ionic Composition”. Energy & Fuels, 2010, 24, 2514–2519.
- [34] Fathi, S.J, Austad, T., and Strand, S., “Water-Based Enhanced Oil Recovery (EOR) by Smart Water in Carbonate Reservoirs”. Paper SPE 154570 presented at the SPE EOR conference at Oil and Gas West Asia, Muscat, Oman, April 16-18, 2012.

- [35] Shariatpanahi, S.F., Strand, S., and Austad, T., "Evaluation of Water-Based Enhanced Oil Recovery (EOR) by Wettability Alteration in a Low-Permeable Fractured Limestone Oil Reservoir". *Energy & Fuels*, 2010, 24, 5997–6008.
- [36] Martin, J.C., "The effects of clay on the displacement of heavy oil by water". Paper SPE 1411-G presented at the SPE of A.I.M.E. Venezuelan 3rd Annual meeting, Caracas, Venezuela, October 14-16, 1959.
- [37] Bernard, G.G., "Effect of floodwater salinity on recovery of oil from cores containing clays". Paper SPE 1725 presented at the SPE of A.I.M.E. 38th Annual California regional meeting, Los Angeles, California, October 26-27, 1967.
- [38] Jadhunandan, P., "Effects of brine composition, crude oil and aging conditions on wettability and oil recovery". PhD Thesis, 1990.
- [39] Jadhunandan, P., and Morrow, N.R., "Effect of wettability on waterflood recovery for crude oil/brine/rock systems". *SPE Reservoir Engineering*, 1995, 40–46.
- [40] Yildiz, H.O., and Morrow, N.R., "Effect of brine composition on recovery of Moutray crude oil by waterflooding". *Petroleum Science and Engineering*, 1996, 14, 159–168.
- [41] Tang, G.Q., and Morrow, N.R., "Salinity, Temperature, Oil composition, and Oil recovery by waterflooding". *SPE Reservoir Engineering*, 1997, 12(4), 269–276.
- [42] Tang, G.Q., and Morrow, N.R., "Influence of brine composition and fines migration on Crude oil/Brine/Rock interactions and oil recovery". *Journal of Petroleum Science and Engineering*, 1999, 24(2-4), 99–111.
- [43] Morrow, N.R., Tang, G.Q., Valat, M., and Xie, X., "Prospects of improved oil recovery related to wettability and brine composition". *Journal of Petroleum Science and Engineering*, 1998, 20(3-4), 267–276.
- [44] Zhang, Y., and Morrow, N.R., "Comparism of secondary and tertiary recovery with change in Injection Brine composition for crude oil/sandstone combinations". Paper SPE 99757 presented at the SPE/DOE symposium on improved oil recovery, Tulsa, USA, April 22-26, 2006.
- [45] Zhang, Y., Xie, X., and Morrow, N.R., "Waterflood performance by injection of brine with different salinity for reservoir cores". Paper SPE 109849 presented at the SPE Annual Technical Conference and Exhibition, Anaheim, California, USA, November 11-14, 2007.
- [46] Patil, S., Dandekar, A.Y., Patil, S.L., and Khataniar, S., "Low salinity brine injection for EOR on Alaska North Slope (ANS)". Paper IPTC 12004 presented at the International Petroleum Technology Conference, Kuala Lumpur, December 3-5, 2008.

- [47] Agbalaka, C.C., Dandekar, A.Y., Patil, S.L., Khataniar, S., and Hemsath, J.R., “Coreflooding studies to evaluate the impact of salinity and wettability on oil recovery efficiency”. *Transport in porous media*, 2009, 76(1), 77–94.
- [48] Lager, A., Webb, K.J., Black, C.J.J., Singleton, M. and Sorbie, K.S.: “Low Salinity Oil Recovery - An Experimental Investigation”. Paper presented at the Society of Core Analysts, Trondheim, Norway, September 12-16, 2006.
- [49] Winoto, W., Loahardjo, N., Xie, X., Yin, P., and Morrow, N.R., “Secondary and Tertiary recovery of crude oil from Outcrop and reservoir rocks by low salinity flooding”. Paper SPE 154209 presented at the 18th SPE symposium on improved oil recovery, Tulsa, USA, April 14-18, 2012.
- [50] Webb, K.J., Black, C.J.J., Al-Ajeel, H., “Low salinity Oil Recovery – Log-Inject-Log,” Paper SPE 81460 presented at the SPE 13th Middle East Oil Show and Conference held in Bahrain, April 5-8, 2003.
- [51] McGuire, P.L., Chatham, J.R., Paskvan, F.K., Sommer, D.M. and Carini, F.H., “Low Salinity Oil Recovery: An Exciting New EOR Opportunity for Alaska’s North Slope”. Paper SPE 93903, presented at the 2005 SPE Western Regional Meeting, Irvine, California, March 30-April 1, 2005.
- [52] Robertson, E.P., “Low-Salinity Waterflooding to Improve Oil Recovery—Historical Field Evidence”. Paper SPE 109965 presented at the SPE Annual Technical Conference and Exhibition, Anaheim, California, USA, 11–14 November, 2007.
- [53] Lager, A., Webb, K.J., Collins, I.R., and Richmond, D.M., “LoSalTM Enhanced Oil Recovery: Evidence of Enhanced Oil Recovery at the Reservoir Scale”. Paper SPE 113976 presented at the SPE/DOE Improved Oil Recovery Symposium, Tulsa, Oklahoma, USA, 19–23 April, 2008.
- [54] Seccombe, J., Lager, A., Jerauld, G., Jhaveri, B., Buikema, T., Bassler, S., Denis, J., Webb, K., Cockin, A., and Fueg, E., “Demonstration of Low-Salinity EOR at Interwell Scale, Endicott Field, Alaska. Paper SPE 129692 presented at the SPE/DOE Improved Oil Recovery Symposium, Tulsa, Oklahoma, USA, 24–28 April, 2010.
- [55] Vledder, P., Fonseca, J.C., Wells, T., Gonzalez, I., and Ligthelm, D., “Low Salinity Water Flooding: Proof of Wettability alteration on a field wide scale”. Paper SPE 129564 presented at the SPE/DOE Improved Oil Recovery Symposium, Tulsa, Oklahoma, USA, 24–28 April, 2010.
- [56] Berg, S., Cense, A.W., Jansen, E., and Bakker, K., “Direct Experimental Evidence of Wettability Modification by Low Salinity”. Paper SCA 2009-12 presented at the 23rd International symposium of the Society of Core Analysts, Noordwijk aan Zee, The Netherlands, September 27-30, 2009.

- [57] Nasralla, R.A., and Nasr-El-Din, H.A., “Double-Layer Expansion: Is it a Primary Mechanism of Improved Oil Recovery by Low-Salinity Waterflooding”. Paper SPE 154334 presented at the 18th SPE symposium on improved oil recovery, Tulsa, USA, April 14-18, 2012.
- [58] Pu, H., Xie, X., Yin, P., and Morrow, N.R., “Low Salinity Waterflooding and Mineral Dissolution”. Paper SPE 134042 presented at the SPE Annual Technical Conference and Exhibition, Florence, Italy, September 19-22, 2010
- [59] Nasralla, R.A., and Nasr-El-Din, H. A., “Coreflood Study of Low Salinity Water Injection in Sandstone Reservoirs”. Paper SPE 149077 presented at SPE/DGS Saudi Arabia Section Technical Symposium and Exhibition held in Al-Khobar, Saudi Arabia, 15-18 May, 2011.
- [60] RezaeiDoust, A., Puntervold, T., Strand, S., and Austad, T., “Smart Water as Wettability Modifier in Carbonate and sandstone: A Discussion of Similarities / Differences in the Chemical Mechanisms”. *Energy & Fuels*, 2009, 23, 4479–4485.
- [61] Zekri, A.Y., Nasr, M., and Zaid, A., “Effect of EOR technology on wettability and oil recovery of Carbonate and Sandstone formation”. Paper IPTC 14131 presented at the International Petroleum Technology Conference, Bangkok, Thailand, February 7-9, 2012.
- [62] Austad,T., RezaeiDoust, A., and Puntervold,T., “Chemical Mechanism of Low Salinity Flooding in Sandstone reservoirs”. Paper SPE 129767 presented at the SPE Improved Oil Recovery Symposium, Tulsa, USA, April 24-28, 2010.
- [63] Alotaibi, M.B., Nasralla, R.A., and Nasr-El-Din, H.A., “Wettability Challenges in Carbonate Reservoirs”. SPE 129972, presented at SPE Improved Oil Recovery Symposium, Tulsa, Oklahoma, 24-28 April 2010.
- [64] Romanuka,J., Hofman,J.P., Ligthelm, D.J., Suijkerbuijk, B.M.J.M., Marcelis, A.H.M., Oedai, S., Brussee,N.J.,Van der Linde, H.A.,Aksulu,H.,and Austad,T., “Low Salinity EOR in Carbonates”. Paper SPE 153869 presented at the 18th SPE Improved Oil Recovery Symposium, Tulsa, USA, April 14-18, 2012.
- [65] Austad, T., Shariatpanahi,S., Strand,S., Black,J., and Webb, K., “Conditions for a Low-Salinity Enhanced Oil Recovery (EOR) effect in Carbonate Oil Reservoirs”. *Energy & Fuels*, 2012, 26(1), 569–575.
- [66] Yousef, A.A., Al-saleh,S., and Al-Jawfi, M., “Improved/Enhanced Oil Recovery from Carbonate Reservoirs by Tuning Injection Water Salinity and Ionic Content”. Paper SPE 154076 presented at the 18th SPE Improved Oil Recovery Symposium, Tulsa, USA, April 14-18, 2012.

- [67] Zahid,A., Shapiro,A., and Skauge,A., “Experimental Studies of Low Salinity Water Flooding in carbonate Reservoirs: A New Promising Approach”. Paper SPE 155625 presented at the SPE EOR conference at Oil and Gas West Asia, Muscat, Oman, April 16-18, 2012.
- [68] Yousef, A.A., Al-Saleh, S., and Al-Jawfi, M., “New Recovery Method for carbonate Reservoirs through Tuning the injection Water Salinity: Smart Waterflooding”. Paper SPE 143550 presented at the SPE EUROPEC/EAGE Annual Conference and exhibition,Vienna, Austria, May 23-26, 2011.
- [69] Alotaibi, M.B., Nasr-El-Din, H. A., and Fletcher, J.J., “Electrokinetics of Limestone and Dolomite Rock Particles”. SPE Reservoir Evaluation & Engineering ,October, 2011, 594–603.
- [70] Jae-Young Yu, Mi-Young Shin, Jin-Hwan Noh, and Jung-Ju Seo, “Adsorption of phenol and chlorophenols on Ca-montmorillonite in aqueous solutions”. Geosciences Journal, 2004, 8(2), 185–189.
- [71] Huang, Y.C., Fowkes,F.M., Lloyd,T.B., and Sanders, N.D., “Adsorption of Calcium Ions from Calcium Chloride Solutions onto Calcium Carbonate Particles ”. Langmuir, 1991, 7, 1742–1748.
- [72] http://en.wikipedia.org/wiki/Dissociation_constant
- [73] <http://www.lenntech.com/ro/index/langelier-explanation.htm>
- [74] http://www-naweb.iaea.org/napc/ih/documents/global_cycle/vol%20I/cht_i_09.pdf
- [75] Skoog, D.A., West, D.M.,Holler,F.J., and Crouch,S.R., “Fundamentals of Analytical Chemistry”, Eighth edition.Thomson Learning Inc,USA, 2004
- [76] Strand, S., Hognesen, E.J., and Austad, T., 2006. “Wettability of Carbonates-effects of potential determining ions (Ca^{2+} and SO_4^{2-}) and temperature”. Colloids and Surfaces A: Physicochem. Eng. Aspects, 273: 1-10.
- [77] Puntervold, T., and Austad, T., “Injection of seawater and mixtures with produced water into North Sea chalk formation: Impact of fluid-rock interactions on wettability and scale formation”. Journal of Petroleum Science and Engineering, 2008, 63, 23–33.
- [78] Vdovic, N., and Biscan, J., 1998. “Electrokinetics of natural and synthetic calcite suspensions” . Colloids and Surfaces A: Physicochemical and Engineering Aspects, 137: 7-14.
- [79] Moulin, P., and Roques, H., “Zeta potential measurement of calcium carbonate”. Journal of Colloid and Interface Science, 2003,261, 115–126.

- [80] Schramm, L.L., Mannhardt, K., and Novosad, J.J., 1991. "Electrokinetic properties of reservoir rock particles". *Colloids and Surfaces*, 55: 309-331.
- [81] Chibowski, E., Hotysz, L., and Szczes, A., 2003. "Time dependent changes in zeta potential of freshly precipitated calcium carbonate". *Colloids and Surfaces A: Physicochem. Eng. Aspects*, 222: 41-54.
- [82] Cicerone, D.S., Regazzoni, A.E., and Blesa, M.A., "Electrokinetic properties of the Calcite/Water Interface in the Presence of Magnesium and Organic Matter". *Journal of Colloid and Interface Science*, 1992, 154, 423–433.
- [83] Rodriguez, K., and Araujo, M., "Temperature and Pressure effects on zeta potential values of reservoir minerals". *Journal of Colloid and Interface Science*, 2006, 300, 788–794.
- [84] Yousef, A.A., Al-saleh, S., and Al-Jawfi, M., "The Impact of the Injection Water Chemistry on Oil Recovery from Carbonate Reservoirs". Paper SPE 154077 presented at the SPE EOR conference at Oil and Gas West Asia, Muscat, Oman, April 16-18, 2012.
- [85] Alotaibi, M.B., and Nasr-El-Din, H.A., "Electrokinetics of Limestone Particles and Crude-Oil Droplets in Saline Solutions". *SPE Reservoir Evaluation and Engineering*, 2011, 604–611.

VITA

Name : Moshood Oluwaseun Kassim

Nationality : Nigerian

Date of Birth : February 11th, 1983

Email : Moshoodk@yahoo.com

Current Address : Petroleum Engineering department, King Fahd
University of Petroleum & Minerals, Dhahran, Saudi-
Arabia

Permanent Address : 6B, Olaitan Sebanjo street, Lekki Phase 1, Lagos, Nigeria

Mobile : +966565134488, +966550921754

Academic Background : MS in Petroleum Engineering (September, 2012) from
King Fahd University of Petroleum and Minerals,
Dhahran, Saudi-Arabia

: B.Sc in Chemical Engineering (November, 2006) from
Obafemi Awolowo University, Ile-Ife, Nigeria